OÉ Gaillimh
NUI Galway

An Examination of the Effects of Viral Priming on Neurotoxin Induced Synapse Dysfunction and Degeneration

By

Laura Olsen, MSc

Supervisor: Dr. Declan McKernan

Co-supervisor: Dr. Eilís Dowd

Department of Pharmacology and Therapeutics,

National University of Ireland, Galway

Doctor of Philosophy

October, 2018

Declaration

I declare that the work presented in this thesis has not been submitted for any degree or diploma at this, or any other university and that the work described herein is my own, except the stereotaxic surgeries for Chapter 5, which were conducted by Silvia Cabre, Veronica Alamilla, and Niamh Moriarty. Chapter 1 was partially published as a review article.

Signed:…… Date:……

Acknowledgements

Firstly, I would like to thank my supervisor Dr. Declan McKernan and my co-supervisor Dr. Eilís Dowd for providing the invaluable opportunity to challenge myself. The guidance and support throughout the PhD process is greatly appreciated. I would also like to thank the collaborators in Umeå, Sweden, specifically Dr. Fredrik Almqvist and Dr. Andrew Cairns. Their zeal for quality science and kindness throughout the collaboration is unmatched.

I would be remiss if I did not acknowledge the amazing group of people that makeup the CNS lab. The supportive atmosphere created by these lovely individuals is unparalleled. Thank you Dr. Conor Hennessy and (soon to be Dr.!) Claire Feerick for all of the chats over 37 West/Mocha Beans breakfast and your patience with my slow morning brain. ☺ Also, a big thank you to my Dowd group half sisters (past and present). I wouldn't have made it to the finish line without you guys! Additionally, I feel enormous gratitude to Dr. Danny Kerr and Amby O'Halloran. You two have been the intellectual pillars of the CNS lab and have always helped us crazy PhD students keep things in perspective.

Finally, I would like to thank my family for the support and encouragement throughout the MSc and PhD. I apologize for all that I have missed over the last 5 years.

Abstract

Over 200 years since its first description, Parkinson's disease (PD) remains the second most common neurodegenerative disorder. Treatments are insufficient and there is still no cure. The continued lack of treatment development is largely due to a lack of understanding of how the disease occurs. Current research suggests that PD develops as a result of an interaction between genes and the environment. Among the environmental factors linked with PD, certain viral infections have been found to be associated with PD. Although this epidemiological association has been documented since the 1970s, limited pre-clinical research has been conducted to investigate the neurological consequences of viral infections and if there is a pathological contribution to PD development. Due to this gap in the literature, we sought to examine the molecular and cellular consequences of viral-mediated inflammation in the context of PD pathology.

This study aimed to investigate the potential influence viral infections might have on the neurodegenerative effects of relevant stimuli using cellular and animal models of PD. Specifically, synthetic viral-like dsRNA (poly I:C) was used to induce an innate immune response in a human SHSY5Y cell line, E14 rat ventral mesencephalic (VM) primary cultures and in an *in vivo* Sprague-Dawley rat model. This viral-like priming was followed by a subsequent neurotoxin treatment of 6-OHDA, rotenone, MPP^+, or FN075 (pre-clinical models of PD). In general, poly I:C priming, in combination with stimuli (such as oxidative stress, mitochondrial dysfunction, or α-synuclein aggregation) used for modelling PD, resulted in the exacerbation of neurotoxin-induced degeneration. In cell culture, synapse related proteins (such as synaptophysin and PSD-95) and autophagy related proteins (such as LC3-a/b-I/II and p62) were altered due to poly I:C priming. *In vivo*, poly I:C priming (in combination with FN075-induced α-synuclein aggregation) in the rat substantia nigra resulted in

exacerbated neuroinflammation (as measured by microgliosis and astrogliosis), motor deficits, and significant dopaminergic cell loss.

The implications of these findings suggest that viral-mediated inflammation may induce significant changes in cell death, autophagy, and synaptic related proteins in neurons. These viral-mediated molecular and cellular alterations might contribute to PD pathology, supporting the epidemiological role of viral infections in PD. Based on these findings, further investigation is needed into how viral infections might induce these changes to identify novel targets for PD treatment and/or prevention.

Publications

Peer Reviewed Manuscript

1. L Olsen, E Dowd, DP McKernan (2018). A role for viral infections in Parkinson's etiology? Neuronal Signaling. 2 (2)

Manuscript Under Review

2. L Olsen, AG Cairns, J Aden, N Moriarty, S Cabre, VR Alamilla, Almqvist, E Dowd, DP McKernan (2018). Priming with a viral mimetic exacerbates α-synuclein induced degeneration *in vivo.* Brain.

Other Research Dissemination

1. L Olsen, AG Cairns, J Aden, N Moriarty, S Cabre, VR Alamilla, Almqvist, E Dowd, DP McKernan. Viral mediated neuroinflammation in combination with α-synuclein aggregation: A novel rat model of Parkinson's disease. Poster Presentation at FENS, 2018.
2. L Olsen, AG Cairns, J Aden, N Moriarty, S Cabre, VR Alamilla, Almqvist, E Dowd, DP McKernan. Pre-clinical Parkinson's model: Neuroinflammation and α-synuclein aggregation. Poster Presentation at BPS, 2017.
3. L Olsen, AG Cairns, J Aden, N Moriarty, S Cabre, VR Alamilla, Almqvist, E Dowd, DP McKernan. A novel Parkinson's disease model: Combined viral mediated neuroinflammation and α-synuclein aggregation. Oral Presentation at NECTAR, 2017.
4. L Olsen, AG Cairns, J Aden, N Moriarty, S Cabre, VR Alamilla, Almqvist, E Dowd, DP McKernan. A novel model of Parkinson's disease including viral mediated neuroinflammation. Poster Presentation at NSI, 2017.
5. L Olsen, E Dowd, DP McKernan. The effects of viral priming on neurotoxin induced neurodegeneration and synapse dysfunction in cell culture models relevant to Parkinson's disease. Poster Presentation MDS Congress, 2015.

List of Abbreviations

6-OHDA = 6-hydroxydopamine

ALS = Amyotrophic lateral sclerosis

AMPA = α-amino-3-hydroxy-5-methyl-4-isoxazolepropionic acid

ANOVA = analysis of variance

ATP = adenosine triphosphate

BBB = blood-brain barrier

CNS = central nervous system

CSF = cerebrospinal fluid

DA = dopamine

DAMP = damage associated molecular patterns

DAPI = 4',6-diamidino-2-phenylindole

DAT = dopamine transporter

EL = Encephalitis Lethargica

ELISA = enzyme-linked immunosorbent assay

ER = endoplasmic reticulum

GFAP = glial fibrillary acidic protein

HIV = human immunodeficiency virus

HSE = herpes simplex encephalitis

HSV-I/II = herpes simplex virus-I/II

IFN-β = interferon beta

IFNAR1 = type 1 interferon receptor

IL-1β = interleukin 1 beta

IL-6 = interleukin 6

IKKε = IκB-Kinase-epsilon

iNOS = inducible nitric oxide synthase

iPD = idiopathic Parkinson's disease

IRF3 = interferon regulatory transcription factor3

ISG = interferon-stimulated gene

ISRE = IFN-stimulated response element

LAT = latency-associated transcripts

LC3-a/b-I/II = light chain 3-a/b-I/II

LPS = lipopolysaccaride

LTP = long-term potentiation

MHC-II = major histocompatibility complex-II

MPP^+ = 1-methyl-4-phenylpyridinium

MTT = 3-(4,5-dimethylthiazol-2-yl)-2,5-diphenyltetrazolium bromide

MyD88 = myeloid differentiation primary response gene 88

NADPH-oxidase = nicotinamide adenine dinucleotide phosphate oxidase

NF-κB = nuclear factor kappa-light-chain-enhancer of activated B cells

NMDA = N-methyl-D-aspartate

NMDAR = N-methyl-D-aspartate receptor

NP = nucleoprotein

NS1 = non-structural protein 1

PAMP = pathogen-associated molecular patterns

PARP = poly (ADP-ribose) polymerase

PBS = phosphate-buffered saline

PD = Parkinson's disease

PEP = post-encephalitic parkinsonism

PFA = paraformaldehyde

PKR = protein kinase R

Poly I:C = polyinosinic-polycytidylic acid

PRR = pattern recognition receptor

PSD-95 = post-synaptic density protein-95

RIG-1 = retinoic acid-inducible gene I

ROS = reactive oxygen species

SDS-PAGE = sodium dodecyl sulfate polyacrylamide gel electrophoresis

SEM = standard error of the mean

SN = substantia nigra

SNARE = Soluble NSF(N-ethylmaleimide-sensitive factor) Attachment Protein Receptor

SNK = Student Newman-Keul's test

STR = striatum

TBK1 = TANK-binding kinase 1

TBS = tris-buffered saline

TG = trigeminal ganglia

TH = tyrosine hydroxylase

TIR = Toll-interleukin-1 binding receptor

TLR2 = toll-like receptor 2

TLR3 = toll-like receptor 3

TNF-α = tumor necrosis factor alpha

TNFR = tumour necrosis factor receptor 1

TRIF = TIR-domain-containing adapter-inducing interferon-β

TUNEL = terminal deoxynucleotidyl transferase dUTP nick end labeling

VM = ventral mesencephalon

Table of Contents

Declaration i
Acknowledgements ii
Abstract iii
Publications v
Other Research Dissemination vi
List of Abbreviations vii
CHAPTER ONE 2
1.1 GENERAL INTRODUCTION 2
1.2 VIRAL INFLAMMATION 3
1.2.1 Innate Immune System 3
1.2.2 Toll-like Receptors 5
1.2.2.1 TLR3 5
1.2.2.2 TLR3 Expression Location 6
1.2.2.3 TLR3 Activation 9
1.2.3 Immune Cells of the CNS: Glial Cells 11
1.3 PARKINSON'S DISEASE 14
1.3.1 Parkinson's Etiology: Risk Factors 14
1.3.1.1 Genetic Predisposition 14
1.3.1.2 Age and Environment 15
1.3.2 Pathophysiology 17
1.3.2.1 Dopaminergic Neurodegeneration 17
1.3.2.2 Abnormal α-synuclein Accumulation 20
1.3.2.3 Synapse Dysfunction 25
1.3.2.4 Oxidative Stress 26
1.3.2.5 Autophagy Disruption 29
1.3.2.6 Neuroinflammation: Glial Cells 32
1.3.2.7 Neuroinflammation: Inflammatory Markers in PD 32
1.4 VIRAL INFECTIONS AND PARKINSON'S DISEASE RISK 34
1.4.1 Historical Perspective 34
1.4.2 Viral Entry into the CNS 37
1.4.3 Neurological Consequences of Viral Infections 41

1.4.3.1 Synapse 41
1.4.3.2 Protein Aggregation and Autophagy Disruption 42
1.4.3.3 Neuroinflammation 45
1.4 PRE-CLINICAL ANIMAL MODELS OF PD AND VIRAL INFECTIONS 48
1.4.1 6-Hydroxydopamine 48
1.4.2 Rotenone 48
1.4.3 MPTP 49
1.4.4 α-synucleinopathy 49
1.4.5 Poly I:C 50
1.5 HYPOTHESES 50
1.6 THESIS OBJECTIVES 50
CHAPTER TWO 53
2.1 MATERIALS 53
2.1.1 Cell Culture 53
2.1.2 Compounds 53
2.1.3 Western Blot 54
2.1.4 Immunocytochemistry 54
2.1.5 Immunohistochemistry 54
2.1.6 qPCR 55
2.1.7 ELISA 55
2.1.8 Antibodies 56
2.2 METHODS 57
2.2.1 Global Experimental Design 57
2.2.2 Cell Culture 58
2.2.2.1 SH-SY5Y Neuroblastoma Cell Line 58
2.2.2.2 SH-SY5Y Maintenance 59
2.2.3 Embryonic Day 14 Ventral Mesencephalic Primary Rat Mixed Culture 60
2.2.3.1 Dissection and Isolation 60
2.2.4 Cell Counting 62
2.2.5 Cell Culture Experiments 65
2.2.6 Animal Experiment 65
2.2.7 Animals 65
2.2.8 Surgery 66

2.2.9 Cell Assays 68
2.2.9.1 MTT Cell Viability Assay 68
2.2.9.2 TUNEL Apoptotic Assay 71
2.2.10 qPCR 73
2.2.10.1 mRNA Isolation 73
2.2.10.2 cDNA Synthesis 73
2.2.10.3 qPCR 74
2.2.10.4 Experimental Design 77
2.2.11 Western Blot 78
2.2.11.1 Protein Lysis 78
2.2.11.2 Bradford 78
2.2.11.3 Gel Electrophoresis 79
2.2.11.4 Wet Transfer 80
2.2.11.5 Antibody Detection 80
2.2.11.6 Experimental Design 84
2.2.11.7 Western Blot Quantification 85
2.2.12 Immunocytochemistry 86
2.2.12.1 Immunostaining 86
2.2.12.2 Experimental Design 86
2.2.12.3 Immunocytochemistry Quantification 88
2.2.13 ELISA 89
2.2.13.1 Cell Culture ELISAs 89
2.2.13.2 Experimental Design 89
2.2.14 Immunohistochemistry 90
2.2.14.1 Immunostaining 90
2.2.14.2 Experimental Design 91
2.2.14.3 Immunohistochemistry Quantification 91
2.2.15 Behavioural Analysis 94
2.2.16 Statistics 96
CHAPTER THREE 98
3.1 INTRODUCTION 98
3.2 METHODS 99
3.3 EXPERIMENTAL DESIGN 99

3.4 RESULTS 101
3.4.1 Cell Viability and Cell Death Assays in SH-SY5Y Cells 101
3.4.1.1 Cell Viability after Neurotoxin Treatment in SH-SY5Y Cells 101
3.4.1.2 Cell Death after Neurotoxin Treatment in SH-SY5Y Cells 104
3.4.2 Poly I:C Activation of TLR3 in SH-SY5Y Cells 106
3.4.3 Poly I:C Priming Modulates Cell Death in SH-SY5Y Cells 109
3.4.3.1 Poly I:C Priming Exacerbates Neurotoxin Induced Decrease in Cell Viability 109
3.4.3.2 Poly I:C Priming Modulates Neurotoxin Induced Increase in $TUNEL^{+}$ Cells 111
3.4.4 Poly I:C Priming Modulates Relative mRNA and Protein Expression SH-SY5Y Cells 113
3.4.4.1 Poly I:C Priming Modulates 6-OHDA Induced Changes in mRNA and Protein Expression 113
3.4.4.2 Poly I:C Priming Modulates Rotenone Induced Changes in mRNA and Protein Expression 121
3.4.4.3 Poly I:C Priming Modulates MPP^{+} Induced Changes in mRNA and Protein Expression 129
3.4.4.4 Poly I:C Priming Modulates FN075 Induced Changes in mRNA and Protein Expression 137
3.6 DISCUSSION 144
CHAPTER FOUR 149
4.1 INTRODUCTION 149
4.2 METHODS 150
4.3 EXPERIMENTAL DESIGN 150
4.4 RESULTS 152
4.4.1 Neurotoxin Optimisation in VM Rat Cells: MTT Cell Viability 152
4.4.2 Poly I:C Activation of TLR3 in VM Cells 154
4.4.3 Poly I:C Priming in VM Cells: Cell Viability and Cell Populations 157
4.4.3.1 Cell Viability after Poly I:C Priming in VM Cells 157
4.4.3.2 Cell Populations after Poly I:C Priming in VM Cells 159
4.4.4 Poly I:C Priming in VM Cells: mRNA and Protein Expression 164
4.4.4.1 Poly I:C Priming 6-OHDA in VM Cells 164
4.4.4.2 Poly I:C Priming Rotenone in VM Cells 170
4.4.4.3 Poly I:C Priming FN075 in VM Cells 176

4.5 DISCUSSION 182
CHAPTER FIVE 187
5.1 INTRODUCTION 187
5.2 METHODS 188
5.3 EXPERIMENTAL DESIGN 188
5.4 RESULTS 191
5.4.1. Motor Dysfunction After Sequential Poly I:C and FN075 Administration. 191
5.4.2. FN075 Promotes Filamentous α-synuclein Aggregation *In vivo* 194
5.4.3. Poly I:C Priming of FN075 Precipitates Nigral Neurodegeneration *In vivo* 197
5.4.4. Poly I:C Priming of FN075 Exacerbates Neuroinflammation *In vivo* 200
5.4.5. Synaptic and Autophagy Changes After Poly I:C Priming *In vivo* 207
5.5 DISCUSSION 212
CHAPTER SIX 216
6.1 SUMMARY OF FINDINGS 216
6.2 CONTRIBUTIONS AND IMPLICATIONS 220
6.3 FUTURE RECOMMENDATIONS 222
References 225
Appendix A. 255

Chapter One: Introduction

CHAPTER ONE

1.1 GENERAL INTRODUCTION

Despite 200 years passing since its first clinical description (Parkinson, 1817, Parkinson, 2002), the etiology of idiopathic Parkinson's disease (PD) remains poorly understood (Schapira and Jenner, 2011). The most widely accepted hypothesis is that the disease manifests after a lifetime of exposures to both protective and detrimental factors in an individual's environment, and their interaction with underlying genetics (Gao and Hong, 2011). Although neuropathological features (such as dopaminergic neurodegeneration, α-synuclein aggregation, neuroinflammation, etc.) have been well described in PD, it is unclear how much environmental factors contribute to PD or PD associated pathology.

Evidence is now beginning to accumulate that suggests that viral infection may drive a chronic neuroinflammatory response in the brain (Bobyn et al., 2012, Bu et al., 2015, Itzhaki et al., 2016, Jang et al., 2009, Lövheim et al., 2015, Marttila et al., 1982, Olsen et al., 2018), which, due to its well established role in the pathogenesis of neurodegenerative disease, could increase the risk of developing PD. Numerous epidemiological studies suggest an association between certain viral infections and the incidence of PD (Bobyn et al., 2012, Bu et al., 2015, Itzhaki et al., 2016, Jang et al., 2009, Lövheim et al., 2015, Marttila et al., 1982, Olsen et al., 2018) . Despite these findings, the contribution of viral infection and/or the viral-mediated neuroinflammatory response in PD has yet to be thoroughly investigated (Deleidi and Isacson, 2012, Olsen et al., 2018). However, previous research suggests that certain viral infections can induce excessive neuroinflammation, synapse dysfunction, and degeneration (Carpentier et al., 2005, Ebrahimie et al., 2015, Menendez et al., 2016, Valyi-Nagy et al., 2000).

With this in mind, the following work detailed in this thesis seeks to investigate the potential molecular and cellular consequences of viral-related inflammation, and if these consequences modulate the degenerative effects of PD related neuropathological features.

1.2 VIRAL INFLAMMATION

1.2.1 Innate Immune System

The human immune system is divided into the adaptive and innate immune systems (Abbas et al., 2014) (see Fig. 1.1). Innate immunity is a genetically conserved, non-specific host defense that attacks foreign antigens. The adaptive immune system is a memory-based specific response that attacks previously encountered antigens with developed B-cells and T-cells (Dutton et al., 1998, Rajewsky and Schittek, 1990).

During an inflammatory response, infected cells release cytokines to recruit neutrophils. The innate immune system uses cytokines, chemokines, complement glycoproteins, and adhesion molecules for phagocytosis. Phagocytosis occurs by myeloid phagocytes that identify foreign bodies, adhere, and degrade invading pathogens. Once a macrophage has ingested a foreign invader, antigen-presenting epitope markers are displayed to alert other immune cells and guide T-cell maturation (Parkin and Cohen, 2001, Turvey and Broide, 2010).

The innate and adaptive immune systems are intertwined through macrophage activity. Macrophages are able to attack pathogenic species due to pattern-recognition receptors (PRRs) that have evolved to recognize the common characteristics of these infectious agents (such as bacterial lipopolysaccharides, pathogenic DNA, viral dsRNA) called pathogen-associated molecular patterns (PAMPs) (Mosser and Edwards, 2008, Schroder et al., 2006). PRRs can also recognize self-debris released from dying cells,

referred to as damage-associated molecular patterns (DAMPs). In this context, the self-debris is degraded and the immune system is alerted to the site of cell death (Miller et al., 2011, Seong and Matzinger, 2004).

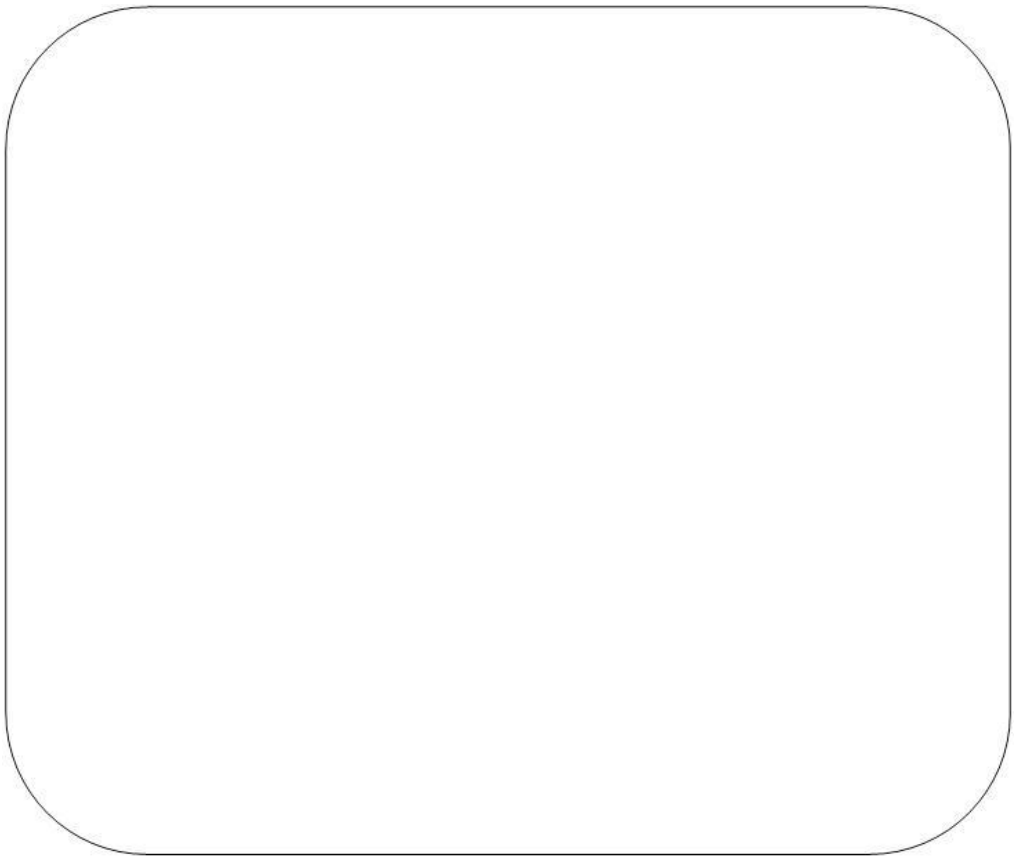

Figure. 1.1 Integrated human immune system. Epithelial tissue is the primary defense system from foreign invaders. Secondly, the innate immune system is an evolutionarily conserved, non-specific host defense system that recognises common pathogenic patterns. The innate immune system interacts with the adaptive immune system via macrophages and dendritic cells. Host cells then degrade and present pathogenic antigens for T- and B- cells to make antibodies that "remember" the infectious agent. Upon further exposure to a similar pathogen, the immunological memory from the adaptive immune system will effectively and immediately attack the invading pathogen. (Turvey and Broide, 2010)

1.2.2 Toll-like Receptors

Toll-like receptors (TLR) are glycoprotein transmembrane receptors that recognize PAMPs (such as lipopolysaccharides, dsDNA/RNA, ssRNA). TLRs are mostly associated with dendritic cells, macrophages, and microglia, but they also present in epithelial cells, endothelial cells, astrocytes, oligodendrocytes, and neurons (Chang, 2010). The downstream effects of TLR activation (see Fig. 1.2) include pro-inflammatory cytokine release, type I interferon (IFN) production, and nuclear factor kappa-light-chain-enhancer (NF-κB) and interferon regulatory factor 3 (IRF3) activation (O'Neill et al., 2013). Cytokine and IFN release due to TLR signaling is controlled by domain-containing adaptor proteins, such as myeloid differentiation primary response protein 88 (MyD88). IFNs have anti-viral properties, while interleukins regulate the expression of cell proteins (such as adhesion molecules and cyclooxygenase type 2) and tumor necrosis factors (TNF) that regulate apoptotic cell death (Dinarello, 2009). NF-κB activation mediates neuroprotective/neurotoxic events through DNA transcription regulation. The transcription activity of NF-κB in neuronal cells is dependent upon the type of NF-κB activated. TLR ligands were unable to induce the RelA/p50 complex in neurons, but the RelA/RelA homodimer complex (activated through TLR3 specific ligands, including Sendai virus) was found to increase IFN-β through selective IFN-β promoter binding in neuronal cells (Jarosinski et al., 2001, Massa et al., 2006, Thanos and Maniatis, 1995).

1.2.2.1 TLR3

TLR3 (a 3,029 bp gene, including 5 exons) is a type I transmembrane receptor structured with a large N-terminal horse-shoe shaped solenoid ectodomain composed of 23 leucine-rich repeats (responsible for ligand binding), a single transmembrane helix, and a C-terminal cytoplasmic Toll-interleukin-1 binding receptor (TIR) domain (Bell et

al., 2006, Choe et al., 2005, Leonard et al., 2008, Rock et al., 1998, Sun et al., 2006). It recognises multiple viruses (such as West Nile virus, Herpes Simplex Virus-I, influenza A) and the synthetic dsRNA known as polyinosinic-polycytidylic (poly I:C) (Alexopoulou et al., 2001, Kawai and Akira, 2006, Lafaille et al., 2012, Lau et al., 2009, Le Goffic et al., 2007, Reinert et al., 2012). The viral dsRNA ligand (as small as 40-50 bp) binds to the glycan-free lateral side of the convex surface of the TLR3 ectodomain, resulting in a stable TLR3 dimerisation (multiple TLR3 dimers for long strands of dsRNA) and receptor activation (Leonard et al., 2008, Rock et al., 1998).

1.2.2.2 TLR3 Expression Location

The cellular location of TLR3 is based on cell type and activation state. Although TLR3 has been found to be intracellular in monocyte-derived immature dendritic cells (DCs), differentiated monocytes, neurons, and microglia; TLR3 was also found to be present on the cell surface of fibroblasts and astrocytes (Alexopoulou et al., 2001, Bsibsi et al., 2002, Farina et al., 2005, Jack et al., 2005, Matsumoto et al., 2002, Matsumoto and Seya, 2008, Menager et al., 2009, Muzio et al., 2000). However, TLR3 is not present in all cell types; including lymphocytes, monocytes, NK cells, human embryonic stem cells, or human induced pluripotent stem cells (Muzio et al., 2000).

The TLR3 ectodomain is suggested to be responsible for governing TLR3 membrane localisation. Immune receptor trafficking helps to control the timing, amplitude, and stability of the host immune response to an invading viral pathogen (Sorkin and Von Zastrow, 2009). Intracellular TLR3 trafficking is usually from the Golgi complex or endoplasmic reticulum (ER) to endosomes. An accessory protein called Unc93B1 (a 12 transmembrane spanning protein) has been found to regulate the trafficking of TLR3, TLR7, and TLR9 (Tabeta et al., 2006). Unc93B1 binds directly to TLR3 at the transmembrane domain/ juxtamembrane region (residues Asp699 and

Glu704) to deliver TLR3 from the ER to the endosomes where TLR3 is proteolytically cleaved to form two fragments for nucleotide sensing and sustained anti-viral response (Brinkmann et al., 2007, Kim et al., 2013b, Qi et al., 2012). Interestingly, the human Unc93B1 gene promoter region was found to have transcriptional factor binding sites for IRF3, NF-κB, AP-1, and ATF-2/c-jun (Pohar et al., 2014).

TLR3 can also be trafficked from intracellular locations to the cell surface after TLR3 stimulation. Cell surface TLR3 was associated with an increase in differentially glycosylated TLR3 and a more potent pro-inflammatory response to dsRNA (Pohar et al., 2014). Maintenance of the intracellular location for TLR3 is suggested to be due to the cytoplasmic 'linker region' at residues Glu727 to Asp749 (Funami et al., 2004, Nishiya et al., 2005). When located at the cell surface, the TLR3 ectodomain can be secreted. It was found that TLR3 ectodomain secretion requires functional Unc93B1 and correlates with full length TLR3 at the cell surface (Qi et al., 2010). In this context, uninfected cells can sense a viral infection via infected cells undergoing cell death which might release both DAMPs and viral dsRNA.

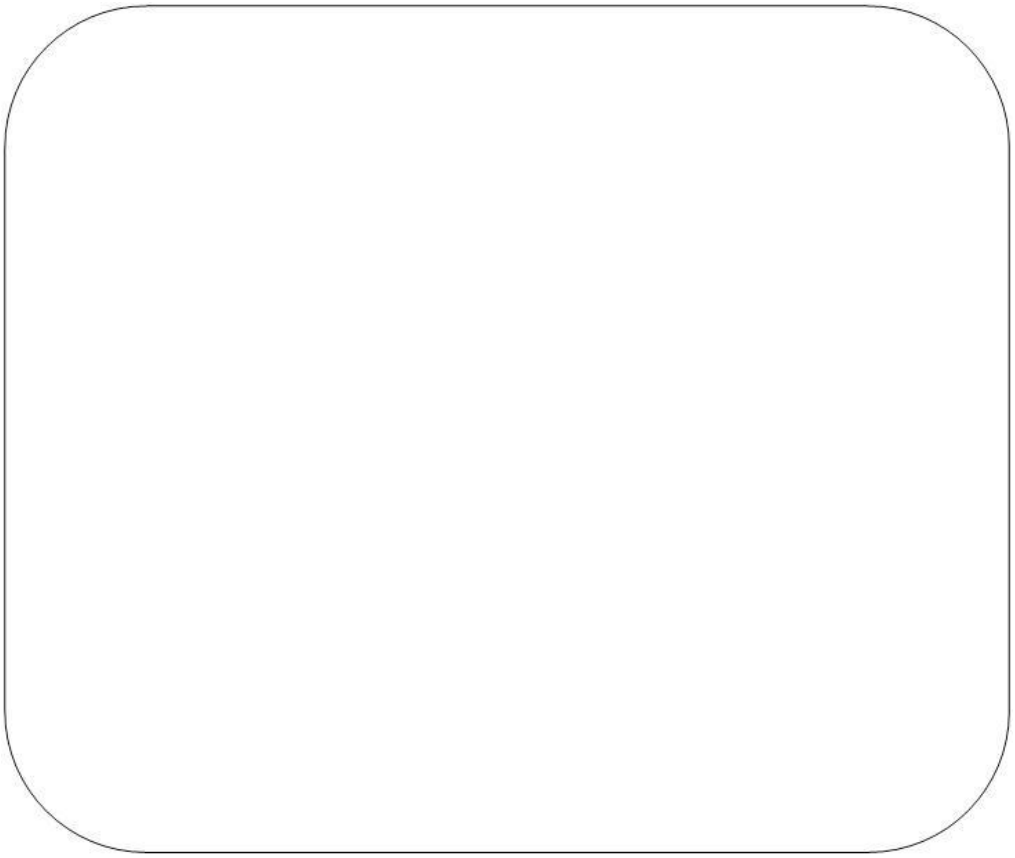

Figure 1.2. TLR3 Signalling Pathway in an Infected Cell. Endosomal TLR3 activation results in multiple cascade events, resulting in NF-κB and IRF3 nuclear translocation and cytokine release. Adapted from (Hennessy and McKernan, 2016).

1.2.2.3 TLR3 Activation

Although most TLRs use MyD88 to induce cascade events, TLR3 uses TIR-domain-containing adaptor inducing IFN-β (TRIF) (Nishiya et al., 2005). TRIF, instead of MyD88, functions in TLR3 (see Fig. 1.2) due to the presence of a proline group instead of an aniline group on the BB loop responsible for intracellular signalling (Oshiumi et al., 2003). TRIF activation causes two separate cascade events. One cascade event recruits tumor necrosis factor receptor (TNFR)-associated factor (TRAF6), protein kinase R (PKR), and other complexes to activate NF-κB (Silva et al., 2004). Release of NF-κB for translocation into the nucleus or mitochondria is due to degrading the inhibitory protein IκB. The other cascade event recruits TANK-binding kinase 1 (TBK1) and IκB kinase-ε (IKKε) to activate interferon regulatory factor 3 (IRF3), which regulates type I IFN activity (Fitzgerald et al., 2003, Sato et al., 1998). IRF3 is phosphorylated at the C-terminus at Ser/Thr residues by IKKε and TBK1, resulting in stable IRF3 dimerisation and nuclear translocation to then associate with co-activator protein CBP/p300 and IFN-stimulated response element (ISRE) for DNA binding at positive regulatory domains III-I near the IFN-β enhancer to initiate type 1 IFN transcription (Escalante et al., 2007, Fitzgerald et al., 2003, Mori et al., 2004, Sharma et al., 2011).

Type I IFNs specific to the anti-viral response include IFN-α and IFN-β, which lead to the transcription of IFN stimulated genes (ISGs) (Isaacs and Lindenmann, 1957, Marcus and Sekellick, 1977). At the IFN-β enhancer site (located -110 and -45 from the transcription start site), the IFN-β enhanceosome is assembled (Panne et al., 2007). The IFN-β enhanceosome contains IRF3/IRF7, NF-κB, and the basic region-leucine zipper protein ATF-2/c-jun (Falvo et al., 2000, Panne et al., 2007). Altogether, the host cell

response to most viral infections results in pro-inflammatory cytokine and IFN release. This evolutionarily conserved immune response can prevent viral replication and spread.

Interleukins (IL) are secreted cytokines which primarily mediate an inflammatory response via communication with leukocytes (Tanaka and Kishimoto, 2014). IL-6 was previously identified as a B-cell-stimulating factor (Kishimoto, 1989). After glycosylation, IL-6 becomes activated and interacts with multiple cells to produce a pro-inflammatory response (Heinrich et al., 1990, Kimura and Kishimoto, 2010, Ma et al., 2012, Tanaka et al., 2012). Another pro-inflammatory member of the IL family is IL-1β (Afonina et al., 2015). Proteolytic maturation of IL-1β allows this cytokine to interact with IL-1 receptor, contributing to the host immune response (Mosley et al., 1987, Dinarello, 2018).

TNF-α plays a significant role in viral immunity and cell death/survival (Victor and Gottlieb, 2002). This cytokine binds to TNF receptor 1 and TNF receptor 2, leading to cascade events which regulate NF-κB activation and caspase activity (Brenner et al., 2015). Depending on other regulatory factors, TNF-α can induce apoptosis or necroptosis (Brenner et al., 2015).

TLR3 activation, and the consequent downstream effects, can have a protective or toxic effect. Viral RNA has been found to translocate IRF3 from the cytosol to the outer membrane of mitochondria, resulting in apoptosis via Bcl-2 family proteins, although this effect was mediated by retinoic acid-inducible gene 1 (RIG-1)-like receptor activation of IRF3 (Chattopadhyay et al., 2011). Instead, TLR3 mediated activation of IRF3 resulted in apoptosis via caspase-3 and caspase-8 activation (McAllister et al., 2012). Synthetic dsRNA (poly I:C) increased PKR and Fas transcription, cytokine release (IFN-β and IL-1β), and apoptosis through caspase-3

activation (Field et al., 2010). PKR was found to be the direct mediator in Fas and BAX expression and apoptosis after dsRNA exposure (Balachandran et al., 1998b). Similar studies found type 1 IFNs to potentiate virus induced apoptosis through PKR activation (Balachandran et al., 2000). As with TRIF, PKR is specific to the TLR3 pathway in the innate immune system. These findings suggest that PKR is selectively activated by TLR3 and that the pro-apoptotic effects of PKR are modulated by type 1 IFNs.

1.2.3 Immune Cells of the CNS: Glial Cells

Glial cells in the CNS mainly function as regulators of the cellular environment for healthy neuronal cell function (see Fig. 1.3). Two glial cells that have are involved in an immune response in the CNS are microglia and astrocytes. Astrocytes (identified by glial fibrillary acidic protein expression- GFAP) regulate the microenvironment by controlling extracellular potassium levels and taking up neurotransmitters (Kandel et al., 2000). Microglial cells (identified by OX42/CD11b expression) act as the resident macrophages in the brain. During a defense response, resting microglia activate and become phagocytic (Banati et al., 1993).

Astrocytes (the most abundant cell type in the CNS) support neuron homeostasis by regulating synaptic activity, assisting in BBB formation, and interacting with immune cells. They regulate neurotransmission and metabolism by controlling extracellular potassium levels, uptake of neurotransmitters (such as glutamate), and storing glycogens/exporting lactate (Kandel et al., 2000). Also, astrocyte-secreted mediators, such as thrombospondins, promote neuronal synapse formation (Allen et al., 2012).

Although the traditional view that the adult central nervous system (CNS) is immunoprivileged has been partially disproven, there are still clear differences in the CNS immunity when compared to other organs. Peripheral immune cells can enter the

CNS and interact with the resident immune cells of the CNS (see Fig. 1.3). Similar to the process in the peripheral immune system, microglia cells respond to pathogenic invasion with phagocytosis and antigen-presentation, while astrocytes produce pro-inflammatory cytokines and chemokines. Microglia cells act as resident immune cells in the CNS, with the capability of sensing, engulfing, and degrading invading pathogen (Banati et al., 1993). The activation of microglia can have neuroprotective or neurotoxic effects depending on their microenvironment. When activated, some microglia release reactive oxygen species (ROS), inducible nitric oxide synthase (iNOS), and cytokines (Zhang et al., 1999). These oxidative species and cytokines interact with dopaminergic neurons to regulate cell fate during stress and neurodegenerative disease, such as PD (Zhang et al., 1999).

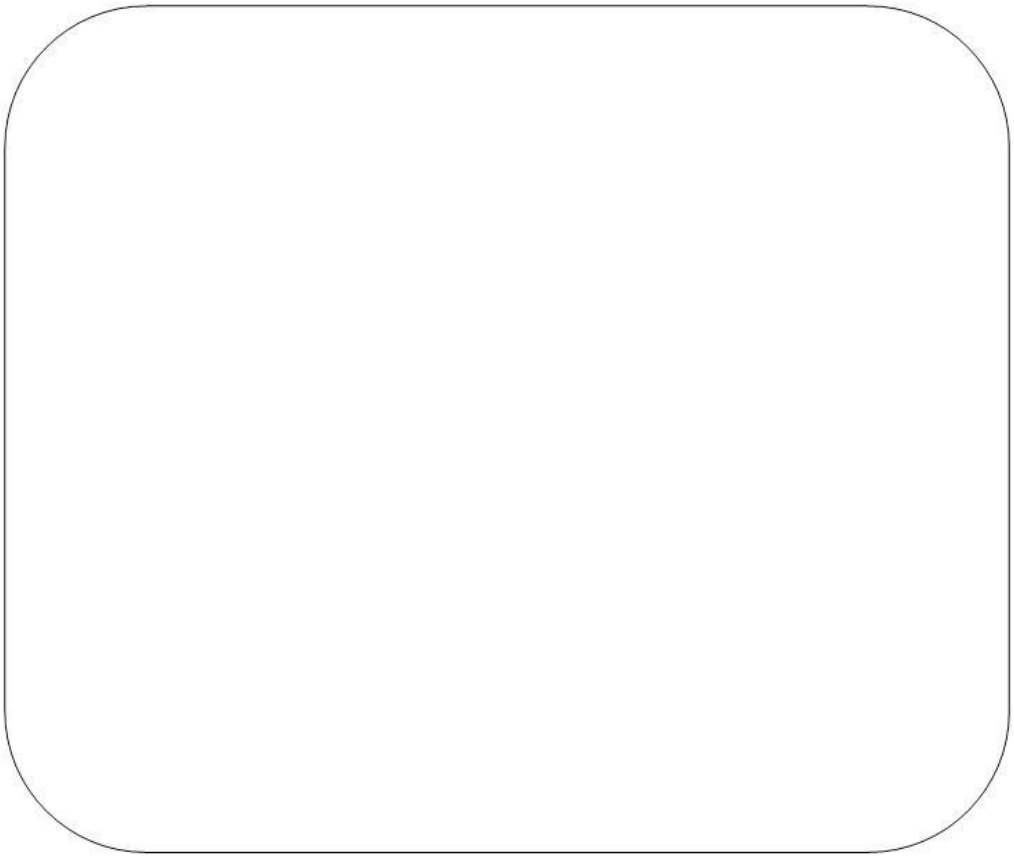

Figure 1.3. Interactions between the Peripheral Immune System and CNS. Within the CNS, resting microglia can become activated during an immune response. From the periphery, other immune cells (such as T-cells and monocytes) can enter the CNS to modulate the immune response in the CNS. 1-2) Resting microglia sense cytokines and cell debris and become activated. 3) Microglia released cytokines can cause healthy neurons to induce neurodegeneration. 4) Peripheral monocytes enter the brain through the BBB. 5) Peripheral monocytes can become monocyte-derived macrophages within the CNS. 6) Macrophage released anti-inflammatory cytokines can suppress activated microglia activity. 7) Immune cells interact with each other within the peripheral immune system. (Schwartz and Shechter, 2010)

1.3 PARKINSON'S DISEASE

Parkinson's disease (PD) is the second most common neurodegenerative disorder; characterised by the selective degeneration of dopaminergic neurons in the substantia nigra (SN) pars compacta of the midbrain, resulting in an overall decrease in dopamine transmission throughout the nigro-striatal pathway. Motor symptoms include resting tremor, instable posture, bradykinesia, rigidity, and freezing (Moustafa et al., 2016, Rao et al., 2003). This progressive neurodegenerative disease can be familial (associated with early on-set) or sporadic, with the common pathological feature of α-synuclein abnormalities/aggregation (Bonifati, 2014).

According to the European Parkinson's Disease Association, 6.3 million people worldwide (and over 9 thousand in Ireland) suffer from PD (parkinsons.ie 2005). Adjusted for age and gender, estimates have found the prevalence of PD in North America for those over the age of 45 year to be 572 per 100,000 people (Marras et al., 2018). This debilitating disease prematurely robs adults of their independence. PD becomes a financial, emotional, and physical burden for the patient and their family. In Europe, the annual cost association with PD is estimated to be 13.9 billion euro (Olesen et al., 2012).

1.3.1 Parkinson's Etiology: Risk Factors

1.3.1.1 Genetic Predisposition

Genetic mutations have been found to contribute to familial and sporadic Parkinsonism. Although there is strong evidence for genetic mutations in familial PD, only 5-10% of all PD patients are diagnosed with the familial condition (Mizuno et al., 2001). Key genes related to sporadic or familial PD (see Table 1.1) are *parkin*, *pink1*, *dj-1*, and *lrrk2* (Alberio and Fasano, 2011). Mutations in these genes have been associated

with α-synuclein mutations and an increase in oxidative stress. There are also five missense α-synuclein genetic mutations that have been linked to PD with various stages of on-set (A30P, E46K, H50Q, G51D, and A53T) (Flagmeier et al., 2016, Fujioka et al., 2014, Krüger et al., 1998, Lesage et al., 2013, Polymeropoulos et al., 1997, Proukakis et al., 2013, Zarranz et al., 2004). Multiplication of the α-synuclein gene also produces PD, with the duplication exhibiting a similar progression to sporadic PD and the triplication leading to early on-set and rapid progression (Olgiati et al., 2015, Ross et al., 2008). The association between these α-synuclein related genes and PD led to the realisation that abnormal α-synuclein accumulate within Lewy Bodies (Goedert et al., 2013).

1.3.1.2 Age and Environment

Age is the most significant risk factor for developing idiopathic PD (iPD). After the age of 65, the incidence of PD increases exponentially with age (Mayeux et al., 2003, Rodriguez et al., 2015). It is unclear why age is associated with an increase in degeneration in the SN, but some processes such as protein aggregation, iron accumulation, and oxidative stress may be due to normal aging (Daugherty and Raz, 2013, Hirsch et al., 1987, Markesbery et al., 2009).

Epidemiological studies have suggested an association between certain environmental factors (such as exposure to pesticides or heavy metals, traumatic brain injury, and previous bacterial or viral infection) and incidence of PD (Lai et al., 2002, Liou et al., 1997, Seidler et al., 1996). Prolonged exposure to specific pesticides (rotenone and paraquat) is believed to cause mitochondrial dysfunction and oxidative stress in humans, possibly leading to the association with PD (Mandel et al., 2012, Tanner et al., 2011).

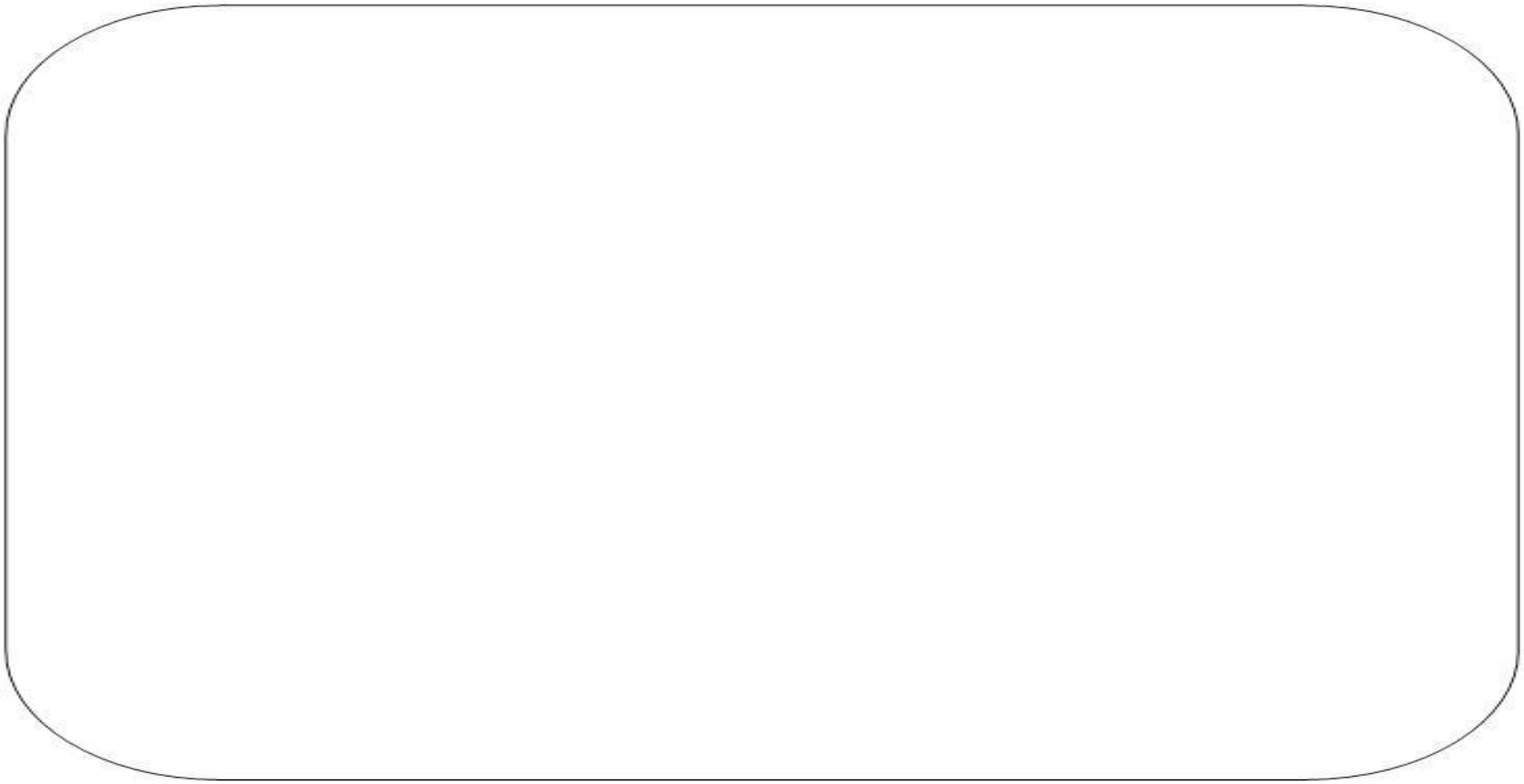

Table 1.1. PD Related Genes. Genes associated with PD have a wide variety of phenotypes (ranging from typical late on-set to aggressive early on-set) and pathological features. Genome wide (GW) association studies found mutations in genes related to α-synuclein and lysosomal pathways led researchers to realise the importance of these cellular proteins in PD pathology. (Bonifati, 2014)

1.3.2 Pathophysiology

1.3.2.1 Dopaminergic Neurodegeneration

Parkinson's patients have a significant loss of dopaminergic neurons in the SN, with motor symptoms present after more than 50% loss (Fearnley and Lees, 1991). The SN is the primary source of dopamine in this pathway (Lucas et al., 2013). Loss of dopaminergic transmission results in cortical-striatal pathway dysfunction, including disruption in the basal ganglia circuit (de la Fuente-Fernández, 2013, Devos et al., 2010, Purves et al., 2001).

The basal ganglia system directly and indirectly regulates the motor neurons in the motor cortex (Purves et al., 2001). Within the direct pathway, transient excitatory D1 type dopaminergic neuronal projections from the SN modulate the transient inhibitory projections from the caudate/putamen to the internal segment of the globus pallidus, which tonically inhibits the excitatory thalamic projections into the premotor cortex (see Fig. 1.4). Conversely, the inhibitory D2 type dopaminergic neuronal projections from the SN regulate the indirect pathway, which relies on the external segment of the globus pallidus and subthalamic nucleus to modulate the activity of the internal segment of the globus pallidus (see Fig. 1.4). Dopaminergic loss in PD results in a lack of inhibition in the basal ganglia pathway, leading to movement disruption (Purves et al., 2001).

Beyond dopaminergic cell death, evidence suggests a wide variety of neuronal populations undergo degeneration (Giguère et al., 2018). A recent review reported significant loss of cholinergic neurons in the pedunculopontine nucleus (41% average), dorsal motor nucleus (55%) and nucleus basalis of meynert (72% average) (Giguère et al., 2018). Although serotonergic loss in the dorsal raphe nucleus and noradrenergic loss in the locus coeruleus was previously suggested to occur in cases of PD, this review

reported non-observational studies which quantified neuronal loss in these regions did not find significant neurodegeneration (Bertrand et al., 1997, Cheshire et al., 2015, Gai et al., 1991, Giguère et al., 2018). The progression and importance of non-dopaminergic neuronal cell loss in PD has yet to be determined.

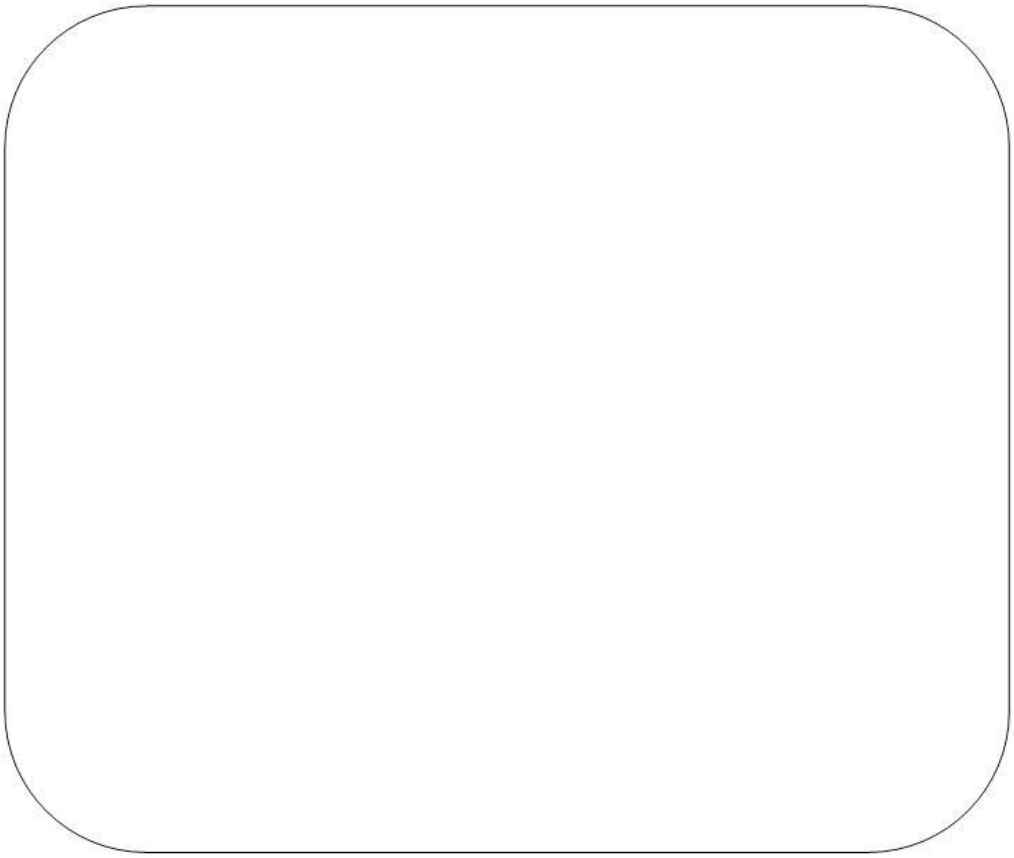

Figure 1.4. The direct and indirect basal ganglia pathways regulating the motor cortex. Excitatory and inhibitory projections from the SN modulate caudate/putamen inhibition of the globus pallidus, leading to disinhibition of thalamic excitatory projections into the motor cortex. The indirect pathway utilises the subthalamic nucleus to oppose the disinhibition of the direct pathway. (Purves et al., 2001)

1.3.2.2 Abnormal α-synuclein Accumulation

Lewy Bodies are pathological protein aggregates characteristic of PD (Fearnley and Lees, 1991). These aggresomes are primarily found in the cytoplasm of neuronal cells in multiple neurodegenerative diseases. Although Lewy Bodies are not present in every PD case, they are strongly associated with dopamine loss, PD, and progressive neurodegeneration (McNaught et al., 2002). Numerous protein types can be found in these Lewy Body inclusions, but α-synuclein aggregates are the most abundant (Garcia-Reitböck et al., 2010).

α-synuclein is a 140 amino acid protein, normally existing as an unfolded monomer in the cytosol or a membrane bound α-helical structure (Maroteaux and Scheller, 1991). In neurons, the α-synuclein protein is believed to be responsible for vesicle/synaptic membrane guidance (as part of the SNARE complex) during exocytosis (Lashuel et al., 2013, Lautenschläger et al., 2017). Genetic studies which deleted α-synuclein found conflicting results, with some finding an increase in dopamine release and others a decrease in dopamine levels (Abeliovich et al., 2000, Cabin et al., 2002, Murphy et al., 2000, Yavich et al., 2006). At the very least, these studies suggest that α-synuclein regulates neurotransmitter release in dopaminergic neurons (see Fig. 1.5).

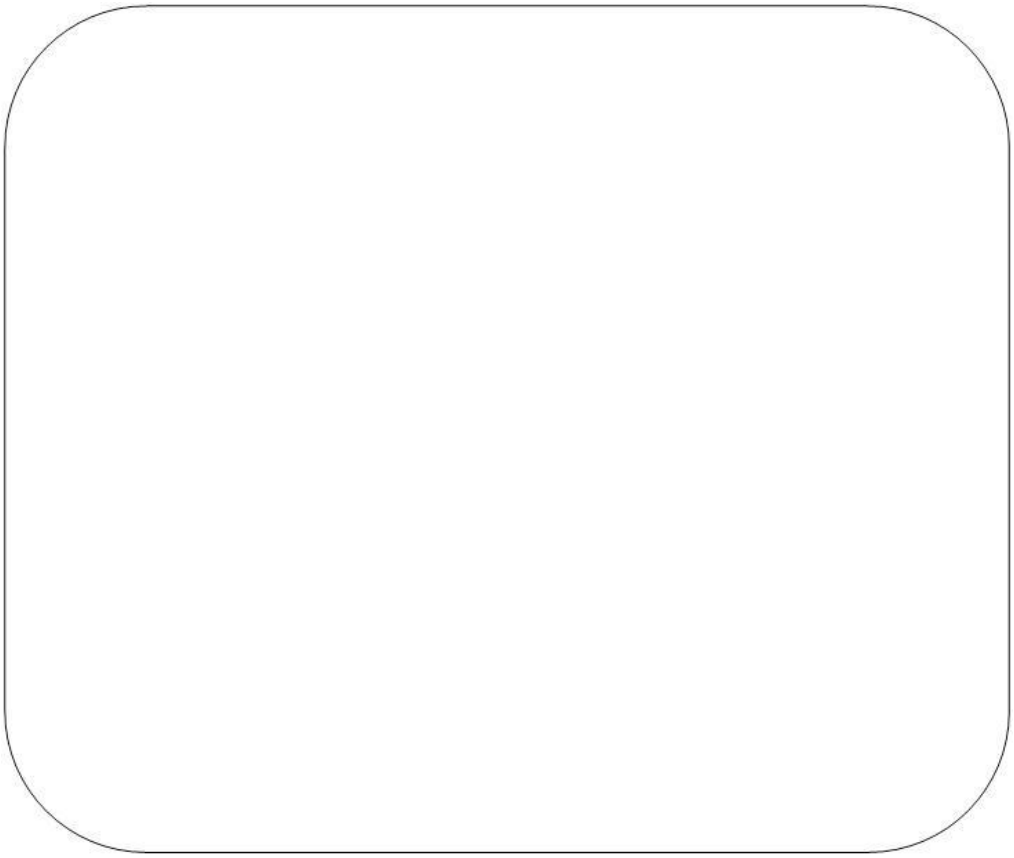

Figure 1.5. α-Synuclein Participation in SNARE Complex Guided Exocytosis. Current research suggests the normal function of α-synuclein to be related to neurotransmitter release via exocytosis. (Lautenschläger et al., 2017)

Although α-synuclein is expressed in many cell types, neurons appear to be far more vulnerable to α-synuclein abnormalities and accumulation (Barbour et al., 2008, Muchowski and Wacker, 2005, Scherzer et al., 2008). Full length isoforms of α-synuclein are found in Lewy Bodies, but post-translational modifications of α-synuclein, such as proteolytic cleavage, may increase the propensity of this protein to aggregate, resulting in more truncated α-synuclein in Lewy Bodies (Baba et al., 1998, Halliday and McCann, 2008). The most common post-translational modification found in Lewy Body α-synuclein is phosphorylation at serine 129 (Anderson et al., 2006, Mbefo et al., 2010). Although less common, nitration and oxidation has also been suggested to enhance pathogenic mis-folding and aggregation of α-synuclein (Liu et al., 2011, Qin et al., 2007). Pathogenic α-synuclein can exist as an array of multiple different conformations, such as soluble oligomers, spherical protofibrils, insoluble fibrils (Ding et al., 2002, Lashuel et al., 2002, Rochet et al., 2000). In general, fibril formation of α-synuclein (see Fig. 1.6) occurs via nucleation and elongation (Cox et al., 2014). Rate limiting oligomeric nuclei formation is followed by elongation of assembled α-synuclein proteins and formation of mature fibrils (Bhak et al., 2009, Wood et al., 1999). The pathogenic disease state, fibrillisation kinetics, and toxicity of α-synuclein has been difficult to study (Koprich et al., 2011). Depending on the method of fibrillisation, pH, or presence of other proteins, α-synuclein can vary widely in structure, toxicity, and ability to propagate (Bousset et al., 2013, Breydo et al., 2012, Peelaerts et al., 2015, Shtilerman et al., 2002, Uversky et al., 2002). It is also unclear which pathogenic α-synuclein structure(s), if any, may be responsible for neurodegeneration.

Post-mortem analysis found most α-synuclein containing Lewy Bodies to be within live neurons, and that they also existed in healthy elderly adults (Gibb and Lees, 1988, Hindle, 2010, Markesbery et al., 2009, Mikolaenko et al., 2005). There are

increased levels of mutated α-synuclein proteins in PD patients. *In vitro* and *in vivo* experiments currently suggest that soluble oligomeric α-synuclein may be far more neurotoxic than mature fibrils (Gosavi et al., 2002, Winner et al., 2011, Xu et al., 2002). If this is true, the end product of Lewy Body protein inclusion might be neuroprotective due to the sequestering of mature less toxic fibrils to prevent their fragmentation back into highly toxic oligomers (Glabe, 2008, Tyedmers et al., 2010). *In vitro* studies using a peptidomemtic to induce α-synuclein oligomerisation (FN075) suggest that α-synuclein fibrils are formed from α-synuclein oligomers (Cegelski et al., 2009, Horvath et al., 2012).

Cremades *et al*. (2012) found normal α-synuclein proteins to convert into β-sheet-rich conformations when introduced to oligomerised α-synucleins (Cremades et al., 2012). The β-sheet-rich conformation of the mutated proteins is more likely to polymerise and form fibril aggregates than the normal α-helical conformation (Cremades et al., 2012). It has also been found that these β-sheet-rich proteins can "infect" healthy cells in a prion-like fashion and propagate the disruptive effects of protein aggregation (Guo and Lee, 2014, Olanow and Brundin, 2013).

Related to the propagation of pathogenic α-synuclein aggregates, the Braak hypothesis was postulated in the early 2000s to describe the clinical staging of PD (Braak et al., 2003). This hypothesis suggests that during the early stages of PD pathogens which enter the nasal cavity and/or gut initiate α-synuclein aggregation, followed by a pattern of pathogenic α-synuclein spread from the nasal cavity and/or gut to the brain (Del Tredici and Braak, 2016, Hawkes et al., 2007). The Braak hypothesis is supported by pre-clinical evidence which has demonstrated the ability of α-synuclein aggregates to transmit along neural tracts and cases of healthy neurons taking up extracellular pathogenic α-synuclein (Angot et al., 2012, Desplats et al., 2009, Kordower

et al., 2011, Lee et al., 2005, Pan-Montojo et al., 2012). Not only are the non-motor symptoms of PD (such as gastronintestinal and olfactory problems, see Fig. 1.7) explained by this hypothesis, but patients who received embryonic stem cell grafts were found to have pathogenic α-synuclein spread from host to graft after 10 years time (Chu and Kordower, 2010, Kordower et al., 2008a, Kordower et al., 2008b, Kurowska et al., 2011, Li et al., 2008, Li et al., 2010).

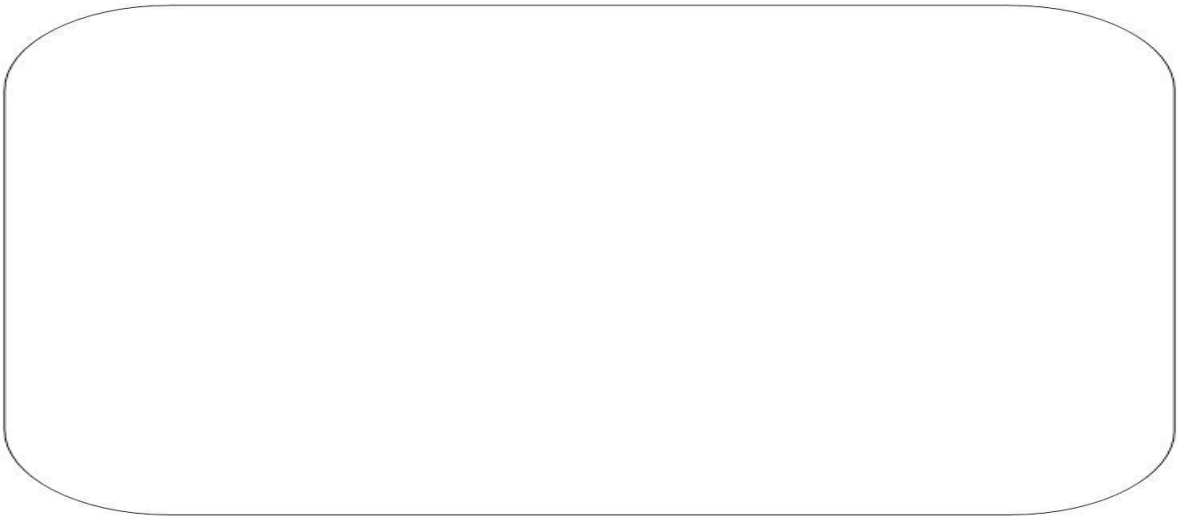

Figure 1.6. α-Synuclein Fibrillisation Kinetics. Under normal conditions, monomeric α-synuclein is believed to exist as a monomer, tetrameric α-helix or a membrane bound structure. Via a nucleation-dependent mechanism, monomers assemble prefibrillar oligomers, which elongate to form mature fibrils. Fibrillised α-synuclein can then be sequestered into protein inclusions, including Lewy Bodies. (Cox et al., 2014)

1.3.2.3 Synapse Dysfunction

Previous models of PD have suggested that synaptic dysfunction (such as alterations to long-term potentiation (LTP)/depression, changes in synaptic proteins, and N-methyl-D-aspartate receptor (NMDAR) subunit composition) in nigrostriatal and corticostriatal pathways could be responsible for the physical manifestations of dopamine loss in the SN (Picconi et al., 2012, Scott et al., 2010, Volpicelli-Daley et al., 2011). Synapse dysfunction, leading to neurodegeneration, occurs years before PD patients experience motor symptoms (see Fig. 1.7). *Post-mortem* studies have found decreases in glutamatergic synapses and α-amino-3-hydroxy-5-methyl-4-isoxazolepropionic acid (AMPA) GluR1 in the striatal regions of PD patients (Bernard et al., 1996, Day et al., 2006). Also, human-induced pluripotent stem cell derived neurons from familial PD patients demonstrated reduced synaptic connectivity and hindered neurite outgrowth (Kouroupi et al., 2017).

In dopaminergic neurons, tyrosine hydroxylase (TH) is the rate-limiting enzyme involved in dopamine synthesis. The monoamine neurotransmitter dopamine is sensitive to degradation into oxidative species such as dopamine quinones and hydroxyl radicals (Caudle et al., 2008). Degradation of dopamine is normally prevented by vesicular monoamine transporters, but these proteins have also been found in Lewy Body aggregates in PD (Yamamoto et al., 2006).

The neuron synapse is a dynamic space with constant neurotransmitter release and re-uptake for cell-cell communication (see Fig. 1.8). As previously mentioned, α-synuclein (as part of the SNARE complex) is suggested to regulate neurotransmitter release (Lautenschläger et al., 2017). Also related to the SNARE complex, synaptophysin (a marker of synaptic plasticity and integrity) is a neuronal glycoprotein crucial for guiding synaptic vesicles (Adams et al., 2017, Gordon et al., 2016,

Wiedenmann and Franke, 1985). Synaptic plasticity is also regulated by post-synaptic density protein 95 (PSD-95), which mediates LTP and dendritic spine structure via its coupling with NMDA receptors at the post-synapse (Clinton et al., 2006, Cousins and Stephenson, 2012, Vickers et al., 2006).

1.3.2.4 Oxidative Stress

Oxidative stress is believed to be a key player in cellular neurodegeneration in PD (Caudle et al., 2008). Reactive oxidative species (ROS) and iNOS are elevated in PD (Hunot et al., 1996, Kouti et al., 2013, Zhang et al., 1999). It is not known whether these toxic species are a cause or result of protein aggregation. It is possible that the disruption in dopamine signalling due to α-synuclein dysfunction may lead to the production of dopamine derived free radicals. Oxidative stress disrupts normal cellular function through oxidising nucleic acids and proteins (Zhang et al., 1999). This stress can alter synaptic transmission and membrane trafficking, likely through nitration of α-synuclein and other proteins (Przedborski et al., 2001). Disruption in dopamine transmission can itself lead to oxidative stress, which confounds the ability to determine the beginning of this destructive cycle.

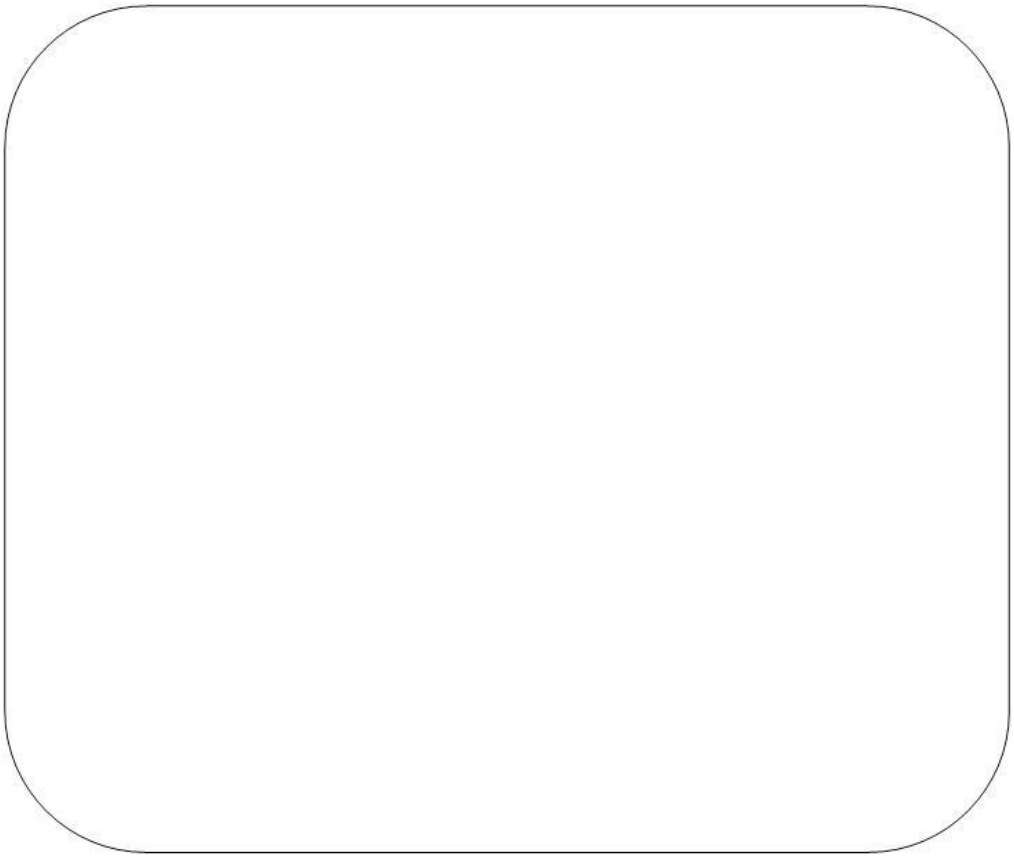

Figure 1.7. Stages of PD Development. Far before PD patients experience symptoms, α-synuclein accumulation and dopaminergic neurodegeneration in the SN has begun. (Mochizuki et al., 2018)

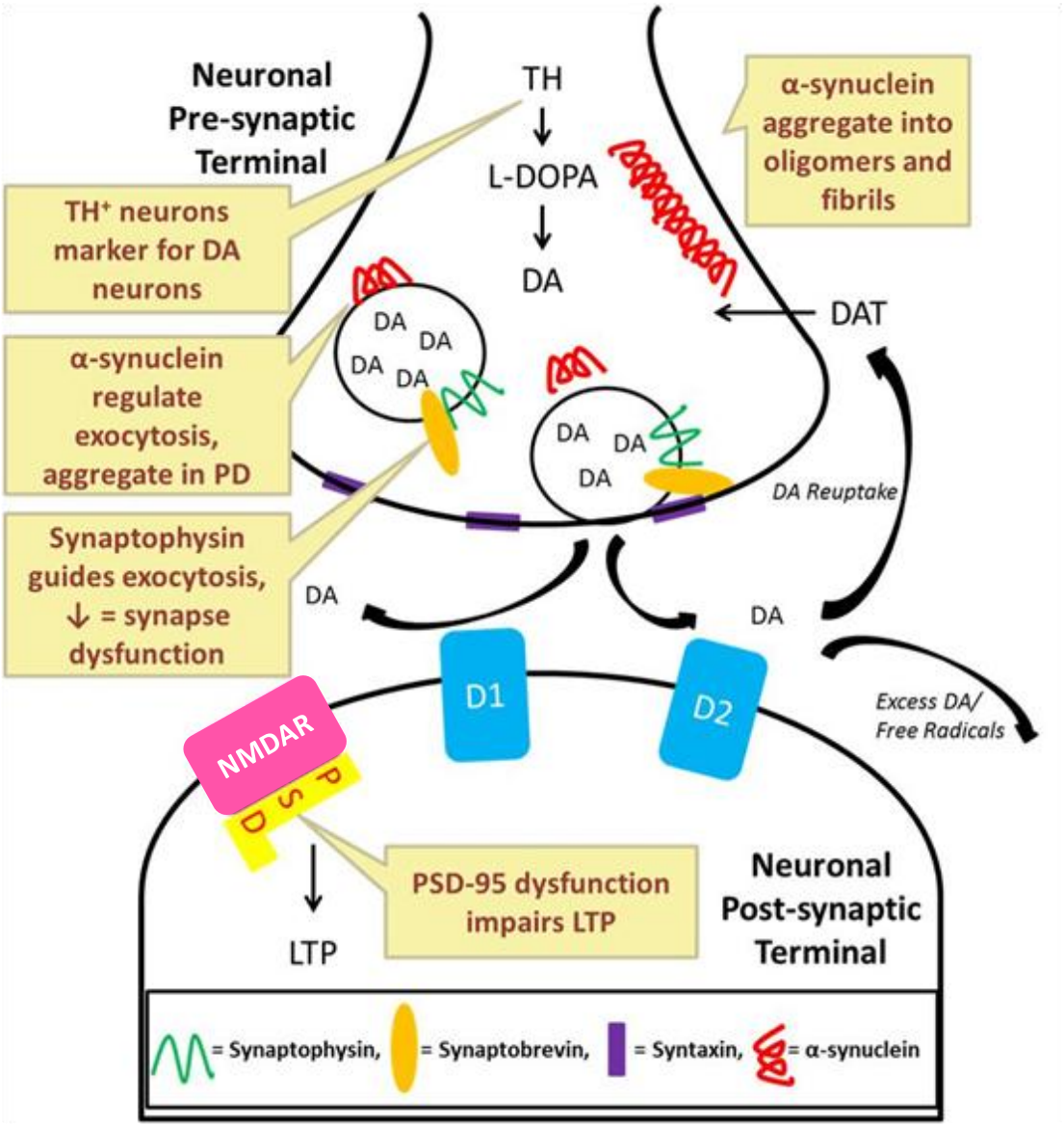

Figure 1.8. Dopaminergic Synapse. Dopamine is synthesised from tyrosine via the rate-limiting TH enzyme in the pre-synapse before collection in synaptic vesicles. Synaptophysin, synaptobrevin, syntaxin, and α-synuclein mediate the exocytosis of the dopamine neurotransmitter into the synapse. Once released into the synapse, dopamine activates post-synaptic dopamine receptors. Dopamine transporter (DAT) is responsible for re-uptake of dopamine, which helps to prevent the production of oxidative species. PSD-95 couples with the NMDA receptor to mediate LTP and dendritic spine formation.

1.3.2.5 Autophagy Disruption

The autophagy process is fundamental for cellular homeostasis. Briefly, unwanted components (mis-folded proteins, foreign structures, dysfunctional proteins, etc.) are engulfed in double-membraned vesicles (autophagosomes) for digestion and substrate recycling (Klionsky et al., 2016). Autophagy pathways have been suggested to be very important for mounting an anti-viral defence in non-replicating cells (Shoji-Kawata and Levine, 2009). Infected epithelial cells, with viruses such as HSV-I, can produce pro-inflammatory cytokines and undergo cell death to prevent viral spread without permanent tissue damage because they can be replaced afterwards. Non-replicating cells, such as neurons, may be more reliant on autophagy processes, referred to xenophagy in the case of degradation of invading pathogens, to limit viral replication and viral spread without undergoing cell death (Levine, 2005, Yordy et al., 2012). To rid the cell of unwanted intracellular components, microtubule-associated protein 1 light chain 3 (LC3-I) undergoes lipidation to produce LC3-II, which binds directly to p62 to form the autophagosome (see Fig. 1.9) (Kabeya et al., 2000, Orvedahl and Levine, 2008, Pankiv et al., 2007). This degradation of invading pathogens reduces replication and facilitates the presentation of pathogenic antigens via major histocompatibility complex class II (MHC-II) (Jordan and Randall, 2012, Schmid et al., 2007).

Crucial for healthy cell aging and relevant to dysfunctional protein in neurodegenerative diseases, autophagy pathways are also responsible for identifying, sequestering, and degrading damaged, mis-folded, or aggregated self proteins (Vilchez et al., 2014). After unwanted proteins are identified and ‘tagged’ via the ubiquitin-proteasome system, proteins undergo lysosomal degradation (Finley, 2009, Nixon, 2013, Tanaka and Matsuda, 2014, Wong and Cuervo, 2010). Ubiquitinated proteins are recognised by p62 (sequestosome 1) and introduced to the autophagosome, which pairs

with the lysosome for protein degradation (Cuervo, 2010, Nixon, 2013). Protein inclusions in neurodegenerative disease have been found to contain ubiquitin, suggesting that autophagy dysfunction may occur in these diseases (Matsuda and Tanaka, 2010, Nixon, 2013, Tanaka and Matsuda, 2014). Familial PD mutations, such as *dj-1* and *lrrk2*, are known to regulate the autophagy pathway, further linking PD and autophagy dysfunction (Irrcher et al., 2010, Plowey et al., 2008). It is currently unclear if the normal slowing of autophagy function that occurs with old age exacerbates PD pathology, or if autophagy directly contributes to PD pathology (Andersson et al., 2013, Ferrington et al., 2005, Grune et al., 2004, Ly et al., 2000).

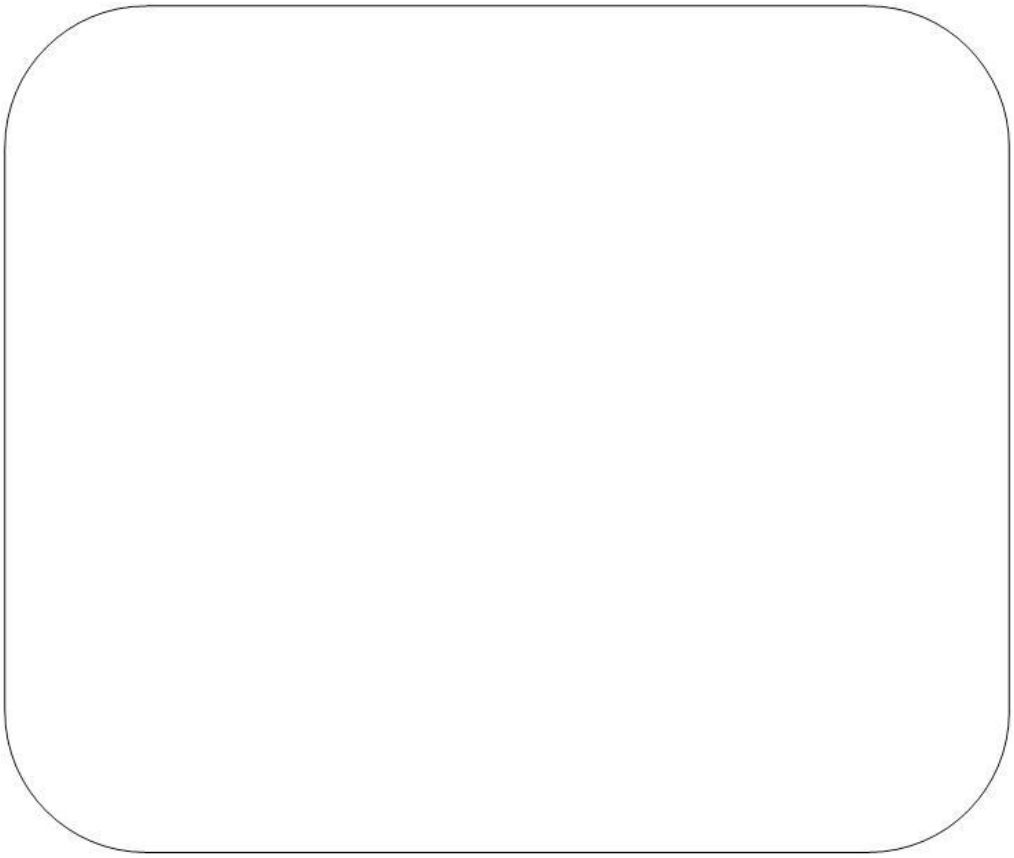

Figure 1.9. Autophagy Activation and Autophagosome Formation. Unwanted structures in the cell (such as abnormal protein or a foreign pathogen) activates the autophagy pathway. This pathway encapsulates unwanted structures in autophagosomes for degradation. Figure adapted from (Orvedahl and Levine, 2008).

1.3.2.6 Neuroinflammation: Glial Cells

The activation of microglia can have neuroprotective or neurotoxic effects depending on their microenvironment. When activated, some microglia release ROS, iNOS, and cytokines (Wu et al., 2005). These oxidative species and cytokines interact with dopaminergic neurons to regulate cell fate during stress. Sawada *et al*. (2006) found that co-culturing ROS producing microglia with neurons resulted in neuronal cell death, and that this was likely due to an increase in nicotinamide adenine dinucleotide phosphate-oxidase (NADPH-oxidase) (Sawada et al., 2006). Increasing the expression of NADPH-oxidase caused neuroprotective microglial cells to become neurotoxic cells. Neurotoxic microglia are suggested to be involved in PD pathology, as an increase in activated microglia have been found in the SN and putamen of PD patients (Sawada et al., 2006). Microglia activation is primarily due to immunological insult or physical stress, although other mediators have been characterised in PD. α-Synuclein aggregates and cytokines have been shown to activate microglia, resulting in enhanced neuronal cell death (Zhang et al., 2005). It is possible that diseased neuronal cells in PD are the primary recruiters of microglia and astrocytes. The role of glial cells in PD requires further research regarding PD and neuroinflammatory processes.

1.3.2.7 Neuroinflammation: Inflammatory Markers in PD

Neuroinflammation in PD patients has previously been investigated to characterise potential biomarkers. Genetic mutations in PD-related genes (*lrrk2* and *parkin*) have been found to regulate the immune system response (Bonifati, 2012, Hakimi et al., 2011, Manzanillo et al., 2013, Satake et al., 2009, Zimprich et al., 2004). Also, single nucleotide polymorphisms in the MHC-II (an antigen-presenting component of specific adaptive immune cells) locus were associated with an increased incidence of PD (Ahmed et al., 2012, Guo et al., 2011, Hamza et al., 2010). *Post-mortem* studies have

found increased levels of pro-inflammatory cytokines (Nagatsu et al., 2000). They also found increased levels of IFNs and p65 subunits of NF-κB (Mogi et al., 1996).

An examination of cytokine levels in PD patients found cytokine levels to be below the sensitivity limits for most lumbar cerebrospinal fluid (CSF) samples when these same cytokines were adequately expressed in the ventricular CSF of the same PD patients (Mogi et al., 1996). It should also be noted that the exchange of proteins between the CSF and plasma is heavily dependent upon the blood-brain barrier (BBB), patient age, and circadian rhythm (Kroksveen et al., 2011, Zhang et al., 2005). Neurodegenerative diseases themselves can cause alterations in the BBB, resulting in confounding variables for CSF/plasma biomarker studies (Abbott and Friedman, 2012). Despite these limitations, examination of ventricular CSF and genetic markers suggest that neuroinflammation is associated with PD. Among PD patients, there was an increase in IL-6 and IL-1β ventricular CSF compared to healthy controls (Mogi et al., 1996). Also, multiple studies found genetic polymorphisms related to cytokines (IL-1β and TNF-α) to be associated with PD development (Arman et al., 2010).

1.4 VIRAL INFECTIONS AND PARKINSON'S DISEASE RISK

1.4.1 Historical Perspective

The very first suggestion of a relationship between viral infections and PD was back in the 1920s. During this time period (1920s-1930s), there was a severe epidemic recognised as Encephalitis Lethargica (EL). EL (also known as von Economo's disease) was first described by the German physician Constantin von Economo in his 1929 monograph publication (later transcribed into English in 1931). Although EL patients showed drastic irregularities in disease progression and displayed 'symptomatological polymorphism,' EL has been described as a type of 'sleeping sickness' which includes headache, nausea, fever, uncontrollable sleepiness, catatonia and sometimes coma (Neal and Bentley, 1932). Von Economo described the most prominent forms of EL as the somnolent-opthalmoplegic form, the hyperkinetic form, and the bulbar-paralytic form (Von Economo, 1931).

The EL epidemic happened to coincide with an equally significant influenza pandemic, leading many clinicians and other prominent scientists from that time to believe there was a causal relationship (or at least epidemiological association) between these conditions (Ravenholt and Foege, 1982). Despite initial speculations, there has been little evidence since the 1930s of such an association. Multiple studies investigating the preserved brain samples of EL patients from the epidemic years (1918-1930) have found no evidence of the 1918 influenza virus in these tissues (Lo et al., 2003, McCall et al., 2001, Taubenberger et al., 1997). It should be noted that these studies relied on detection of nucleotides, which can easily degrade *post-mortem* before brain samples can be prepared for preservation (especially before the availability of refrigeration pre-1930s). Even so, 1918 influenza derived sequences revealed mutations in two surface protein-encoding genes that suggest this viral strain was incapable of replicating outside

of the respiratory system (Reid et al., 1999, Reid et al., 2000). Von Economo himself did not believe the influenza and EL epidemics to be related. He instead suggested that the EL condition may be of viral origin, but that this virus must be specific to EL and the EL epidemic (Von Economo, 1931). There is some support for this theory due to the slight success of a herpes vaccine and an EL brain tissue derived vaccine from 'hyperimmune rabbit brains' for treating EL patients in clinical trials (Neal, 1942). Reports from more current cases of EL have suggested EL may be an auto-antibody disorder (Anderson et al., 2009, Dale et al., 2004, Dale et al., 2009, Lopez-Alberola et al., 2009, Rail et al., 1981, Singer et al., 2005, Vincent et al., 2004, Von Economo, 1931).

Parkinsonism is characterised by similar symptomology to Parkinson's disease, but with more complex and varied etiology than PD. There have been numerous case reports of post-encephalitic parkinsonism (PEP) after certain viral infections (H5N1, coxsackie virus, Japanese encephalitis B., St. Louis viral encephalopathy, HIV), but these cases of parkinsonism often do not exhibit the same cellular or molecular pathologies as seen in PD and are suggested to be 'phenocopies' of PD (De Jong et al., 2005, Jang et al., 2009, Mattos et al., 2002, Poser et al., 1969, Pranzatelli et al., 1994, Tse et al., 2004, Walters, 1960). Gamboa *et al.* (1974) noted a presence of neurotropic strains of influenza A in the hypothalamus and midbrain in a couple of PEP cases, but no viral presence (influenza A, measles, or HSV) in any cases of idiopathic PD brain tissue (Gamboa et al., 1974). Further differentiating EL and PEP, analysis of EL and PEP brain tissues found drastically different histological characteristics (McCall et al., 2001).

Although EL and PEP may have associations with viral infections (albeit EL appears to be either its own viral strain or not related to any virus at all), the relationship between viruses and these motor disorders seems to be limited to these very specific conditions. Any inferences relating to iPD based on these phenomena should be

considered with caution, especially since the evidence for these relationships is primarily based on a limited number of case studies.

Based on the intriguing relationship between viral infections and cases of PEP (and then accepted relationship with EL), multiple clinical studies (see Table 1.2) were conducted in the late 1970s and early 1980s to determine if there was also a relationship between viral infections and PD. Influenza A, HSV, CMV, and measles were the primary viruses investigated during this time (Elizan et al., 1979, Marttila et al., 1977, Marttila et al., 1988, Marttila and Rinne, 1978, Marttila et al., 1981, Marttila et al., 1982, Rail et al., 1981, Wetmur et al., 1979). A study by Elizan *et al*. (1979) found a significant relationship between viruses (HSV, measles, and influenza A) and iPD, but these findings should be disregarded since their control group included ALS and Alzheimer's disease (AD) patients (conditions which are now believed to possibly be related to viral infections themselves). Multiple studies by Martilla *et al*., using a variety of antibody detection techniques (complement fixation, radioimmunoassay, indirect immunofluorescent assay, microindirect hemagglutination), found a significant increase in HSV antibody titres and mean titre in iPD patient serum (Marttila et al., 1977, Marttila et al., 1988, Marttila and Rinne, 1978, Marttila et al., 1981, Marttila et al., 1982). The study using the microindirect hemagglutination test was able to differentiate between HSV-I and HSV-II; finding that increases in antibody titres and mean titre in iPD was specific to HSV-I only (not HSV-II) (Marttila et al., 1981).

Other studies have questioned iPD patients for their history of HSV infection with conflicting results, but the conclusions drawn from these studies are not very dependable since they rely on accurate patient memory and interpretation of their condition (patients cannot be expected to correctly diagnose their previous exposure or infection with viruses) (Harris et al., 2012, Vlajinac et al., 2013). One recent study that

examined patient serum did confirm the increased existence of HSV-I infections among iPD patients (Bu et al., 2015) . Although some other viruses (mumps, influenza A, measles, and CMV) were found to have a small (but significant) relationship with iPD, the interpretability of these studies is limited since they relied on self-report patient data (Harris et al., 2012, Vlajinac et al., 2013).

1.4.2 Viral Entry into the CNS

Among the viruses associated with PD, some have the ability to enter the CNS (see Table 1.2 and Fig. 1.10). The two viruses which have the most epidemiological support for a significant association with PD (HSV-I and influenza A) have very different life cycles, which leads to different neurovirulence and survival/replication strategies in the host. Generally, a transient influenza A infection usually lasts a few weeks (Samji, 2009). Conversely, initial infection with HSV-I is followed by anterograde transport into the trigeminal ganglia, where it maintains viral latency (Kumar et al., 2016). The trigeminal ganglia innervates the brainstem and cerebellum (see Fig. 1.10), providing opportunity for the chronic HSV-I infection to enter the CNS, especially during reactivation (Marfurt and Rajchert, 1991, Miller et al., 2016). Although influenza A primarily resides within the respiratory system during infection, the olfactory nerve within the nasal cavity does provide opportunity for a transient influenza A infection to enter the brain (Kuiken and Taubenberger, 2008). Previously investigated *in vivo*, influenza A was found to be axonally transported via cytoskeleton intermediate filaments along olfactory neural projections through the cribiform into the olfactory bulbs and olfactory tracts within the CNS (Matsuda et al., 2005, van Riel et al., 2015).

In the past, viral entry into the CNS was been considered to have fatal consequences with conditions such as herpes simplex encephalitis (HSE) or acute encephalitis (due to HSV-I or influenza A, respectively) (De Jong et al., 2005, Esiri,

1982, Shoji et al., 1994). More recently, studies suggest that viral entry into the CNS may not produce a fatal immune response. Although *post-mortem* studies of PD patients have not found the presence of HSV-I DNA or antigens in the CNS, multiple studies of healthy aged or AD patients have found HSV-I DNA in the CNS (Fraser et al., 1981, Gordon et al., 1996, Hemling et al., 2003, Lövheim et al., 2015, Olsson et al., 2016, Wetmur et al., 1979). In some of these studies, HSV-I DNA in the CNS was associated with an increase in age and the existence of amyloid-β-plaques among AD patients (Olsson et al., 2016, Wozniak et al., 2009). Due to the transient nature of influenza A, it has been more difficult to study its neurovirulence. Although partially determined by the route of influenza A infection, *in vivo* murine studies found neurovirulent strains of influenza A to enter the CNS around day ten post-infection and localise within the SN, hippocampus, thalamus, locus coeruleus, olfactory bulbs, thoracic spinal cord, and ganglia (trigeminal, vagal, sympathetic trunk, and spinal) (Jang et al., 2009, Park et al., 2002, Reinacher et al., 1983, Takahashi et al., 1995). Also, influenza A antigens appeared to preferentially infect catecholaminergic neurons, meninges, and ependymal areas (Yamada et al., 1996). Although influenza A was able to infect the CNS in these models, viral replication ended by week two post-infection and was no longer detected in the CNS by day twenty-one post-infection. Even after influenza A could no longer be detected within the CNS, neurotropic H5N1 influenza A induced chronic microglia activation and α-synuclein phosphorylation/aggregation in the SN post-infection (Jang et al., 2012, Jang et al., 2009). A *post-mortem* study found macrophages infected with influenza A to be present within the brainstem, with a significant increase in these infected macrophages among PD patients (Rohn and Catlin, 2011).

Along with an increased risk of PD due to aging, there is also an increased sensitivity to respiratory infection (De Lau and Breteler, 2006, Jamieson et al., 1992,

Nicholson et al., 1997). Also, the BBB becomes more permeable with age, resulting in increased infiltration of peripheral proteins into the CNS (Kleine et al., 1992). Immune system compromise and BBB disruption among the aged may lead to an increased risk of viral entry into the CNS in this population (Kleine et al., 1992, Valiathan et al., 2016).

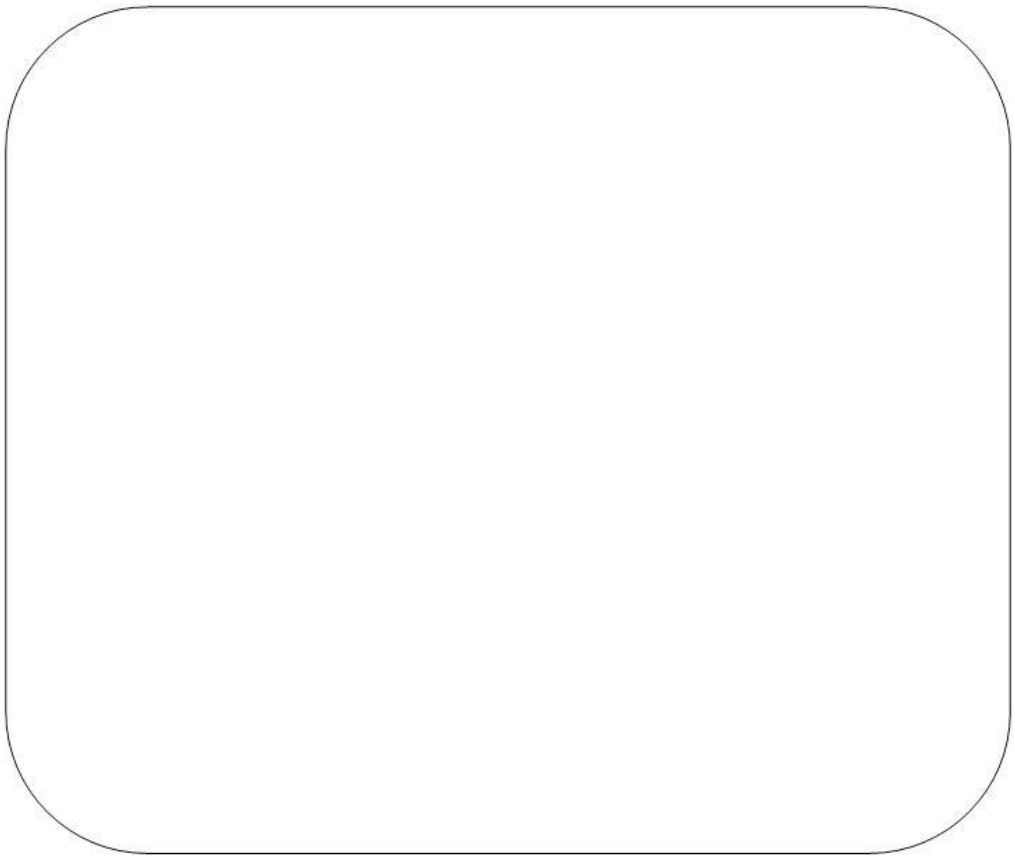

Table 1.2. Viral Infections Associated with Parkinson's Disease. Multiple viral infections have been suggested to be associated with PD. The most frequent findings suggest that HSV-I and influenza A are associated with PD. (Olsen et al., 2018)

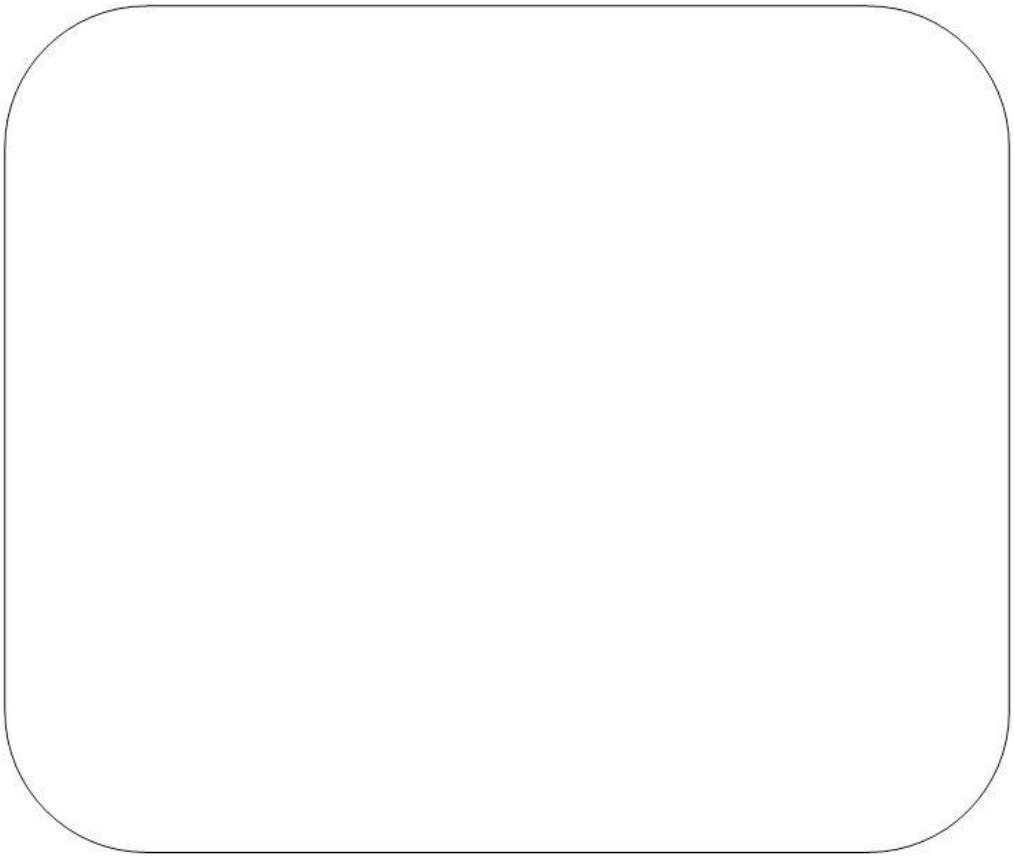

Figure 1.10. Neurological Consequences of Viral Entry into the CNS. Viral infections have the potential to induce molecular and cellular changes that may alter healthy neuron function. After entry into the CNS, viral transcripts/proteins may cause inflammation, autophagy disruption, and synapse dysfunction. These viral-related changes in the CNS could contribute to Parkinson's disease-like pathology. (Olsen et al., 2018)

1.4.3 Neurological Consequences of Viral Infections

1.4.3.1 Synapse

Viral infections may reduce or disrupt normal synapse function. Influenza A infection has been found to disrupt synaptic activity through modulation of host gene expression and interaction with synaptic related proteins. Pandemic and seasonal influenza A infections were examined for their modulation of genes in the CNS (Ebrahimie et al., 2015). Pandemic influenza strains were associated with down-regulation of 'neuron projection,' 'synapse assembly,' and 'calcium channel activity' related genes (Ebrahimie et al., 2015). Genes that were down-regulated compared with the seasonal flu strain included glycoprotein M6A, protocadherin α-subfamily C2, and cAMP-regulated phosphoprotein. Influenza A non-structural protein 1 (NS1) and nucleoprotein (NP) were also found to modify the host synapse. The influenza A NP was found to localise within the dendritic spine-like structures of hippocampal neurons, resulting in reduced spontaneous excitatory synaptic frequency and decreased amplitude of excitatory post-synaptic currents (Brask et al., 2005). Also in hippocampal neurons, the PSD-95/discs-large/ZO-1 (PDZ) motif of the C-terminus of H5N1 influenza A NS1 (not H1N1 influenza A NS1) was found to bind to PSD-95 (Zhang et al., 2011). NS1 binding to PSD-95 was suggested to prevent normal post-synaptic processes. More related to chronic infection, a murine model of HSV-I infection of cortical neurons resulted in decreased synapsin-1 and synaptophysin proteins, and disrupted synaptic transmission (Piacentini et al., 2015). Also, intra-striatal injection of a viral synthetic mimetic in rats resulted in a drastic increase in striatal PSD-95 and NMDAR1 (Deleidi et al., 2010). Interestingly, NMDAR antibodies were found in patients with HSE, with reduced NMDAR and synapsin protein in murine hippocampal neurons after treatment with serum isolated from HSE patients (Piacentini et al., 2015).

1.4.3.2 Protein Aggregation and Autophagy Disruption

Although α-synuclein abnormality and accumulation is well researched with regards to PD, far less is known about the relationship between α-synuclein and viral infections. *Post-mortem* analysis of the brains of AD patients found a majority of HSV-I DNA positive neurons to also have amyloid-β-plaques (Olsson et al., 2016; Wozniak et al., 2009; Mori et al., 2002). These findings are further supported by cell culture studies which found HSV-I infection to increase amyloid-β aggregation accumulation (Santana et al., 2012). In a study examining the CNS of long surviving aged adults with HIV, there was an increase in α-synuclein and amyloid-β expression, but no clear pathological protein aggregation (Khanlou et al., 2009). It is possible that other viral infections might also increase α-synuclein or α-synuclein aggregation, but this needs further investigation.

Pre-clinical studies suggest that viral infections may modify α-synuclein. In mice, the neurotropic H5N1 influenza A virus induced the phosphorylation of α-synuclein (at Ser129) in the brainstem, midbrain, hippocampus, and cortex (Jang et al., 2009). This study suggested that influenza A might directly stimulate a cellular kinase to phosphorylate α-synuclein since there was no phosphorylated α-synuclein within uninfected structures (Jang et al., 2009). Also possibly relevant to infections, an *in vitro* study with purified α-synuclein protein found the presence of a bacterial endotoxin, lipopolysaccharide (LPS), to influence α-synuclein aggregate conformation (Kim et al., 2016). With the addition of LPS, the α-synuclein protein aggregated into a more ribbon-like, flat and straight conformation compared to the curvy and flexible fibrils under normal conditions (Kim et al., 2016). This change in α-synuclein aggregate fibril morphology was accompanied with no disruption in self-propagation, but intra-striatal injection of these pre-formed fibrils found fibrils formed in the presence of LPS induced

significantly more microglia activation (Kim et al., 2016). Intriguingly, normal non-pathogenic α-synuclein may influence the immune response to viral infections. In mice, the presence of α-synuclein was required to inhibit West Nile Virus replication and entry into the CNS (Beatman et al., 2015).

As mentioned, the immune system interacts with autophagy pathways to facilitate the clearance of pathogens without undergoing cell death. In retaliation, some viruses have evolved mechanisms for evading this autophagy clearance. Previous studies have identified ICP34.5 as a crucial HSV-I protein for inhibiting autophagic degradation of virion structures (Alexander et al., 2007, Tallóczy et al., 2006). Multiple HSV-I and influenza A proteins are able to disrupt autophagy. HSV-I ICP34.5 is able to indirectly inhibit RNA activated PKR, while HSV-I US11 directly binds to PKR to prevent activation (He et al., 1997, Mulvey et al., 1999, Poppers et al., 2000). Influenza A NS1 and NP also inhibit PKR (Lussignol et al., 2013). This PKR activation inhibition prevents PKR-mediated autophagy activation (Lussignol et al., 2013, Tallóczy et al., 2006). Also, HSV-I ICP34.5 has been found to bind directly to Beclin-1 (Orvedahl et al., 2007). Beclin-1 binds with other autophagy components to promote the formation of autophagosomes (Kang et al., 2011). The amino acid region 68-87 of ICP34.5 binds to Beclin-1, leaving the section that functions to inhibit PKR signaling to remain open (Orvedahl et al., 2007). HSV-I ICP34.5 inhibition of autophagy through Beclin-1 binding also prevents antigen presentation and $CD4^+$ T-cell response (Leib et al., 2009). Further investigation into the consequences of ICP34.5-mediated autophagy disruption needs to be done to understand the effects on host neuron homeostasis beyond increased neurovirulence of HSV-I.

Some viruses have evolved to express proteins which disrupt autophagy to prevent the clearance of viral components from host cells during latency and replication.

Viral mediated autophagy disruption or suppression could lead to a decrease in the clearance of mis-folded/ aggregated proteins. Studies examining *post-mortem* AD brains found HSV-I DNA to be associated with amyloid-β plaques (Mori et al., 2002, Olsson et al., 2016, Wozniak et al., 2009). Although a majority of HSV-I DNA positive CNS neurons were found to have amyloid-β plaques, there was no correlation between amyloid-β plaque containing neurons and the presence of HSV-I DNA (Olsson et al., 2016). These findings suggest that HSV-I infection may cause an increase in amyloid protein aggregation. Further investigation should be conducted to determine if there may also be an association between HSV-I DNA positive neurons and α-synuclein aggregation.

A study by Santana *et al*. found HSV-I infection in neuronal cell cultures to cause an increase in amyloid-β aggregation accumulation, along with an increase in LC3-II (Santana et al., 2012). This study further supports the theory that HSV-I may contribute to amyloid protein aggregation, but does not refute the possibility that this is related to HSV-I mediated autophagy disruption since ICP34.5 disrupts autophagy through Beclin-1 binding, not LC3-II. Also, the lack of correlation between amyloid-β plaque containing neurons and HSV-I DNA positivity may be due to cross-seeding. HSV-I may cause autophagy disruption in innervating neurons (possibly latent sensory neurons), leading to amyloid fibril accumulations that may have the capability of spreading to other non-HSV-I DNA positive neurons. These protein aggregates may then be transported to innervating neurons or be exocytosed for extracellular cross-seeding. In general, autophagy disruption has been previously found to cause an increase in neurodegeneration, pre-synaptic α-synuclein accumulation, neuronal inclusions, and dopaminergic axon and dendritic degeneration (Friedman et al., 2012, Komatsu et al., 2006).

1.4.3.3 Neuroinflammation

Neurotropic viruses may increase glial cell activation and increase inflammation within the CNS, while non-neurotropic viruses may still activate an immune response in the CNS due to an increase in peripheral inflammatory mediators, such as cytokines/chemokines. Of importance to HSV-I, $CD8^+$ T-cells have been found to have HSV-I epitopes and block reactivation (Khanna et al., 2003, Leger et al., 2013). Although involved in hindering HSV-I reactivation, there are suggestions that these T-cells lead to chronic inflammation. Residual lymphocytes were found to recognise HSV-I during latency in the TG, resulting in cytokine release, T-cell exhaustion, and eventual allowing of viral reactivation (Benmohamed et al., 2016, Halford et al., 1996, Theil et al., 2003). The H5N1 influenza A strain was also found to induce excessive peripheral T-cell activation (Perrone et al., 2008). There is evidence of T-cell population modulation in PD as well. T-cell population increase/decrease and impairment in PD depends on T-cell type, and more recently T-cells have been found to recognise α-synuclein epitopes (Saunders et al., 2012, Sulzer et al., 2017). Interestingly, recent studies identified homologous cross-reactivity between HSV-I and α-synuclein, suggesting that HSV-I may induce an autoimmune response (Caggiu et al., 2016). Indeed, auto-antibodies against an HSV-I peptide were cross-reactive with an α-synuclein epitope (Caggiu et al., 2016). While lymphocytes are involved in the adaptive immune response, the innate immune system also initiates an immediate response due to PAMPs (Chang, 2010). Of significance to HSV-I and influenza A, the PRR TLR3 is known to recognise viral dsRNA (and experimentally poly I:C) that is present during the viral life cycle within infected host cells (Alexopoulou et al., 2001, Matsumoto et al., 2002).

Although the host immune system is well evolved to combat viral infections through type 1 IFNs and IFN-stimulated genes (ISGs), HSV-I and influenza A have also evolved ways to evade this host immune response. HSV-I proteins inhibit NF-κB and IRF3 activation (Antrobus and Boutell, 2008, Lin et al., 2004, Preston et al., 2001). The influenza A NS1 prevents the host innate immune response and cellular apoptosis of infected cells by suppressing IFN activation through multiple routes (Thulasi Raman and Zhou, 2016). Also, NS1 regulates IFN-α/β receptor subunit 1 (IFNAR1) surface expression (Wang et al., 2017). Due to suppression of the innate immune system, influenza A infection of neurons only leads to increases in TNF-α release, not IL-6 or IFNs (Pringproa et al., 2015). Despite multiple HSV-I proteins working to dampen IFN signalling, there is still evidence of IFN signalling and regulation of viral replication in HSV-I infected cells. This is not surprising since HSV-I inhibition or activation of IRF3 appears to be cell-type dependent (Preston et al., 2001). In sensory neurons, where HSV-I latency is generally maintained, some level of IFN signaling may be required for HSV-I reactivation. Latency-associated transcripts (LATs) have not been found to produce an inflammatory cytokine/IFN response themselves, but instead may require some cytokines/IFNs to initiate reactivation (Carr et al., 1998, Rosato et al., 2016). One study suggested that IFNs regulate LAT expression in a way that benefits HSV-I infection; by promoting neuron cell survival throughout latency, HSV-I is provided an opportunity for reactivation and viral spread later (Rosato et al., 2016). Interestingly, neuronal IFN-β suppression was associated with α-synuclein accumulation and PD-like neurodegeneration (Ejlerskov et al., 2015).

Although HSV-I and influenza A viruses have evolved ways to circumvent neuronal innate immune sensing of infection, other CNS cells can still sense and defend against pathogens. Astrocytes and microglia participate in the defense against viral

spread throughout the CNS (Hauwel et al., 2005). Although HSV-I may find a safe haven in sensory neurons, replication in these neurons for reactivation may alert neighbouring astrocytes. These cells recognise extracellular dsRNA since they can express cell surface TLR3 (Farina et al., 2005). Indeed, previous studies have found astrocytes to be reactive to a synthetic mimetic of dsRNA, albeit with conflicting conclusions (Bsibsi et al., 2006, Carpentier et al., 2005, Farina et al., 2005, Jack et al., 2005, Park et al., 2006, Zhao et al., 2006). One study found synthetic dsRNA to produce an anti-inflammatory response in astrocytes (Bsibsi et al., 2006), while others found a pro-inflammatory response (Carpentier et al., 2005; Zhao et al., 2006). The reasons for these differences may be due to astrocyte source (fetal or adult). Overall, synthetic dsRNA treatment in human astrocytes *in vitro* was found to cause increases in IFNs, IL-6, and a down-regulation in connexin 43 (a crucial protein for intercellular gap junctions between astrocytes and maintaining BBB integrity) (Carpentier et al., 2005; Zhao et al., 2006; Ezan et al., 2012). Interestingly, a rat study also found synthetic dsRNA to attenuate astrocytic L-glutamate uptake by inhibiting EAAT1/GLAST transporter gene transcription (Scumpia et al., 2005). Studies examining HSV-I infection in the mouse CNS found increased inflammation and ROS (Kavouras et al., 2007, Valyi-Nagy et al., 2000). These studies suggest viral infection and replication in neurons near astrocytes could cause an inflammatory response and disrupt healthy astrocyte function, possibly leading to neuronal signaling dysfunction and cell death. Of relevance to HSV-I and glial activity, a study describing a mouse model of HSE found lytic genes (ICP0 and ICP27) to sustain their expression long into ‘latency’ within the brain ependymal after HSE recovery (Menendez et al., 2016). This HSV-I gene expression profile differs from its life in the TG and was associated with a loss of effector T-cell function and an increase in microglia in the region. Although most humans infected with HSV-I never

experience an episode of HSE during their lifetime, the present study not only further demonstrates that not all cell types respond in the same way to HSV-I, but that HSV-I can infect regions of the CNS without lethal consequences.

1.4 PRE-CLINICAL ANIMAL MODELS OF PD AND VIRAL INFECTIONS

Since PD is not known to occur in other species, models of PD have been developed to study the disease and identify treatment targets/strategies. Most of these models were designed based on the current understanding of the disease at the time of development, resulting in a wide range of models with differing advantages and limitations.

1.4.1 6-Hydroxydopamine

6-Hydroxydopamine (6-OHDA) induces dopaminergic cell death with high specificity due to its reuptake into dopamine neurons via the dopamine transporter (DAT) protein (Javoy et al., 1976, Jonsson, 1980). This neurotoxin is used to model the dopaminergic cell loss found in PD (but not other pathological features) by direct injection into the nigrostriatal pathway (Sakai and Gash, 1994, Ungerstedt, 1968). 6-OHDA is believed to induce dopaminergic neuronal cell death via oxidation into ROS (Mazzio et al., 2004).

1.4.2 Rotenone

Pesticide based models of PD were first investigated due to their epidemiological association with PD. The most commonly used pesticide in pre-clinical models of PD is rotenone (Heikkila et al., 1985). Rotenone disrupts normal mitochondrial function via inhibition of complex I, resulting in oxidative stress (Sherer et al., 2003). In addition to dopaminergic cell death, rotenone also produces intraneuronal α-synculein inclusions (Alam et al., 2004, Cannon et al., 2009, Pan-Montojo et al., 2012).

1.4.3 MPTP

MPTP was first discovered due to a recreational drug mishap, resulting in the users rapidly developing parkinsonism (Langston et al., 1984). In the brain, MPTP is converted into MPP^+, which can be taken up by DAT (Langston et al., 1983). Similar to rotenone, this active metabolite disrupts mitochondrial ATP production and increases oxidative stress, resulting in dopaminergic cell death (Javitch et al., 1985, Karunakaran et al., 2008, Nicklas et al., 1987). MPTP is able to produce these effects in non-human primates and mice, but not rats (Bové and Perier, 2012, Madras et al., 2006, Porras et al., 2012).

1.4.4 α-synucleinopathy

The α-synucleinopathy in PD has been modeled multiple ways in animals and cell culture. The phenotype of transgenic α-synuclein mutations vary based on mutation type (Koprich et al., 2017). Over-expression of α-synuclein results in progressive α-synuclein aggregation and eventual dopaminergic cell death (Kirik et al., 2003). Synthetic pre-formed fibrils can propagate α-synuclein aggregation when introduced to normal α-synuclein (Bousset et al., 2013, Guo and Lee, 2014, Koprich et al., 2017). A more recent model of α-synucleinopathy utilised a synthetic peptidomimetic (FN075) to promote α-synuclein fibrillisation via accelerated formation of soluble oligomers *in vitro* (Cegelski et al., 2009, Horvath et al., 2012, Pedersen et al., 2015). Although α-synucleinopathies recapitulate the α-synuclein aggregation found in PD, the neurotoxicity of these models depends on the model type and animals used (Koprich et al., 2017).

1.4.5 Poly I:C

Poly I:C is a synthetic mimetic of viral dsRNA and a known ligand for TLR3 (Chang, 2010). This compound is used experimentally to mimic viral infections (Balachandran et al., 1998a, Field et al., 2010). The advantage of using this compound is that the direct effect of viral-like dsRNA can be measured. However, using this compound limits the interpretation with regards to mimicking viral infections. Viral infections produce multiple viral proteins and LATs throughout their viral live cycle which do not exist when using poly I:C. Also, poly I:C selectively stimulates the innate immune system versus actual viral infections which stimulate the innate and adaptive immune system.

1.5 HYPOTHESES

Based on the epidemiological association between viruses and PD and the neurological consequences of some viral infections, there is suggestion that viral infections may contribute to PD pathology. Currently, there has been little investigation into the neurological effects and molecular consequences of viral/viral-mediated inflammation in the context of PD pathology. Therefore, this study aimed to investigate the potential influence viral infections might have on the neurodegenerative effects of PD related neuropathology using multiple models of PD. We hypothesise that viral infections may exacerbate the neurodegenerative effects of other underlying contributors to PD development.

1.6 THESIS OBJECTIVES

Using cell culture and animal models, we investigated effects of viral-like priming on PD-related neurotoxin induced neurodegeneration and synaptic dysfunction.

Specifically, we aimed to:

1. Assess the inflammatory effects of viral-like poly I:C alone or in combination with pre-clinical models of PD (including 6-OHDA, rotenone, MPP^+, and FN075 induced α-synucleinopathy) in cell culture and *in vivo*.
2. Determine if viral-like poly I:C priming in combination with PD related neuropathology (such as oxidative stress or α-synuclein aggregation) induces neurodegeneration in cell culture or *in vivo*.
3. Determine if viral-like poly I:C priming in combination with PD related neuropathology (such as oxidative stress or α-synuclein aggregation) induces synaptic dysfunction in cell culture or *in vivo*.
4. Determine if viral-like poly I:C priming in combination with PD related neuropathology (such as oxidative stress or α-synuclein aggregation) induces autophagy dysfunction in cell culture or *in vivo*.

Chapter Two: Materials and Methods

CHAPTER TWO

2.1 MATERIALS

2.1.1 Cell Culture

Product	Code	Supplier
DMEM/F12	D6421	Sigma
FBS	10270-106	Gibco
Penn/Strep	P0781	Sigma
L-glut	G7513	Sigma
D-glucose	G7021	Sigma
B-27	12587-010	Gibco
Trypsin	T4174	Sigma
PBS	D8537	Sigma
Hank's red	H9394	Sigma
Hank's clear	H6648	Sigma
Trypan	T8154	Sigma
DMSO	D8418	Sigma

2.1.2 Compounds

Product	Code	Supplier
6-OHDA	H4381	Sigma
Rotenone	R8875	Sigma
MPP+	D048	Sigma
FN075	Gift from Dr. Almqvist	Umea, Sweden
Poly I:C	tlrl-pic	Invivogen

2.1.3 Western Blot

Abbreviation	Code	Supplier
Ammonium Persulfate	A3678	Sigma
Trisma	T1503	Sigma
Sodium Chloride	S/3160/60	Fisher Chemical
Glycine	G8898	Sigma
Acrylamide	A3699	Sigma
SDS	71736	Sigma
Bovine Serum Albumen	A8022	Sigma
Bradford Reagent	71729	Sigma
Protease inhibitor cocktail	P8340	Sigma
TEMED	T9281	Sigma
Tween 20	P1379	Sigma
β-mercaptoethanol	M6250	Sigma

2.1.4 Immunocytochemistry

Product	Code	Source
Trisma	T1503	Sigma
Sodium Chloride	S/3160/60	Fisher Chemical
Triton-X	T8787	Sigma
Bovine Serum Albumen	A8022	Sigma
Goat Serum	G9023	Sigma
Sodium Azide	S/2380/48	Fisher Chemical
PFA	F8775	Sigma

2.1.5 Immunohistochemistry

Product	Code	Source
Trisma	T1503	Sigma
Sodium Chloride	S/3160/60	Fisher Chemical
Methanol	322415	Sigma
Hydrogen Peroxide (30%)	H1009	Sigma
Triton-X	T8787	Sigma
Normal Goat Serum	G9023	Sigma
Normal Horse Serum	H1138	Sigma
ABC Complex	ZE0501	Vectastain
DAB	11718096001	Sigma
Ethanol	362808	Sigma
Xylene	214736	Sigma
DPX	44581	Sigma

2.1.6 qPCR

Product	Code	Source
H. β-actin	143636	Roche
H. α-synuclein	137142	Roche
H. PSD-95	145168	Roche
H. Synaptophysin	136197	Roche
H. TH	144999	Roche
R. β-actin	500152	Roche
R. α-synuclein	503549	Roche
R. PSD-95	502414	Roche
R. Synaptophysin	503981	Roche
R. TH	503274	Roche
RNA Isolation Kit	11828665001	Roche
cDNA Synthesis Kit	4368813	Applied Biosystems
PCR Mastermix	04707494001	Roche

2.1.7 ELISA

Product	Code	Source
Human IL-6 Kit	900-T16	Peprotech
Human IFN-β Kit	8499-IF	RnD Systems
Rat IL-6 Kit	900-K86	Peprotech
Rat TNF-α	900-K73	Peprotech
Rat IL-1β	900-K91	Peprotech

2.1.8 Antibodies

Product	Code	Source
TH	MAB318	Millipore
GFAP	Z033401	Dako
CD116/ OX42	CBL1512	Chemicon
Agg-synuclein	209538	Abcam
Synaptophysin	5461	Cell Signalling
PSD-95	3450	Cell Signalling
TH	2792	Cell Signalling
Alpha-synuclein	2644	Cell Signalling
PARP/cPARP	9542	Cell Signalling
cCASP-3	9661	Cell Signalling
LC3-a/b-I/II	4108	Cell Signalling
p62	56416	Abcam
p-IRF3	4947	Cell Signalling
p-IκB	2859	Cell Signalling
p-NF-κB	3003	Cell Signalling
Alexa Flour 546 Goat-anti-rabbit	A11035	Life Technologies
Alexa Flour 488 Goat-anti-mouse	A11001	Life Technologies

2.2 METHODS

2.2.1 Global Experimental Design

The aim of this thesis was to investigate the potential of viral-like poly I:C priming to modulate synapse dysfunction and degeneration when combined with pre-clinical models of PD. These effects were first examined in a human neuronal cell line (Chapter 3), followed by investigation in primary rat VM cells (Chapter 4). Finally, the findings from Chapter 3 and 4 were translated into an *in vivo* study to determine if viral-like poly I:C priming in combination with a novel model of α-synucleinopathy resulted in synaptic dysfunction and/or degeneration (Chapter 5).

In Chapter 3, a human neuroblastoma cell line (SH-SY5Y) was primed with viral-like poly I:C to induce a TLR3 mediated pro-inflammatory response. Following poly I:C priming, cells were treated with a range of compounds used to model PD to determine if priming exacerbated the degenerative effects of these models. Synaptic, autophagy, and cell death markers were measured.

In Chapter 4, a similar experimental design of poly I:C priming in combination with models of PD from Chapter 3 was investigated in primary rat VM cells. Again, synaptic, autophagy, and cell death markers were measured to determine if viral-like poly I:C priming/TLR3 mediated inflammation exacerbated the degenerative effects of the PD models.

In Chapter 5, viral-like poly I:C priming was investigated *in vivo*. Sprague-Dawley rats received uni-lateral intra-nigral injections of poly I:C followed by subsequent intra-nigral injections of a novel small peptidomimetic molecule that is known to induce α-synuclein oligomerisation and fibril formation. Motor behaviour was

assessed throughout, followed by *post-mortem* analysis of the nigra for degeneration, synaptic dysfunction, neuroinflammation, and autophagy activation.

2.2.2 Cell Culture

2.2.2.1 SH-SY5Y Neuroblastoma Cell Line

SH-SY5Y is a thrice cloned human neuroblastoma mixed adherent/suspension cell line from the SK-N-SH cell line obtained from ATCC (CRL-2266). These cells were originally isolated in 1970 from a metastatic bone marrow tumor from a four year old female (see Fig. 2.1). SH-SY5Y cells express dopaminergic-like neuronal markers, such as dopamine and DAT (Lopes et al., 2017). Due to their rapid growth and neuronal expression, these cells are ideal for measuring changes in neuronal proteins and mRNA in cell culture.

Figure 2.1. SH-SY5Y Neuroblastoma Cells from ATCC. SH-SY5Y human neuroblastoma cells were purchased from ATCC for all neuronal cell culture experiments. (ATCC, 2016)

2.2.2.2 SH-SY5Y Maintenance

SH-SY5Y cells were maintained in Dulbecco's Modified Eagle's Medium with F12 (DMEM/F12, D6421, Sigma, Ireland), supplemented with 10% FBS (10270-106, Gibco, USA), 1% L-glutamine (G7513, Sigma, Ireland), and 1% Penicillin-Streptomycin (P0781, Sigma, Ireland). They were grown in a T-75 flask (83.3911.002, Sarstedt, Germany) in a sterile incubator (Hera Cell 150, Kendro, Germany) at 37^{o}C with 5% CO_2. Cells were sub-cultured approximately every 2-3 days after reaching 80% confluency. For counting, extraction, and preservation, cells were sub-cultured. In a sterile flow-hood (Hera Safe, Kendro, Germany), old medium was removed and discarded from the T-75 flask. Then, adherent cells were washed with sterile PBS (D8537, Sigma, Ireland), followed by 5 min incubation in warmed trypsin media (1 ml trypsin (T4174, Sigma, Ireland) + 9 ml Hank's Balanced Salt Solution (H9394, Sigma, Ireland)). After the 5 min incubation in the trypsin media in the incubator at 37^{o}C, the flask was tapped to ensure cell suspension before adding warmed media to neutralise the trypsin. The suspended cells were then centrifuged at 1400 rpm for 5 min. Afterwards, the neutralised trypsin was discarded and the pelleted cells were re-suspended in fresh warmed media before returning the cells back to the T-75 flask for storage in the incubator.

To store cells for later, cells were re-suspended as describe above using trypsin once the T-75 flask reached ~80% confluency. In this case, after the neutralised trypsin was removed, cells from one flask were re-suspended in 1 ml of cryopreservation media (DMEM/F12 with 5% DMSO (D8418, Sigma, Ireland)). Re-suspended cells were transferred to a sterile preservation tube (72.380, Sarstedt, Germany) and frozen using a Mr. Frosty Freezing Container (5100-0001, Thermo Fisher, Ireland) to control the rate of

freezing in the -80. After the cells reached -80^{o}C, cells were transferred to a liquid nitrogen tank for long term storage.

2.2.3 Embryonic Day 14 Ventral Mesencephalic Primary Rat Mixed Culture

Primary cells isolated from the ventral mesencephalon (VM) of embryonic day 14 (E14) rats were grown in cell culture for treatment. These primary mixed cell cultures were chosen for their TH^{+} rich population (Clayton and Sullivan, 2007).

2.2.3.1 Dissection and Isolation

Time-mated Sprague-Dawley female rats weighing 225 kg (Charles River, UK) were terminally anaesthesised by isoflurane inhalation, followed by decapitation. Embryos were then obtained by laporatomy. Embryonic sacs were washed in cold Hank's Balanced Salt Solution (HBSS, H6648, Sigma, Ireland). The embryos were removed from the yolk sac and the head was removed. To extract the VM, an incision was made along the dorsal midline. The dorsal portion of the mesencephalon and meninges were discarded (see Fig. 2.2). All embryos were collected together for dissociation and cell isolation (Clayton and Sullivan, 2007).

HBSS was removed from VM tissue by centrifugation (1400 rpm for 5 min). VM tissue was incubated in warmed (37^{o}C) dissociation medium (2 ml trypsin + 3 ml HBSS) for 4 min at 37^{o}C. The trypsin in the dissociation medium was neutralised using FBS. Dissociation medium and FBS were removed by centrifugation (1400 rpm for 5 min). The pelleted cells were re-suspended in DMEM/F12. Cells were fully dissociated by pipetting with a P1000, followed by a 25 gauge needle with a 1 ml syringe. After determining the cell concentration using a haemocytometer (Blaubrand, Neubauer Improved, Germany), 50 µl of cells were plated in a poly-l-lysine coated 24-well plate (83.3922.300, Sarstedt, Germany) at 2,000,000 cells/ml. Cells were incubated at 37^{o}C

with 5% CO_2 for 1 hr. After the 1 hr incubation, wells were topped up with 450 µl of DMEM/F12. Medium was changed every 3 days by removing 250 µl of medium and adding 300 µl of fresh DMEM/F12. Cells were allowed 5 days for maturation and differentiation.

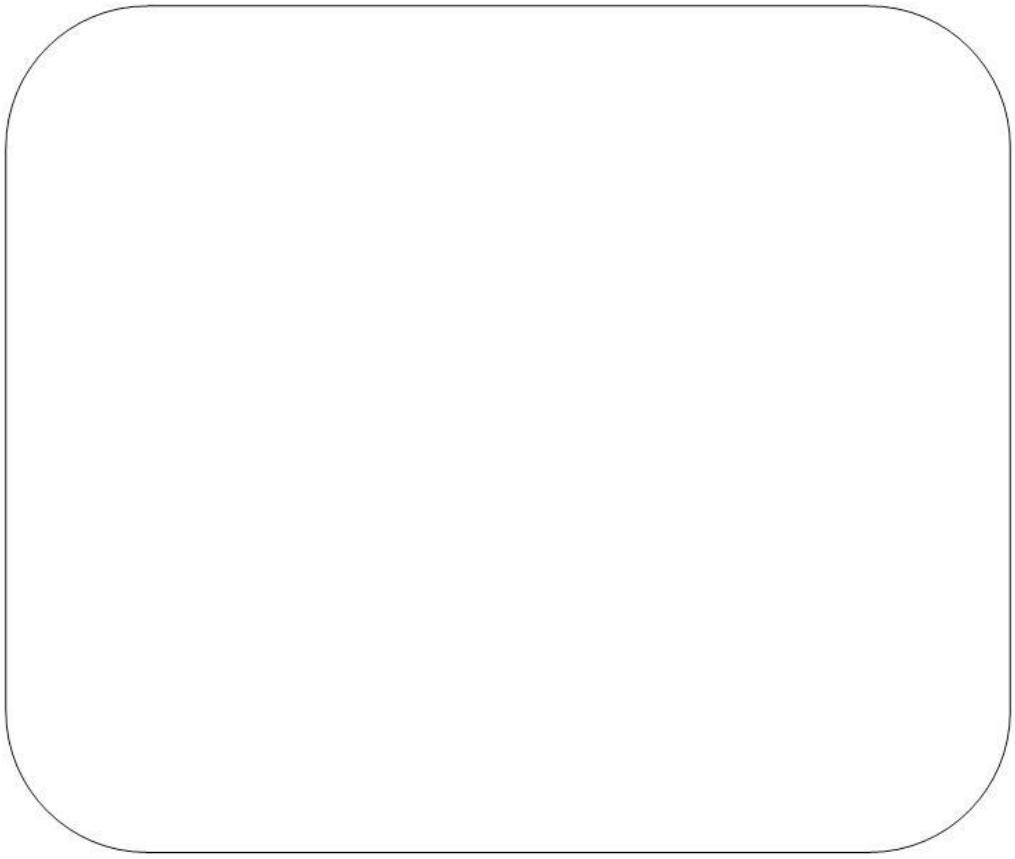

Figure 2.2. E14 VM Rat Dissection Schematic. The ventral mesencephalon was dissected from the neural tube of day 14 rat embryos. First, the dorsal midline was cut to reveal the ventral midline. Meninges and excess tissue was removed from the ventral mesencephalon. (Clayton and Sullivan, 2007)

2.2.4 Cell Counting

After re-suspension, cells can be sub-cultured or counted for seeding. A small sample is taken from the main stock of cells for counting. The cell sample is used to make a 1:1 mixture of cells in medium and trypan blue. Immediately after creating the mixture, ten microlitres is pipetted under a glass coverslip placed on top of a haemocytometer (see Fig. 2.3). Trypan blue stains dead cells, therefore the number of unstained cells is counted using an inverted microscope. The grid of the haemocytometer is used as a reference for counting the cells. All cells within the four large squares (see Fig. 2.4) were counted. The volume of one large square is 1 x 10^{-4} cm3. Therefore, the volume of cells is calculated as per the calculation below:

$$Cell\ Concentration\ (cells/ml) = \left(\frac{Counts}{4}\right) \times 2\ \times (1\ x\ 10^{4})$$

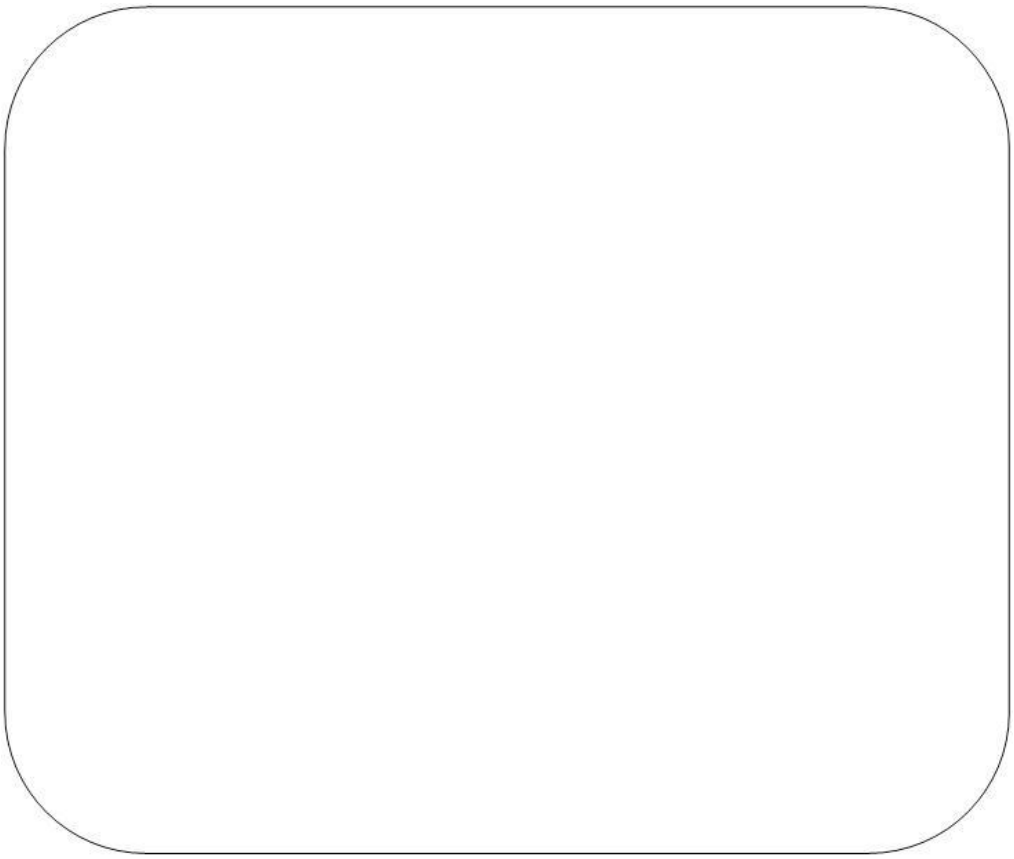

Figure 2.3. Haemocytometer for cell counting. A glass cover slip (B) is placed on top of the middle section of the slide (A) where a microscopic grid (C) can be used for cell counting.

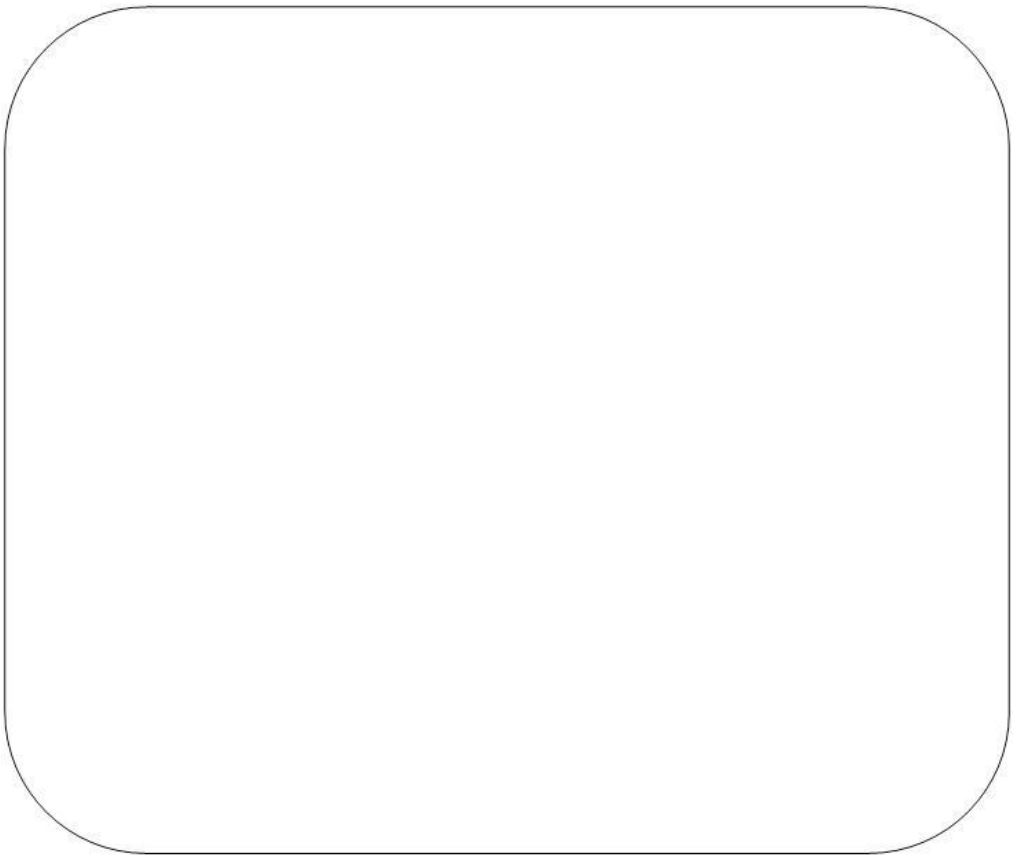

Figure 2.4. Haemocytometer Grid Lines. Above is an example of the view through the microscope (when using a 10X power lens) when counting cells. Cells located in the corner four squares were counted to determine the concentration.

2.2.5 Cell Culture Experiments

Cell culture experiments were conducted by sub-culturing cells from a T-75 flask, re-suspending, counting, and seeding into experiment plates at specific concentrations. Twenty-four hours after seeding in experiment plates, cells were treated with drugs for experiments. Cells were treated with a combination of poly I:C (tlrl-pic, Invivogen, USA) (prepared in endotoxin free water), 6-OHDA (H4381, Sigma, prepared in sterile media), Rotenone (R8875, Sigma, prepared in sterile media supplemented with DMSO and cremaphor), MPP^+ (D048, Sigma, prepared in sterile media), and FN075 (gift from Dr. Almqvist at Umea University, Sweden, prepared in sterile PBS supplemented with DMSO). For concentration-response experiments, cells were treated at various time points (see Tables 2.1, 2.2, 2.9, 2.16, 2.18, 2.19, 2.22, 2.23). Poly I:C priming experiments were conducted by priming cell cultures with poly I:C (20 µg/ml) for 24 hr before proceeding with a neurotoxin treatment of 6-OHDA, Rotenone, MPP^+, or FN075 (see Tables 2.3, 2.4, 2.6, 2.10, 2.11, 2.17, 2.20, 2.21).

2.2.6 Animal Experiment

Proceeding from cell culture experiments, an animal study was conducted using rats. Similar to the poly I:C priming paradigm in the cell culture experiments, rats were primed with poly I:C for 2 weeks before injection of the neurotoxin FN075 (see Table 2.24).

2.2.7 Animals

Thirty-two male Sprague-Dawley rats (Charles Rivers UK, 200-225 g on arrival) were housed in groups of 4 per cage on a 12:12 hr light/dark cycle, with 19-23^{o}C temperature, and 40-70% humidity. Throughout the duration of the study, rats were allowed access to food and water ad libitum. Procedures carried out on animals were approved by the Animal Care and Research Ethics Committee of the National University

of Ireland Galway, licensed by the Irish Department of Health and Children and the Irish Health Products Regulatory Authority, and were in agreement with European Union Directive 2010/63/EU and S.I. No. 543 of 2012.

2.2.8 Surgery

All surgeries were conducted under isofluorane anaesthesia (5% in O^2 for induction, followed by 2% in O^2 for maintenance) in a stereotaxic frame with the nose bar set at -2.3 mm. A total of 30 µg of poly I:C (7.5 µg/ml in a total volume of 4 µl) or vehicle (sterile saline, 4 µl) was infused at a rate of 1 µl/min for 4 min, followed by 3 min diffusion time at stereotaxic coordinates AP -5.3, ML +2.0 (from bregma), and DV -7.2 below dura (see Fig. 2.5). Two weeks later, 4 µl of FN075 (1 mM) or vehicle (0.25% DMSO in PBS) was infused at a rate of 1 µl/min for 4 min, followed by a 2 min diffusion time at the same site.

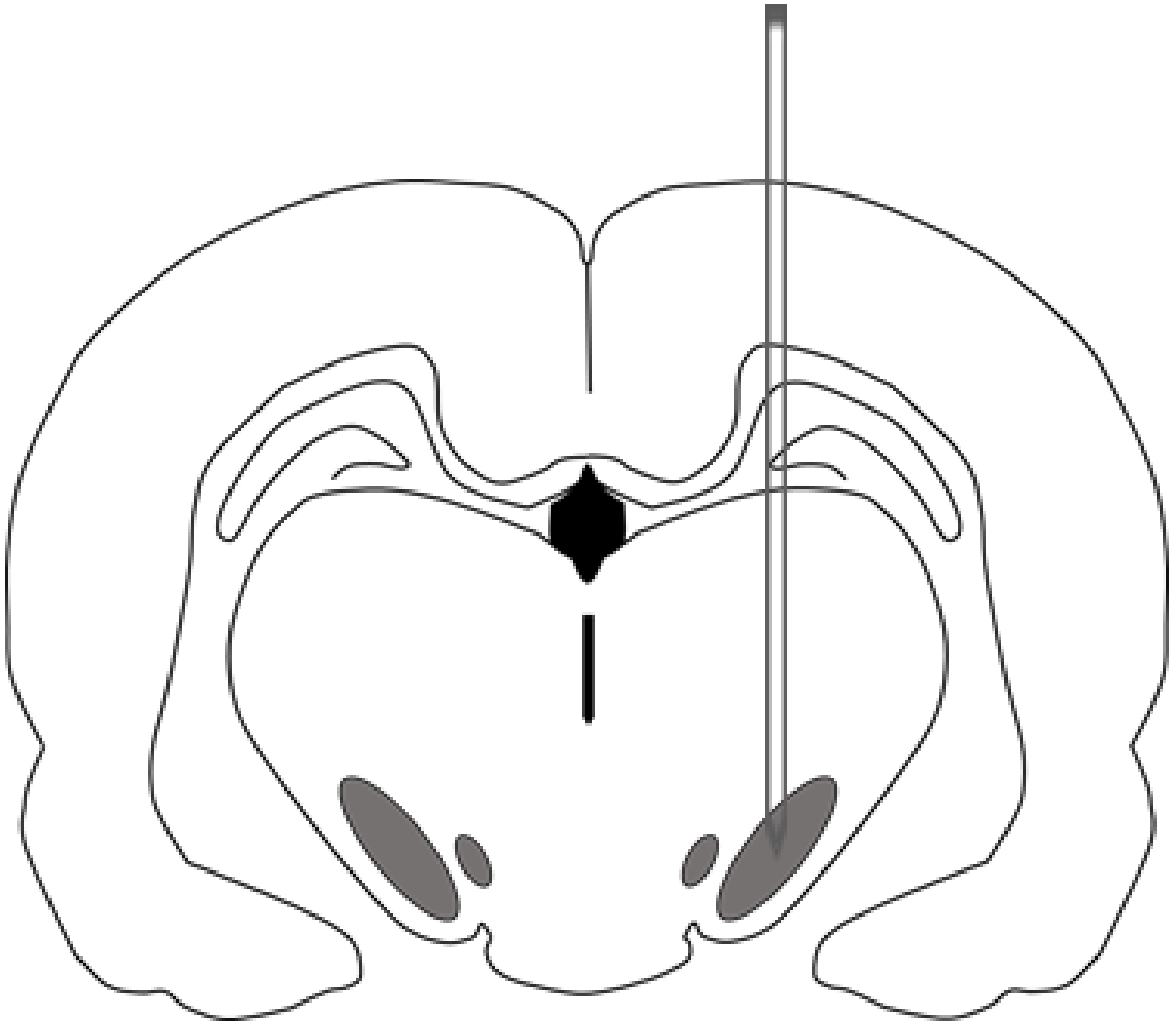

Figure 2.5. Intra-nigral Injection in the Rat Brain. A stereotaxic frame was used with the nose bar set at -2.3 mm for intra-nigral injections (stereotaxic coordinates AP -5.3, ML +2.0 from bregma, DV -7.2 below dura). (Paxinos and Ashwell, 2018)

2.2.9 Cell Assays

2.2.9.1 MTT Cell Viability Assay

2.2.9.1.1 Methodology

The MTT cell viability assay is based on the phenomenon that mitochondrial dehydrogenases cleave the tetrazolium ring of yellow MTT (3-(4,5-Dimethylthiazol-2-yl)-2,5-diphenyltetrazolium bromide) (M2128, Sigma, Ireland), causing it to reduce to a purple MTT formazan crystal. This crystal can be dissolved in isopropanol (I9516, Sigma, Ireland) and quantified by colourimetric spectrophotometer (570 nm wavelength) to measure mitochondrial respiration. For this assay, the mitochondrial respiration of the treated groups were compared to the untreated control group to indirectly measure cell viability.

After cells were treated, MTT solution (5 mg/ml of Thiazolyl Blue Tetrazolium Bromide dissolved in PBS) was added directly to the cell culture medium at a 1:10 dilution factor. Cells (and the blank with no cells) were incubated in MTT solution for 2-2.5 hr in the incubator at 37^{o}C with 5% CO_2. Before adding 150 µl of MTT solvent, medium and remaining MTT solution was removed (carefully so as to not disturb the adherent cells). Cells were gently agitated using an orbital shaker for 15 min before reading the absorbance. The blank was subtracted from all measurements before relating all samples to the control group. Data was presented as a percentage of the control group.

2.2.9.1.2 Experimental Design

Drug	Concentration(s)	Time Point(s)
Poly I:C	0, 5, 10, 20, 50 µg/ml	6, 24, 48 hr
6-OHDA	0, 10, 20, 50, 100 µM	6, 24, 48, hr
Rotenone	0, 50, 100, 250, 500 nM	6, 24, 48 hr
MPP^+	0, 100, 200, 500, 1000 µM	18, 24, 48 hr
FN075	0, 12.5, 25, 50, 100 µM	12, 24, 48 hr

Table 2.1. Experimental Design: SH-SY5Y MTT Concentration and Time Response Experiments.

Drug	Concentration(s)	Neurotoxin Time Point
Poly I:C	0, 10, 20, 50 µg/ml	24 hr
6-OHDA	0, 10, 20, 50 µM	24 hr
Rotenone	0, 50, 100, 250 nM	24 hr
FN075	0, 25, 50, 75 µM	48 hr

Table 2.2. Experimental Design: E14 Rat VM MTT Concentration Response Experiments.

Poly I:C Priming	Neurotoxin	Neurotoxin Concentration	Neurotoxin Time Point
20 µg/ml, 24 hr	6-OHDA	20 µM	24 hr
20 µg/ml, 24 hr	Rotenone	250 nM	24 hr
20 µg/ml, 24 hr	MPP^+	1 mM	24 hr
20 µg/ml, 24 hr	FN075	25 µM	48 hr

Table 2.3. Experimental Design: SH-SY5Y MTT Poly I:C Priming of Neurotoxin Experiments.

Poly I:C Priming	Neurotoxin	Neurotoxin Concentration	Neurotoxin Time Point
20 µg/ml, 24 hr	6-OHDA	20 µM	24 hr
20 µg/ml, 24 hr	Rotenone	100 nM	24 hr
20 µg/ml, 24 hr	FN075	25 µM	48 hr

Table 2.4. Experimental Design: E14 Rat VM MTT Poly I:C Priming of Neurotoxin Experiments.

2.2.9.2 TUNEL Apoptotic Assay

2.2.9.2.1 Methodology

An *In Situ* Cell Death Detection Kit (11684795910, Roche, Germany) was used to detect TUNEL positive DNA strand breaks. SH-SY5Y cells were fixed with 4% PFA (F8775, Sigma, Ireland) for 1 hr before washing with PBS. Fixed cells were then incubated in permeabilisation solution (PBS with 0.1% TritonX-100 and 0.1% sodium citrate) for 2 min at 4^{o}C. TUNEL Reaction Mixture was prepared by combining the TdT Enzyme Solution and Nucleotide Label Solution. After washing twice with PBS, cells were incubated in TUNEL Reaction Mixture for 1 hr at 37^{o}C. Cells were again washed twice in PBS, followed by DAPI (1 µg/ml in TBS) incubation for 5 min at room temperature. Afterwards, fluorescent cells were washed, coverslipped, and imaged using an Optigrid fluorescent microscope. TUNEL stained cells were counted and calculated as a percentage of total number of DAPI stained cells. Data was presented as total percentage.

2.2.9.2.2 Experimental Design

Drug	Concentration(s)	Time Point(s)
Poly I:C	0, 10, 20, 50 µg/ml	24 hr
6-OHDA	0, 10, 20, 50 µM	24 hr
Rotenone	0, 100, 250, 500 nM	24 hr
MPP^+	0, 100, 500, 1000 µM	24 hr
FN075	0, 25, 50, 75 µM	48 hr

Table 2.5. Experimental Design: SH-SY5Y TUNEL Concentration Response Experiments.

Poly I:C Priming	Neurotoxin	Neurotoxin Concentration	Neurotoxin Time Point
20 µg/ml, 24 hr	6-OHDA	20 µM	24 hr
20 µg/ml, 24 hr	Rotenone	250 nM	24 hr
20 µg/ml, 24 hr	MPP^+	1 mM	24 hr
20 µg/ml, 24 hr	FN075	25 µM	48 hr

Table 2.6. Experimental Design: SH-SY5Y TUNEL Poly I:C Priming of Neurotoxin Experiments.

2.2.10 qPCR

2.2.10.1 mRNA Isolation

A Roche high pure RNA isolation kit (11828665001, Roche, Germany) was used for RNA isolation. RNA lysis buffer was used to lyse cells/tissue by vortexing for 15 s. Lysate cells/tissues were transferred to a high pure filter tube and centrifuged for 15 s at 8,000 g. The flow-through was discarded before incubating in DNase I mix (1 U/µl) for 15 min at room temperature. Cells were then centrifuged for 15 s at 8,000 g with 500 µl of Wash Buffer I. Flow-through was discarded, followed by centrifugation for 15 s at 8,000 g with 500 µl of Wash Buffer II. Again flow-through was discarded and sample was centrifuged for 2 min at 13,000 g with 200 µl of Wash Buffer II. After the final flow-through discard, elution buffer was added and the sample was centrifuged for 1 min at 8,000 g to collect the purified RNA flow-through. RNA was quantified using a NanoDrop (purity range: A260/A280 = 1.837-2.957) and stored at -80^{o}C until ready for cDNA synthesis.

2.2.10.2 cDNA Synthesis

Isolated mRNA was synthesised into cDNA using a High Capacity cDNA reverse transcription kit (4368814, Roche, Germany). For SH-SY5Y experiments, RNA was normalised to 250 ng per reaction, while RNA was normalised to 200 ng per reaction for E14 VM experiments due to lower VM cell mRNA yields. Reactions were carried out using RNase/DNase free tubes and distilled water. For a standard reaction volume of 20 µl (see Master Mix in Table 2.7) reactions were heated in a thermocycler (LightCycler 480 by Roche) for 8 min (95^{o}C), followed by maintenance for 2 hr at 37^{o}C and then held at 4^{o}C up to 12 hr until storage at -20^{o}C for qPCR experiments.

cDNA Master Mix
2 µl reverse transcriptase (50 U/µl)
4 µl 10X RT Buffer
4 µl 10X Random Primers
1.6 µl dNTPs (100 mM)
8.4 µl nuclease free water

Table 2.7. Master Mix for cDNA Synthesis.

2.2.10.3 qPCR

Synthesised cDNA was used to quantify relative mRNA levels. The specific primer sequences of the probe targets are found in table 2.8. Reactions of 10 µl (0.5 µl probe, 1 µl cDNA, 3.5 µl nuclease free water, 5 µl of 2x Roche Master Mix (04707494001, Roche, Germany)) were carried out in triplicate in Roche 96 well plates (04729692001, Roche, Germany) and measured using the Roche LightCycler 480. Reactions in the LightCycler underwent a 10 min pre-incubation (95^{o}C), followed by 45 cycles of 10/30 s amplification (95^{o}C/60^{o}C), and 10 s of cooling (40^{o}C). After the cycles were completed, cycle threshold (Ct) was calculated for each replicate by analysing the fluorescence vs cycle measured by the theramocycler. Δ^{Ct} values were generated by transforming the cycles (see Fig. 2.5) using the $2^{-\Delta ct}$ method (Livak and Schmittgen, 2001, Rodríguez-Lázaro and Hernández, 2013). These values were then normalised to the loading control (β-actin). The relative fold change of Δ^{Ct} was used to compare treatment groups and data was presented as such.

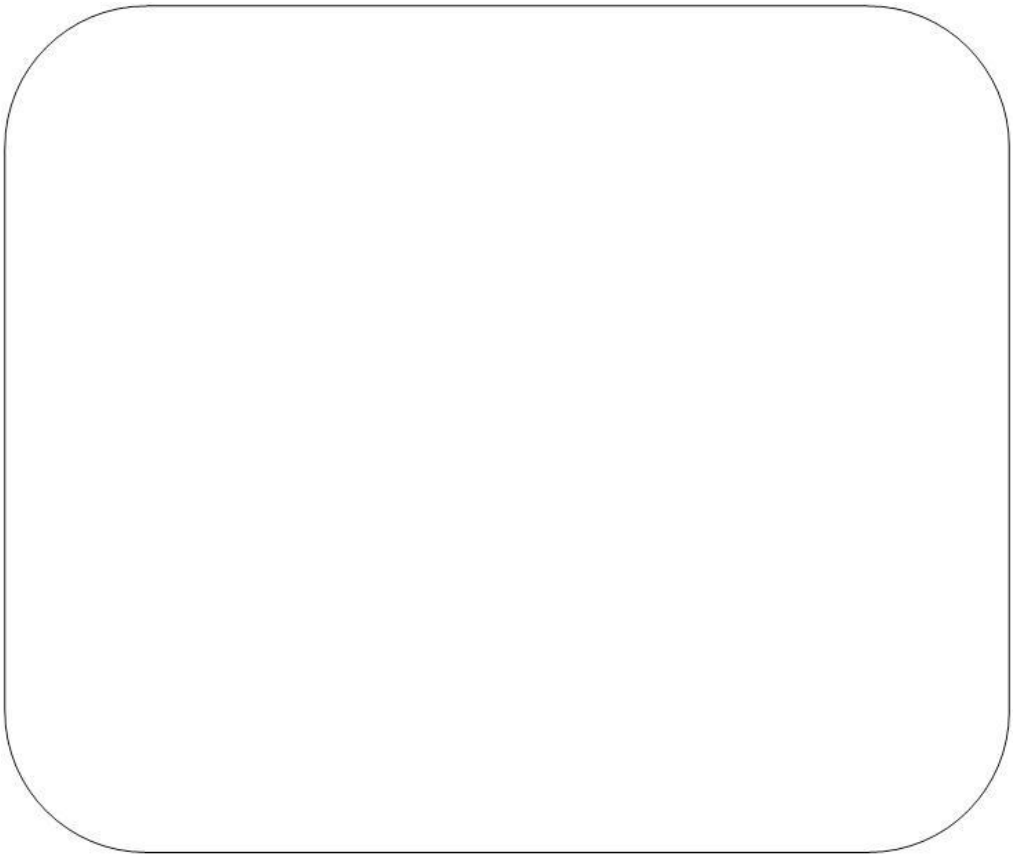

Figure 2.5. qPCR Amplification Curve. Relative fold change of Δ^{Ct} was determined using the qPCR amplification curve. (Adams, 2015)

Target Gene	Assay ID
H. β-actin	143636
H. α-synuclein	137142
H. PSD-95	145168
H. Synaptophysin	136197
H. TH	144999
R. β-actin	500152
R. α-synuclein	503549
R. PSD-95	502414
R. Synaptophysin	503981
R. TH	503274

Table 2.8 PCR Probes. Target genes were purchased from Roche (see Assay ID for each Roche probe).

2.2.10.4 Experimental Design

Drug	Concentration(s)	Time Point(s)
Poly I:C	0, 10, 20, 50 µg/ml	24 hr

Table 2.9. Experimental Design: SH-SY5Y qPCR Concentration Response Experiments.

Poly I:C Priming	Neurotoxin	Neurotoxin Concentration	Neurotoxin Time Point
20 µg/ml, 24 hr	6-OHDA	20 µM	24 hr
20 µg/ml, 24 hr	Rotenone	250 nM	24 hr
20 µg/ml, 24 hr	MPP+	1 mM	24 hr
20 µg/ml, 24 hr	FN075	25 µM	48 hr

Table 2.10. Experimental Design: SH-SY5Y qPCR Poly I:C Priming of Neurotoxin Experiments.

Poly I:C Priming	Neurotoxin	Neurotoxin Concentration	Neurotoxin Time Point
20 µg/ml, 24 hr	6-OHDA	20 µM	24 hr
20 µg/ml, 24 hr	Rotenone	100 nM	24 hr
20 µg/ml, 24 hr	FN075	25 µM	48 hr

Table 2.11. Experimental Design: E14 Rat VM qPCR Poly I:C Priming of Neurotoxin Experiments.

2.2.11 Western Blot

2.2.11.1 Protein Lysis

After treatment, cells were washed in PBS. PBS was removed by centrifugation for 5 min at 1400 rpm. Protease inhibitor cocktail (P8340, Sigma, Ireland) (10 µl) was added to 990 µl of lysis buffer (1 M Tris-HCl, NP-40/Igepal CA-630, 0.25% of sodium deoxycholate, 5 M NaCl, 50 mM EGTA, 1 mM sodium orthovanadate, 50 mM NaF) before adding to the pelleted cells (25 µl). Cells were lysed by vortexing on ice every 10 min for the duration of 40 min. The lysed cells were centrifuged for 15 min at 13,000 rpm at 4^{o}C. Supernatant was transferred to a new eppendorf and stored at -20^{o}C.

2.2.11.2 Bradford

Supernatant protein concentration was determined using the Bradford assay. A BSA standard was prepared by dissolving 2 mg of BSA in 1 ml of distilled water, followed by a series dilution as depicted in table 2.12. A 1:5 dilution of each sample was prepared using distilled water. Each sample (treatment samples and standards) was pipetted in triplicate (5 µl) into a 96-well plate. Bradford reagent (B6916, Sigma, Ireland) (250 µl) was added to each sample. The 96-well plate was then covered in tin foil and gently agitated using an orbital shaker for 15 min. Absorbance reading using a spectrophotometer was taken at 595 nm wavelength.

Concentration of BSA(µg/mL)	BSA stock (µL)	dH_2O (µL)
Blank	0	200
100	10	190
250	25	175
500	50	150
750	75	125
1000	100	100
1500	150	50

Table 2.12. Bradford Standard BSA Concentrations.

2.2.11.3 Gel Electrophoresis

Sodium dodecyl sulfate polyacrylamide gel electrophoresis (SDS-PAGE) was used to separate lysed proteins. Gel percentage was dependent on protein of interest (see Table 2.13). Sample lysates were normalised to 20 µg (unless otherwise stated) using distilled water. Each 20 µl sample prepared in 1.5 ml eppendorfs for SDS-PAGE included 5 µl of 4x Sample Buffer (63.81 mM SDS, 50 mM Tris-HCl pH 6.8, 8% v/v glycerol, 0.02% Bromophenol Blue). β-mercaptoethanol (07604, Sigma, Ireland) (50 µl) was added to 950 µl of 4x sample buffer before adding to the samples. Samples were briefly centrifuged before boiling for 7-8 min at 95^{o}C. After boiling, samples were cooled on ice and briefly centrifuged again before loading onto gels that were previously prepared based on protein size (see Table 14).

Samples (and ladder) were run on gel at 80 V through the stacking gel (5% Acrylamide, 375 mM Tris-HCl pH 6.8, 01% SDS, 0.1% APS, 0.17% TEMED). Once the samples reached the resolving gel, voltage was increased to 120 V. Samples were run

until proteins were adequately separated on the gel, but the dye front was not run off the bottom of the gel.

2.2.11.4 Wet Transfer

Once the SDS-PAGE was complete, the separated proteins were transferred from the gel to a nitrocellulose membrane using a wet transfer. A working transfer buffer was prepared by diluting 10X Transfer Buffer (247.65 mM Tris-HCl, 1.92 M Glycine) to 1X supplemented with 20% Methanol. The nitrocellulose membrane and filter paper were soaked in working transfer buffer previous to transfer cassette set-up. The transfer cassette of the Bio-Rad system was set up as follows:

- Case (red)
- Filter paper
- Nitrocellulose Membrane
- Gel
    - Front of the gel face down on the membrane
- Filter Paper
- Case (black)

The transfer cassette was then placed in the Bio-Rad transfer tank with an ice pack and magnetic flea. Voltage and transfer time was dependent on protein size (see Table 2.13). To confirm a successful transfer, Ponceau stain was used to stain for proteins present on the nitrocellulose membrane.

2.2.11.5 Antibody Detection

After the transfer, the nitrocellulose membrane was incubated for 1 hr in blocking solution (5% milk or BSA in TBS) on a rocker set to 34 rpm at room temperature. The blocking solution was then discarded and the membrane was incubated

overnight in primary antibody (prepared as per Table 2.13) at 4^{o}C on a rocker set to 34 rpm. The following day, the primary antibody was removed and the membrane was washed for 5 min three times in TBS-T (0.05% Tween in TBS) on a rocker set to 34 rpm. After the washes, the membrane was incubated in secondary antibody (prepared as per Table 2.13) for 1 hr at room temperature on a rocker set to 34 rpm. The membrane was then washed again for 5 min three times in TBS-T before storing membrane in distilled water at 4^{o}C until ready for imaging.

Antibody	Type	Antibody Dilution	Concentration	Gel (%)	Transfer Time	Transfer Voltage
TH	Rabbit	Milk	1:1000	10	3 h	20 V
Synaptophysin	Rabbit	Milk	1:800	10	3 h	20 V
PSD-95	Rabbit	Milk	1:1000	10	3 h	20 V
PARP	Rabbit	Milk	1:1000	10	3 h	20 V
c-CASP3	Rabbit	Milk	1:1000	12	1 h 45 min	70 V
LC3-a/b-I/II	Rabbit	BSA	1:1000	12	1 h 45 min	70 V
p62	Mouse	Milk	2 µg/ml	10	1 h 45 min	70 V
p-NF-κB p65	Rabbit	LICOR	1:1000	10	1 h 45 min	70 V
NF-κB p65	Rabbit	LICOR	1:1000	10	1 h 45 min	70 V
p-IκB	Rabbit	LICOR	1:1000	10	1 h 45 min	70 V
IκB	Rabbit	LICOR	1:1000	10	1 h 45 min	70 V
p-IRF3	Rabbit	LICOR	1:1000	10	1 h 45 min	70 V
IRF3	Rabbit	LICOR	1:1000	10	1 h 45 min	70 V
β-actin	Mouse	As above	1:10000	N/A	N/A	N/A
Anti-Rabbit	Goat	As above	1:10000	N/A	N/A	N/A
Anti-Mouse	Goat	As above	1:10000	N/A	N/A	N/A

Table 2.13. Western Blot. The SDS-PAGE gel percentage, transfer time, transfer voltage, antibody concentration, and protein solution were optimised for each antibody. Antibodies for the house-keeping protein (β-actin) and secondary were able to be used with any previously used condition (such as gel percentage or transfer time), as denoted in the table by 'N/A.' For antibody dilution, secondary antibodies were made in the same diluent as the primary antibody indicated by 'As above'.

10% Resolving Gel	
	10% Acrylamide
	375 mM Tris-HCl, pH 8.8
	0.1% SDS
	0.1% APS
	0.1%TEMED*
12% Resolving Gel	12% Acrylamide
	375 mM Tris-HCl, pH 8.8
	0.1% SDS
	0.1% APS
	0.1% TEMED

Table 2.14. Gel Preparation.

5X Running Buffer	
	0.12 M Tris
	1.44 M Glycine
	0.5% SDS
10X Tris-Buffered Saline Solution (TBS), pH 7.6	
	50 mM Tris
	150 mM NaCl
Stripping Solution, pH 2.0	
	5 mM Glycine
	2% SDS

Table 2.15. Buffers.

2.2.11.6 Experimental Design

Drug	Concentration(s)	Time Point(s)
Poly I:C	0, 10, 20 µg/ml	1 hr

Table 2.16. Experimental Design: SH-SY5Y Western Blot Concentration Response Experiments.

Poly I:C Priming	Neurotoxin	Neurotoxin Concentration	Neurotoxin Time Point
20 µg/ml, 24 hr	6-OHDA	20 µM	24 hr
20 µg/ml, 24 hr	Rotenone	250 nM	24 hr
20 µg/ml, 24 hr	MPP+	1 mM	24 hr
20 µg/ml, 24 hr	FN075	25 µM	48 hr

Table 2.17. Experimental Design: SH-SY5Y Western Blot Poly I:C Priming of Neurotoxin Experiments.

2.2.11.7 Western Blot Quantification

Fluorescent protein bands were imaged using Licor Odyssey. Images were then quantified using densitometry collected with Image Studio Lite (LICOR, Lincoln, NE) (see Fig. 2.6). Relative protein expression was calculated as relative to the loading control (β-actin or total protein for phosphorylated proteins). Data was then expressed as fold change compared to the control group.

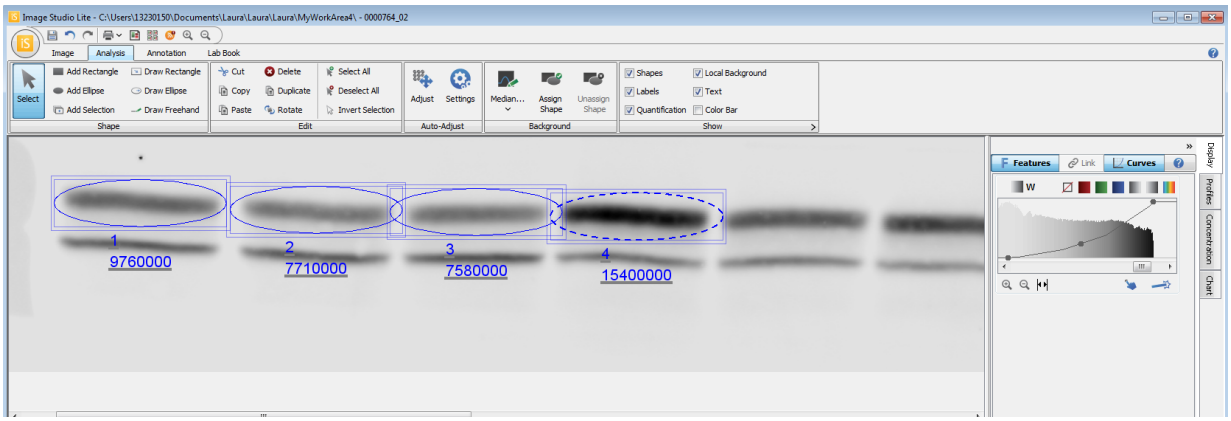

Figure 2.6. Western Blot Quantification. Above is an example of Western Blot quantification for PSD-95 as conducted by the experimenter using Image Studio Lite.

2.2.12 Immunocytochemistry

2.2.12.1 Immunostaining

Cells (SH-SY5Y or rat VM primary cells) were fixed with 4% PFA within chamber slides (89626, Ibidi, Germany) for 30 min before washing with PBS. Fixed cells were then washed with tris-buffered saline (TBS) before 1 hr room temperature incubation in blocking serum (TBS + 1% BSA, 5% normal goat serum, 0.3% Triton X-100, 0.01% Sodium Azide), followed by overnight room temperature incubation in primary antibody (Mouse anti-TH, 1:800, Millipore MAB318; Rabbit anti-GFAP, 1:2000, Dako Z033401; Rabbit anti-phos-NF-κB-p65 @Ser536, 1:100, Cell Signalling 3033; Rabbit anti-synaptophysin, 1:100, Cell Signalling 5461; Mouse anti-α/β-synuclein, 1:50, Cell Signalling 2644; Rabbit anti-α-synuclein-filament-conformation-specific, 1:5000, Abcam 209538) prepared with TBS + 1% BSA, 0.01% Sodium Azide. After washing with TBS, cells were then incubated for 3 hr at room temperature with secondary antibodies (Goat anti-rabbit A.F. 546, 1:1000, Biosciences; Goat anti-mouse A.F. 488, 1:1000, Biosciences) prepared with TBS + 1% normal goat serum. Cells were washed in TBS before 5 min incubation with DAPI (1 µg/ml in TBS) counterstain, followed by further washes with TBS.

2.2.12.2 Experimental Design

Drug	Concentration(s)	Time Point(s)
Poly I:C	0, 20 µg/ml	24 hr
FN075	0, 25, 50 µM	6, 24, 48 hr

Table 2.18. Experimental Design: SH-SY5Y ICC Concentration Response Experiments.

Drug	Concentration(s)	Neurotoxin Time Point
Poly I:C	0, 10, 20, 50 µg/ml	24 hr
6-OHDA	0, 10, 20, 50 µM	24 hr
Rotenone	0, 50, 100, 250 nM	24 hr
FN075	0, 25, 50, 75 µM	48 hr

Table 2.19. Experimental Design: E14 Rat VM ICC Concentration Response Experiments.

Poly I:C Priming	Neurotoxin	Neurotoxin Concentration	Neurotoxin Time Point
20 µg/ml, 24 hr	6-OHDA	20 µM	24 hr
20 µg/ml, 24 hr	Rotenone	250 nM	24 hr
20 µg/ml, 24 hr	MPP^+	1 mM	24 hr
20 µg/ml, 24 hr	FN075	25 µM	48 hr

Table 2.20. Experimental Design: SH-SY5Y ICC Poly I:C Priming of Neurotoxin Experiments.

Poly I:C Priming	Neurotoxin	Neurotoxin Concentration	Neurotoxin Time Point
20 µg/ml, 24 hr	6-OHDA	20 µM	24 hr
20 µg/ml, 24 hr	Rotenone	100 nM	24 hr
20 µg/ml, 24 hr	FN075	25 µM	48 hr

Table 2.21. Experimental Design: E14 Rat VM ICC Poly I:C Priming of Neurotoxin Experiments.

2.2.12.3 Immunocytochemistry Quantification

All immunocytochemistry quantification was completed using ImageJ (open source). Cell counts were measured as number of cells in a designated field of view (FOV) (see Fig. 2.7). The cell counts were then calculated as a percentage of total cell population. To quantify immunofluorescent staining, the region of interest manage in ImageJ was used to select the cell of interest before quantifying mean fluorescence (after subtracting mean background fluorescence). Data was presented as total percentage or fold-change compared to the control group.

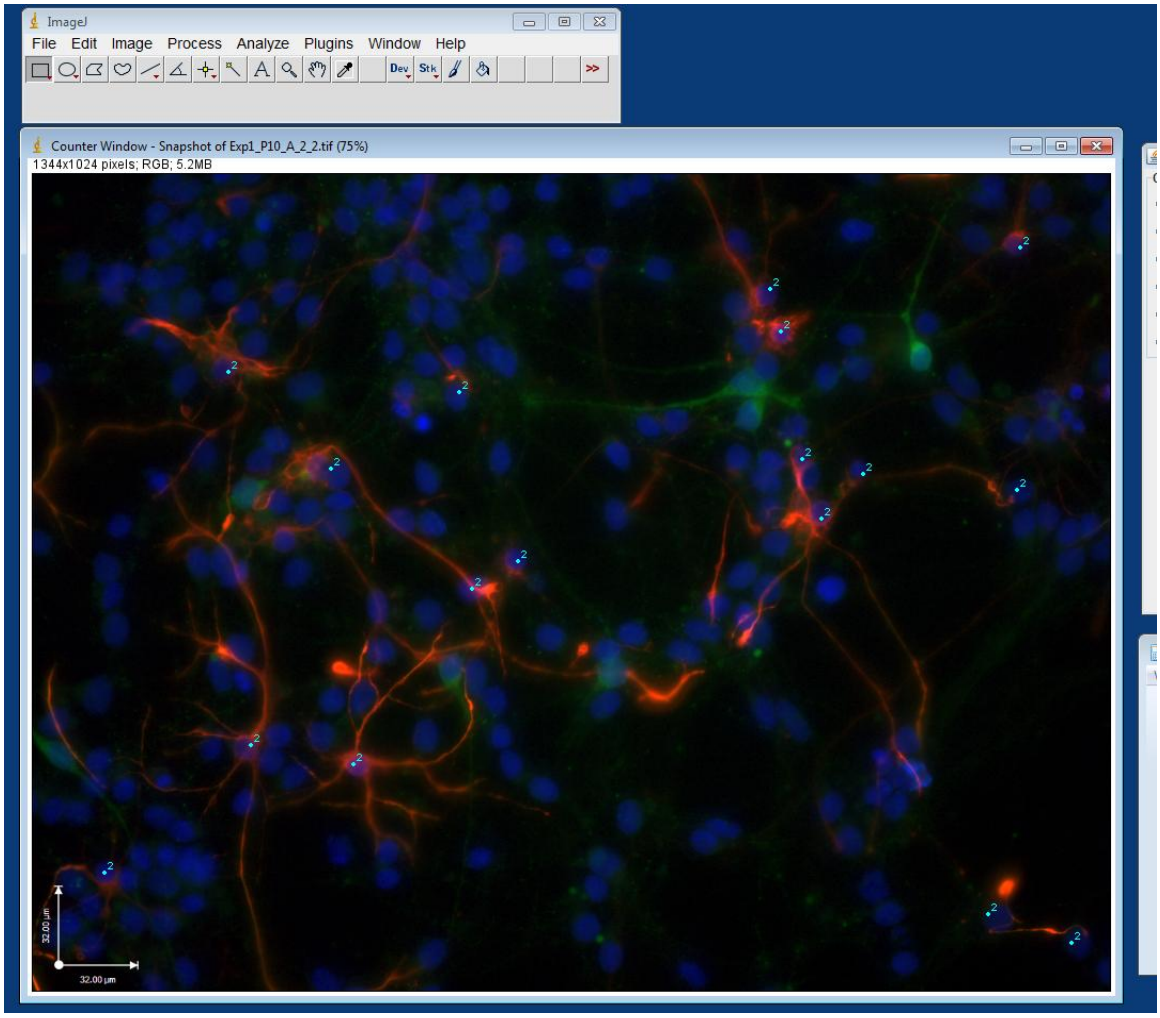

Figure 2.7. Cell Counting using ImageJ. Above is an example of ICC quantification for counting the number of GFAP immunopositive cells in one FOV as conducted by the experimenter using ImageJ.

2.2.13 ELISA

2.2.13.1 Cell Culture ELISAs

Peprotech ELISA kits were conducted for rat IL-6 (900-K86), TNF-α (900-K73), and IL-1β (900-K91) and human IL-6 (900-T16). RnD Systems ELISA kit was used for human IFN-β (8499-IF). Nunc MaxiSorp 96-well microplates were incubated in capture antibody (diluted in PBS) overnight. Plates were aspirated four times with wash buffer (PBS with 0.05% Tween-20) before incubating in blocking solution (PBS with 1% bovine serum albumin) for 1 hr. After blocking, plates were aspirated four times, followed by standard/sample incubation for 2 hr. Plates were then aspirated four times again, followed by 1 hr detection antibody incubation. After aspirating four times, samples were incubated for 30 min in Avidin-HRP Conjugate, followed by another wash and incubation with ABTS or TMB until colour development. Readings were collected using a colourimetric plate reader at 405 nm wavelength. Samples were compared to the standard for quantification. The standards were plotted and analysed using a spline fit line and unknowns were determined from this equation using GraphPad Prism. Data was presented as absolute values.

2.2.13.2 Experimental Design

Drug	Concentration(s)	Time Point(s)
Poly I:C	0, 10, 20, 50 µg/ml	24 hr

Table 2.22. Experimental Design: SH-SY5Y ELISA Concentration Response Experiments.

Drug	Concentration(s)	Time Point(s)
Poly I:C	0, 10, 20, 50 µg/ml	24 hr

Table 2.23. Experimental Design: E14 Rat VM ELISA Concentration Response Experiments.

2.2.14 Immunohistochemistry

2.2.14.1 Immunostaining

Animals were sacrificed by terminal anaesthesia (50 mg/kg pentobarbital intraperitoneal) and transcardial perfusion-fixation with 4% PFA. Brains were extracted, fixed overnight in 4% PFA, and stored in 25% sucrose for post-mortem analysis. Serial coronal sections (30 µm) were sliced using a freezing stage sledge microtome (Bright Series 8000, Hacker). Free floating tissue sections were quenched using distilled water + 3% hydrogen peroxide, 10% methanol. After washing with TBS, tissue was blocked for 1 hr at room temperature in TBS + 3% normal horse/goat serum, 0.2% Triton X-100. Primary antibody incubation was overnight at room temperature. After washing with TBS, sections were incubated in biotinylated secondary antibody (Horse anti-mouse, 1:200, Vector; Goat anti-rabbit, 1:200, Jackson ImmunoResearch) for 3 hr at room temperature, followed by washes with TBS. The tissue was then incubated in streptavidin-biotin-horseradish peroxidase solution for 2 hr at room temperature. A 0.5% solution of diaminobenzidine tetra hydrochloride (DAB) in TNS + 0.3 µl/ml hydrogen peroxide was used to develop the tissue staining. For the Rabbit anti-α-synuclein filament conformation specific stained tissue, a 0.125% DAB solution was used. Stained tissue sections were mounted onto gelatin-coated slides, dehydrated in a series of alcohols and xylene and coverslipped with DPX mountant. Slides were imaged using an Olympus VS120 slide scanner.

2.2.14.2 Experimental Design

Group	Surgery One	Surgery Two	N
Control	Vehicle	Vehicle	7
Poly I:C	Poly I:C	Vehicle	8
FN075	Vehicle	FN075	8
Poly I:C & FN075	Poly I:C	FN075	8

Table 2.24. Experimental Design: Rat IHC Intra-nigral Poly I:C Priming of FN075 Experiment.

2.2.14.3 Immunohistochemistry Quantification

All immunohistochemistry quantification was completed using ImageJ. Cell counts were measured as number of cells in the SN tissue section (see Fig. 2.8). The number of cells in the SN were counted manually using ImageJ across at least three brain tissue sections per animal. Both the injected (ipsilateral) and un-injected (contralateral) sides of the SN were counted for each tissue section. The cell counts were then calculated as the percentage of cells compared to the contralateral side for each tissue section and the average percentage across all tissue sections were determined for each animal. Although this technique is valid, it is worth noting that this method lacks the ability to account for the three-dimensional space of the original structure. The currently accepted methodological approach to account for the geometrical parameters of three-dimensional structures is the stereological technique (Garcia et al., 2007).

Optical density was quantified by measuring the mean grey value in the tissue area of interest (the whole SN or the rostro-caudal axis of the striatum) as previously described (Hoban et al., 2013) across at least three brain tissue sections per animal (see Fig. 2.9). The optical density was quantified for both the ipsilateral and contralateral

sides of the SN and STR for each tissue section. The mean grey values were transformed using the following formula:

$$\text{optical density} = \log_{10} 255/(mean\ grey\ value)$$

After transformation, the optical density was calculated as a percentage compared to the contralateral side and the average percentage across all tissue sections was determined for each animal. Data for the counted cells and optical density cells were presented as percentages compared to the contralateral side.

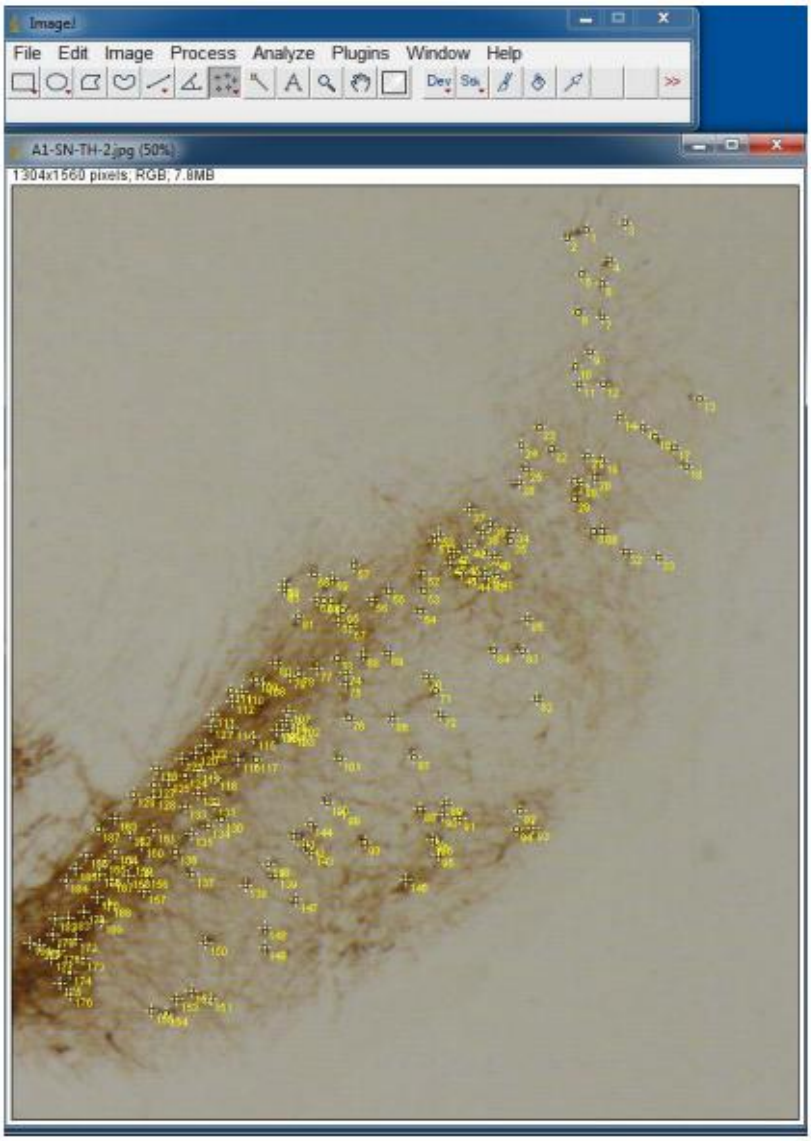

Figure 2.8. Cell Counting of Rat SN using ImageJ.

Figure 2.9. Optical Density of Rat Striatum using ImageJ.

2.2.15 Behavioural Analysis

The Stepping Test of forelimb akinesia was conducted as previously described (Hoban et al., 2013, Olsson et al., 1995). Briefly, both hindlimbs and one forelimb were restrained while the rat was guided across the table top in a horizontal position (see Fig. 2.10). The unrestrained forelimb was assessed for the number of paw adjustment steps (forepaw and backpaw) while going across 90 cm in 5 s. This assessment was conducted for both the ipsilateral and contralateral sides of the body.

The Whisker Test of sensorimotor integration was conducted as previously described (Hoban et al., 2013, Schallert et al., 2000). Briefly, both hindlimbs and one forelimb were restrained while the rat was brushed against the side of a table top (see Fig. 2.11). Number of vibrissae-elicited forelimb placement steps of the unrestrained forelimb out of 10 tests was recorded for both the ipsilateral and contralateral sides of the body.

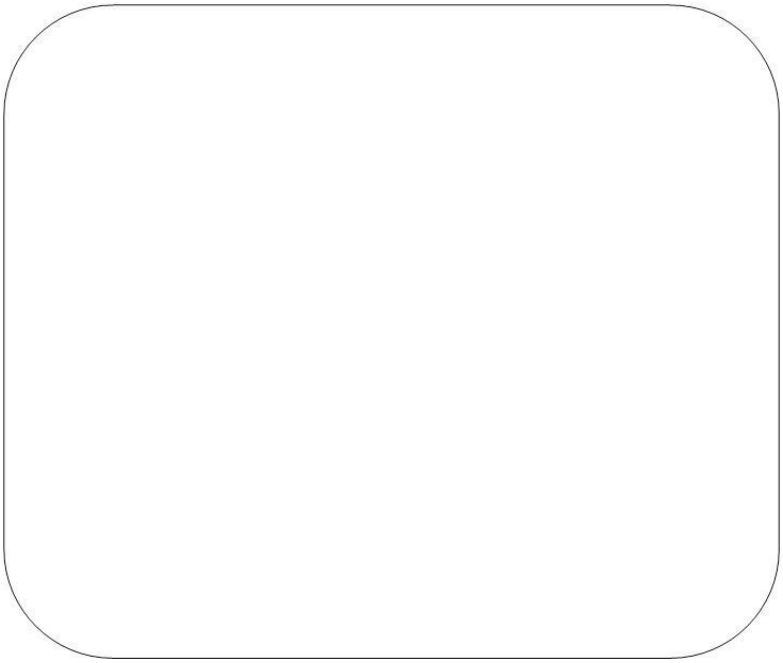

Figure 2.10. Stepping Test of Forelimb Akinesia. The hindlimbs and one forelimb were restrained while the free forelimb was guided across a 90 cm space for 5 s. The number of free forelimb repositions during the 5 s was recorded.

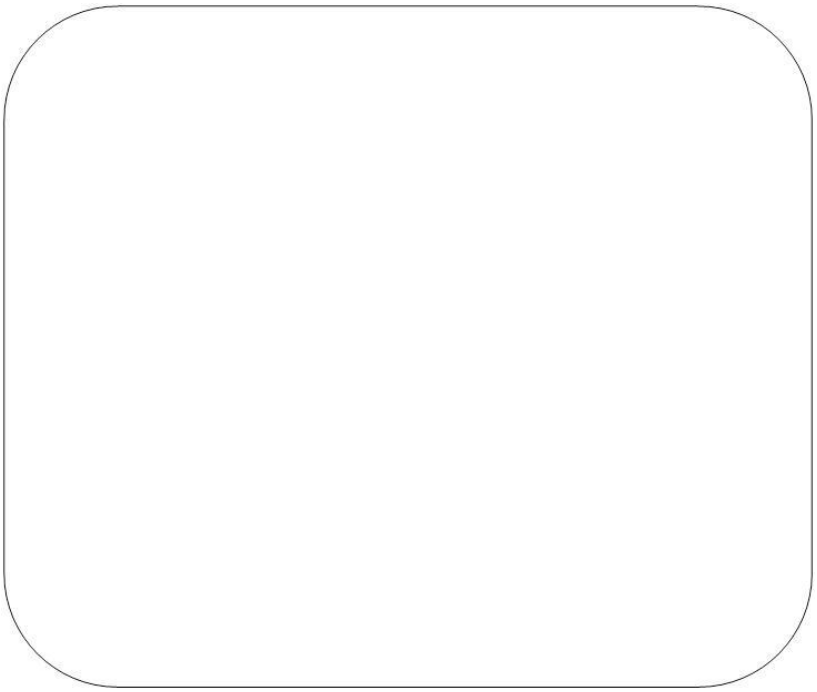

Figure 2.11. Whisker Test of Sensorimotor Integration. The hindlimbs and one forelimb were restrained while the rat's whiskers (of the free forelimb) were brushed against the edge of a table consecutively for 10 tests. The number of forelimb placements on the edge of the table was recorded as a score out of 10 tests.

2.2.16 Statistics

Statistics was conducted using SPSS (IBM, USA) and GraphPad Prism (GraphPad, USA). All data were tested for normality by Shapiro-Wilk's test and homogeneity of variance by Levene's test to determine the appropriate statistical test. Depending on the parametric nature of the data, experiments with only two groups were analysed using an independent samples t-test, or Mann-Whitney U-test. Where appropriate, cell culture concentration response experiments with more than two groups were analysed using a One-way ANOVA or Kruskal-Wallis test, followed by a Student Newman-Keul's (SNK) or non-parametric-Bonferroni *post-hoc* test, respectively. *Post-mortem* IHC analyses were conducted using a One-way ANOVA, followed by a SNK *post-hoc* test. The Stepping Test was analysed using a Two-way ANOVA, followed by Bonferroni *post-hoc* tests. A Kruskal-Wallis test, followed by a Dunn's multiple comparison *post-hoc* test, was used to analyse the Whisker Test. The Pearson Correlation test was used to determine significant associations between neuropathological features. Significance tests were two-tailed with $\alpha = 0.05$ significance level. Graphical error bars represent standard error of the mean (SEM), while box plots include min/max whiskers.

Chapter Three: SH-SY5Y Results

CHAPTER THREE

3.1 INTRODUCTION

Since an epidemiological association between certain viral infections and PD has become apparent (Bu et al., 2015, Marttila and Rinne, 1978, Marttila et al., 1981, Vlajinac et al., 2013), pre-clinical investigation into the molecular and cellular consequences of viral infections in neurons was undertaken. As previously described in Chapter 1, certain viral infections have been found to disrupt host autophagy, decrease synaptic function and increase neuroinflammation in the CNS (Carpentier et al., 2005, Ebrahimie et al., 2015, Lussignol et al., 2013, Piacentini et al., 2015, Tallóczy et al., 2006, Valyi-Nagy et al., 2000, Zhang et al., 2011). Some of these studies utilised specific viruses (such as HSV-I or influenza A) to examine these neurological effects, while some used viral-like synthetic dsRNA (poly I:C). Proceeding on from these studies, experiments were designed to investigate the potential for viral-like poly I:C to prime or sensitise neurons to the toxic effects of compounds that induce pathological features known to occur in PD (such as oxidative stress, mitochondrial dysfunction, and α-synuclein aggregation).

Although the primary cells of interest in PD are dopaminergic neurons, obtaining and maintaining human primary dopaminergic neurons for research is not practical. Therefore, established neuronal cell lines are often used to study PD (Heusinkveld and Westerink, 2017, Xicoy et al., 2017). Due to their expression of dopaminergic neuron markers (such as TH), one of the more commonly used cell lines for PD research is the neuroblastoma SH-SY5Y cell line (Biedler et al., 1978, Ross and Biedler, 1985, Xicoy et al., 2017). These cells are ideal for molecular/cellular investigation of poly I:C priming in combination with PD pathological features induced via the use of PD models (such as 6-OHDA or rotenone). The experiments in this chapter utilise SH-SY5Y cells to

determine if poly I:C priming modulates the neurotoxicity of 6-OHDA, rotenone, MPP^+ and FN075.

3.2 METHODS

The methods used in this chapter did not differ in any way from those outlined in chapter two, unless otherwise stated.

3.3 EXPERIMENTAL DESIGN

Due to the epidemiological association between viral infections and development of PD, molecular and cellular changes in neurons after viral-like priming were investigated. The beginning of this chapter covers concentration response experiments for poly I:C and other neurotoxins to determine the optimal concentration for poly I:C priming experiments. Cell death as measured by MTT cell viability and $TUNEL^+$ staining are examined for all neurotoxins. Poly I:C is also investigated for TLR3 activation (as measured by cytokine/chemokine release and phosphorylation of proteins downstream from TLR3). The remaining experiments examine the effects of poly I:C priming in combination with 6-OHDA, rotenone, MPP^+, and FN075 (see Fig. 3.1). In this context, 6-OHDA is used to model oxidative stress, rotenone and MPP^+ are used to model mitochondrial dysfunction, and FN075 is used to model α-synuclein aggregation. A relatively new model of α-synucleinopathy, FN075 is a small molecule peptidomimetic which has been found to promote α-synuclein fibril formation via acceleration of α-oligomerisation (Horvath et al., 2012, Pedersen et al., 2015). FN075 was selected from a group of related peptidomimetics for these experiments due to its affinity for α-synuclein fibril formation *in vitro* (see Appendix A).

After poly I:C priming in combination with 6-OHDA, rotenone, MPP^+, or FN075, changes in inflammation, neurodegeneration/cell death, the synapse, and

autophagy were examined. Cell viability, TUNEL^{+} staining, qPCR, Western Blot, and qualitative immunocytochemical staining were conducted to determine the consequences of poly I:C priming in SH-SY5Y neurons. All experiments were repeated a minimum of three times. The viral-like priming experiments were designed following the diagram below:

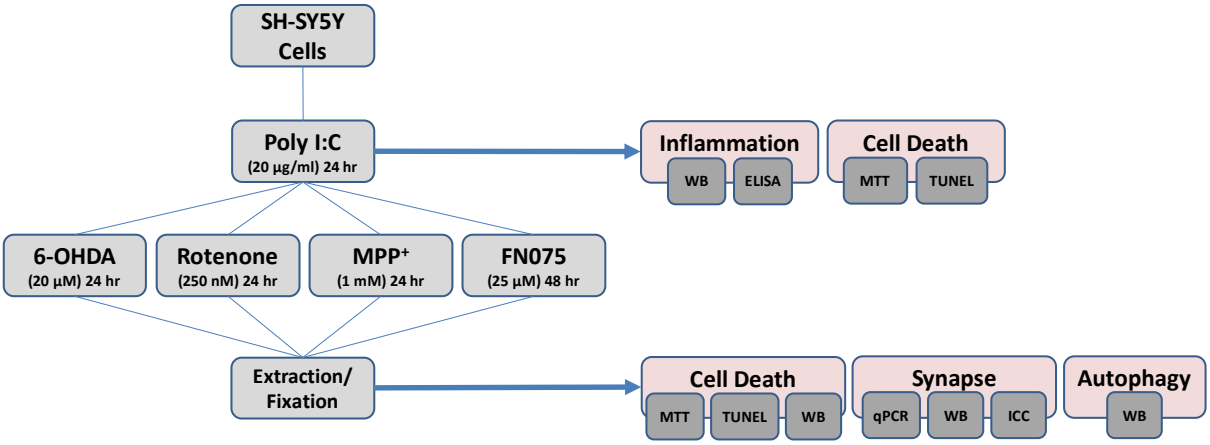

Figure 3.1. Chapter 1 Experimental Design. SH-SY5Y cells were primed with poly I:C (20 µg/ml) for 24 hr, followed by 6-OHDA (20 µM for 24 hr), rotenone (250 nM for 24 hr), MPP^{+} (1 mM for 24 hr), or FN075 (25 µM for 48 hr) treatment. Cells were extracted or fixed for analysis; n = 3 or 6 per group.

3.4 RESULTS

3.4.1 Cell Viability and Cell Death Assays in SH-SY5Y Cells

3.4.1.1 Cell Viability after Neurotoxin Treatment in SH-SY5Y Cells

The optimal concentration and treatment time for poly I:C and other neurotoxins was determined using the MTT cell viability assay. Mitochondrial respiration in live cells reduces MTT into formazan, which produces a purple colour that can be measured by a spectrophotometer. A change in the amount of formazan produced (purple colour present) has been demonstrated to be proportional to the number of live cells (Gerlier and Thomasset, 1986). According to this assay, there was a significant concentration-dependent decrease in cell viability for all neurotoxins (see Fig. 3.2). 6-OHDA reduced cell viability after 6 hr ($F_{(4,25)} = 31.9$, $p < 0.0010$), 24 hr ($F_{(4,25)} = 85.2$, $p < 0.001$), and 48 hr ($F_{(4,25)} = 89.7$, $p < 0.001$) of treatment. The highest concentration of 100 µM appeared to immediately reduce cell viability, with 42% reduction after 6 hr ($p < 0.001$). Lower concentrations, such as 20 µM, did not reduce cell viability until hr 24 (25% reduction, $p < 0.001$). Similarly, rotenone reduced cell viability after 6 hr ($F_{(4,25)} = 12.5$, $p < 0.001$), 24 hr ($F_{(4,25)} = 7.0$, $p = 0.001$), and 48 hr ($F_{(4,24)} = 58.1$, $p < 0.001$) of treatment. A consistent reduction in cell viability after rotenone was not apparent until hour 24, with the highest concentration of 500 nM inducing a 15% reduction ($p < 0.05$). By hour 48, this 500 nM rotenone reduction in cell viability was increased to an 82% reduction ($p < 0.001$). Unlike 6-OHDA and rotenone, only the highest concentration of 1 mM of MPP^+ induced significant reduction in cell viability after 18 hr ($F_{(4,25)} = 7.4$, $p < 0.001$) and 24 hr ($F_{(4,25)} = 15.2$, $p < 0.001$) treatment. After 48 hr, all concentrations of MPP^+ reduced cell viability ($F_{(4,25)} = 75.0$, $p < 0.001$), with 1000 µM reducing cell viability by 37% ($p < 0.001$). FN075 reduced cell viability after 12 hr ($F_{(4,25)} = 9.0$, $p < 0.001$), 24 hr ($F_{(4,25)} =$

13.7, $p < 0.001$), and 48 hr ($F_{(4,25)} = 28.9$, $p < 0.001$). Consistent reduction in cell viability after FN075 treatment was not seen until hour 48 ($p < 0.001$).

Based on the above results, the optimal concentration and time for all neurotoxin treatments after poly I:C were determined. After a 24 hour treatment, 6-OHDA 20 µM (74.41%, $p < 0.001$), rotenone 250 nM (79.99%, $p < 0.01$), and MPP^+ 1000 µM (74.91%, $p < 0.001$) induced a significant reduction in cell viability while retaining enough live cells for experimental analysis (such as for mRNA for qPCR or protein for Western Blot). A similar level of cell viability was the case for FN075 25 µM after 48 hr (79.54%, $p < 0.05$).

The optimal concentration of poly I:C for priming SH-SY5Y cells was not determined using the MTT assay, but cell viability was used to measure neurotoxicity. Although poly I:C did reduce cell viability after 6 hr ($F_{(4,25)} = 5.1$, $p = 0.004$), 24 hr ($F_{(4,25)} = 6.0$, $p = 0.002$), and 48 hr ($F_{(4,25)} = 17.6$, $p < 0.001$), poly I:C did not reduce cell viability beyond a 33% loss even at the highest concentration (see Fig. 3.2). The highest concentration of 50 µg/ml reduced cell viability by 33% after 48 hr ($p < 0.01$), while 20 µg/ml reduced cell viability by 28% ($p < 0.01$).

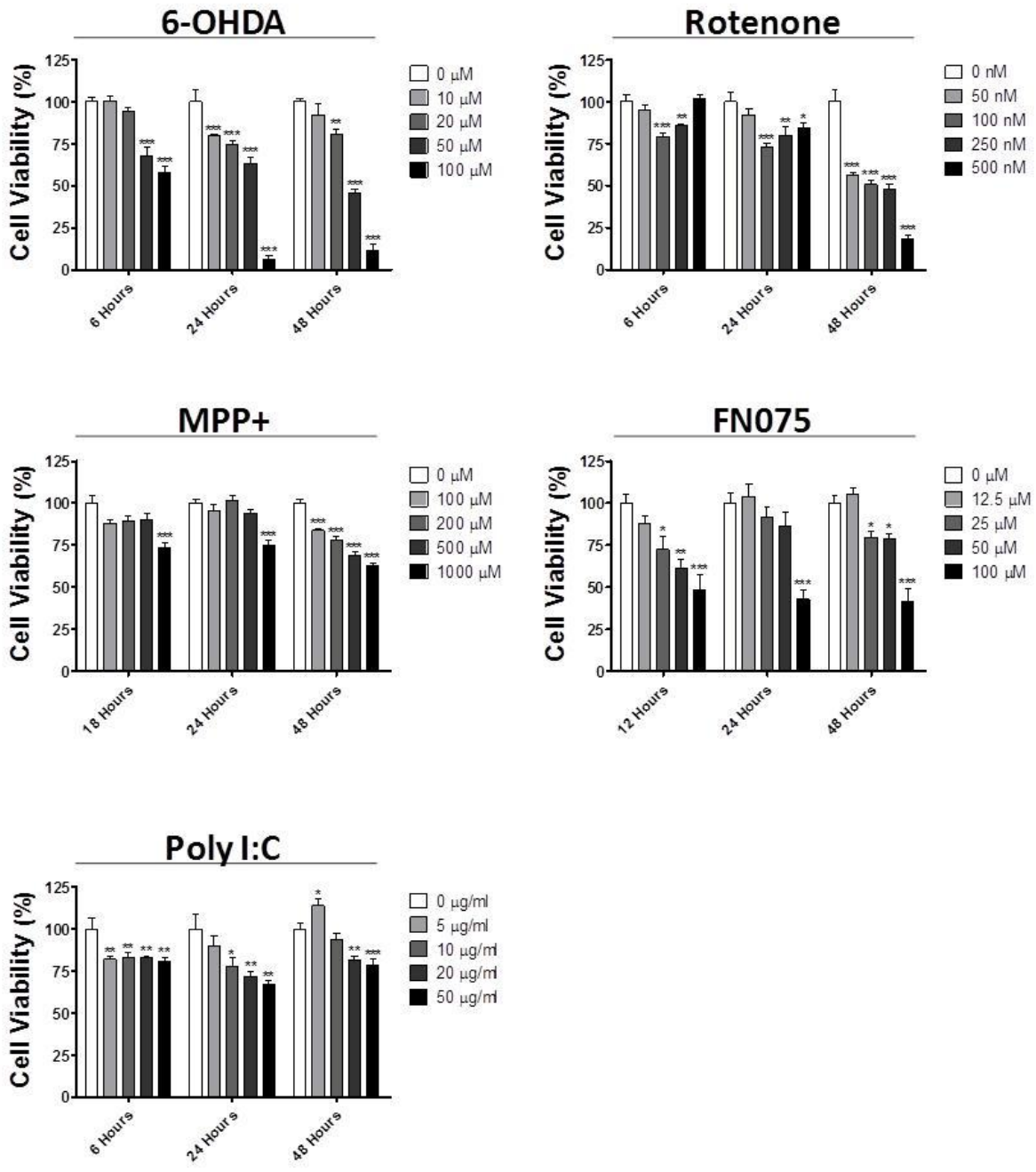

Figure 3.2. Cell Viability after Neurotoxin Treatment in SH-SY5Y Cells: Concentration Response at Multiple Time Points. Cells were treated once with various neurotoxins. All neurotoxins demonstrated a concentration-dependent decrease in cell viability. Data are expressed as means and standard deviations. All analyses were conducted using a One-way ANOVA, followed by SNK *post-hoc* test. For readability, only *post-hoc* comparisons to the untreated group were denoted in the graphs. *$p < 0.05$ vs untreated, **$p < 0.01$ vs untreated, ***$p < 0.001$ vs untreated

3.4.1.2 Cell Death after Neurotoxin Treatment in SH-SY5Y Cells

Neuronal cell death was also measured to determine the toxicity of poly I:C and neurotoxins (see Fig. 3.3). SH-SY5Y cells were treated with 6-OHDA (0-50 µM), rotenone (0-500 nM), MPP^+ (0-1000 µM), or poly I:C (0-50 µg/ml) for 24 hr, or FN075 (0-75 µM) for 48 hr. The TUNEL cell death assay measures DNA fragmentation by staining nicks within the DNA (Kyrylkova et al., 2012). DNA fragmentation suggests that cells are undergoing apoptotic cell death. Although all neurotoxins demonstrated a concentration-dependent decrease in cell viability, not all neurotoxins exhibited a concentration-dependent increase in $TUNEL^+$ stained cells (see Fig. 3.3). MPP^+ ($F_{(3,16)} = 4.0$, $p < 0.05$), FN075 ($F_{(3,16)} = 42.3$, $p < 0.001$), and poly I:C ($F_{(3,16)} = 5.7$, $p < 0.01$) were found to induce a concentration-dependent increase in apoptotic cell death according to the TUNEL assay. MPP^+ (1000 µM), FN075 (25 µM), and poly I:C (50 µg/ml) produced approximately a 10% increase in $TUNEL^+$ staining. Although 6-OHDA was reported to have a significant change in $TUNEL^+$ staining ($F_{(3,16)} = 3.7$, $p < 0.05$), SNK *post-hoc* analysis found no significant changes. Only the highest concentration of rotenone (500 nM) induced a 5% increase in apoptotic-like cell death ($p < 0.05$).

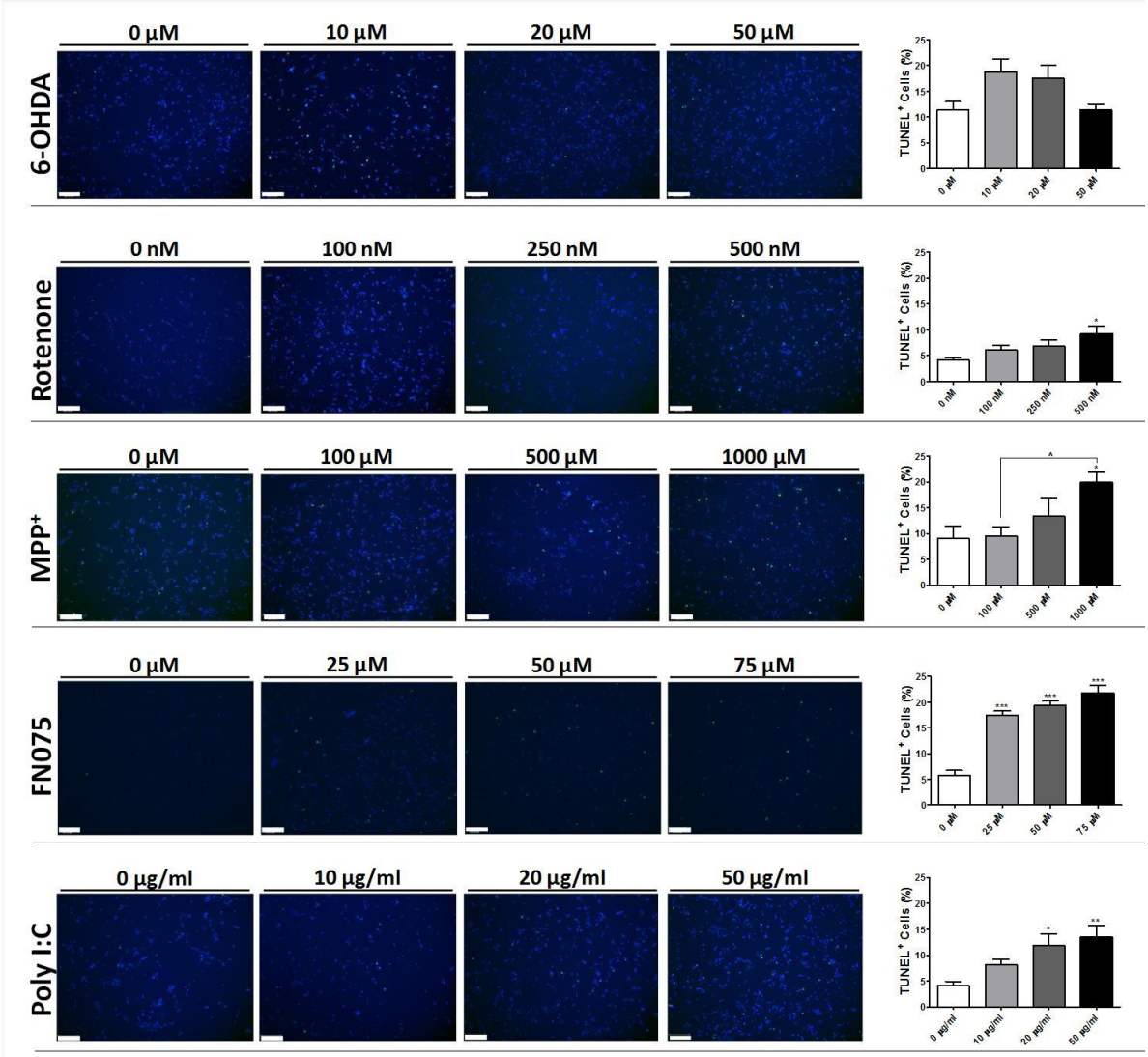

Figure 3.3. TUNEL Assay in SH-SY5Y Cells: Dose Response after Neurotoxin Treatment. SH-SY5Y cells were treated with 6-OHDA, rotenone, MPP^+, or poly I:C for 24 hr, or FN075 for 48 hr. Cells were fixed with 4% PFA for $TUNEL^+$ (green) and DAPI nuclear staining (blue). Images were taken with an Olympus microscope using the 20X objective lens. Analyses were conducted using One-way ANOVA, followed by SNK *post-hoc* test. Data are presented as means and standard error of the means. Scale bar = 200 µm. *p < 0.05 vs Control, **p < 0.01 vs Control, ***p < 0.001 vs Control, ^p < 0.05 vs poly I:C

3.4.2 Poly I:C Activation of TLR3 in SH-SY5Y Cells

For these experiments, poly I:C was used to activate TLR3. As described in Chapter 1, TLR3 activation results in NF-κB/IRF3 phosphorylation and cytokine/interferon release (O'Neill et al., 2013). Therefore, relative phosphorylated NF-κB/IRF3 expression and cytokine/interferon release was measured after poly I:C treatment to determine the poly I:C concentration required to activate TLR3 in SH-SY5Y cells. Media and cells were extracted from poly I:C treated SH-SY5Y cells for protein analysis to determine poly I:C mediated activation of TLR3 in neurons. Western Blot analysis for phosphorylated proteins after 1 hr poly I:C treatment (see Fig. 3.4) found no significant changes in phosphorylated-p65 NF-κB ($F_{(2,6)} = 0.001$, $p > 0.05$) or phosphorylated I-κB ($F_{(2,6)} = 1.3$, $p > 0.05$). However, there was a trend of a poly I:C induced increase in phosphorylated IRF3 ($F_{(2,6)} = 4.5$, $p = 0.065$). Poly I:C (20 µg/ml) induced a 1.6-fold increase in phosphorylated IRF3, suggesting TLR3 activation. Further supporting TLR3 activation, ELISA analysis found poly I:C treatment to increase cytokine and interferon release, with a significant increase in IL-6 ($F_{(2,6)} = 80.9$, $p < 0.001$) and IFN-β ($F_{(2,6)} = 137.5$, $p < 0.001$) release (see Fig. 3.5). After 24 hr, poly I:C (20 µg/ml) produced increases in IL-6 (30.48 ± 18.80 pg/ml) and IFN-β (10.85 ± 2.44 pg/ml), as compared to the untreated group. The poly I:C mediated increase in cytokine/interferon release suggests that both NF-κB and IRF3 downstream pathways of TLR3 were activated with 20 µg/ml of poly I:C.

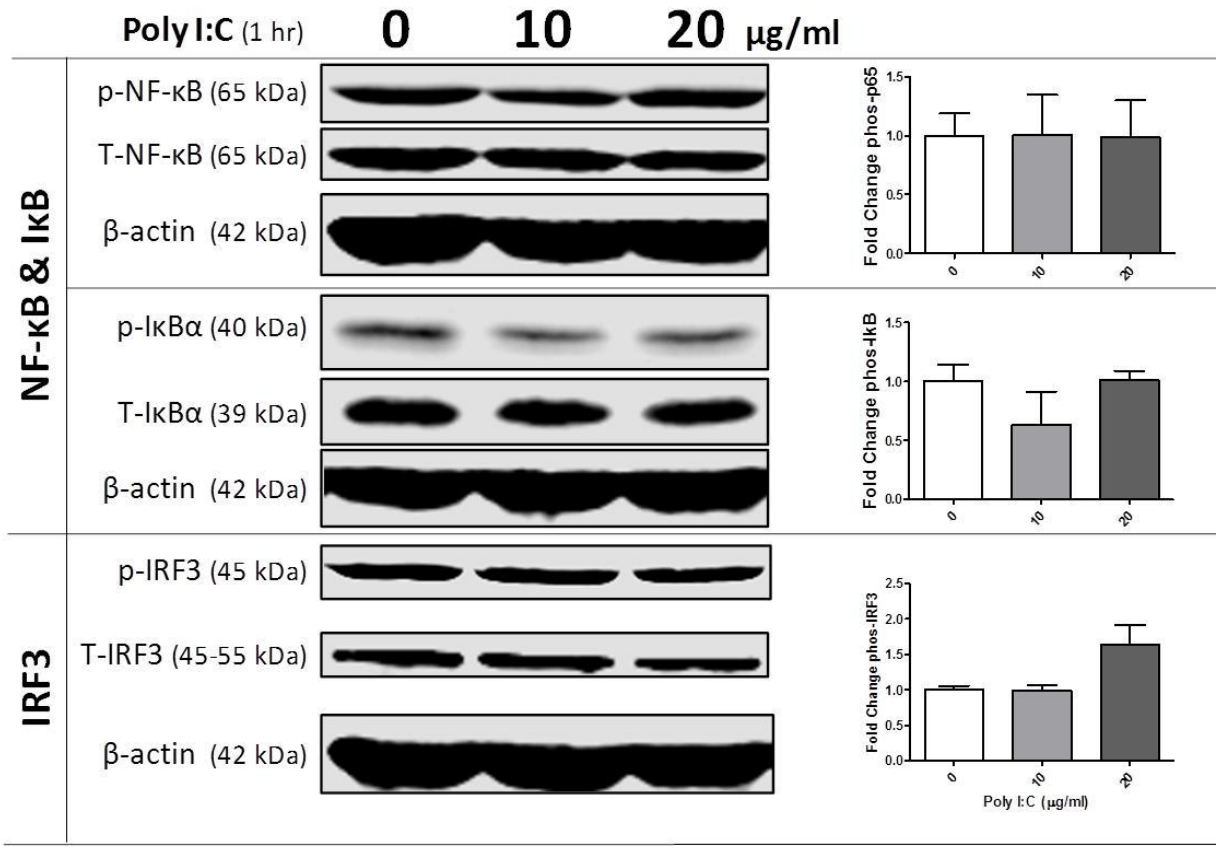

Figure 3.4. Poly I:C Dose Response: Phosphorylated Protein Expression. After SH-SY5Y cells were treated with poly I:C for 1 hr, cells were extracted for Western Blot analysis. Optical density was quantified using Image Studio Lite and calculated as relative to total protein levels. Data were analysed using One-way ANOVA, followed by SNK *post-hoc* test, and presented as means and standard error of the means.

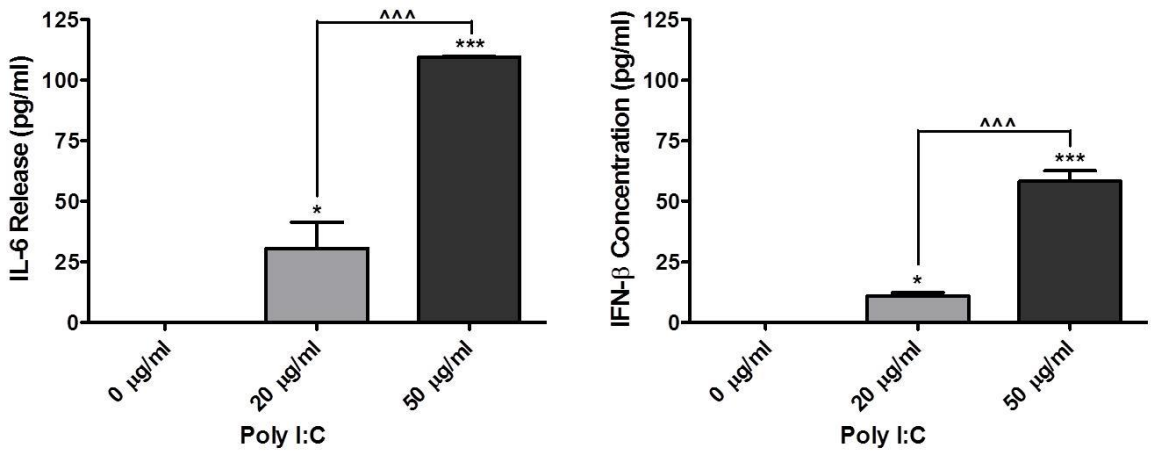

Figure 3.5. Poly I:C Dose Response: Cytokine and Interferon Release. Media was collected after SH-SY5Y cells were treated with poly I:C for 24 hr. ELISA analysis for IL-6 and IFN-β were conducted. Concentration in the media was determined by comparison to a standard. Data are presented as means and standard error of the means. Analysis was conducted using One-way ANOVA and SNK *post-hoc* test. *$p < 0.05$ vs Control, ***$p < 0.001$ vs Control, ^^^$p < 0.001$ vs 20 µg/ml

3.4.3 Poly I:C Priming Modulates Cell Death in SH-SY5Y Cells

3.4.3.1 Poly I:C Priming Exacerbates Neurotoxin Induced Decrease in Cell Viability

Based on the previous concentration-dependent experiments, the poly I:C priming experiments were designed to determine if priming altered the neurotoxicity of multiple neurotoxins. SH-SY5Y cells were primed with poly I:C (20 µg/ml) for 24 hr, followed by a 24 or 48 hr treatment with 6-OHDA (20 µM), rotenone (250 nM), MPP^+ (1 mM), and FN075 (25 µM). According to the MTT assay, poly I:C priming of 6-OHDA ($F_{(3,16)} = 13.2$, $p < 0.001$), rotenone ($F_{(3,20)} = 47.0$, $p < 0.001$), and MPP^+ ($F_{(3,20)} = 34.8$, $p < 0.001$) exacerbated the neurotoxin induced decrease in cell viability (see Fig. 3.6). Poly I:C priming in combination with 6-OHDA (76.52%, $p < 0.05$), rotenone (58.71%, $p < 0.001$), and MPP^+ (41.17%, $p < 0.001$) resulted in a more significant decrease in cell viability compared to the neurotoxins alone (6-OHDA (87.74%), rotenone (76.10%), and MPP^+ (78.08%)). Although poly I:C (89.00%, $p < 0.05$) and FN075 (80.59%, $p < 0.01$) alone induced a decrease in cell viability for the poly I:C+FN075 experiment ($F_{(3,20)} = 7.5$, $p < 0.01$), poly I:C priming did not exacerbate this effect (79.69%, $p > 0.05$). Changing the media in between poly I:C and neurotoxin treatment modulated the toxic effects of 6-OHDA (94.85%), rotenone (90.25%), and FN075 (105.85%) (see Fig. 3.6). Although poly I:C priming followed by media change before treatment with rotenone (88.42%) or FN075 (84.40%) resulted in a decrease in cell viability, this reduction was not as drastic as when the media was retained (see Fig. 3.6). Conversely, the effects of MPP^+ and poly I:C priming with MPP^+ follow the same trend regardless of media change ($F_{(3,20)} = 34.3$, $p < 0.001$).

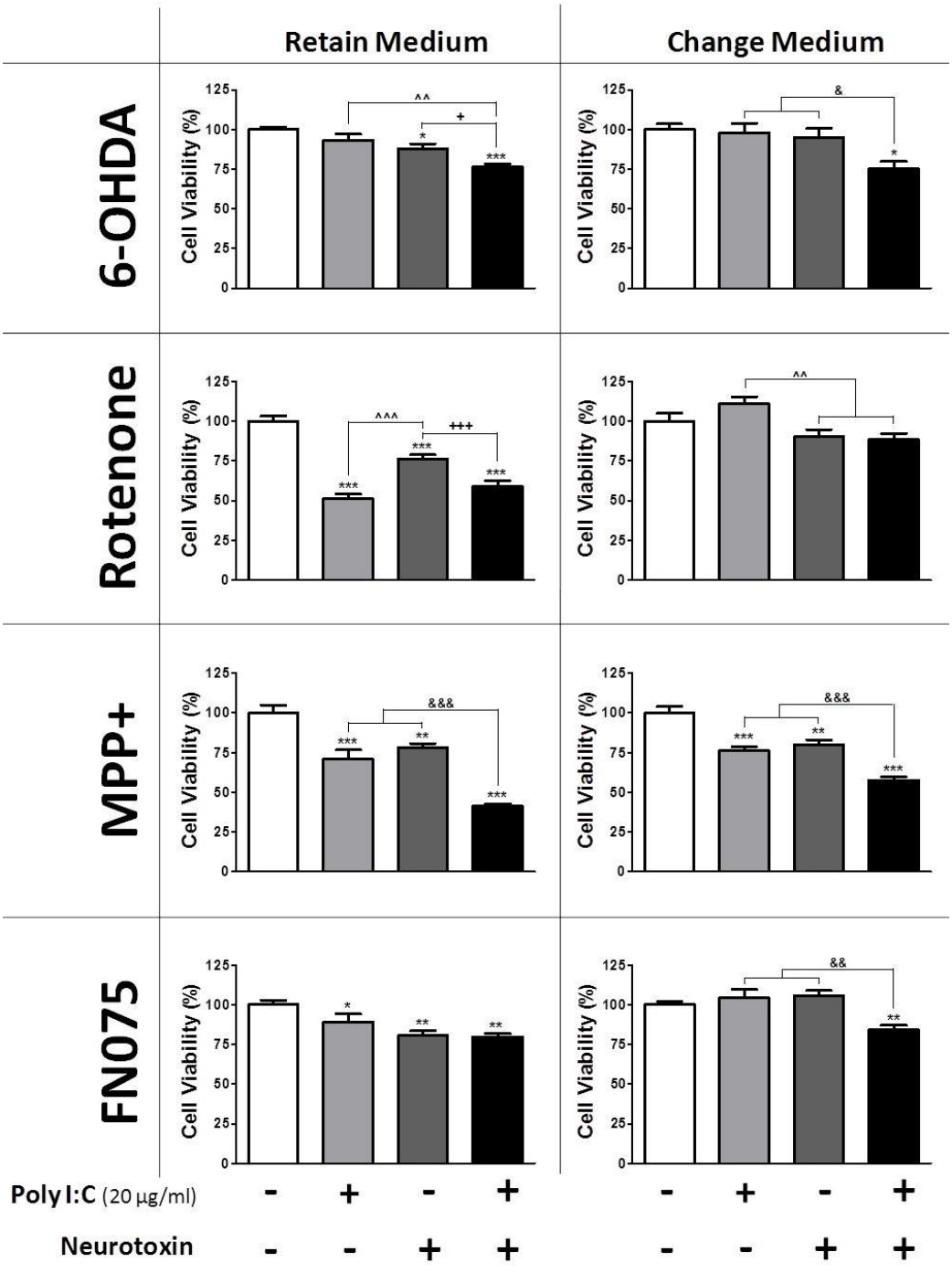

Figure 3.6. Cell Viability after Poly I:C Priming of Neurotoxins in SH-SY5Y Cells. Cells were primed with poly I:C, followed by neurotoxin treatment. The media was either retained or changed in between the poly I:C and neurotoxin treatment. MTT cell viability was analysed using One-way ANOVA, followed by SNK post-hoc test. Data are presented as means and standard error of the means. *p < 0.05 vs Control, **p < 0.01 vs Control, ***p < 0.001 vs Control, ^^p < 0.01 vs poly I:C, ^^^p < 0.001 vs poly I:C, $^{+}$p < 0.05 vs neurotoxin, $^{+++}$p < 0.001 vs neurotoxin, $^{\&}$p < 0.05 vs poly+neurotoxin, $^{\&\&}$p < 0.01 vs poly+neurotoxin, $^{\&\&\&}$p < 0.001 vs poly+neurotoxin

3.4.3.2 Poly I:C Priming Modulates Neurotoxin Induced Increase in TUNEL$^+$ Cells

The TUNEL assay was used to examine changes in DNA fragmentation, a marker of apoptotic-like cell death, after poly I:C priming. Similar to the MTT experiments, SH-SY5Y cells were primed with poly I:C (20 µg/ml) previous to neurotoxin treatment. For all these experiments, the media was retained in between the poly I:C and neurotoxin treatment. In these experiments, poly I:C priming exacerbated MPP$^+$ ($F_{(3,8)} = 80.2$, $p < 0.001$) and FN075 ($F_{(3,8)} = 40.9$, $p < 0.001$) induced increase in TUNEL$^+$ stained cells (see Fig. 3.7). Priming increased the percentage of TUNEL$^+$ cells from 24.10% (MPP$^+$ 1 mM for 24 hr) and 17.50% (FN075 25 µM for 48 hr) to 33.42% and 23.91%, respectively. There was no poly I:C priming effect of 6-OHDA ($F_{(3,8)} = 1.1$, $p > 0.05$) or rotenone ($F_{(3,8)} = 2.9$, $p > 0.05$).

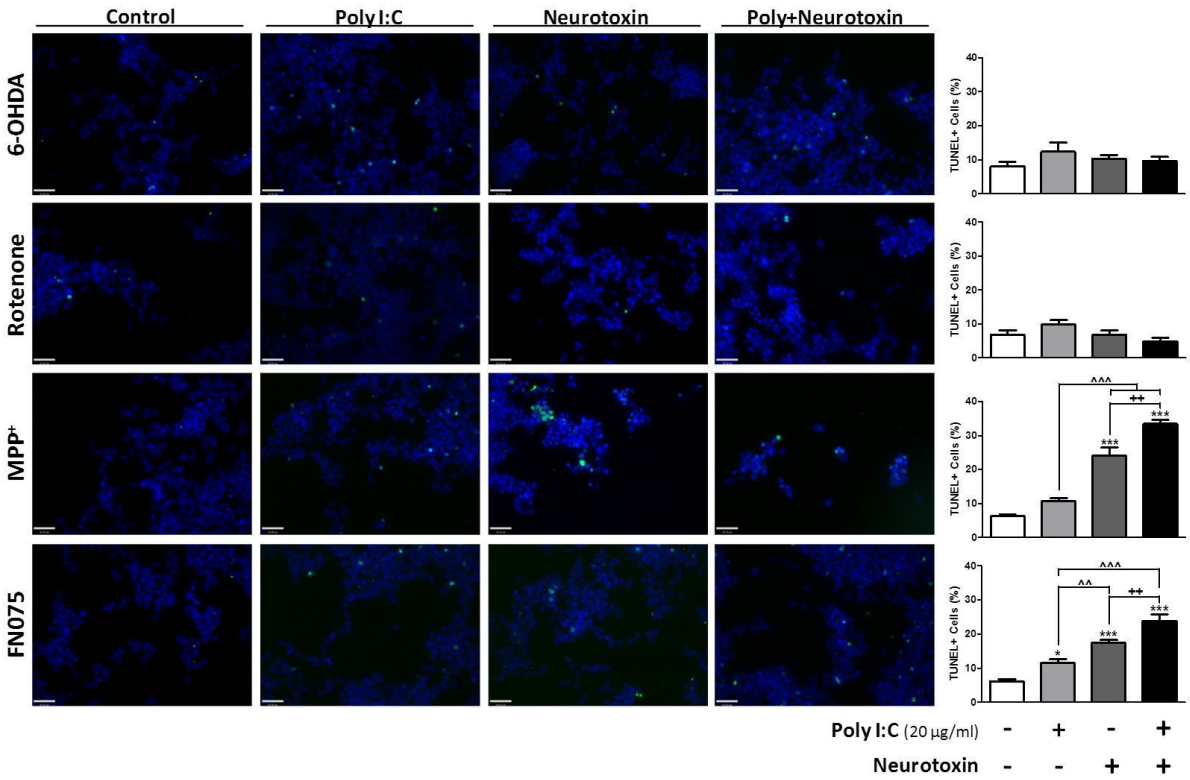

Figure 3.7. TUNEL Assay in SH-SY5Y Cells: Poly I:C Priming of Neurotoxins. Poly I:C priming (20 µg/ml) for 24 hr preceded neurotoxin (6-OHDA 20 µM, rotenone 250 nM, MPP^+ 1 mM, or FN075 25 µM) treatment. SH-SY5Y cells were fixed with 4% PFA for $TUNEL^+$ (green) and DAPI nuclear staining (blue). Images were taken with an Olympus microscope using the 40X objective lens. Analyses were conducted using One-way ANOVA, followed by SNK *post-hoc* test. Data are presented as means and standard error of the means. Scale bar = 42 µm. *$p < 0.05$ vs Control, ***$p < 0.001$ vs Control, ^^$p < 0.01$ vs poly I:C, ^^^$p < 0.001$ vs poly I:C, $^{++}p < 0.01$ vs neurotoxin

3.4.4 Poly I:C Priming Modulates Relative mRNA and Protein Expression SH-SY5Y Cells

We hypothesised that poly I:C priming would exacerbate neurotoxin induced neurodegeneration, synaptic dysfunction, and autophagy disruption in SH-SY5Y cells. Increases in cell death related proteins and decreases in synapse related mRNA/proteins are expected, along with a change (increase or decrease) in autophagy related proteins.

3.4.4.1 Poly I:C Priming Modulates 6-OHDA Induced Changes in mRNA and Protein Expression

For these experiments, SH-SY5Y cells were poly I:C primed (20 µg/ml) for 24 hr followed by another 24 hr treatment with 6-OHDA (20 µM). Then the cells were extracted for protein or mRNA analysis. For all Western Blot protein analyses, the media was retained or changed in between the poly I:C and neurotoxin treatment. Conversely, the media was retained in between treatments for all qPCR and immunocytochemistry analyses.

Apoptosis related proteins (caspase-3 and PARP) were examined to investigate possible modulation of neurodegeneration. As previously discussed, caspase activation has been found to inactivate PARP, inhibiting the DNA repair activity of PARP. Along with PARP inactivation, cleavage of the protease caspase-3 leads to apoptotic mediated cell death. Although there was over a 20-fold increase in relative cleaved caspase-3 ($F_{(3,8)} = 170.0$, $p < 0.001$) after poly I:C treatment (see Fig. 3.8), there was no significant change in cleaved PARP ($F_{(3,8)} = 3.0$, $p > 0.05$). Interestingly, changing the media in between drug treatments slightly modulated this poly I:C induced increase in cleaved caspase-3 ($F_{(3,8)} = 13.6$, $p < 0.01$). When the media was retained, poly I:C alone (22-fold, $p < 0.001$) and poly I:C combined with 6-OHDA (24-fold, $p < 0.001$) produced a much

larger increase in cleaved caspase-3 compared to when the media was changed (poly I:C alone (13-fold, $p < 0.01$), poly I:C+6-OHDA (9-fold, $p < 0.05$)).

Autophagy related proteins (LC3-a/b-I/II and p62) were also examined after cells were primed with poly I:C and treated with 6-OHDA to determine changes in proteins that might contribute to cell death and/or protein clearance. These proteins were of interest due to their participation in autophagic vesicle formation for degradation of mis-folded/abnormal proteins. Treatment with poly I:C was found to induce a significant 0.5-fold decrease in relative fold change of LC3-a/b-I ($F_{(3,8)} = 10.2$, $p < 0.01$, see Fig. 3.9). Conversely, the LC3-a/b-II isoform was significantly enhanced after treating with 6-OHDA ($F_{(3,8)} = 7.9$, $p < 0.01$), with a 1.6-fold increase. Also, media retention was required for the significant reduction in LC3-a/b-I after poly I:C treatment alone (0.5-fold, $p < 0.05$) or poly I:C in combination with 6-OHDA (0.5-fold, $p < 0.05$) to occur, since there was no significant difference in LC3-a/b-I after changing the media ($F_{(3,8)} = 0.8$, $p > 0.05$). When the media was retained, there was a trend for poly I:C alone to decrease p62, but this did not reach significance ($F_{(3,8)} = 3.4$, $p > 0.05$). Conversely, poly I:C alone (0.4-fold, $p < 0.05$) decreased the relative fold change in p62 when the media was changed ($F_{(3,8)} = 7.3$, $p < 0.05$).

Synapse related proteins (and corresponding mRNA) were examined after poly I:C priming in combination with 6-OHDA (see Fig. 3.10 and Fig. 3.11). To examine both the pre- and post-synapse, synaptophysin and PSD-95 were investigated for changes in relative mRNA and protein expression. Also, TH (the rate limiting enzyme for dopamine synthesis) and α-synuclein were measured via qPCR and Western Blot or qualitative immunocytochemistry. Except a significant reduction in relative TH mRNA (0.2-fold, $p < 0.05$) after poly I:C treatment ($F_{(3,8)} = 5.6$, $p < 0.05$), there were no other significant changes in relative mRNA expression (α-synuclein ($F_{(3,8)} = 1.4$, $p > 0.05$) and

synaptophysin ($F_{(3,8)}$ = 1.4, $p > 0.05$)). Although according to the One-way ANOVA, there was a significant difference in relative PSD-95 mRNA between groups ($F_{(3,8)}$ = 5.4, $p < 0.05$), SNK *post-hoc* test found no differences between groups ($p > 0.05$). Unlike qPCR mRNA analysis, poly I:C priming in combination with 6-OHDA resulted in significant changes in relative synapse related protein expression (see Fig. 3.11), but not TH expression ($F_{(3,20)}$ = 0.2, $p > 0.05$). When the media was retained between treatments, poly I:C priming in combination with 6-OHDA resulted in a significant increase in relative PSD-95 ($F_{(3,20)}$ = 4.0, $p < 0.05$) and synaptophysin ($F_{(3,20)}$ = 9.5, $p < 0.001$). With poly I:C priming in combination with 6-OHDA, PSD-95 was increased by 1.5-fold ($p < 0.05$), while synaptophysin was increased by over 3-fold ($p < 0.001$). These significant changes only occurred when the media was retained, with no significant changes in protein expression when the media was changed in between treatments (PSD-95 ($F_{(3,20)}$ = 0.7, $p > 0.05$), synaptophsyin ($F_{(3,20)}$ = 1.5, $p > 0.05$)). Qualitative immunocytochemistry was conducted for synaptophysin and α/β-synuclein to investigate protein localisation (see Fig. 3.12). Some α/β-synuclein inclusions were found in the cytosol after 6-OHDA, while the combination of poly I:C and 6-OHDA appeared to produce synaptophysin inclusions that co-localised with α/β-synuclein (see Fig. 3.12).

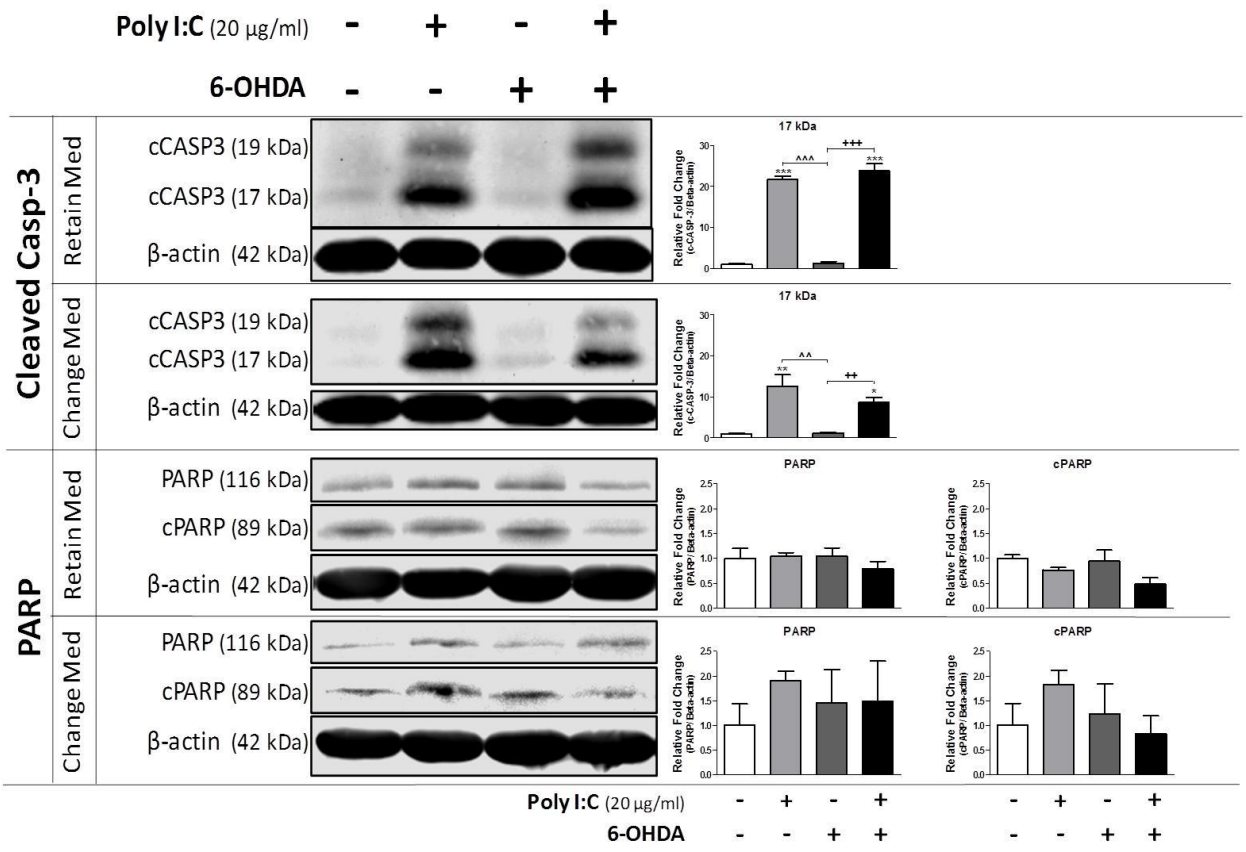

Figure 3.8. Poly I:C Priming 6-OHDA in SH-SY5Y Cells: Apoptotic Related Protein Expression. SH-SY5Y cells were primed with poly I:C (20 µg/ml) for 24 hr prior to treatment with 6-OHDA (20 µM) for 24 hr. Cells were extracted, lysed, and probed for apoptotic related proteins. Data are presented as means and standard error of the means, and analysed using One-way ANOVA (followed by SNK *post-hoc* test). *p < 0.05 vs Control, **p < 0.01 vs Control, ***p < 0.001 vs Control, ^^p < 0.01 vs poly I:C, ^^^p < 0.001 vs poly I:C, $^{++}$p < 0.01 vs 6-OHDA, $^{+++}$p < 0.001 vs 6-OHDA

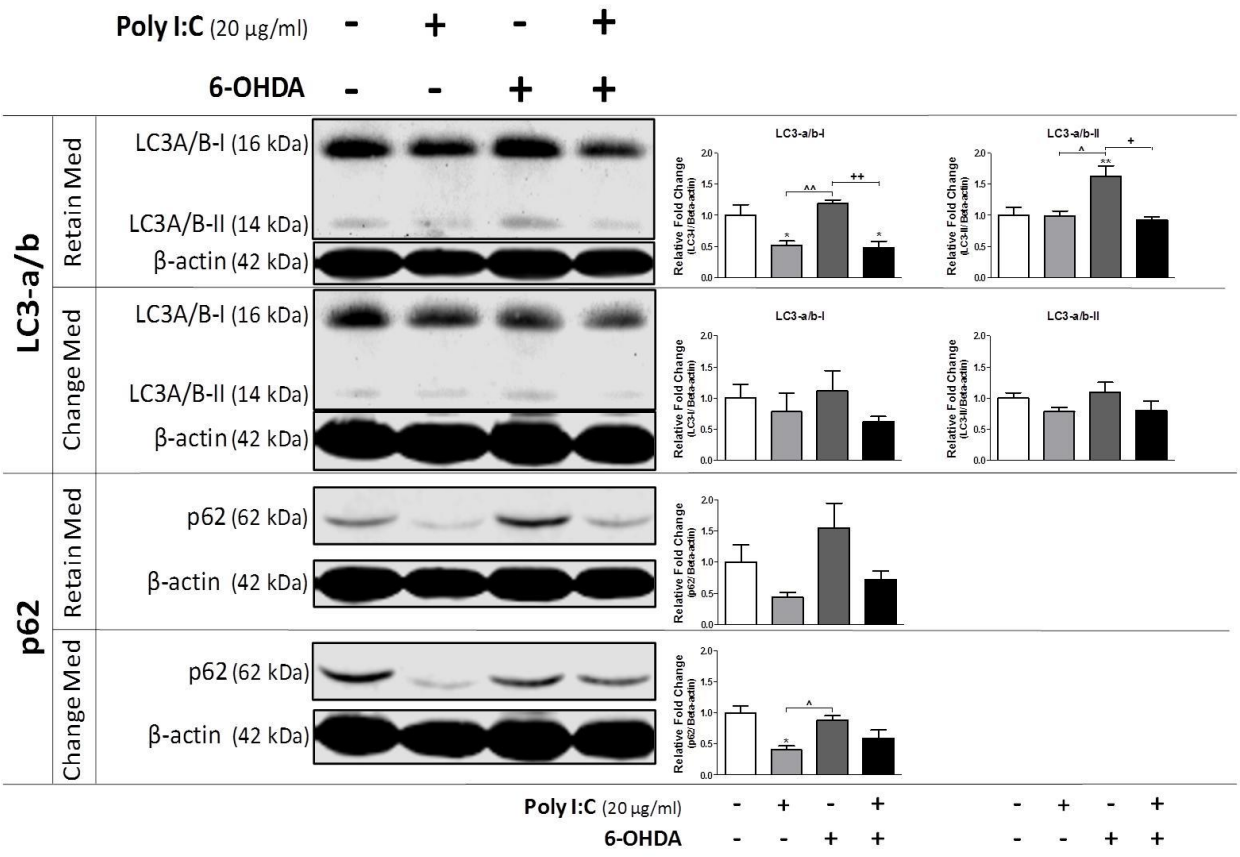

Figure 3.9. Poly I:C Priming 6-OHDA in SH-SY5Y Cells: Autophagy Related Protein Expression. SH-SY5Y cells were primed with poly I:C (20 µg/ml) for 24 hr prior to treatment with 6-OHDA (20 µM) for 24 hr. Cells were extracted, lysed, and probed for autophagy related proteins. Data are presented as means and standard error of the means, and analysed using One-way ANOVA (followed by SNK *post-hoc* test). *$p < 0.05$ vs Control, **$p < 0.01$ vs Control, ^$p < 0.05$ vs poly I:C, ^^$p < 0.01$ vs poly I:C, $^{+}p < 0.05$ vs 6-OHDA, $^{++}p < 0.01$ vs 6-OHDA

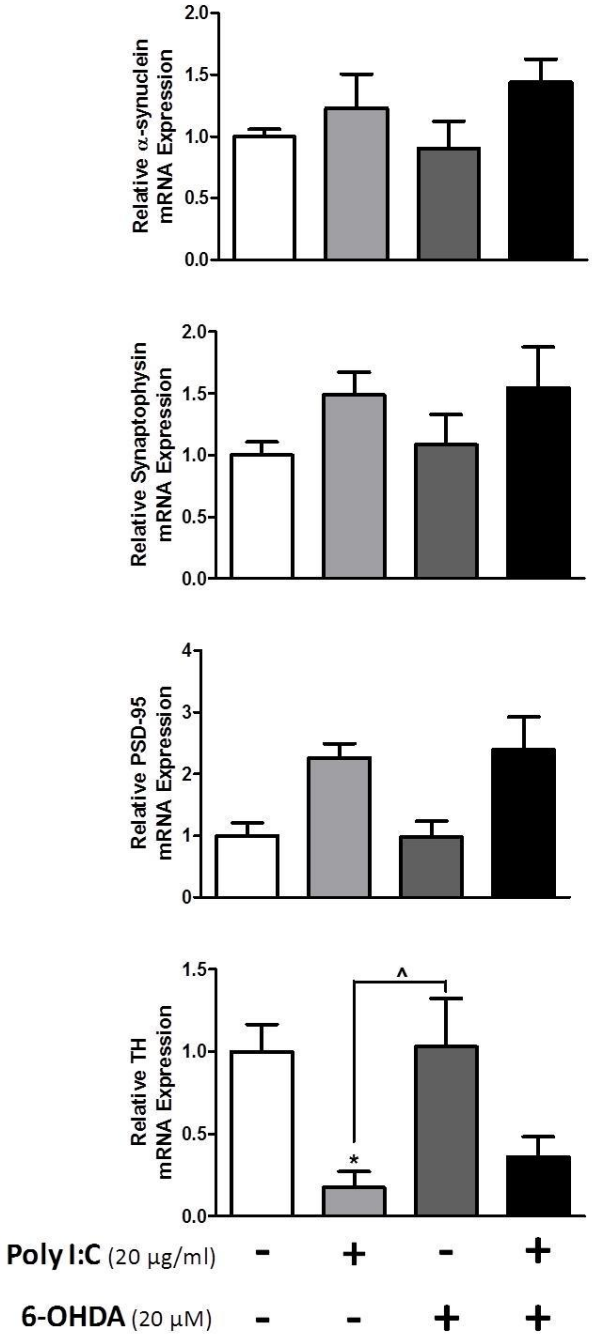

Figure 3.10. Poly I:C Priming 6-OHDA in SH-SY5Y Cells: Synaptic Related mRNA Expression. SH-SY5Y cells were primed with poly I:C (20 µg/ml) for 24 hr prior to treatment with 6-OHDA (20 µM) for 24 hr. The media was retained in between poly I:C and 6-OHDA treatment. Cells were extracted, lysed for mRNA, and probed with synapse related primers. Data are presented as means and standard error of the means, and analysed using One-way ANOVA (followed by SNK *post-hoc* test). *$p < 0.05$ vs Control, ^$p < 0.05$ vs poly I:C

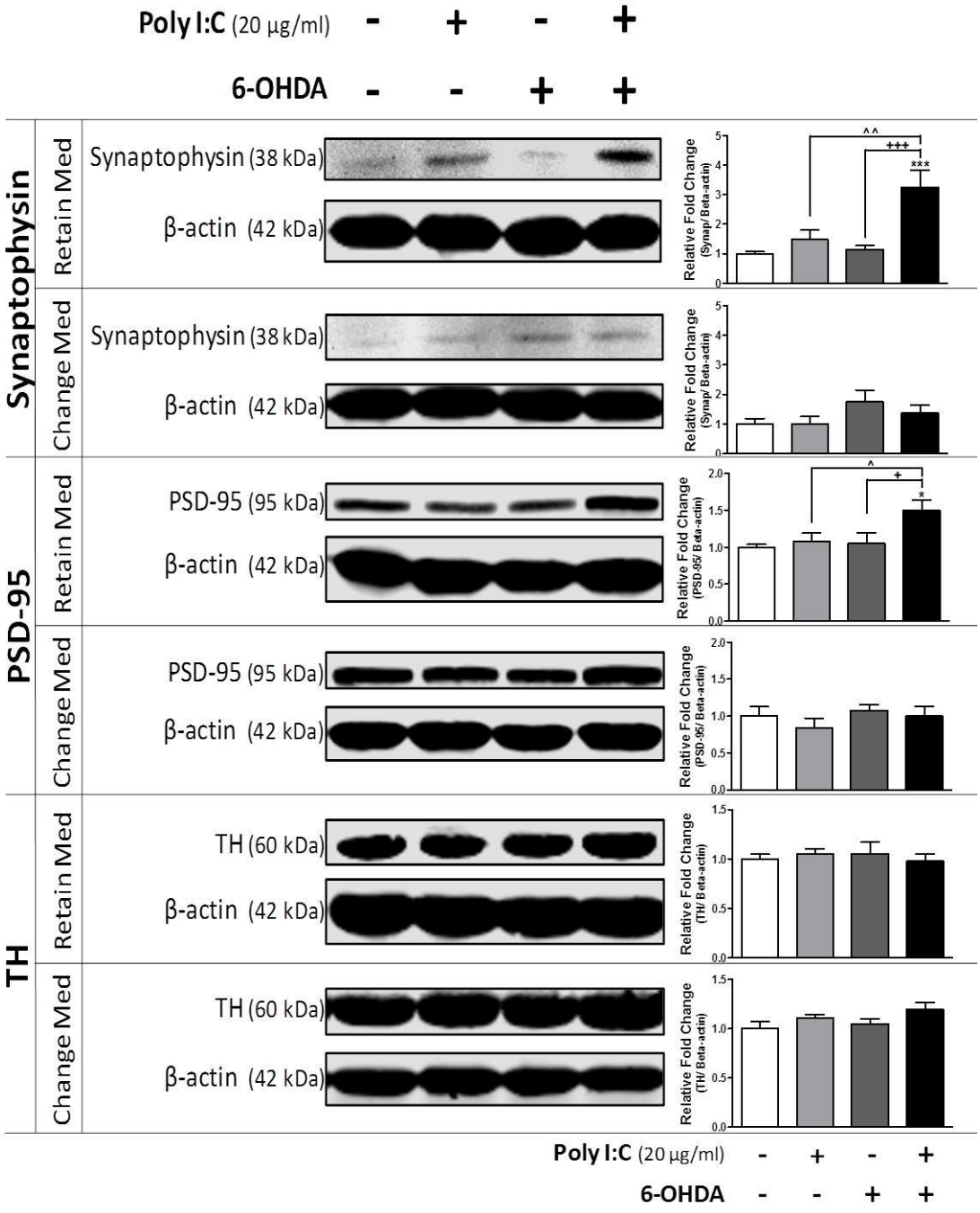

Figure 3.11. Poly I:C Priming 6-OHDA in SH-SY5Y Cells: Synaptic Related Protein Expression. SH-SY5Y cells were primed with poly I:C (20 µg/ml) for 24 hr prior to treatment with 6-OHDA (20 µM) for 24 hr. Cells were extracted, lysed, and probed for synapse related proteins. Data are presented as means and standard error of the means, and analysed using One-way ANOVA (followed by SNK *post-hoc* test). *$p < 0.05$ vs Control, ***$p < 0.001$ vs Control, ^$p < 0.05$ vs poly I:C, ^^$p < 0.01$ vs poly I:C, $^{+}p < 0.05$ vs 6-OHDA, $^{+++}p < 0.001$ vs 6-OHDA

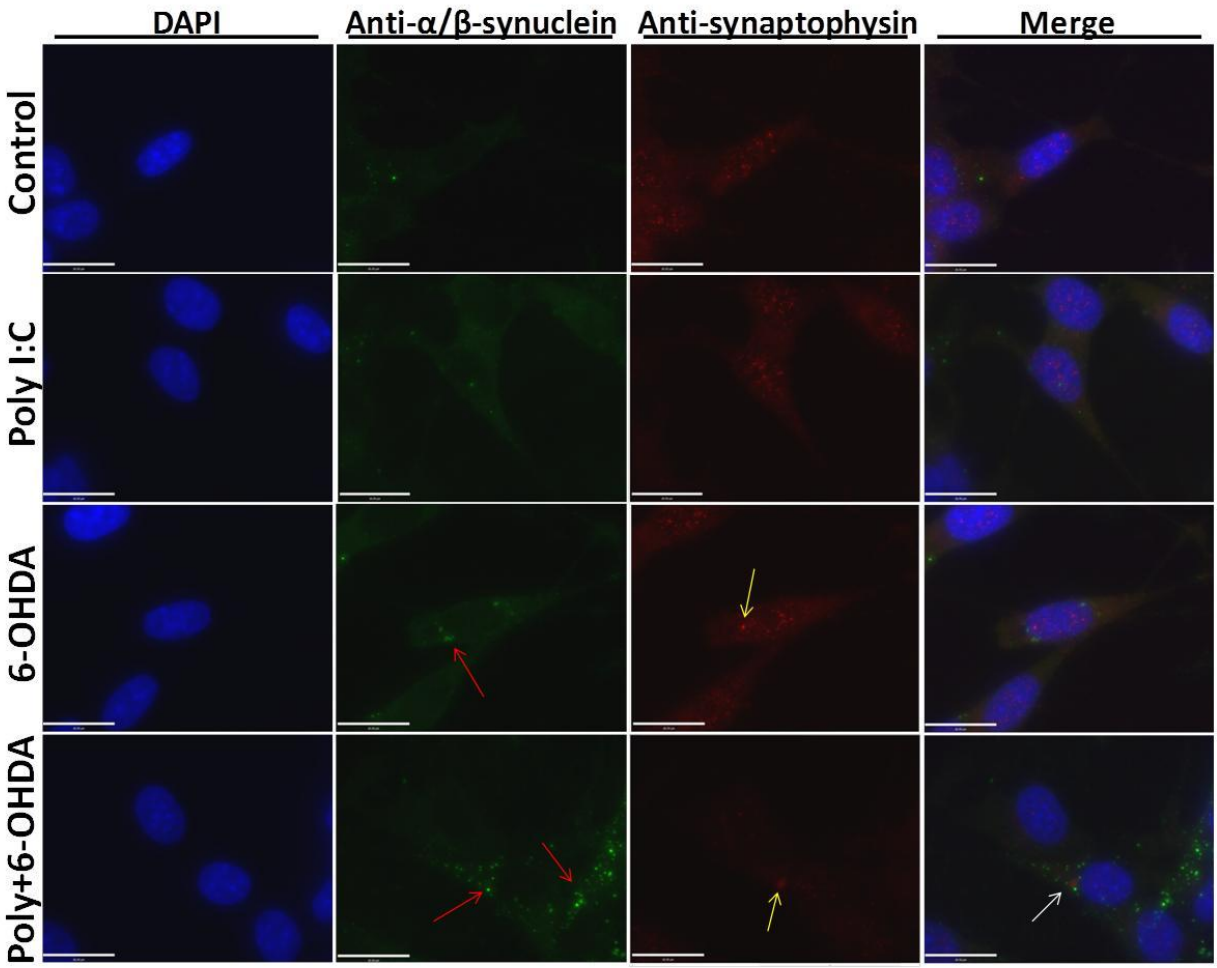

Figure 3.12. Poly I:C Priming 6-OHDA in SH-SY5Y Cells: Immunofluorescent α/β-synuclein. Poly I:C (20 µg/ml for 24 hr) primed cells were treated with 6-OHDA (20 µM) for 24 hr. The media was retained in between poly I:C and 6-OHDA treatment. After treatments, 4% PFA fixed cells were stained for α/β-synuclein (green), synaptophysin (red), and DAPI (blue). Qualitative immunocytochemistry images demonstrated some α/β inclusions after 6-OHDA treatment (red arrows), while the combination of poly I:C and 6-OHDA seemed to produce synaptophysin aggregates (yellow arrow) that co-localized with α/β-synuclein (white arrow). Scale bar = 18 µm.

3.4.4.2 Poly I:C Priming Modulates Rotenone Induced Changes in mRNA and Protein Expression

Similar to the poly I:C+6-OHDA experiments, SH-SY5Y cells were primed with poly I:C (20 µg/ml) for 24 hr before a 24 hr rotenone treatment (250 nM). Cells were extracted for mRNA or protein analysis via qPCR or Western Blot, respectively.

To investigate changes in apoptotic-like cell death, relative changes in protein markers related to apoptosis were examined via Western Blot (see Fig. 3.13). Treatment with poly I:C resulted an 18-fold increase in cleaved caspase-3 ($F_{(3,8)} = 17.9$, $p < 0.01$). *Post-hoc* analyses found this poly I:C mediated increase in cleaved caspase-3 to be significant ($p < 0.001$), but poly I:C priming in combination with rotenone only produced an 8-fold increase in cleaved caspase-3 that was not statistically different from the control group ($p > 0.05$). Changing the media previous to the rotenone treatment ($F_{(3,8)} = 48.2$, $p < 0.001$) reduced the relative increase in cleaved caspase-3 for poly I:C alone to only 6-fold ($p < 0.001$), with poly I:C priming in combination with rotenone reduced to 3-fold ($p < 0.01$). Relative changes in cleaved PARP were also measured (see Fig. 3.13). Although there was a significant difference between the poly I:C alone (1.5-fold vs control) treatment and the rotenone (0.5-fold vs control) treatment ($F_{(3,8)} = 5.9$, $p < 0.05$), no group demonstrated a significant change in cleaved PARP compared to the control group ($p > 0.05$). This was also true when the media was changed in between the poly I:C and rotenone treatment ($F_{(3,8)} = 3.7$, $p > 0.05$).

The autophagy pathway was also investigated to determine if poly I:C priming alters any rotenone induced changes in protein clearance or autophagy-mediated cell death prevention (see Fig. 3.14). Poly I:C treatment seemed to reduce the relative expression of LC3-a/b-I ($F_{(3,8)} = 9.9$, $p < 0.01$), with a 0.3-fold reduction after poly I:C alone ($p < 0.05$) and poly I:C priming rotenone ($p < 0.05$) treatments. Interestingly, poly

I:C did not seem to have any effect on the expression of the activated isoform LC3-a/b-II ($F_{(3,8)}$ = 2.0, p > 0.05). There were no significant changes in LC3-a/b-I ($F_{(3,8)}$ = 1.5, p > 0.05) or LC3-a/b-II ($F_{(3,8)}$ = 1.1, p > 0.05) when the media was changed in between poly I:C and rotenone treatments. Similar to LC3-a/b-I, poly I:C reduced the relative expression of p62 ($F_{(3,8)}$ = 5.8, p < 0.05). Although SNK *post-hoc* tests found no significant differences in any of the groups compared to the control group (p > 0.05), the slight increase in p62 after rotenone treatment (1.3-fold) was significantly reduced when poly I:C priming was introduced (0.7-fold, p < 0.05). This trend of a rotenone induced increase in p62 (1.3-fold), with a reducing poly I:C priming effect (0.7-fold), was maintained when the media was changed in between treatments (see Fig. 3.14), but was not found to be significant ($F_{(3,8)}$ = 3.1, p > 0.05).

Synaptic integrity after poly I:C priming was examined by measuring mRNA and protein expression for specific synapse-related markers. Relative PSD-95 expression was upregulated at the mRNA ($F_{(3,8)}$ = 9.1, p < 0.01) and protein ($F_{(3,20)}$ = 4.7, p < 0.05) level after poly I:C priming (see Fig. 3.15 and Fig. 3.16), with a 3.6-fold increase at the mRNA level and a 1.9-fold increase at the protein level. Although there was a trend for poly I:C to decrease TH mRNA (0.2-fold) and increase TH protein expression (1.9-fold), these trends only approach statistical significance (TH mRNA ($F_{(3,8)}$ = 3.5, p = 0.068) andTH protein ($F_{(3,20)}$ = 2.9, p = 0.061). This trend was not seen when the media was changed in between treatments ($F_{(3,20)}$ = 1.3, p > 0.05). Although poly I:C priming had no effect on relative synaptopysin mRNA expression ($F_{(3,8)}$ = 3.1, p > 0.05), poly I:C alone treatment was found to reduce protein expression by 0.3-fold ($F_{(3,20)}$ = 6.1, p < 0.01). Qualitative immunostaining for synaptophysin didn't suggest any changes in protein localisation after poly I:C treatment, but poly I:C priming in combination with rotenone appeared to induce synaptophysin inclusions (see Fig. 3.17). Although the One-

way ANOVA reported significant changes in α-synuclein mRNA expression due to treatment group ($F_{(3,8)} = 4.161$, $p < 0.05$), SNK *post-hoc* analysis found no significant changes in relative expression between any of the groups ($p > 0.05$). However, immunostaining for α/β-synuclein found protein inclusions developing in the synaptic terminal region of some cells, including some localisation with synaptophysin inclusions (see Fig. 3.17).

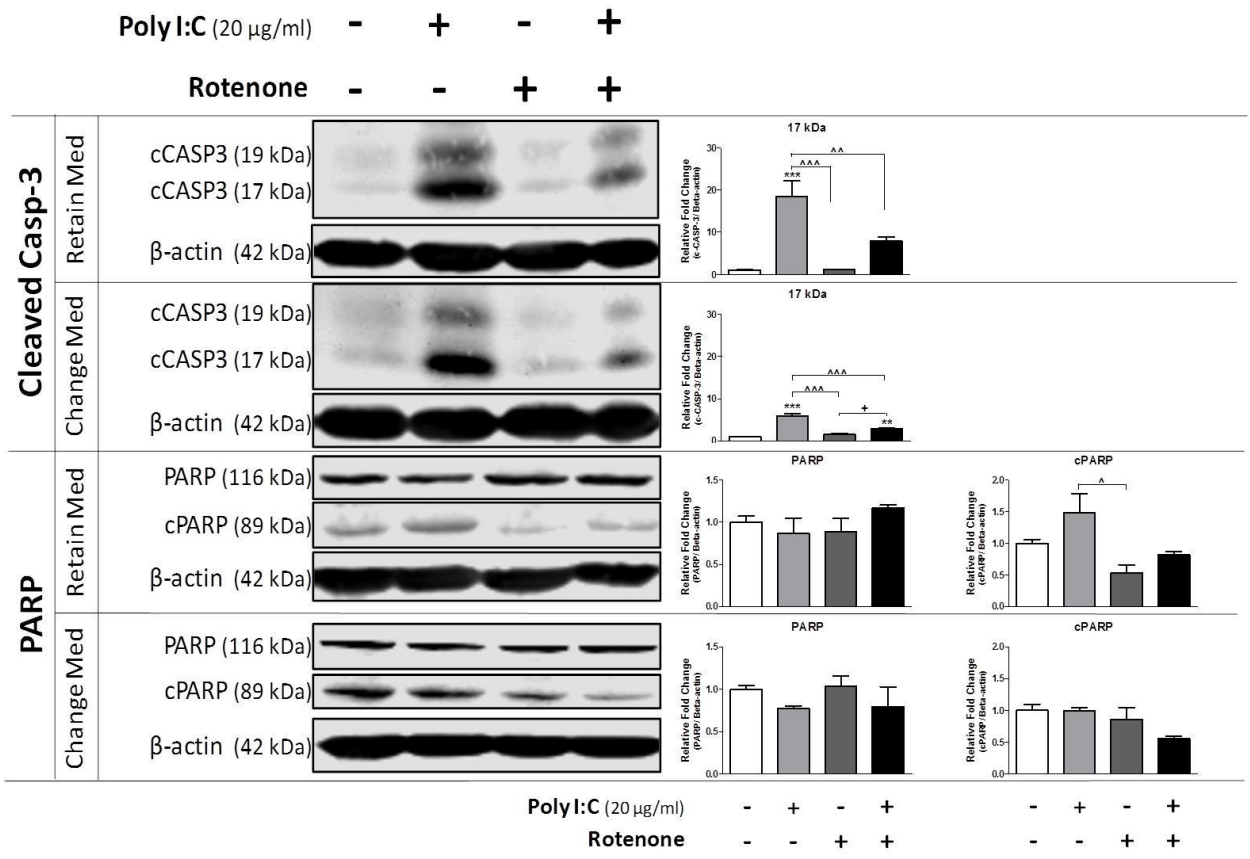

Figure 3.13. Poly I:C Priming Rotenone in SH-SY5Y Cells: Apoptotic Related Protein Expression. SH-SY5Y cells were primed with poly I:C (20 µg/ml) for 24 hr prior to treatment with rotenone (250 nM) for 24 hr. Cells were extracted, lysed, and probed for apoptotic related proteins. Data are presented as means and standard error of the means, and analysed using One-way ANOVA (followed by SNK *post-hoc* test). **p < 0.01 vs Control, ***p < 0.001 vs Control, ^p < 0.05 vs poly I:C, ^^p < 0.01 vs poly I:C, ^^^p < 0.001 vs poly I:C, $^{+}$p < 0.05 vs rotenone

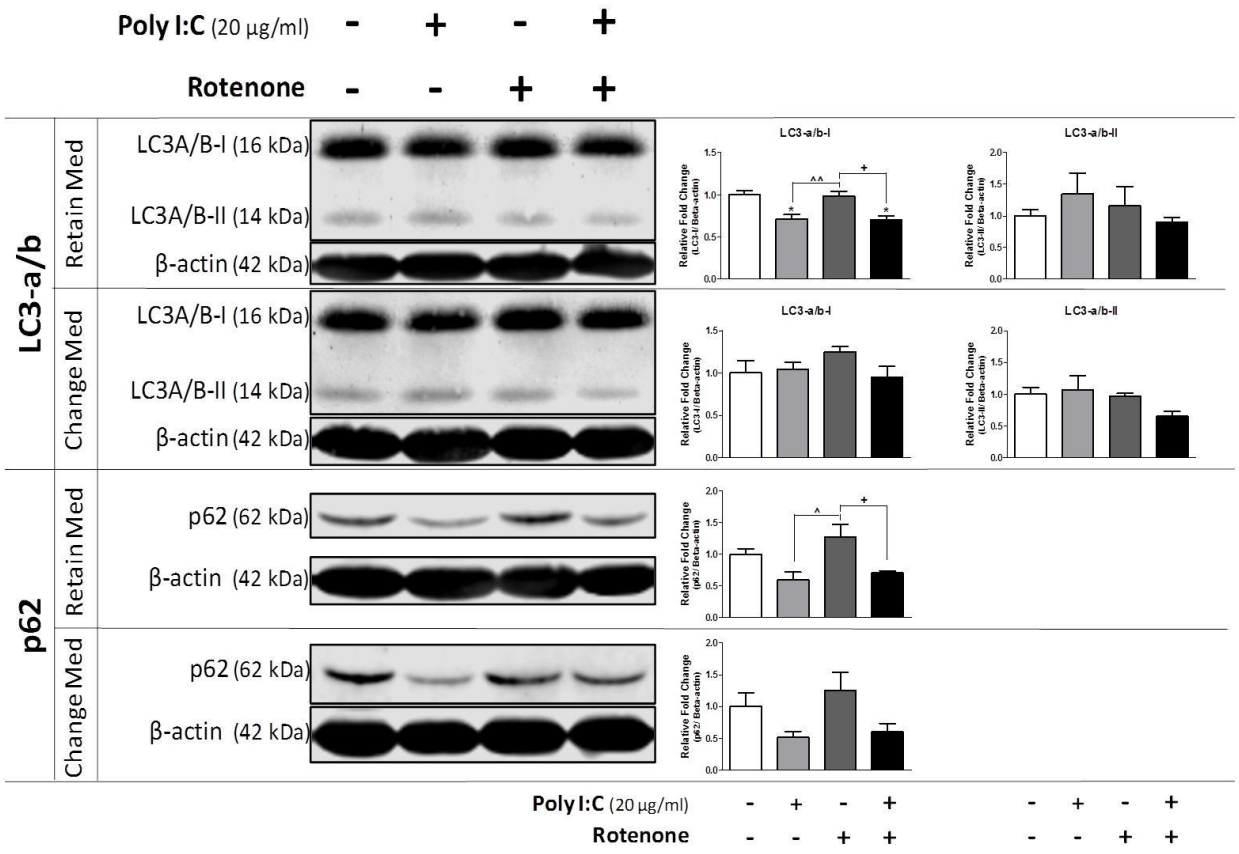

Figure 3.14. Poly I:C Priming Rotenone in SH-SY5Y Cells: Autophagy Related Protein Expression. SH-SY5Y cells were primed with poly I:C (20 µg/ml) for 24 hr prior to treatment with rotenone (250 nM) for 24 hr. Cells were extracted, lysed, and probed for autophagy related proteins. Data are presented as means and standard error of the means, and analysed using One-way ANOVA (followed by SNK *post-hoc* test). *$p < 0.05$ vs Control, ^$p < 0.05$ vs poly I:C, ^^$p < 0.01$ vs poly I:C, $^{+}p < 0.05$ vs rotenone

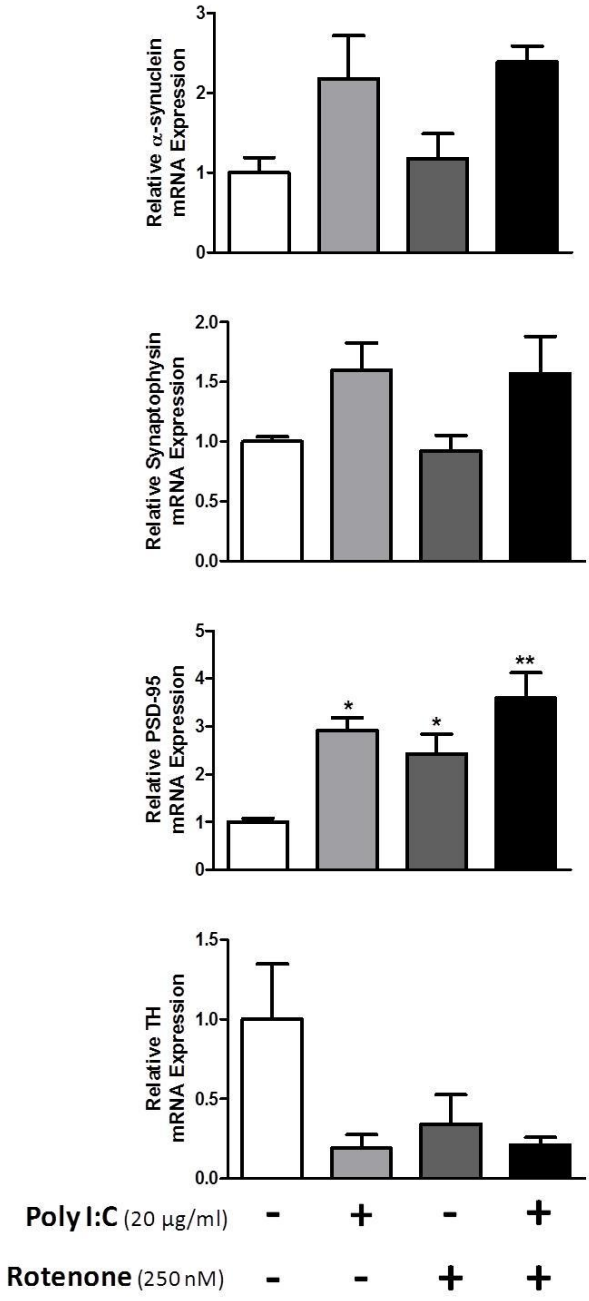

Figure 3.15. Poly I:C Priming Rotenone in SH-SY5Y Cells: Synaptic Related mRNA Expression. SH-SY5Y cells were primed with poly I:C (20 µg/ml) for 24 hr prior to treatment with rotenone (250 nM) for 24 hr. The media was retained in between poly I:C and rotenone treatment. Cells were extracted, lysed for mRNA, and probed with synapse related primers. Data are presented as means and standard error of the means, and analysed using One-way ANOVA (followed by SNK *post-hoc* test). *$p < 0.05$ vs Control, **$p < 0.01$ vs Control

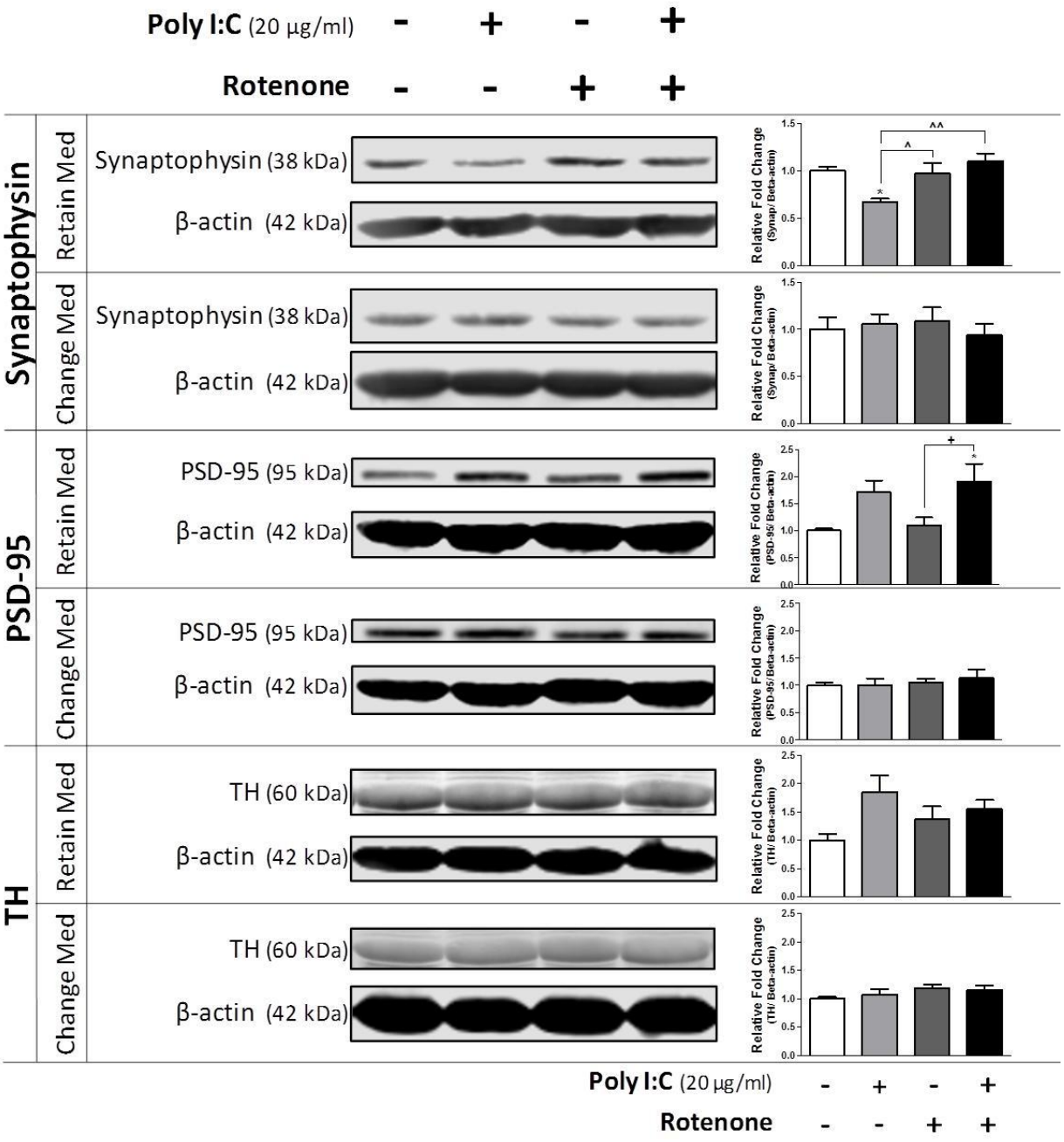

Figure 3.16. Poly I:C Priming Rotenone in SH-SY5Y Cells: Synaptic Related Protein Expression. SH-SY5Y cells were primed with poly I:C (20 µg/ml) for 24 hr prior to treatment with rotenone (250 nM) for 24 hr. Cells were extracted, lysed, and probed for synapse related proteins. Data are presented as means and standard error of the means, and analysed using One-way ANOVA (followed by SNK *post-hoc* test). *$p < 0.05$ vs Control, ^$p < 0.05$ vs poly I:C, ^^$p < 0.01$ vs poly I:C, $^{+}p < 0.05$ vs rotenone

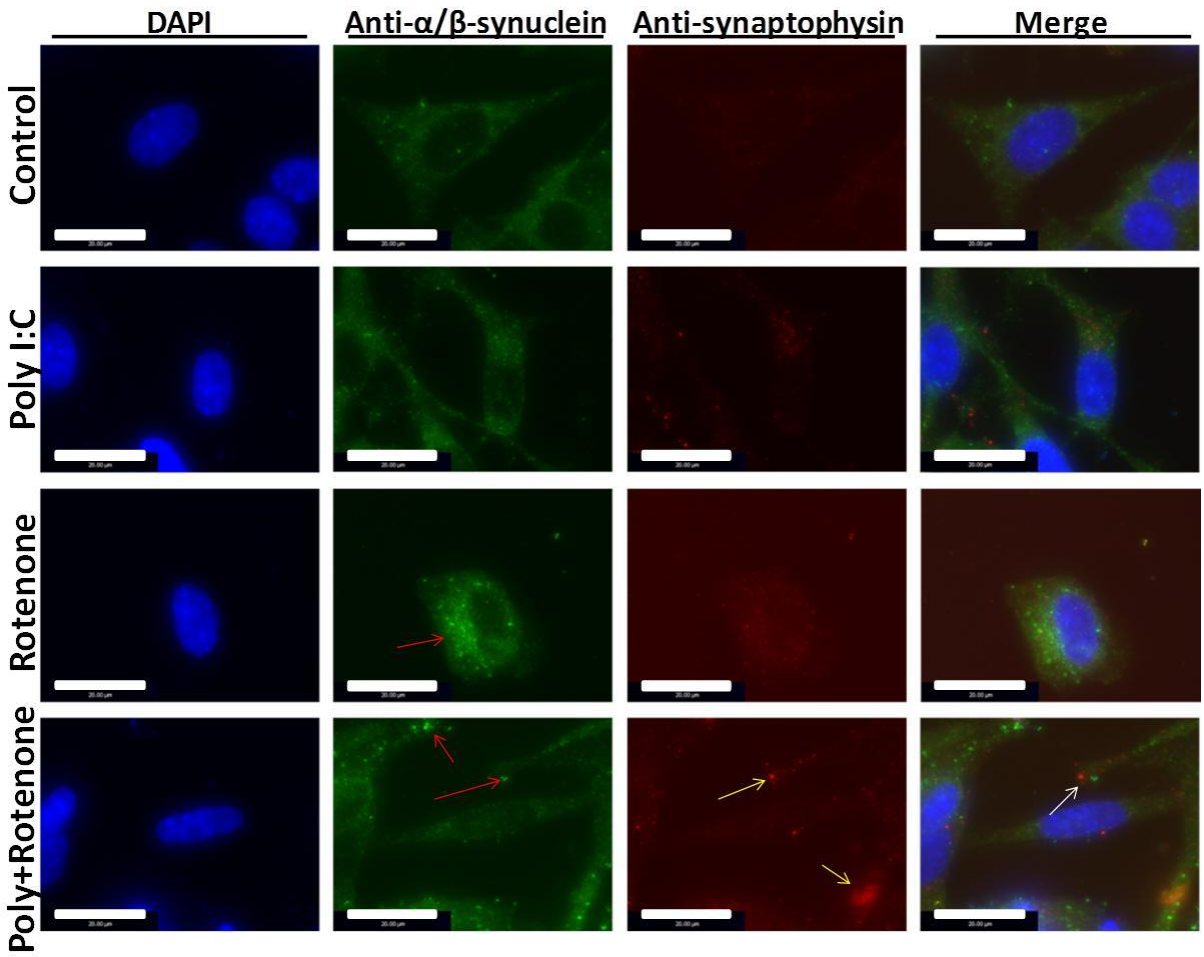

Figure 3.17. Poly I:C Priming Rotenone in SH-SY5Y Cells: Immunofluorescent α/β-synuclein. Cells were treated with poly I:C (20 µg/ml) for 24 hr preceding a 24 hr rotenone treatment (250 nM). The media was retained in between poly I:C and rotenone treatment. After treatments, cells were fixed with 4% PFA and stained for α/β-synuclein (green), synaptophysin (red), and DAPI (blue). Protein inclusions of α/β-synuclein (red arrows) and synaptophysin (yellow and white arrows) were found. Scale bar = 20 µm.

3.4.4.3 Poly I:C Priming Modulates MPP^+ Induced Changes in mRNA and Protein Expression

After poly I:C priming (20 µg/ml for 24 hr), SH-SY5Y cells were treated with MPP^+ (1 mM) for 24 hr. Cells were extracted for protein and mRNA expression quantification, which was measured by Western Blot and qPCR, respectively.

Extracted protein from the treated cells was examined for changes in apoptotic related proteins (see Fig. 3.18). Consistent with previous experiments, poly I:C treatment increased relative cleaved caspase-3 expression ($F_{(3,8)} = 25.3$, $p < 0.001$). Alone, poly I:C induced a 13-fold increase in cleaved caspase-3 ($p < 0.001$), while poly I:C priming with MPP^+ resulted in an 11-fold increase ($p < 0.01$). Interestingly, changing the media after poly I:C priming did not drastically alter the poly I:C priming effect on cleaved caspase-3 ($F_{(3,8)} = 37.1$, $p < 0.001$), with a 10-fold increase ($p < 0.001$). Very similar to the cleaved caspase-3 findings, poly I:C increased relative cleaved PARP expression ($F_{(3,8)} = 35.8$, $p < 0.001$), with a 2.3-fold increase after poly I:C treatment ($p < 0.001$) and a 1.5-fold increase after poly I:C priming was combined with MPP^+ ($p < 0.05$). Surprisingly, changing the media in between treatments exacerbated the poly I:C (4.4-fold, $p < 0.01$) and poly I:C priming with MPP^+ (6.1-fold increase, $p < 0.001$) effect on cleaved PARP expression ($F_{(3,8)} = 24.9$, $p < 0.001$).

Probing for autophagy related proteins was used to determine any significant changes due to poly I:C priming. There was a significant change in relative LC3-a/b-II expression ($F_{(3,8)} = 4.1$, $p < 0.05$). The active form of LC3-a/b-II was decreased after MPP^+ treatment (0.5-fold, $p < 0.05$). MPP^+ decreased LC3-a/b-II to a similar degree (0.6-fold) when the media was changed (see Fig. 3.19), but this did not reach statistical significance ($F_{(3,8)} = 1.1$, $p > 0.05$). Conversely, neither poly I:C nor MPP^+ had a significant effect on LC3-a/b-I when the media was retained ($F_{(3,8)} = 3.9$, $p > 0.05$) or

when the media was changed ($F_{(3,8)}$ = 1.6, $p > 0.05$) in between treatments. Although poly I:C priming had no effect on LC3-a/b-I/II, priming before MPP^+ treatment produced a drastic increase (3.6-fold, $p < 0.05$) in relative p62 expression ($F_{(3,8)}$ = 5.1, $p < 0.05$). Changing the media in between treatments did not change the pattern of increased p62 expression for the group primed with poly I:C previous to MPP^+ treatment, but the increase in relative p62 was twice as drastic (8.9-fold, $p < 0.05$) in this experimental condition ($F_{(3,8)}$ = 5.9, $p < 0.05$).

To investigate synaptic alterations due to poly I:C priming with MPP^+, relative mRNA and protein expression was measured. Similar to previous experiments, poly I:C was found to reduce relative TH mRNA expression by 0.7-fold (see Fig. 3.20), but this trend did not reach statistical significance in this experiment ($F_{(3,8)}$ = 2.6, $p > 0.05$). Also, relative TH protein was not found to significantly change based on poly I:C or MPP^+ treatment ($F_{(3,20)}$ = 1.3, $p > 0.05$), including when the media was changed in between treatments ($F_{(3,20)}$ = 0.2, $p > 0.05$). Poly I:C priming before MPP^+ treatment (but not poly I:C or MPP^+ alone) seemed to modulate the relative expression level of multiple mRNA transcripts, namely PSD-95 ($F_{(3,8)}$ = 16.3, $p < 0.01$), α-synuclein ($F_{(3,8)}$ = 36.9, $p < 0.001$), and synaptophysin ($F_{(3,8)}$ = 14.5, $p < 0.01$). Poly I:C priming led to a 6.3-fold increase in relative PSD-95 mRNA ($p < 0.001$). This trend for PSD-95 mRNA is consistent with the results for PSD-95 protein ($F_{(3,20)}$ = 3.4, $p < 0.05$), with a 1.4-fold increase in relative PSD-95 (see Fig. 3.21). Changing the media did not alter the poly I:C priming effect on PSD-95 expression ($F_{(3,20)}$ = 4.1, $p < 0.05$). Conversely, the significant 2.6-fold increase in synaptophysin mRNA after poly I:C priming ($p < 0.01$) was not seen at the protein level (see Fig. 3.21). Instead, poly I:C priming of MPP^+ induced a drastic 0.7-fold decrease in relative synaptophysin protein levels ($F_{(3,20)}$ = 7.4, $p < 0.01$). The decrease in synaptophysin was unique to the group which received poly I:C priming and

MPP^+ since there was no significant decrease after poly I:C (0.8-fold, $p > 0.05$) or MPP^+ (0.9-fold, $p > 0.05$) treatment. Although a statistically significant effect was found for synaptophysin protein for the experimental condition in which the media is changed ($F_{(3,20)} = 4.1$, $p < 0.05$), SNK *post-hoc* analysis found no group differences in relative protein expression ($p > 0.05$). The opposing findings for synaptophysin mRNA and protein levels seems counter-intuitive, but immunostaining suggests that poly I:C priming with MPP^+ induces excessive synaptophysin aggregation (see Fig. 3.22). Unlike the 3.9-fold increase in α-synuclein mRNA expression ($p < 0.001$), poly I:C priming with MPP^+ did not seem to change α/β-synuclein cellular localisation (see Fig. 3.22).

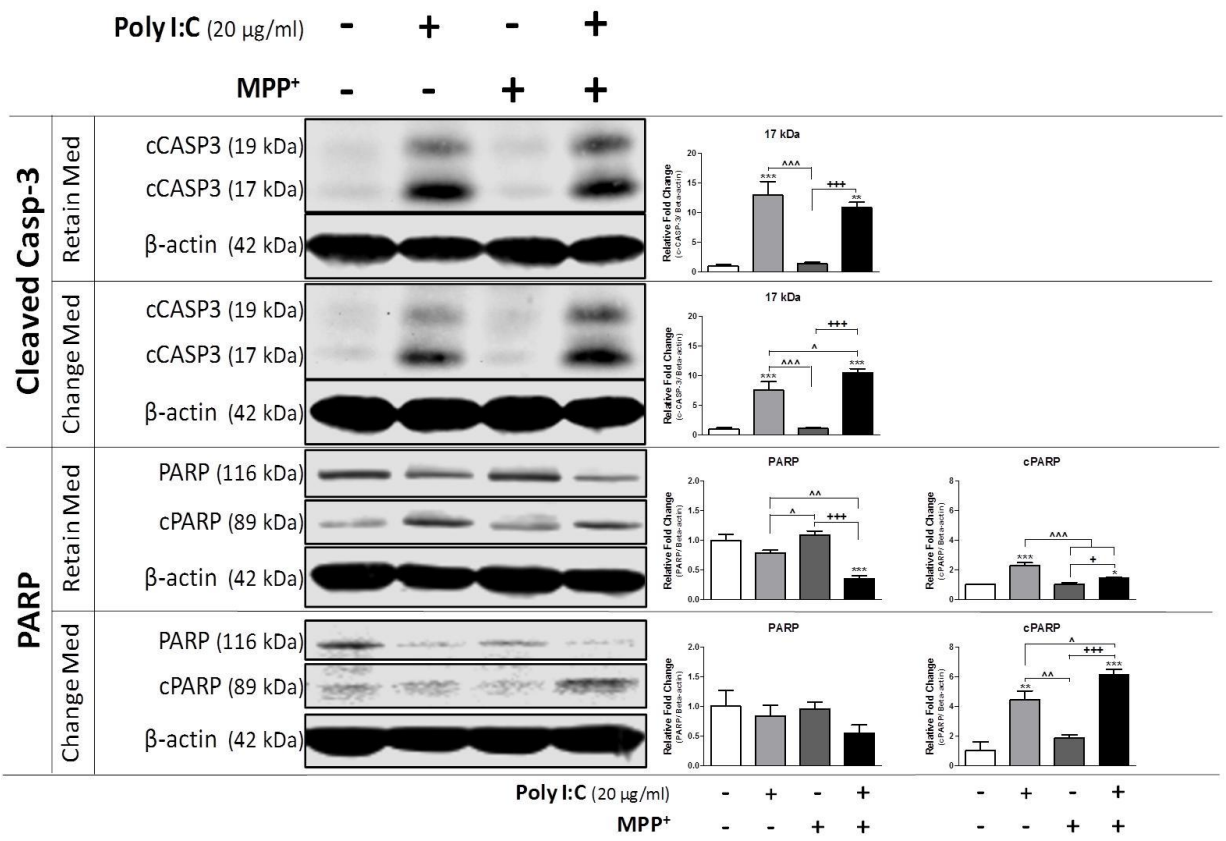

Figure 3.18. Poly I:C Priming MPP^+ in SH-SY5Y Cells: Apoptotic Related Protein Expression. SH-SY5Y cells were primed with poly I:C (20 µg/ml) for 24 hr prior to treatment with MPP^+ (1 mM) for 24 hr. Cells were extracted, lysed, and probed for apoptotic related proteins. Data are presented as means and standard error of the means, and analysed using One-way ANOVA (followed by SNK *post-hoc* test). *$p < 0.05$ vs Control, **$p < 0.01$ vs Control, ***$p < 0.001$ vs Control, ^$p < 0.05$ vs poly I:C, ^^$p < 0.01$ vs poly I:C, ^^^$p < 0.001$ vs poly I:C, $^{+}p < 0.05$ vs MPP^+, $^{+++}p < 0.001$ vs MPP^+

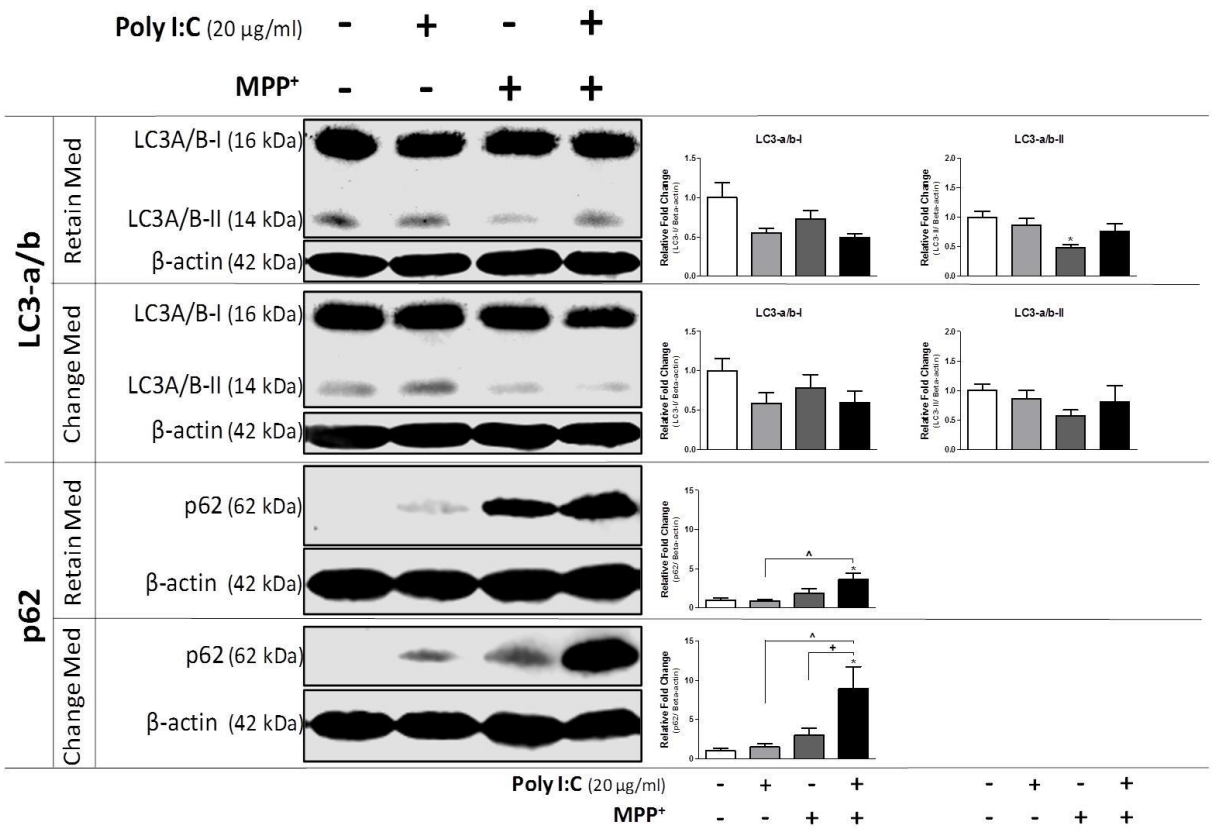

Figure 3.19. Poly I:C Priming MPP$^+$ in SH-SY5Y Cells: Autophagy Related Protein Expression. SH-SY5Y cells were primed with poly I:C (20 µg/ml) for 24 hr prior to treatment with MPP$^+$ (1 mM) for 24 hr. Cells were extracted, lysed, and probed for autophagy related proteins. Data are presented as means and standard error of the means, and analysed using One-way ANOVA (followed by SNK *post-hoc* test). *$p < 0.05$ vs Control, ^$p < 0.05$ vs poly I:C, $^+p < 0.05$ vs MPP$^+$

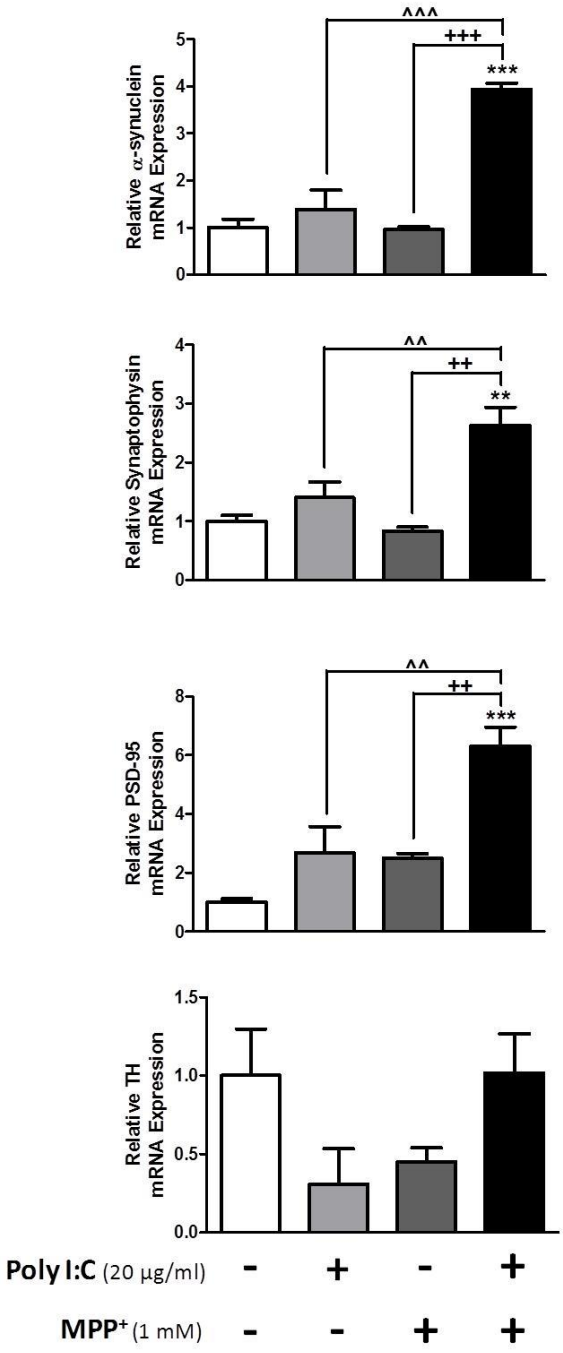

Figure 3.20. Poly I:C Priming MPP^+ in SH-SY5Y Cells: Synaptic Related mRNA Expression. SH-SY5Y cells were primed with poly I:C (20 µg/ml) for 24 hr prior to treatment with MPP^+ (1 mM) for 24 hr. The media was retained in between poly I:C and MPP^+ treatment. Cells were extracted, lysed for mRNA, and probed with synapse related primers. Data are presented as means and standard error of the means, and analysed using One-way ANOVA (followed by SNK *post-hoc* test). **$p < 0.01$ vs Control, ***$p < 0.001$ vs Control, ^^$p < 0.01$ vs poly I:C, ^^^$p < 0.001$ vs poly I:C, $^{++}p < 0.01$ vs MPP^+, $^{+++}p < 0.001$ vs MPP^+

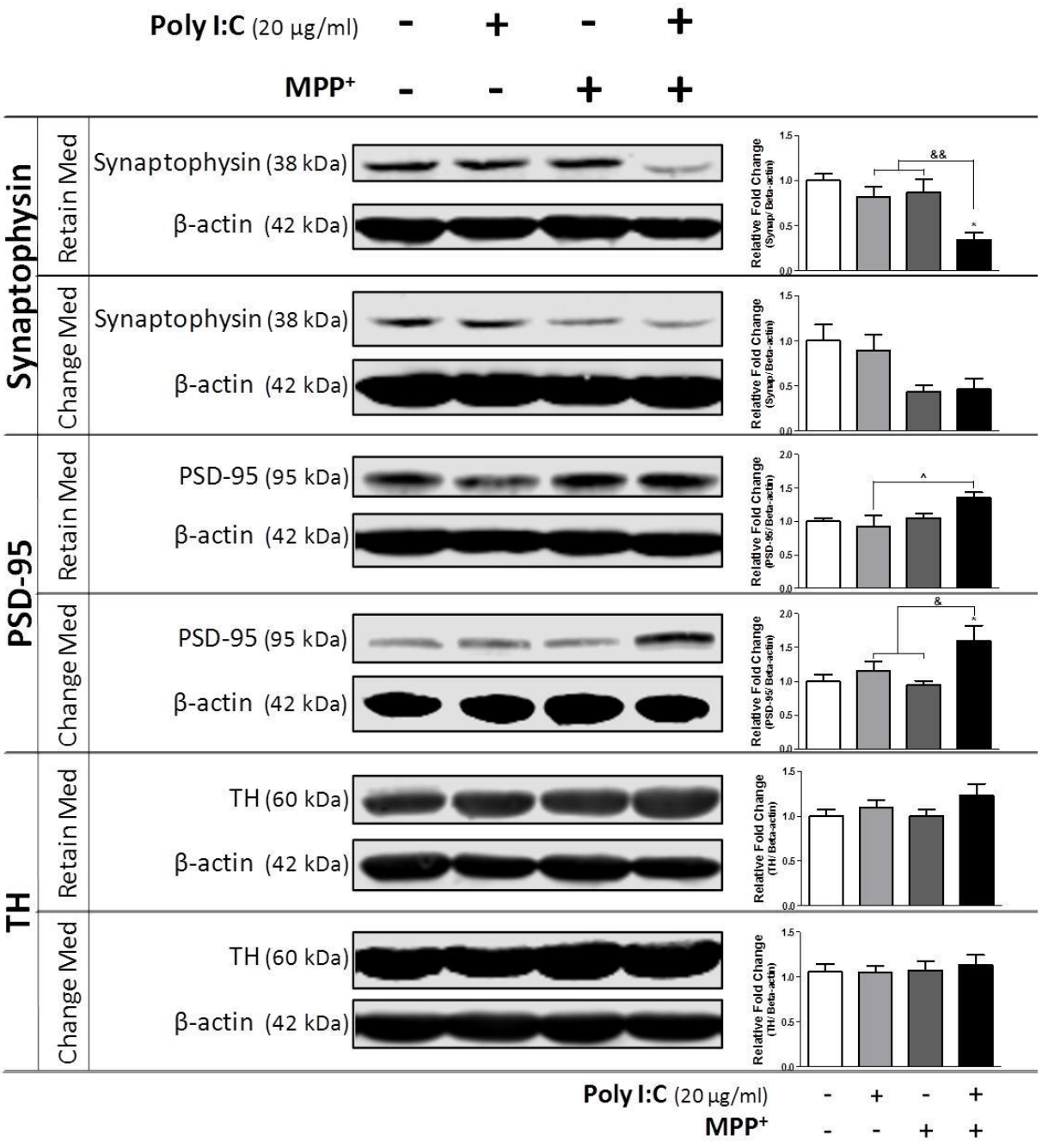

Figure 3.21. Poly I:C Priming MPP^+ in SH-SY5Y Cells: Synaptic Related Protein Expression. SH-SY5Y cells were primed with poly I:C (20 µg/ml) for 24 hr prior to treatment with MPP^+ (1 mM) for 24 hr. Cells were extracted, lysed, and probed for synapse related proteins. Data are presented as means and standard error of the means, and analysed using One-way ANOVA (followed by SNK *post-hoc* test). *$p < 0.05$ vs Control, ^$p < 0.05$ vs poly I:C, $^{\&}p < 0.05$ vs poly+MPP^+, $^{\&\&}p < 0.01$ vs poly+MPP^+

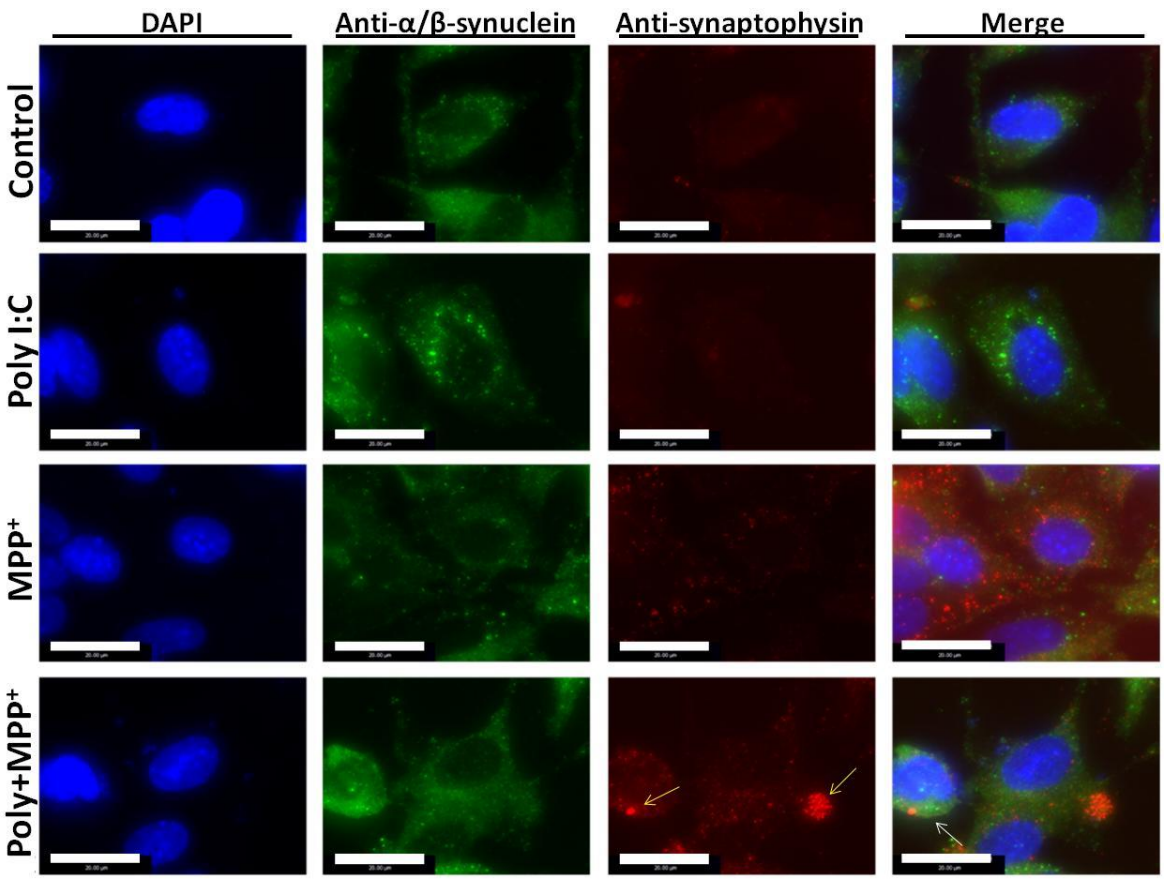

Figure 3.22. Poly I:C Priming MPP^+ in SH-SY5Y Cells: Immunofluorescent α/β-synuclein. Cells were treated with poly I:C (20 µg/ml) for 24 hr, followed by a 24 hr MPP^+ treatment (1 mM). The media was retained in between poly I:C and MPP^+ treatment. After treatments, cells were fixed with 4% PFA and stained for α/β-synuclein (green), synaptophysin (red), and DAPI (blue). Large synaptophysin protein inclusions (yellow and white arrows) were found. Scale bar = 20 µm.

3.4.4.4 Poly I:C Priming Modulates FN075 Induced Changes in mRNA and Protein Expression

SH-SY5Y cells were treated with FN075 for 48 hr after priming with poly I:C (20 µg/ml) for 24 hr. Extracted cells were lysed and used for molecular analysis. Autophagy, apoptotic, and synapse related proteins were probed using Western Blot, while synapse related mRNA transcripts were examined using qPCR.

Apoptotic related cell death proteins were modulated by cell treatment (see Fig. 3.23). Consistent with all other experimental conditions, poly I:C increased relative cleaved caspase-3 expression ($F_{(3,8)} = 19.3$, $p < 0.01$). Poly I:C alone resulted in a 12-fold increase in cleaved caspase-3 ($p < 0.001$), while poly I:C priming in combination with FN075 resulted in only a 6-fold increase in cleaved caspase-3 ($p < 0.05$). Similar to all previous experiments, changing the media in between treatments did not alter the effect of poly I:C ($F_{(3,8)} = 44.9$, $p < 0.001$), with poly I:C alone increasing relative cleaved caspase-3 9-fold ($p < 0.001$) and poly I:C priming increasing cleaved caspase-3 7-fold ($p < 0.001$). Conversely, neither poly I:C nor FN075 altered relative cleaved PARP ($F_{(3,8)} = 2.3$, $p > 0.05$) or PARP expression ($F_{(3,8)} = 0.8$, $p > 0.05$). This was also true when the media was changed in between treatments (cleaved PARP ($F_{(3,8)} = 1.6$, $p > 0.05$) and PARP ($F_{(3,8)} = 1.5$, $p > 0.05$).

Lysed cells were also examined for autophagy related proteins. Poly I:C was found to have an effect on relative LC3-a/b-I ($F_{(3,8)} = 6.8$, $p < 0.05$) and LC3-a/b-II ($F_{(3,8)} = 13.1$, $p < 0.01$) expression (see Fig. 3.24). Poly I:C alone was found to reduce relative LC3-a/-I (0.5-fold, $p < 0.05$) and LC3-a/b-II (0.7-fold, $p < 0.05$) expression. LC3-a/b-I (0.6-fold, $p < 0.05$) and LC3-a/b-II (0.6-fold, $p < 0.05$) expression was also reduced with poly I:C priming of FN075. Changing the media before FN075 treatment did not alter the effect of poly I:C on LC3-a/b-II ($F_{(3,8)} = 8.6$, $p < 0.001$) expression but did aberrate

the changes seen in LC3-a/b-I ($F_{(3,8)} = 0.8$, $p > 0.05$). FN075 treatment increased relative p62 expression by 2.6-fold ($F_{(3,8)} = 22.7$, $p < 0.001$). Poly I:C priming before FN075 treatment (1.1-fold, $p > 0.05$) attenuated this FN075 induced increase (2.6-fold, $p < 0.001$) in p62 (see Fig. 3.24).

Synapse dysfunction was then investigated in poly I:C primed cells. As expected, FN075 induced α-synuclein aggregate inclusions (see Fig. 3.27). This aggregation is likely a direct effect of FN075, since α-synuclein mRNA levels did not change due to FN075 treatment ($F_{(3,8)} = 0.5$, $p > 0.05$). As measured by qPCR (see Fig. 3.25), FN075 induced α-synuclein aggregates resulted in a 3.2-fold increase in relative TH mRNA ($F_{(3,8)} = 16.8$, $p < 0.01$). Although poly I:C priming with FN075 did not change TH mRNA expression ($p > 0.05$), priming did significantly increase TH protein expression ($F_{(3,20)} = 7.6$, $p < 0.01$). Priming resulted in a 1.5-fold increase in TH (see Fig. 3.26), which was attenuated when the media was changed in between treatments ($F_{(3,20)} = 0.3$, $p > 0.05$). Although poly I:C (2.3-fold, $p < 0.05$) and poly I:C priming of FN075 (2.8-fold, $p < 0.05$) resulted in an increase in PSD-95 mRNA ($F_{(3,8)} = 7.5$, $p < 0.05$), only poly I:C priming produced a 1.5-fold increase in relative PSD-95 protein levels ($F_{(3,20)} = 4.6$, $p < 0.05$). No changes in PSD-95 were found when the media was changed in between treatments ($F_{(3,20)} = 0.3$, $p > 0.05$). Similar to the effects of poly I:C priming in combination with MPP^+, priming in combination with FN075 led to a 2-fold increase ($p < 0.05$) in relative synaptophysin mRNA ($F_{(3,8)} = 4.7$, $p < 0.05$), but a 0.8-fold ($p < 0.001$) decrease in synaptophysin protein ($F_{(3,20)} = 16.6$, $p < 0.001$). Changing media in between treatments attenuated this decrease in synaptophysin ($F_{(3,20)} = 0.2$, $p > 0.05$). Although not as excessive, qualitative immunostaining resulted in some synaptophysin aggregation (see Fig. 3.27).

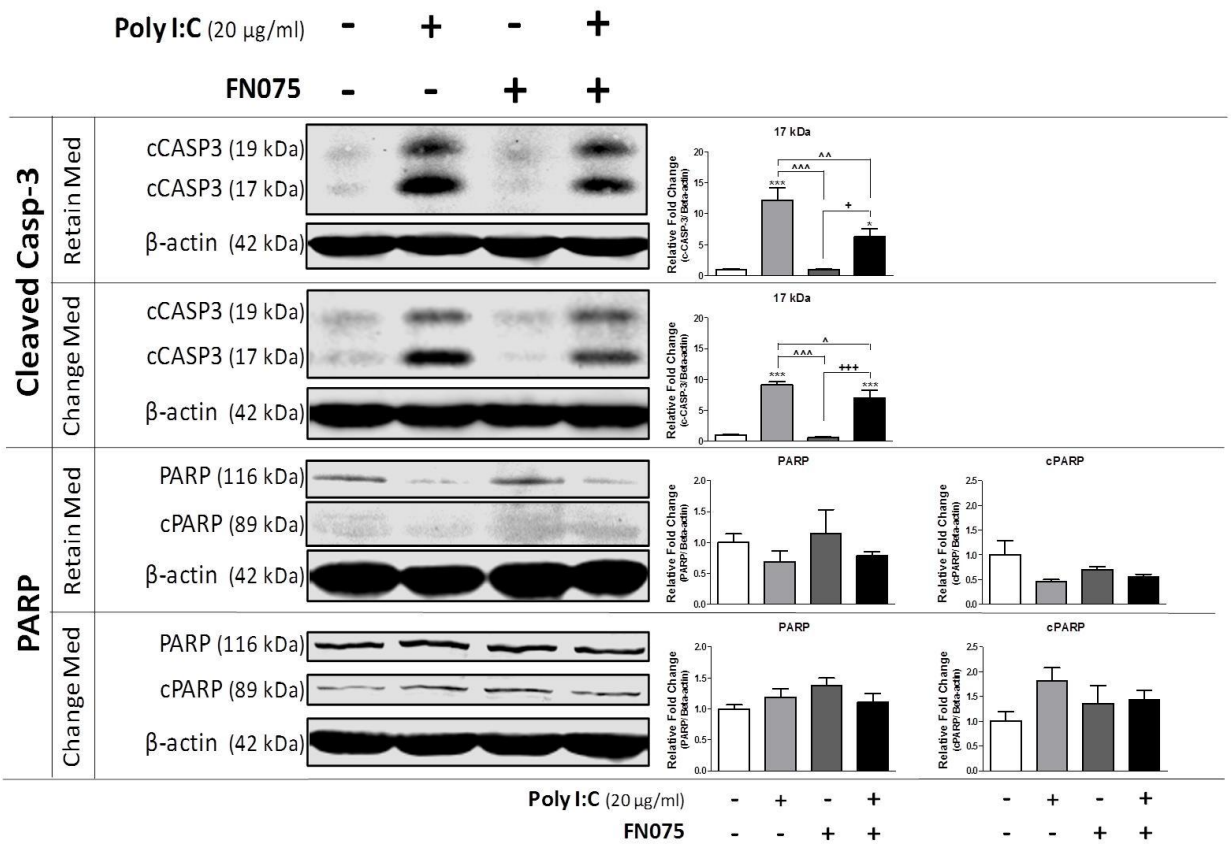

Figure 3.23. Poly I:C Priming FN075 in SH-SY5Y Cells: Apoptotic Related Protein Expression. SH-SY5Y cells were primed with poly I:C (20 µg/ml) for 24 hr prior to treatment with FN075 (25 µM) for 48 hr. Cells were extracted, lysed, and probed for apoptotic related proteins. Data are presented as means and standard error of the means, and analysed using One-way ANOVA (followed by SNK *post-hoc* test). *$p < 0.05$ vs Control, ***$p < 0.001$ vs Control, ^$p < 0.05$ vs poly I:C, ^^$p < 0.01$ vs poly I:C, ^^^$p < 0.001$ vs poly I:C, $^{+}p < 0.05$ vs FN075, $^{+++}p < 0.001$ vs FN075

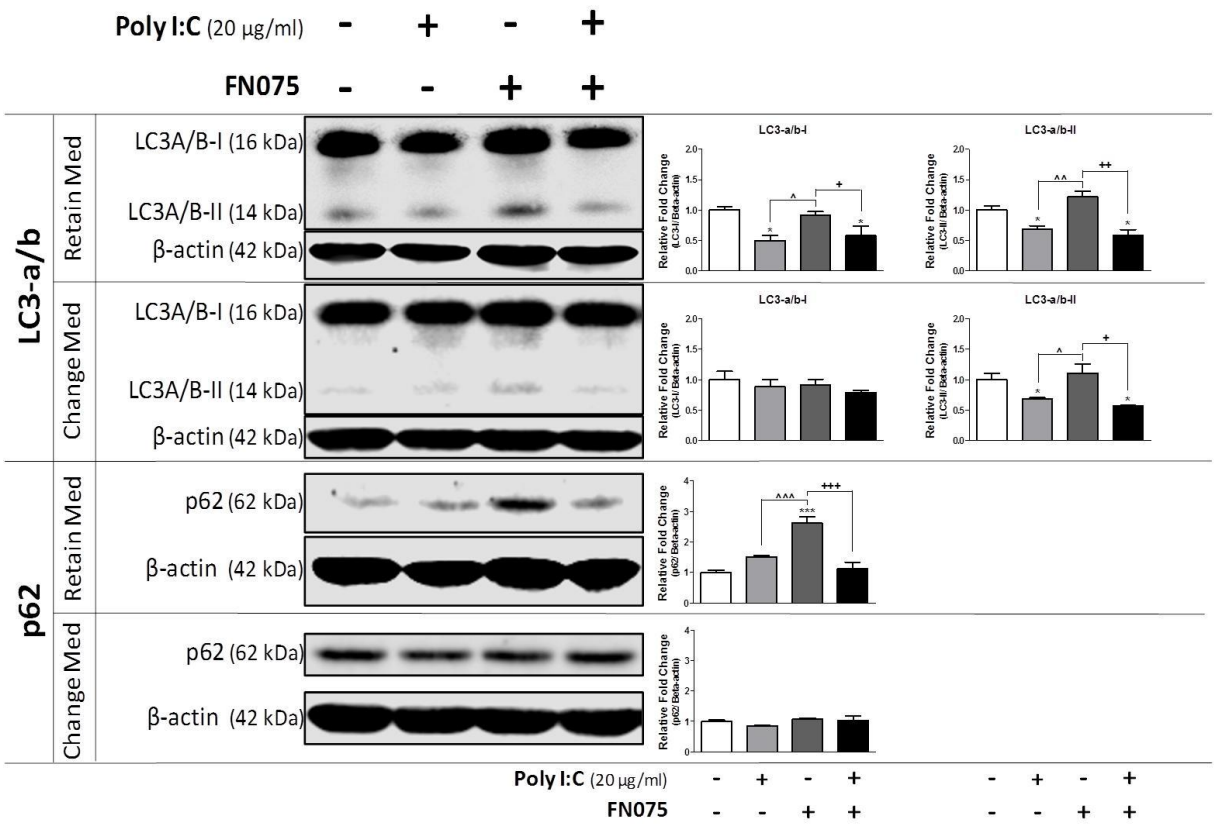

Figure 3.24. Poly I:C Priming FN075 in SH-SY5Y Cells: Autophagy Related Protein Expression. SH-SY5Y cells were primed with poly I:C (20 µg/ml) for 24 hr prior to treatment with FN075 (25 µM) for 48 hr. Cells were extracted, lysed, and probed for autophagy related proteins. Data are presented as means and standard error of the means, and analysed using One-way ANOVA (followed by SNK *post-hoc* test). *$p < 0.05$ vs Control, ***$p < 0.001$ vs Control, ^$p < 0.05$ vs poly I:C, ^^$p < 0.01$ vs poly I:C, ^^^$p < 0.001$ vs poly I:C, $^{+}p < 0.05$ vs FN075, $^{++}p < 0.01$ vs FN075, $^{+++}p < 0.001$ vs FN075

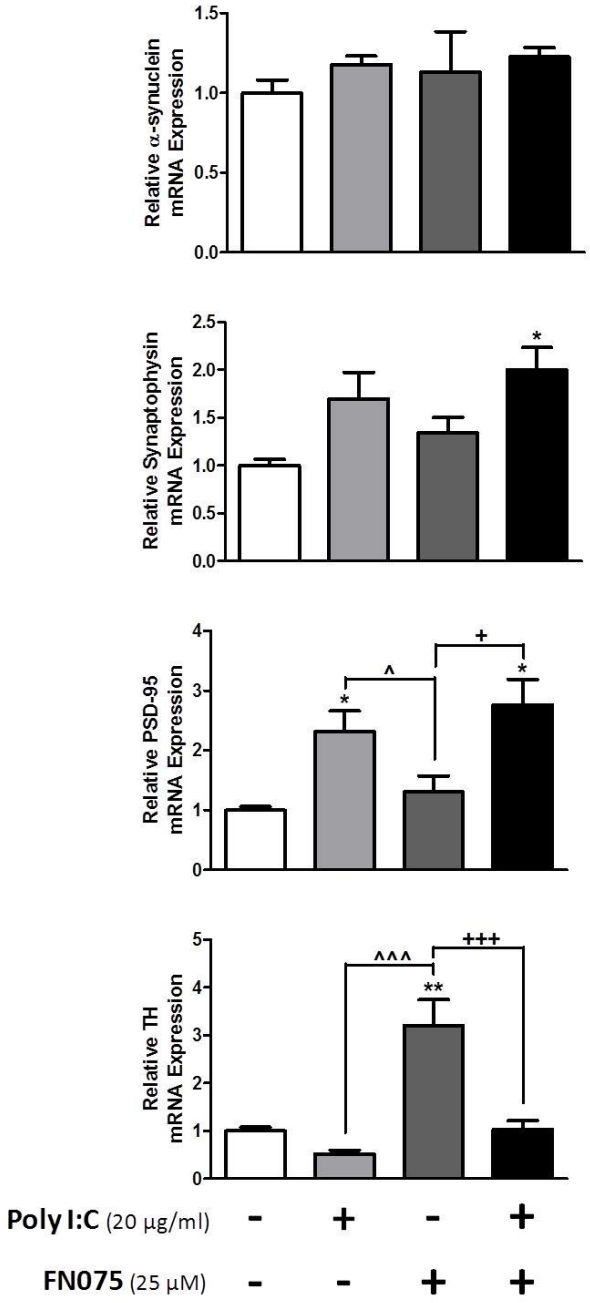

Figure 3.25. Poly I:C Priming FN075 in SH-SY5Y Cells: Synaptic Related mRNA Expression. SH-SY5Y cells were primed with poly I:C (20 µg/ml) for 24 hr prior to treatment with FN075 (25 µM) for 48 hr. The media was retained in between poly I:C and FN075 treatment. Cells were extracted, lysed for mRNA, and probed with synapse related primers. Data are presented as means and standard error of the means, and analysed using One-way ANOVA (followed by SNK *post-hoc* test). *$p < 0.05$ vs Control, **$p < 0.01$ vs Control, ^$p < 0.05$ vs poly I:C, ^^^$p < 0.001$ vs poly I:C, $^{+}p < 0.05$ vs FN075, $^{+++}p < 0.001$ vs FN075

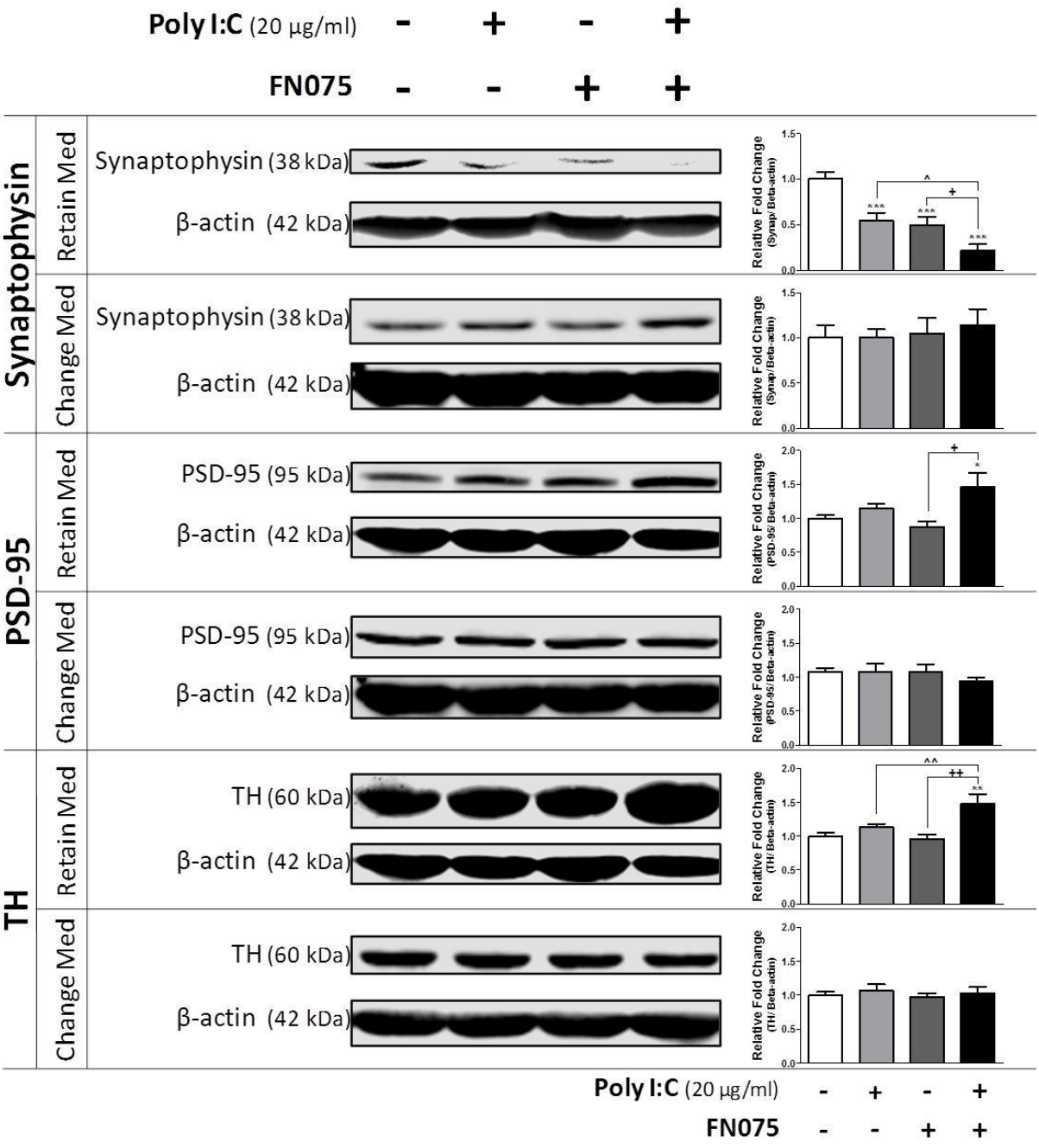

Figure 3.26. Poly I:C Priming FN075 in SH-SY5Y Cells: Synaptic Related Protein Expression. SH-SY5Y cells were primed with poly I:C (20 µg/ml) for 24 hr prior to treatment with FN075 (25 µM) for 48 hr. Cells were extracted, lysed, and probed for synapse related proteins. Data are presented as means and standard error of the means, and analysed using One-way ANOVA (followed by SNK *post-hoc* test). *$p < 0.05$ vs Control, **$p < 0.01$ vs Control, ***$p < 0.001$ vs Control, ^$p < 0.05$ vs poly I:C, ^^$p < 0.01$ vs poly I:C, $^{+}p < 0.05$ vs FN075, $^{++}p < 0.01$ vs FN075

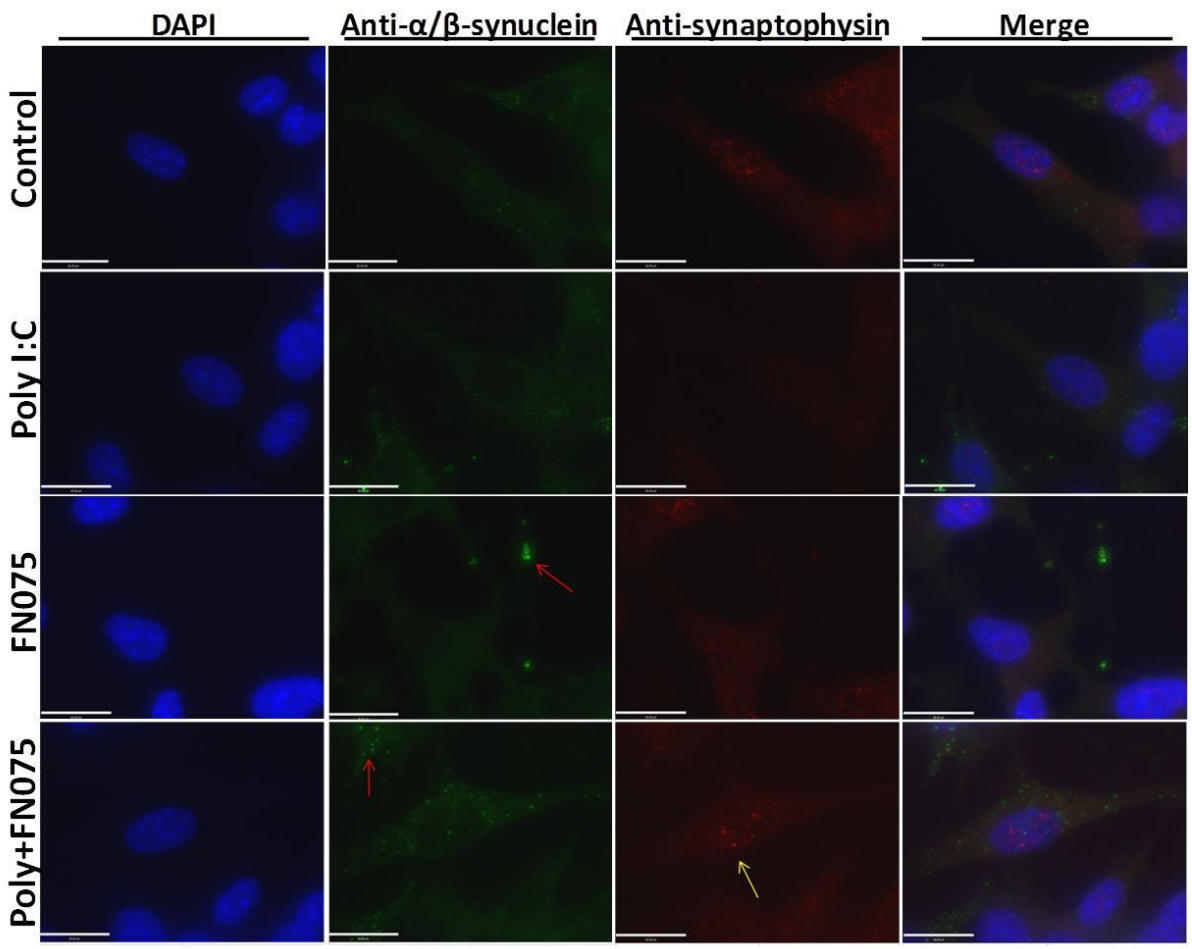

Figure 3.27. Poly I:C Priming FN075 in SH-SY5Y Cells: Immunofluorescent α/β-synuclein. Poly I:C (20 µg/ml for 24 hr) primed cells were treated with FN075 (25 µM) for 48 hr. The media was retained in between poly I:C and FN075 treatment. After treatments, cells were fixed with 4% PFA and stained for α/β-synuclein (green), synaptophysin (red), and DAPI (blue). Protein inclusions of α/β-synuclein (red arrows) and synaptophysin (yellow arrows) were found. Scale bar = 18 µm.

3.6 DISCUSSION

Although it has been established that SH-SY5Y cells express TLR3, few studies have investigated the effects of poly I:C in these cells (Larouche et al., 2008, Nessa et al., 2006). Among the experiments that have measured TLR3 activation in SH-SY5Y cells after poly I:C treatment, there is consistency between our findings and the literature. Similar to our findings, poly I:C was found to increase phosphorylated IRF3, but not phosphorylated NF-κB or NF-κB nuclear translocation in SH-SY5Y cells (Larouche et al., 2008, Lawrimore and Crews, 2017). Also similar to our findings, TLR3 stimulation with poly I:C in SH-SY5Y cells resulted in cytokine and interferon release (Boes and Meyer-Wentrup, 2015, Lawrimore and Crews, 2017, Zhou et al., 2009).

Toxin	**6-OHDA**			**Rotenone**			**MPP+**			**FN075**		
Result	P	6	P+6	P	R	P+R	P	M	P+M	P	F	P+F
TUNEL	NC	NC	NC	NC	NC	NC	NC	↑	↑↑	↑	↑	↑↑
cCASP3	↑	NC	↑	↑	NC	↑	↑↑	NC	↑	↑↑	NC	↑
cPARP	NC	NC	NC	NC	NC	NC	↑	NC	↑	NC	NC	NC
p62	NC	↑	NC	NC	↑	NC	NC	↑	↑↑	NC	↑	NC
LC3	NC	↑	NC	NC	NC	NC	NC	↓	NC	↓	↑	↓
PSD-95	NC	NC	↑	NC	NC	↑	NC	NC	↑	NC	NC	↑
Synap	NC	NC	↑	NC	NC	NC	NC	NC	↓	↓	↓	↓↓

Table 3.1. Summary of Protein/TUNEL Assay Changes.

In our experiments, poly I:C was found to modulate cell death in SH-SY5Y cells. Poly I:C consistently increased cleaved caspase-3 expression. Although previously published research has not investigated apoptotic markers in SH-SY5Y cells after poly I:C treatment, some published studies suggest TLRs in general modulate apoptotic cell death in SH-SY5Y cells (Ulbrich et al., 2015). Beyond poly I:C induced increases in cleaved caspase-3 expression, poly I:C priming was found to exacerbate MPP^+ and

FN075 induced increases in TUNEL staining (see Table 3.1), suggesting poly I:C or poly I:C-mediated neuroinflammation exacerbates MPP^+ and FN075-induced α-synuclein stimulated apoptotic-like cell death. Conversely, poly I:C priming exacerbated 6-OHDA and rotenone induced decreases in cell viability, but not TUNEL staining. Although rotenone and MPP^+ are both complex I inhibitors, they appear to induce very different neurodegenerative effects. This may be due to the mode of neurotoxin uptake (DAT is required for MPP^+ uptake) or their different effects on cellular bioenergetic capacity (Giordano et al., 2012, Langston et al., 1984). A previous study found rotenone to inhibit reserve capacity (the difference between basal and maximal oxygen consumption rates), while MPP^+ increased reserve capacity in SH-SY5Y cells (Giordano et al., 2012). Also, these findings suggest that poly I:C exacerbation of 6-OHDA and rotenone induced cell death may be mediated by a mode of cell death other than apoptosis.

Poly I:C was also found to mediate changes in synaptic related proteins. A consistent finding from these experiments was an increase in PSD-95 when poly I:C priming was combined with neurotoxins used for modeling PD. This finding is contradictory to what was hypothesised, but still demonstrates that poly I:C priming can alter the expression of synaptic proteins. Although this effect was consistent, poly I:C in combination with 6-OHDA produced the strongest synergistic effect on PSD-95 expression. This finding is supported by the literature since a previous animal model found intra-nigral poly I:C priming in combination with 6-OHDA to significantly increase PSD-95 expression in the STR (Deleidi et al., 2010). It is striking that this finding was so consistent, but very little research has investigated the effects of poly I:C on PSD-95, especially in cell culture. One study found pre-natal administration of poly

I:C to modulate the expression of NMDA receptor subunits, but not PSD-95 expression (Forrest et al., 2012).

Similar to the TUNEL staining experiments, poly I:C in combination with both MPP^+ and FN075 reduced synaptophysin expression. It is possible that there is a common neuropathological factor between MPP^+ and FN075 that interacts with viral-like inflammation to result in increased DNA fragmentation and reductions in synaptophysin. Although poly I:C priming in combination with MPP^+ or FN075 has not been previously investigated, one study found pre-natal poly I:C to induce synaptic dysfunction, but not neurodegeneration, in neurons (Oh-Nishi et al., 2010). Also, a viral infection in combination with MPP^+ was found to exacerbate MPP^+ induced dopaminergic cell death in mice (Sadasivan et al., 2017). However, the results from this thesis found a disparity between the findings for synaptophysin mRNA expression, Western Blot protein expression, and immunocytochemistry localisation after poly I:C priming of MPP^+ in SH-SY5Y cells. According to the Western Blot results, there was a decrease in relative protein expression, but immunostaining suggested protein accumulation and an increase in relative expression. One possible explanation for this contradictory finding could be that the relative synaptophysin protein expression is decreased, but that the accumulation of synaptophysin misleadingly looks like a protein increase. It is also possible that the synaptophysin protein which is accumulated into a protein inclusion is not able to be properly elongated for SDS-PAGE gel electrophoresis and so is lost in the stacking gel before antibody detection, resulting in what appears to be a relative decrease in synaptophysin protein. Another possibility is that following cell lysis, the target protein forms part of an inclusion that subsequently makes the protein unavailable for antibody detection. Further experimentation is required to determine if there truly is a decrease in synaptophysin protein expression after poly I:C priming in

combination with MPP^+, but first it is suggested that quantitative (instead of qualitative) immunocytochemistry be conducted to properly measure intracellular protein expression.

Alone, poly I:C did not appear to modulate autophagy processes. Also, poly I:C priming did not show any consistent changes in LC3-a/b-II. However, all the examined neurotoxins tended to increase p62 expression, which was attenuated with poly I:C priming (except in the case of poly I:C priming MPP^+). It is possible that increases in p62 may be a neuroprotective response to neurotoxin insults in SH-SY5Y cells, and that poly I:C or poly I:C mediated inflammation disrupts this process. Indeed, autophagy activation has been found to be neuroprotective and prevent apoptotic-like cell death in SH-SY5Y cells experiencing oxidative stress or mitochondrial dysfunction (Heo et al., 2009, Park et al., 2013).

It is worth noting that the cells used in this study are only dopaminergic-like neurons. Although they express multiple dopaminergic markers, they are not fully mature dopamine neurons. Also, they are a sub-cloned neuroblastoma cell line. Normal mature adult neurons, which undergo neurodegeneration in PD, do not replicate. It is also worth noting that the SH-SY5Y cells used in this study were not differentiated. Differentiated SH-SY5Y cells might respond differently to the neurotoxins used in this study since certain dopaminergic markers (such as DAT) increase their expression after differentiation (Lopes et al., 2017).

Overall, poly I:C priming was found to exacerbate neurodegeneration. Poly I:C priming also was found to induce changes in synaptic and autophagy related proteins that might contribute to changes in cell death or synaptic function.

Chapter Four: Primary Rat VM Results

CHAPTER FOUR

4.1 INTRODUCTION

Based on the results of the poly I:C priming experiments in SH-SY5Y cells, there is suggestion that viral-like priming in combination with oxidative stress, mitochondrial dysfunction, or α-synuclein aggregation modulates neurodegeneration/cell death, synaptic function, and autophagy. Due to these findings, further investigation was conducted to determine if similar changes would occur in primary dopaminergic neurons.

Although E14 primary rat VM cells have been widely used to explore neuronal transplantation (Björklund and Lindvall, 2017, Moriarty et al., 2017), they have also been utilised to investigate PD pathology (Clayton and Sullivan, 2007, Zhu et al., 2015). These cells provide an opportunity to not only investigate non-replicating primary dopaminergic neurons, but also the potential interactions between glial and neuronal cells. E14 primary rat VM cell cultures include a mixture of neurons, microglia, and astrocytes (Zhu et al., 2015). Since glial cells (such as microglia and astrocytes) mediate inflammation in the CNS, this model is ideal for investigating the effects of viral-like poly I:C priming in dopaminergic neurons.

Similar to chapter 3, experiments were designed to determine if viral-like poly I:C priming sensitises primary dopaminergic neurons to the effects of neurotoxins used in pre-clinical models of PD. Neurodegeneration, synaptic function, and autophagy markers were measured in these primary rat neurons after poly I:C priming in combination with 6-OHDA, rotenone and FN075.

4.2 METHODS

The methods used in this chapter did not differ in any way from those outlined in chapter two, unless otherwise stated.

4.3 EXPERIMENTAL DESIGN

Similar to the beginning of chapter 3, the optimum concentration for poly I:C priming was determined by measuring markers of TLR3 activation (such as cytokine release and NF-κB nuclear translocation). The optimum concentration for 6-OHDA, rotenone, and FN075 was determined by measuring MTT cell viability and previous investigation into FN075 induced α-synuclein aggregation (see Appendix A). Following the optimisation experiments, poly I:C priming experiments were conducted by pre-treating with poly I:C followed by 6-OHDA, rotenone, or FN075. Cell death was assessed by measuring MTT cell viability and changes in the TH neuronal population. Synaptic integrity was examined by qPCR, Western Blot, and immunocytochemistry. Autophagy was also measured via Western Blot and immunocytochemistry. All experiments were repeated a minimum of three times. The experimental design is detailed in the following diagram:

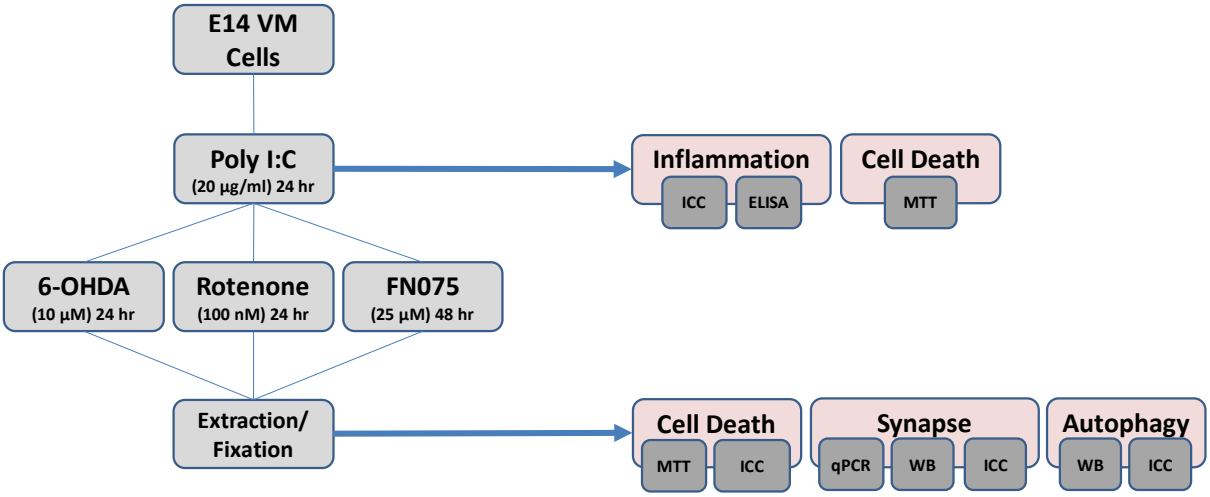

Figure 4.1. Chapter 4 Experimental Design. E14 primary rat VM cells were isolated for cell culture. Cells were primed with poly I:C (20 µg/ml) for 24 hr, followed by 6-OHDA (10 µM for 24 hr), rotenone (100 nM for 24 hr), or FN075 (25 µM for 48 hr) treatment. After the treatment, cells were extracted or fixed for analysis; n = 3-6 per group.

4.4 RESULTS

4.4.1 Neurotoxin Optimisation in VM Rat Cells: MTT Cell Viability

Similar to the SH-SY5Y experiments, the MTT cell viability assay was used to determine the optimal neurotoxin concentration for poly I:C priming experiments in primary E14 rat VM cells. According to this assay, there was a significant decrease in cell viability after 24 hr 6-OHDA ($F_{(3,20)} = 271.2$, $p < 0.001$) and rotenone ($F_{(3,20)} = 74.6$, $p < 0.001$) treatment (see Fig. 4.2). 6-OHDA at 10 µM reduced cell viability by 27% ($p < 0.001$), while rotenone at 100 nM reduced cell viability by 33% ($p < 0.001$). FN075, however, did not significantly reduce cell viability after 48 hr at any of the tested concentrations ($F_{(3,16)} = 1.2$, $p > 0.05$). Based on these findings, the optimal neurotoxin concentrations for poly I:C priming experiments to investigate alterations to cell death, synapse, and autophagy makers was determined to be 10 µM for 6-OHDA and 100 nM for rotenone. Since there was no significant change in cell viability after FN075 treatment, further preliminary investigation was conducted to determine the optimal FN075 concentration to induce α-synuclein aggregation.

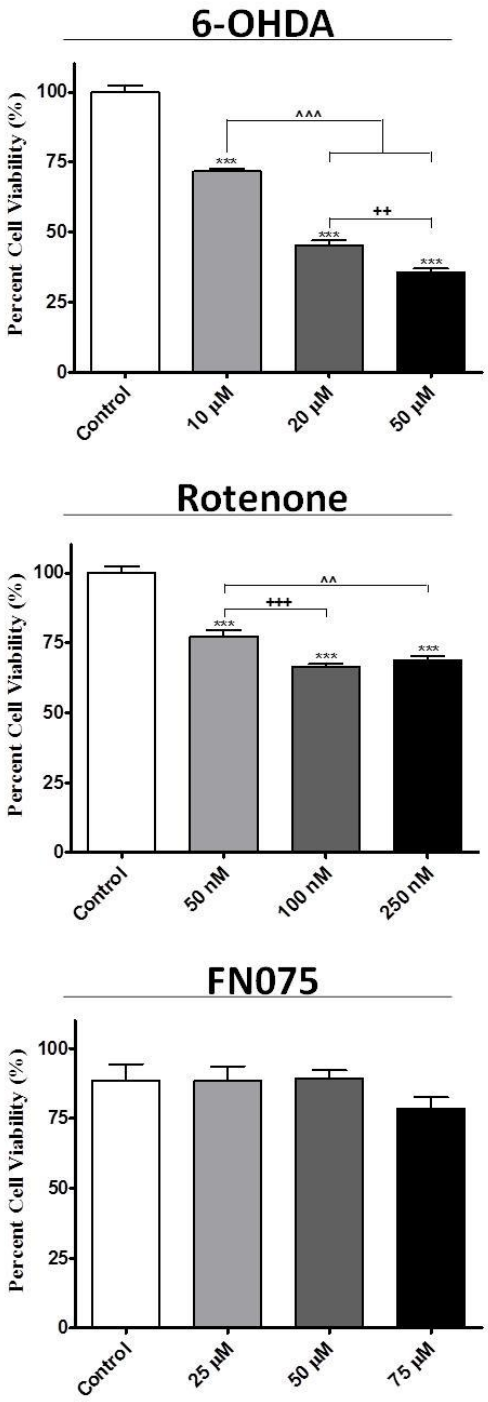

Figure 4.2. Cell Viability in E14 VM Primary Cells: Neurotoxin Dose Response. After neurotoxin treatment, E14 rat primary VM cells were tested for MTT cell viability. Analyses were conducted using a One-way ANOVA, followed by SNK *post-hoc* test. Data are presented as means and standard error of the means. ***p < 0.001 vs Control, ^^p < 0.01 vs 250 nM rotenone, ^^^p < 0.001 vs 10 µM 6-OHDA, ++p < 0.01 vs 20 µM 6-OHDA, +++p < 0.001 vs 100 nM rotenone

4.4.2 Poly I:C Activation of TLR3 in VM Cells

As previously mentioned, TLR3 activation leads to NF-κB/IRF3 nuclear translocation and cytokine/interferon release (O'Neill et al., 2013). The E14 primary rat VM cells were studied to determine reactivity to poly I:C. First, immunostaining for phosphorylated-p65 NF-κB was quantified in poly I:C treated cells. TH^+ cells were selected and phosphorylated-p65 fluorescent density was measured for the whole cell and the nucleus to determine changes in NF-κB phosphorylation and NF-κB nuclear translocation (see Fig. 4.3). Poly I:C (20 µg/ml) 24 hr treatment did not significantly increase NF-κB phosphorylation in TH^+ neurons ($t_{(9)} = 0.1$, $p > 0.05$), but poly I:C did induce significant nuclear translocation of phosphorylated NF-κB ($U = 2.7$, $p < 0.01$).

Activation of TLR3 should also lead to cytokine release. After 24 hr poly I:C treatment, there was a significant increase in cytokine release (see Fig. 4.4). ELISA measurement of the media from poly I:C treated mixed primary VM rat cells found increases in IL-6 ($F_{(2,6)} = 21.6$, $p < 0.01$), TNF-α ($F_{(2,6)} = 14.6$, $p < 0.01$), and IL-1β ($F_{(2,6)} = 28.4$, $p < 0.01$). IL-6 (151.49 ± 27.81 pg/ml), TNF-α (334.27 ± 59.82 pg/ml), and IL-1β (3019.60 ± 565.10 pg/ml) was released into the media after cells were treated in 20 µg/ml poly I:C (see Fig. 4.3). When cells were treated with only 10 µg/ml poly I:C, there was no significant increase IL-6 ($p > 0.05$), TNF-α ($p > 0.05$), or IL-1β ($p > 0.05$), suggesting that 20 µg/ml of poly I:C is required for TLR3 activation of primary rat VM cells.

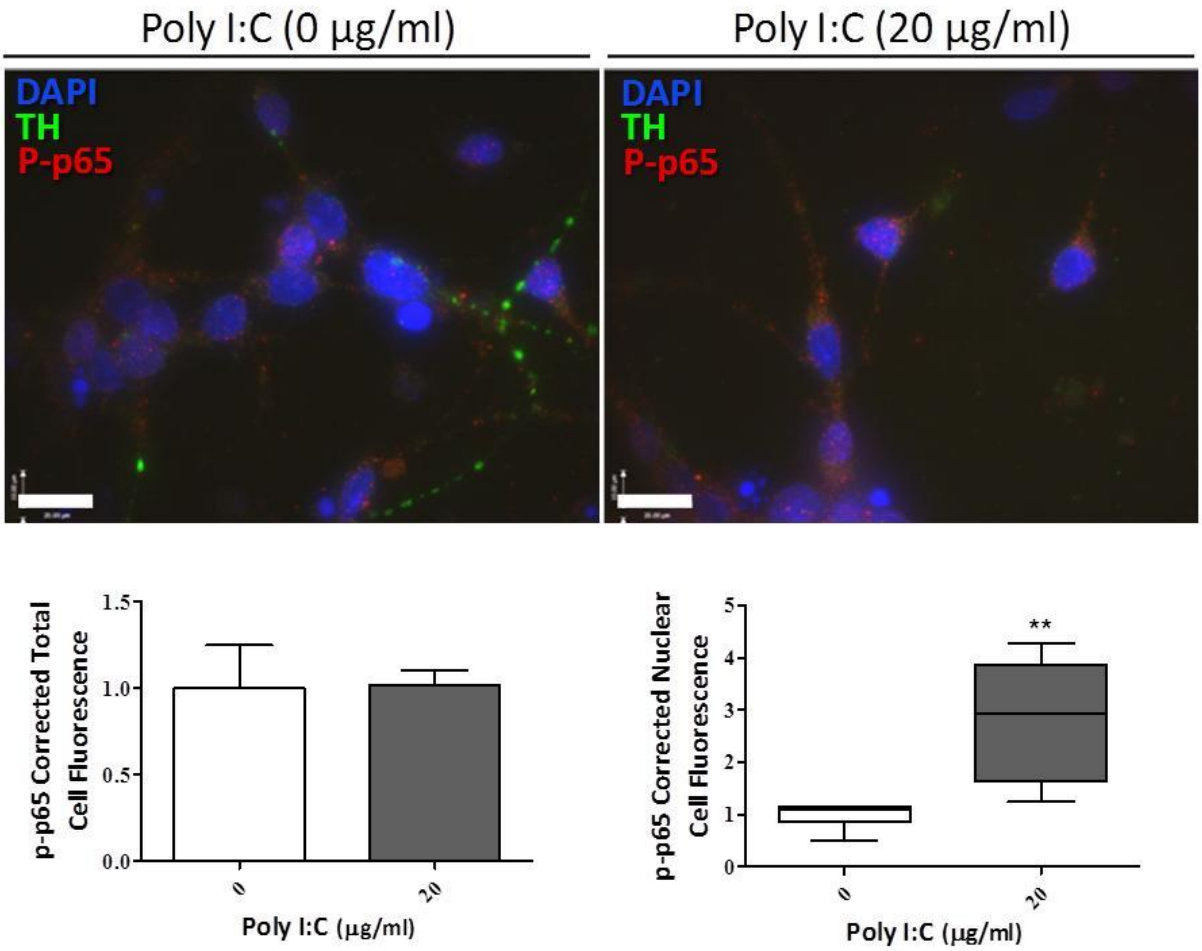

Figure 4.3. Poly I:C Dose Response: Immunofluorescence of Phosphorylated Proteins. E14 rat VM cells were treated with poly I:C (20 µg/ml) for 24 hr. Cells were fixed with 4% PFA and immunostained for TH (green), phosphorylated-p65 NF-κB (red), and DAPI (blue). Images were obtained using an Olympus microscope (100X lens). Analysis was conducted using independent samples t-test for relative total p65 expression and Mann-Whitney U-test for relative nuclear p65 expression. Data are presented as means and standard error of the means or median ± min and max, respectively. Scale bar = 20 µm. **p < 0.01 vs 0 µg/ml

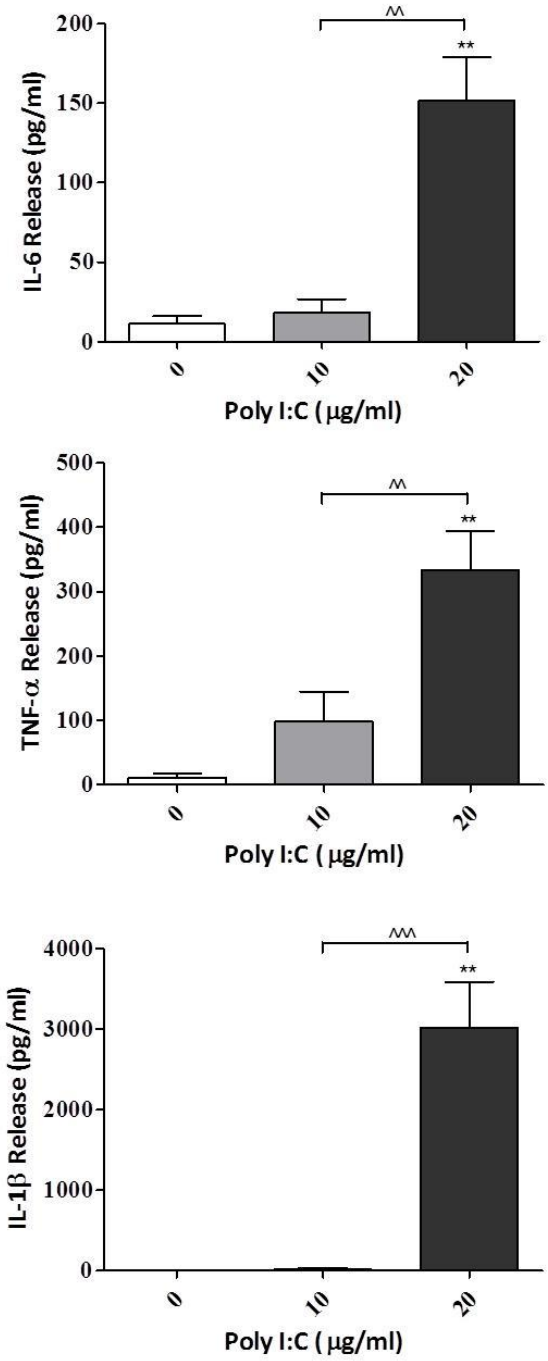

Figure 4.4. Poly I:C Dose Response: Cytokine Release. After 24 hr poly I:C treatment, media from E14 primary rat VM cells was collected for ELISA analysis. IL-6, TNF-α, and IL-1β concentration in the media was determined by spline fit regression analysis to the standard. Analysis was conducted using One-way ANOVA and SNK *post-hoc* test. Data are presented as means and standard error of the means. **p < 0.01 vs 0 µg/ml, ^^p < 0.01 vs 10 µg/ml, ^^^p < 0.001 vs 10 µg/ml

4.4.3 Poly I:C Priming in VM Cells: Cell Viability and Cell Populations

4.4.3.1 Cell Viability after Poly I:C Priming in VM Cells

Based on the previous experiments, poly I:C priming experiments were designed to examine the effects of viral-like priming (and resulting inflammatory response) in mixed VM primary cell culture. E14 rat VM cells were primed with poly I:C 20 µg/ml for 24 hr, followed by treatment with a 6-OHDA (10 µM for 24 hr), rotenone (100 nM for 24 hr), or FN075 (25 µM for 48 hr) (see Fig. 4.5). A significant reduction in cell viability was seen after poly I:C priming of 6-OHDA ($F_{(3,15)} = 39.0$, $p < 0.001$), rotenone ($F_{(3,20)} = 31.7$, $p < 0.001$), and FN075 ($F_{(3,16)} = 34.5$, $p < 0.001$). As expected based on the concentration-dependent experiments, cell viability was reduced after 6-OHDA (33% reduction, $p < 0.001$) and rotenone (32% reduction, $p < 0.001$) treatments. FN075 did not significantly change cell viability compared to the control group (114%, $p > 0.05$). Poly I:C itself was found to consistently reduce cell viability by 38-50% across all experiments ($p < 0.001$). Priming with poly I:C was found to further exacerbate 6-OHDA (27% more reduction, $p < 0.001$) and rotenone (14% more reduction, $p < 0.05$) induced decrease in cell viability. Although priming with poly I:C further reduced the cell viability of the VM mixed cultures when compared to the neurotoxin treatment group, this reduction was not significantly different from the reduction induced by poly I:C alone ($p > 0.05$), suggesting that the poly I:C priming effect is due to poly I:C alone and not a synergistic effect with any of the neurotoxins.

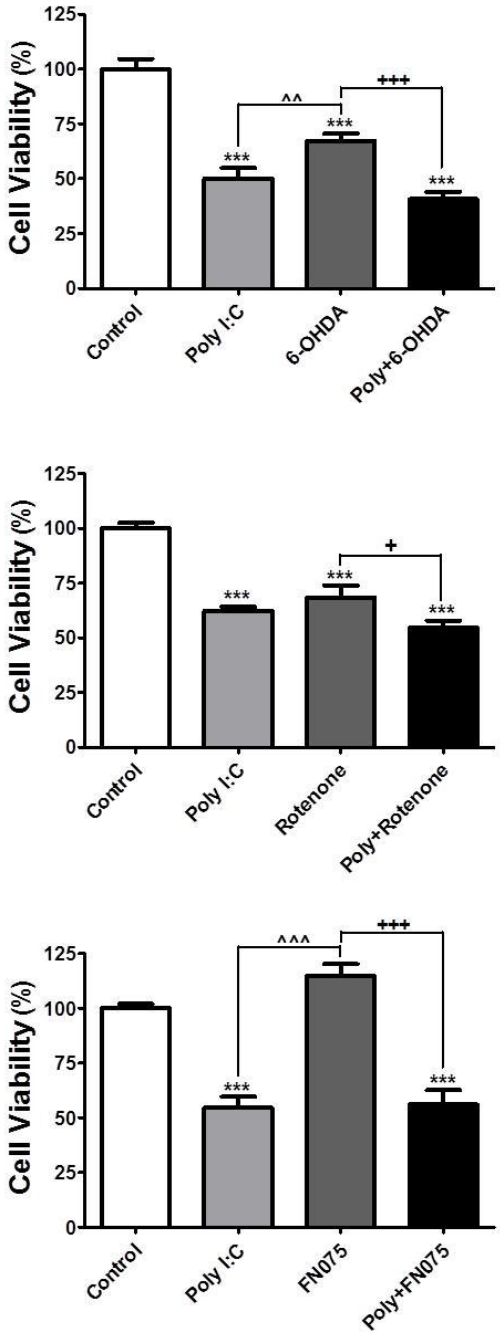

Figure 4.5. Poly I:C Priming Neurotoxin Treatment in E14 VM Primary Cells: Cell Viability. E14 Rat VM cells were primed with poly I:C (20 µg/ml) for 24 hr before treatment with 6-OHDA 10 µM (24 hr), rotenone 100 nM (24 hr), or FN075 µM (48 hr). MTT cell viability was analysed using One-way ANOVA, followed by SNK post-hoc test. Data are presented as means and standard error of the means. ***$p < 0.05$ vs Control, ^^$p < 0.01$ vs poly I:C, ^^^$p < 0.001$ vs poly I:C, $^{+}p < 0.05$ vs neurotoxin, $^{+++}p < 0.001$ vs neurotoxin

4.4.3.2 Cell Populations after Poly I:C Priming in VM Cells

Based on the optimisation experiments, E14 primary rat VM cells were primed with 20 µg/ml poly I:C to induce a TLR3 mediated inflammatory response, followed by 6-OHDA (10 µM for 24 hr), rotenone (100 nM for 24 hr), or FN075 (25 µM for 48 hr). VM cells were then immunostained for tyrosine hydroxylase to identify TH^+ cells, an indication of dopaminergic neurons. Across all experiments, a significant change in the percentage of TH^+ cells was found (6-OHDA ($F_{(3,8)} = 9.6$, $p < 0.01$, see Fig. 4.6), rotenone ($F_{(3,8)} = 12.6$, $p < 0.01$, see Fig. 4.7), FN075 ($F_{(3,8)} = 10.7$, $p < 0.01$, see Fig. 4.8)).

Treatment with poly I:C (20 µg/ml) consistently reduced the percentage of TH^+ cells in the VM mixed culture population (6-10% reduction compared to the control group, $p < 0.05$) across all experiments (see Fig. 4.6-4.8). This poly I:C induced reduction in percentage of TH^+ cells is slightly more than the previous concentration-response experiments, which found only a 4% decrease in TH^+ cell after 20 µg/ml of poly I:C. The increase in poly I:C induced neurotoxicity for TH^+ neurons may be due to the extended exposure to poly I:C and/or poly I:C induced inflammatory response for these cells. An additional 24-48 hr incubation time for poly I:C was required to account for the neurotoxin (6-OHDA, rotenone, FN075) incubation time.

As expected, each neurotoxin produced a significant reduction in percentage of TH^+ neurons in the VM mixed culture. FN075 (25 µM) was found to be the least toxic to dopaminergic neurons, with only a 7% decrease in TH^+ neurons ($p < 0.05$, see Fig. 4.8). 6-OHDA (10 µM) reduced the dopaminergic neuronal population by over 10% ($p < 0.01$, see Fig. 4.6). Demonstrating the highest neurotoxicity, rotenone (100 nM) was found to decrease the TH^+ neuronal population by 14% ($p < 0.01$, see Fig. 4.7).

The purpose of these experiments was to determine if priming with poly I:C before neurotoxin administration (6-OHDA, rotenone, FN075) exacerbated neurotoxin induced neurodegeneration of dopaminergic neurons. Although all groups which were primed with poly I:C in combination with a neurotoxin demonstrated a reduction in percentage of TH^+ neurons compared to the control group (poly I:C+6-OHDA: 13% decrease, $p < 0.01$; poly I:C+rotenone: 15% decrease, $p < 0.01$; poly I:C+FN075: 11% decrease, $p < 0.01$), none of the poly I:C primed groups had a further reduction in TH^+ neurons compared to their corresponding neurotoxin alone treatment group ($p > 0.05$). These experiments indicate that priming with poly I:C did not exacerbate the dopaminergic neurotoxicity of 6-OHDA, rotenone, or FN075.

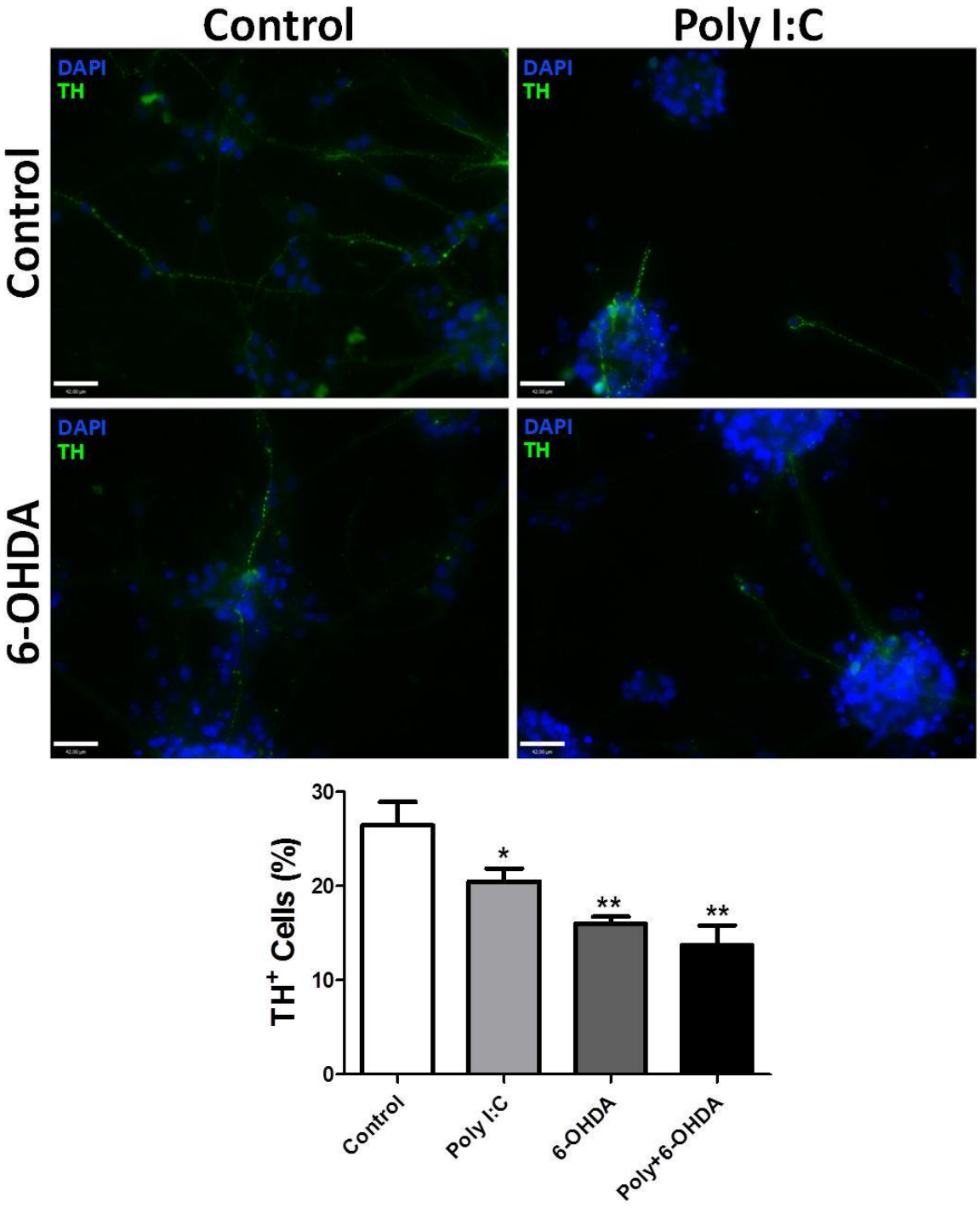

Figure 4.6. Poly I:C Priming 6-OHDA Treatment: Percent TH^+ Population in E14 VM Primary Cells. E14 VM cells were primed with poly I:C (20 µg/ml) followed by a subsequent treatment with 6-OHDA (10 µM). Cells were fixed with 4% PFA and immunostained for TH (green) and DAPI (blue). Images were obtained using an Olympus microscope (40X lens). Data were analysed using One-way ANOVA, followed by SNK *post-hoc* test, and presented as means and standard errors of the mean. Scale bar = 42 µm. *$p < 0.05$ vs Control, **$p < 0.01$ vs Control

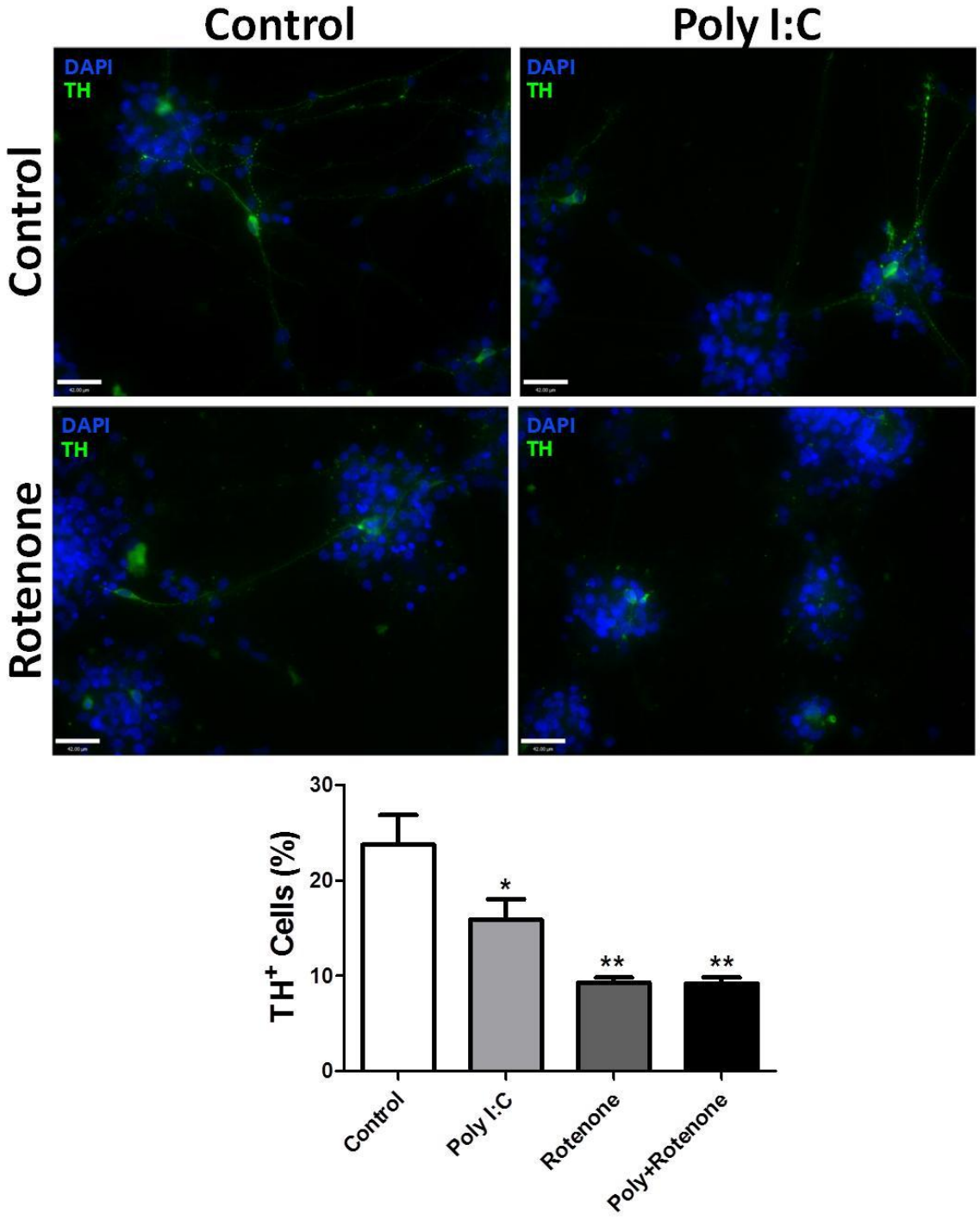

Figure 4.7. Poly I:C Priming Rotenone Treatment: Percent TH^+ Population in E14 VM Primary Cells. E14 VM cells were primed with poly I:C (20 µg/ml) followed by a subsequent treatment with rotenone (100 nM). Cells were fixed with 4% PFA and immunostained for TH (green) and DAPI (blue). Images were obtained using an Olympus microscope (40X lens). Data were analysed using One-way ANOVA, followed by SNK *post-hoc* test, and presented as means and standard errors of the mean. Scale bar = 42 µm. *$p < 0.05$ vs Control, **$p < 0.01$ vs Control

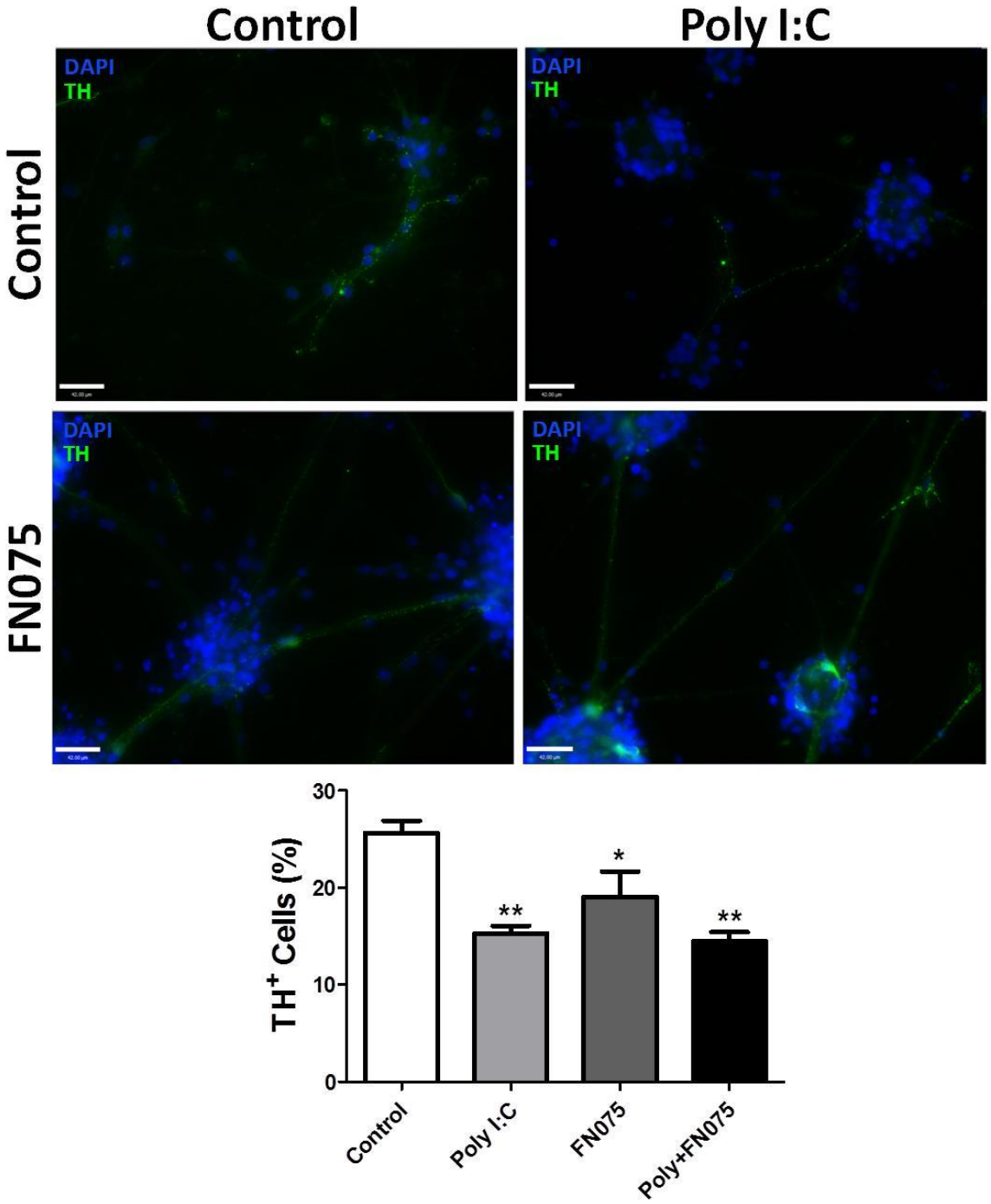

Figure 4.8. Poly I:C Priming FN075 Treatment: Percent TH^+ Population in E14 VM Primary Cells. E14 VM cells were primed with poly I:C (20 µg/ml) followed by a subsequent treatment with FN075 (25 µM). Cells were fixed with 4% PFA and immunostained for TH (green) and DAPI (blue). Images were obtained using an Olympus microscope (40X lens). Data were analysed using One-way ANOVA, followed by SNK *post-hoc* test, and presented as means and standard errors of the mean. Scale bar = 42 µm. *$p < 0.05$ vs Control, **$p < 0.01$ vs Control

4.4.4 Poly I:C Priming in VM Cells: mRNA and Protein Expression

4.4.4.1 Poly I:C Priming 6-OHDA in VM Cells

In addition to investigating poly I:C mediated changes to neurotoxin induced neurodegeneration in rat primary E14 VM cells, synaptic and autophagy dysfunction were also measured. Relative mRNA/protein expression of synaptic related markers were quantified to determine if viral-like poly I:C priming reduced synapse function or integrity. Autophagy related proteins were investigated to examine poly I:C induced changes to autophagic protein clearance.

Although TH immunostaining found 6-OHDA and poly I:C to reduce the percentage of TH^+ neurons in VM mixed cultures (see Fig. 4.6), these treatments did not alter relative TH mRNA expression as measured by qPCR ($F_{(3,8)} = 2.0$, $p > 0.05$, see Fig. 4.9). There was also no change in relative α-synuclein mRNA expression due to 6-OHDA or poly I:C treatment ($F_{(3,8)} = 0.4$, $p > 0.05$). Although there was no change in α-synuclein mRNA expression, immunostaining for filamentous α-synuclein found 6-OHDA to induce a significant 2-fold increase in filamentous α-synuclein ($F_{(3,25)} = 12.0$, $p < 0.001$, see Fig. 4.10). Poly I:C did not induce any changes in relative filamentous α-synuclein levels in VM mixed cultures, but priming with poly I:C previous to 6-OHDA did result in a total 3-fold increase in filamentous α-synuclein ($p < 0.001$), which was a significantly greater than the 6-OHDA induced 2-fold increase ($p < 0.05$).

Synapse related proteins other than α-synuclein were also investigated after poly I:C priming of 6-OHDA in VM mixed cultures. Western Blot and qPCR found 6-OHDA and poly I:C to slightly increase synaptophysin protein and mRNA expression, respectively. Poly I:C and 6-OHDA both induced a 2-fold increase in synaptophysin mRNA, but this increase was not found to be statistically significant ($F_{(3,8)} = 1.4$, $p >$

0.05, see Fig. 4.9). Similarly, 6-OHDA induced a 2-fold increase in synaptophysin protein which was not statistically significant (see Fig. 4.11). However, poly I:C did induce a significant 3-fold increase in relative synaptophysin protein expression in VM mixed culture rat primary cells ($F_{(3,8)} = 5.2$, $p < 0.05$). Although poly I:C increased synaptophysin expression, there was no significant change in the combined poly I:C plus 6-OHDA group ($p > 0.05$, see Fig. 4.11). Conversely, priming with poly I:C in combination with 6-OHDA did result in a significant 4-fold increase in relative PSD-95 mRNA expression ($F_{(3,8)} = 4.2$, $p < 0.05$, see Fig. 4.9). Despite this change in PSD-95 mRNA, neither poly I:C nor 6-OHDA significantly changed PSD-95 protein expression ($F_{(3,8)} = 2.1$, $p > 0.05$).

Autophagy related p62 and LC3-a/b-I/II proteins were also measured after poly I:C priming with 6-OHDA. Immunostaining found 6-OHDA to induce a 2-fold increase in p62 expression in rat VM primary cells ($F_{(3,25)} = 11.1$, $p < 0.001$, see Fig. 4.8). The addition of poly I:C previous to 6-OHDA treatment did not alter this 2-fold increase in p62 ($p > 0.05$). Western Blot analysis of lysed primary VM cells found poly I:C to produce a 4-fold increase in the active LC3-a/b-II isoform, but this did not reach statistical significance ($F_{(3,8)} = 2.7$, $p > 0.113$, see Fig. 4.12). Similarly, neither poly I:C nor 6-OHDA resulted in a statistically significant change in LC3-a/b-I expression ($F_{(3,8)} = 2.2$, $p > 0.05$).

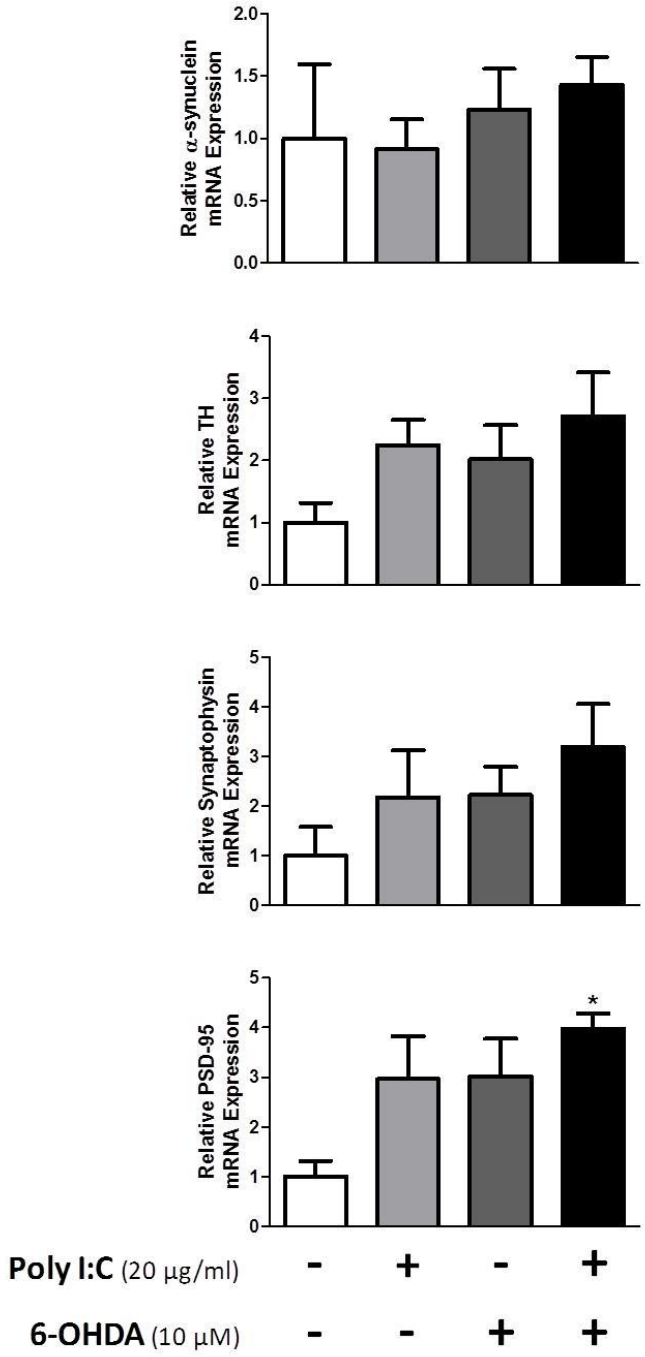

Figure 4.9. Poly I:C Priming 6-OHDA in E14 VM Primary Cells: Synaptic Related mRNA Expression. E14 rat VM cells were primed with poly I:C (20 µg/ml) for 24 hr prior to 6-OHDA (10 µM) 24 hr treatment. Cells were extracted, lysed for mRNA, and probed with synapse related primers. The data was transformed by calculating the relative change in ΔCp values. Analysis was conducted using One-way ANOVA, followed by SNK *post-hoc* test. Data are presented as means and standard error of the means. *$p < 0.05$ vs Control

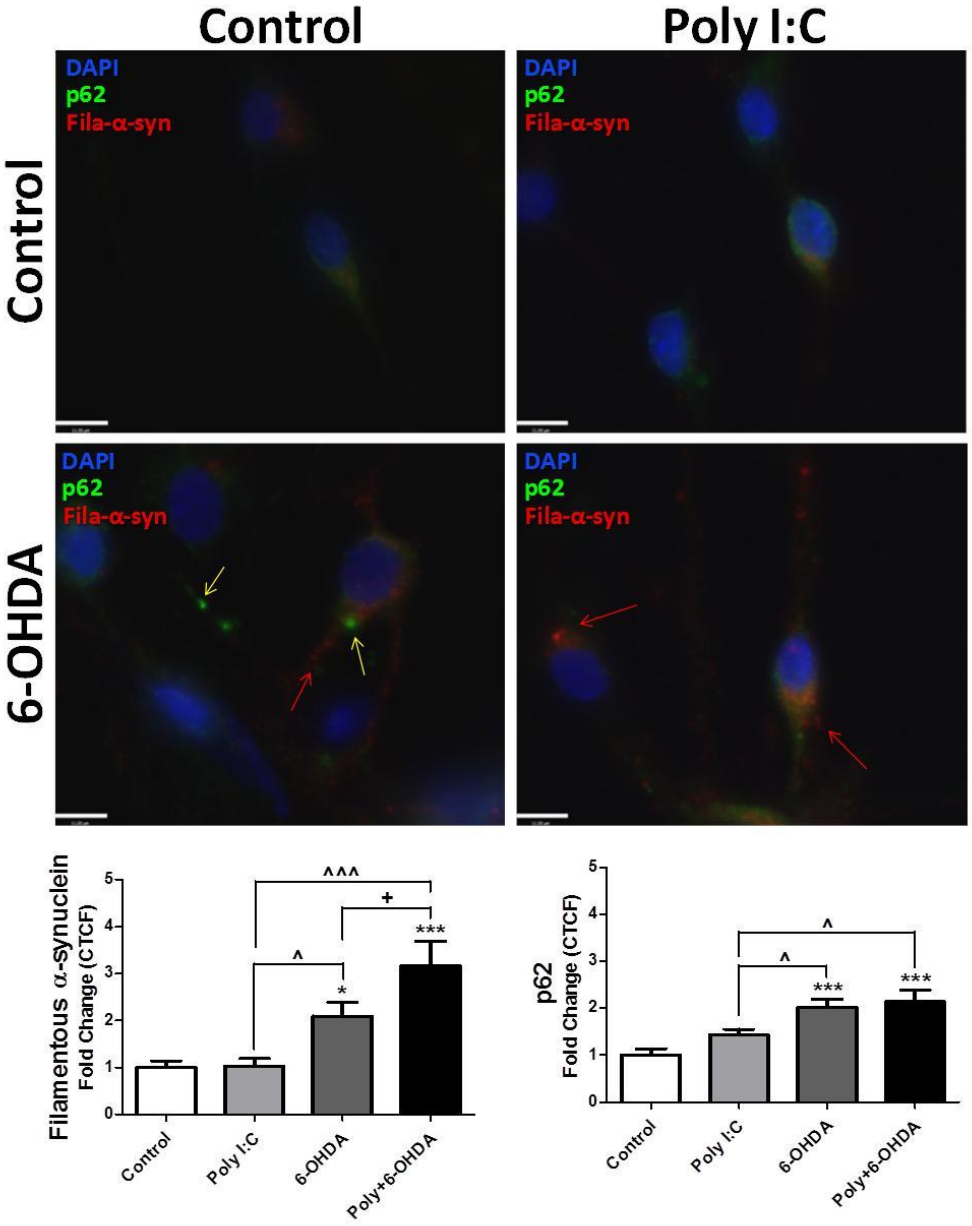

Figure 4.10. Poly I:C Priming 6-OHDA in E14 VM Primary Cells: Filamentous-α-synuclein and p62. Following poly I:C priming (20 µg/ml for 24 hr) in combination with 6-OHDA (10 µM for 24 hr), E14 rat VM cells were fixed with 4% PFA, permeabilised wiTriton-X100, and immunostained for filamentous α-synuclein (red), p62 (green), and DAPI (blue). 6-OHDA treatment resulted in p62 inclusions (yellow arrows) and filamentous α-synuclein (red arrows). Images were collected with an Olympus microscope using the 40X objective lens. Analysis was conducted using One-way ANOVA, followed by SNK *post-hoc* test. Data are presented as means and standard error of the means. Scale bar = 11 µm. *$p < 0.05$ vs Control, ***$p < 0.001$ vs Control, ^$p < 0.05$ vs poly I:C, ^^^$p < 0.001$ vs poly I:C, $^{+}p < 0.05$ vs 6-OHDA

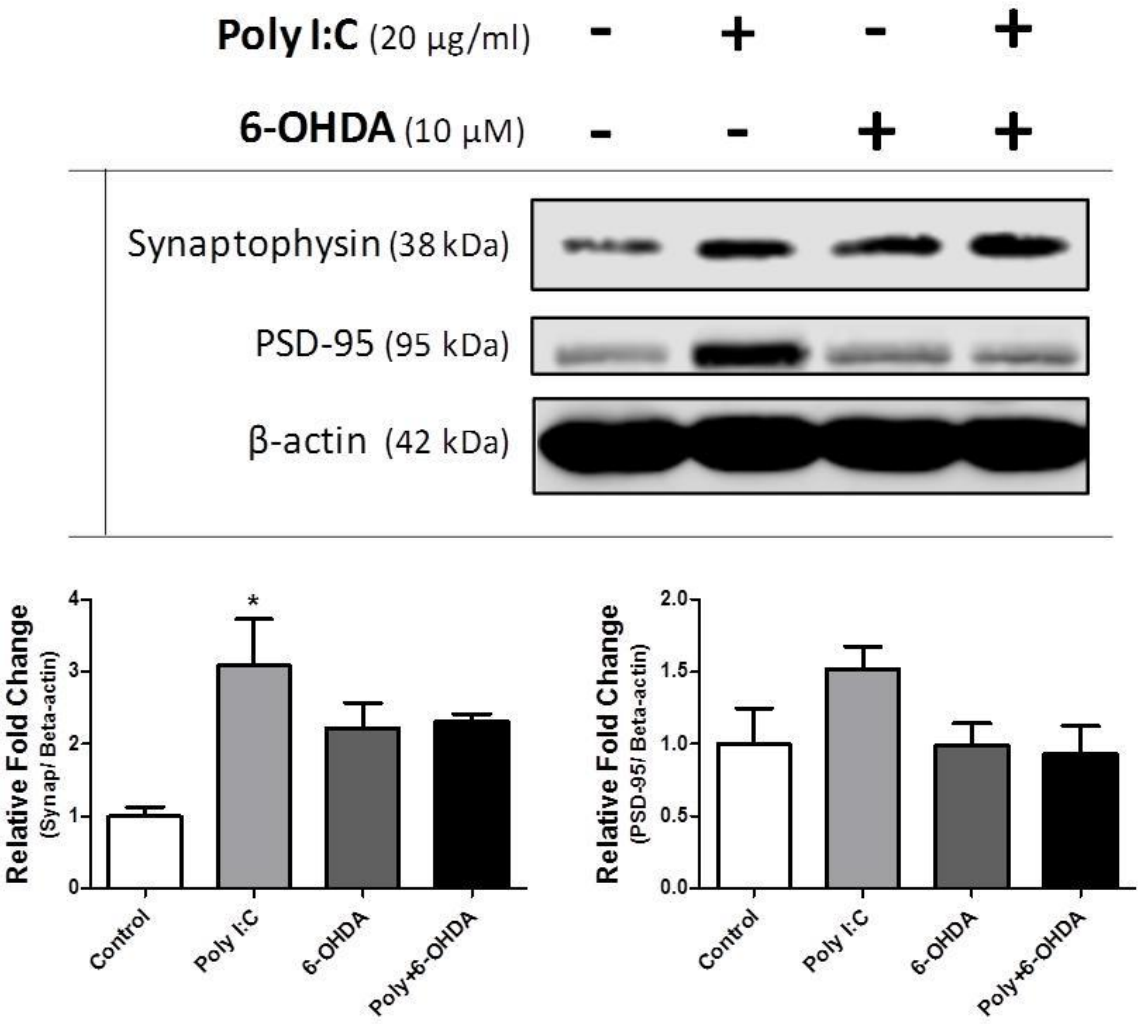

Figure 4.11. Poly I:C Priming 6-OHDA in E14 VM Primary Cells: Synapse Related Proteins. Following 24 hr poly I:C priming (20 µg/ml) in combination with 6-OHDA (10 µM for 24 hr), E14 rat VM cells were extracted, lysed, and probed for synapse related proteins. Analysis was conducted using One-way ANOVA, followed by SNK *post-hoc* test. Data are presented as means and standard error of the means. *$p < 0.05$ vs Control

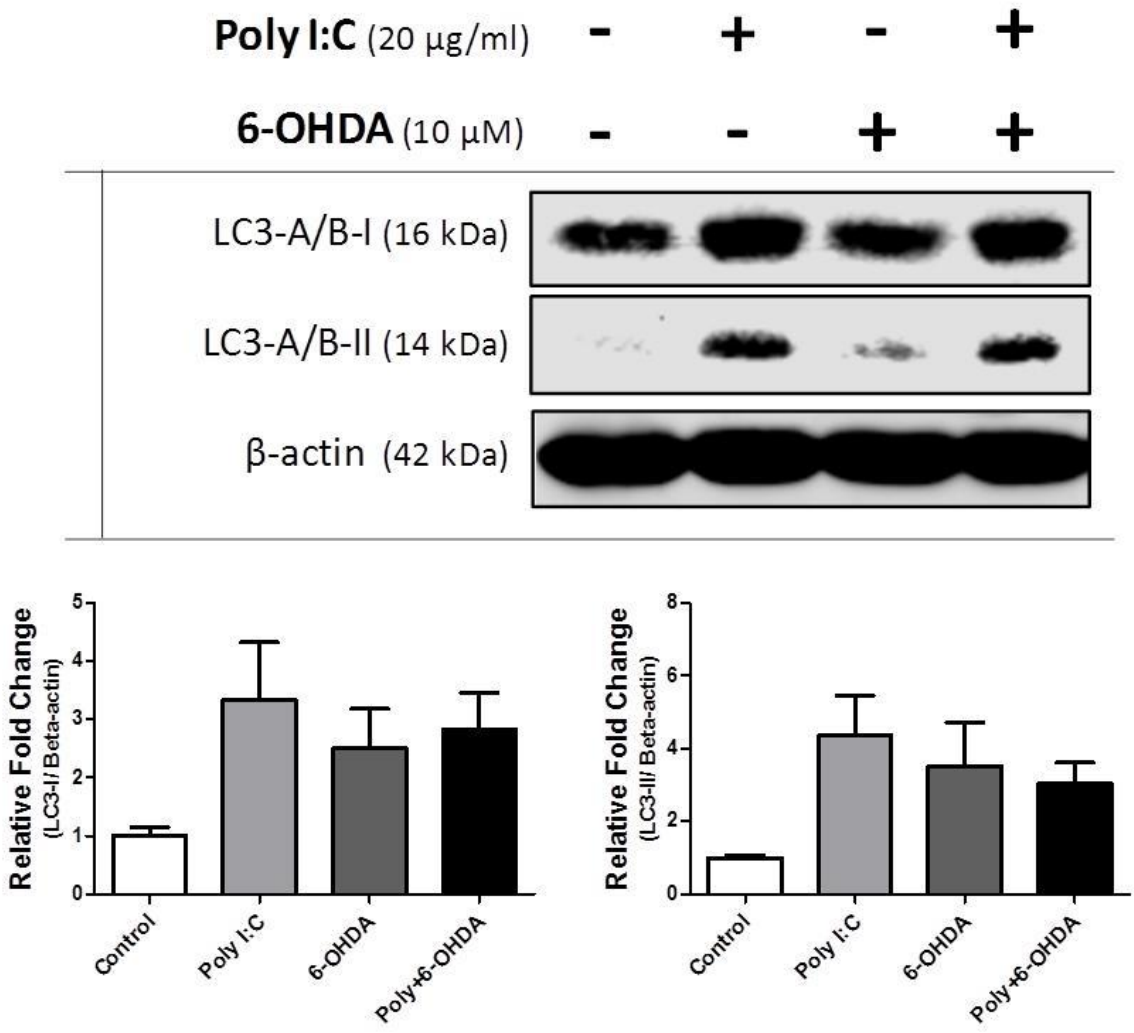

Figure 4.12. Poly I:C Priming 6-OHDA in E14 VM Primary Cells: LC3-a/b-I/II. Following 24 hr poly I:C priming (20 µg/ml) in combination with 6-OHDA (10 µM for 24 hr), E14 rat VM cells were extracted, lysed, and probed for LC3-a/b-I/II. Analysis was conducted using One-way ANOVA, followed by SNK *post-hoc* test. Data are presented as means and standard error of the means.

4.4.4.2 Poly I:C Priming Rotenone in VM Cells

Similar to the poly I:C/6-OHDA experiments, synaptic and autophagy related markers were investigated in E14 rat VM primary cells after poly I:C (20 µg/ml for 24 hr) primed cells were treated with rotenone (100 nM for 24 hr). Again, although both poly I:C and rotenone resulted in a decrease in TH^+ immunostained neurons in the primary mixed cultures (see Fig. 4.7), there was no significant change in relative TH mRNA expression ($F_{(3,8)} = 0.5$, $p > 0.05$, see Fig. 4.13). Although there was no significant change in relative α-synuclein mRNA expression ($F_{(3,8)} = 0.4$, $p > 0.05$), treatment with rotenone induced a significant 3-fold increase in filamentous α-synuclein expression in rat primary VM cells ($F_{(3,25)} = 9.2$, $p < 0.001$, see Fig. 4.14). Interestingly, poly I:C priming attenuated this rotenone mediated increase in filamentous α-synuclein, with a reduction back to control levels (see Fig. 4.14).

Further investigation into the synapse of the rat VM cells, qPCR found no clear change in relative synaptophysin mRNA expression ($F_{(3,8)} = 2.4$, $p > 0.05$, see Fig. 4.13). Similar to the poly I:C/6-OHDA experiments, poly I:C did induce a 3-fold increase in synaptophysin protein expression ($F_{(3,8)} = 5.4$, $p < 0.05$, see Fig. 4.15). Similarly, poly I:C, when combined with rotenone, had no effect on synaptophysin expression ($p > 0.05$). Although there was a 2-fold increase in relative PSD-95 mRNA expression in the cells after rotenone treatment, this did not reach statistical significance ($F_{(3,8)} = 1.8$, $p > 0.05$, see Fig. 4.13) and there was no change in PSD-95 protein expression ($F_{(3,8)} = 0.8$, $p > 0.05$, see Fig. 4.15).

While poly I:C priming in combination with rotenone did not modulate synapse related markers in rat primary VM cells, there were significant changes in autophagy related markers. Treatment with rotenone resulted in a 2.7-fold increase in immunostained p62 expression in these cells ($K = 13.2$, $p < 0.01$, see Fig. 4.14). Similar

to the rotenone mediated increase in filamentous α-synuclein, priming with poly I:C appeared to attenuate this increase in p62 expression (see Fig. 4.14). However, poly I:C priming in combination with rotenone did lead to a drastic 5.8-fold increase in the active LC3-a/b-II isoform ($F_{(3,8)} = 5.7$, $p < 0.05$, see Fig. 4.16). Individually, poly I:C increased LC3-a/b-II by 4.4-fold and rotenone increase it by 3.5-fold but these values did not reach statistical significance ($p > 0.05$), suggesting that the increase found after poly I:C priming in combination with rotenone is a synergistic effect. Although poly I:C appeared to increase LC3-a/b-I, there was no statistically significant change in protein expression due to poly I:C or rotenone ($F_{(3,8)} = 2.1$, $p > 0.05$, see Fig. 4.16).

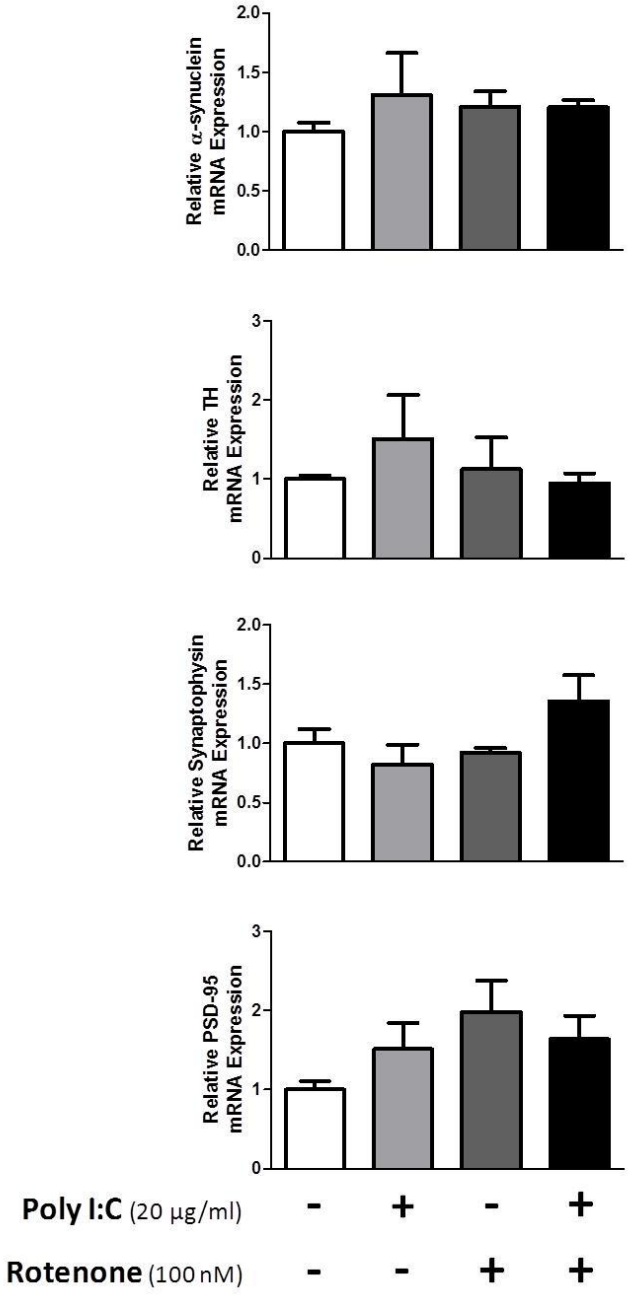

Figure 4.13. Poly I:C Priming Rotenone in E14 VM Primary Cells: Synaptic Related mRNA Expression. E14 rat VM cells were primed with poly I:C (20 µg/ml) for 24 hr prior to a 24 hr rotenone (100 nM) treatment. Cells were extracted, lysed for mRNA, and probed with synapse related primers. The data was transformed by calculating the relative change in ΔCp values. Analysis was conducted using One-way ANOVA, followed by SNK *post-hoc* test. Data are presented as means and standard error of the means.

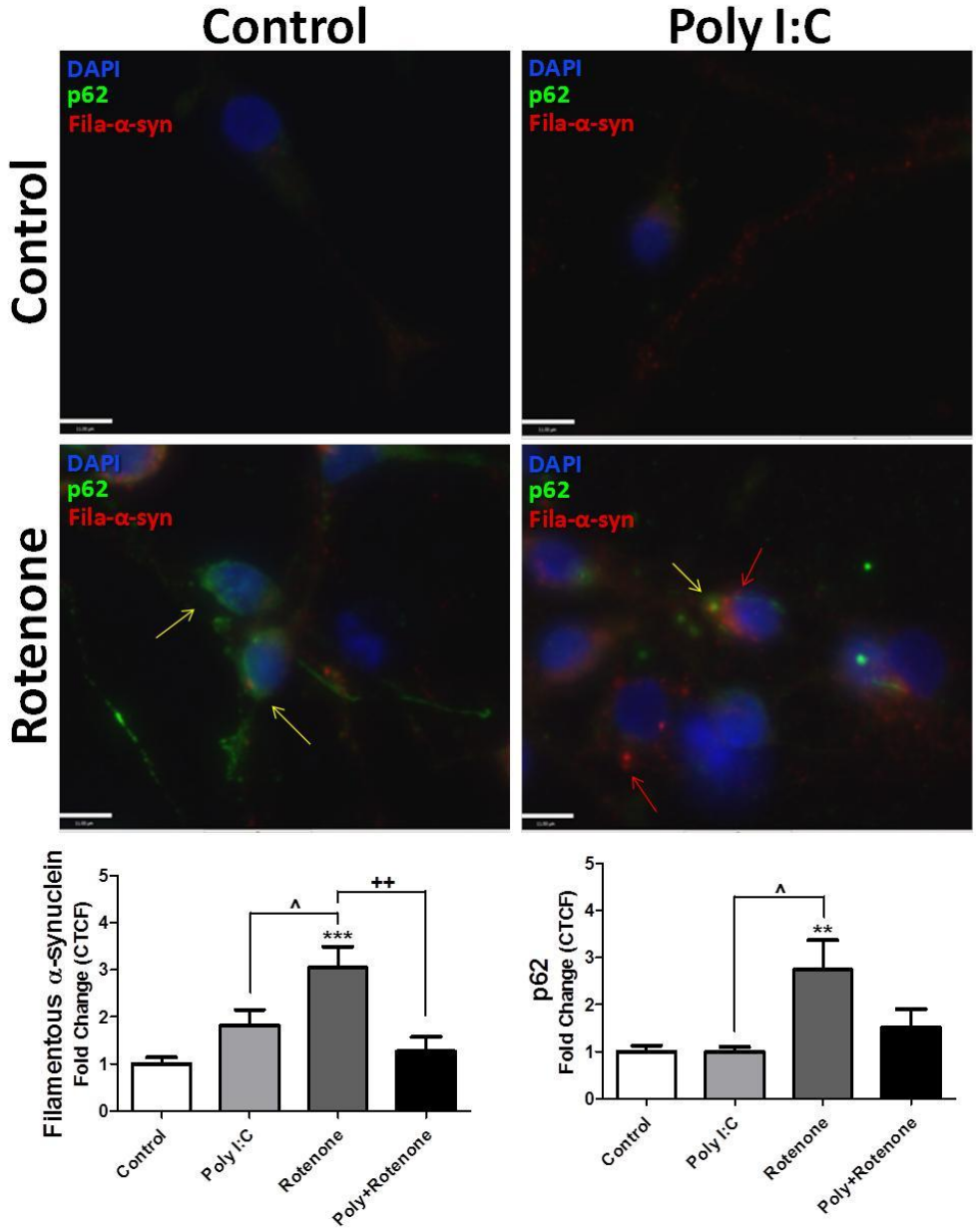

Figure 4.14. Poly I:C Priming Rotenone in E14 VM Primary Cells: Filamentous-α-synuclein and p62. Following poly I:C priming (20 µg/ml for 24 hr) in combination with rotenone (100 nM for 24 hr), E14 rat VM cells were fixed with 4% PFA, permeabilised wiTriton-X100, and immunostained for filamentous α-synuclein (red), p62 (green), and DAPI (blue). Rotenone treatment resulted in increases in p62 (yellow arrows) and filamentous α-synuclein (red arrows). Images were collected with an Olympus microscope using the 40X objective lens. Analysis was conducted using One-way ANOVA, followed by SNK *post-hoc* test. Data are presented as means and standard error of the means. Scale bar = 11 µm. **p < 0.01 vs Control, ***p < 0.001 vs Control, ^p < 0.05 vs poly I:C, $^{++}$p < 0.01 vs rotenone

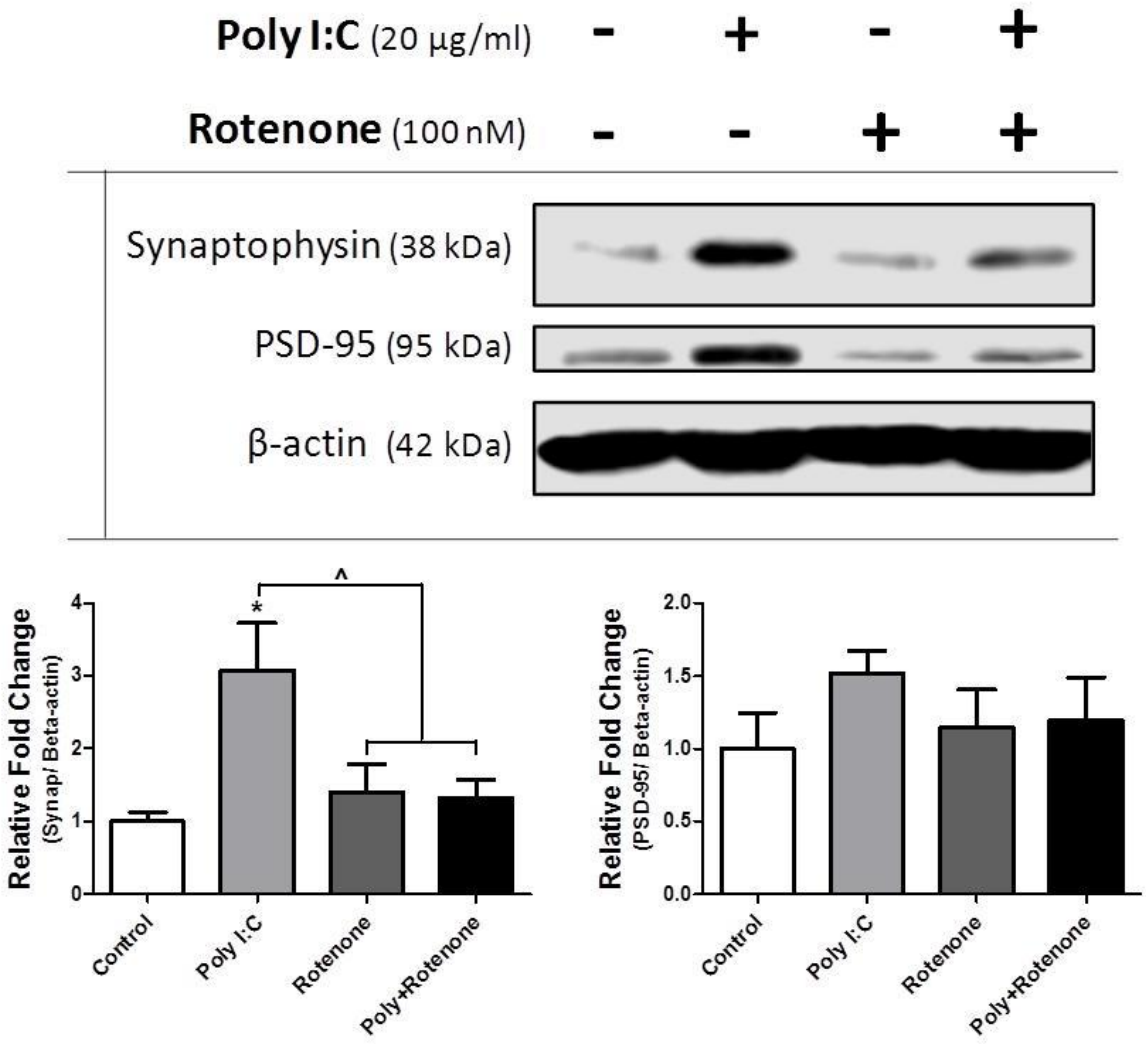

Figure 4.15. Poly I:C Priming Rotenone in E14 VM Primary Cells: Synapse Related Proteins. Following 24 hr poly I:C priming (20 µg/ml) in combination with rotenone (100 nM for 24 hr), E14 rat VM cells were extracted, lysed, and probed for synapse related proteins. Analysis was conducted using One-way ANOVA, followed by SNK *post-hoc* test. Data are presented as means and standard error of the means. *$p < 0.05$ vs Control, ^$p < 0.05$ vs poly I:C

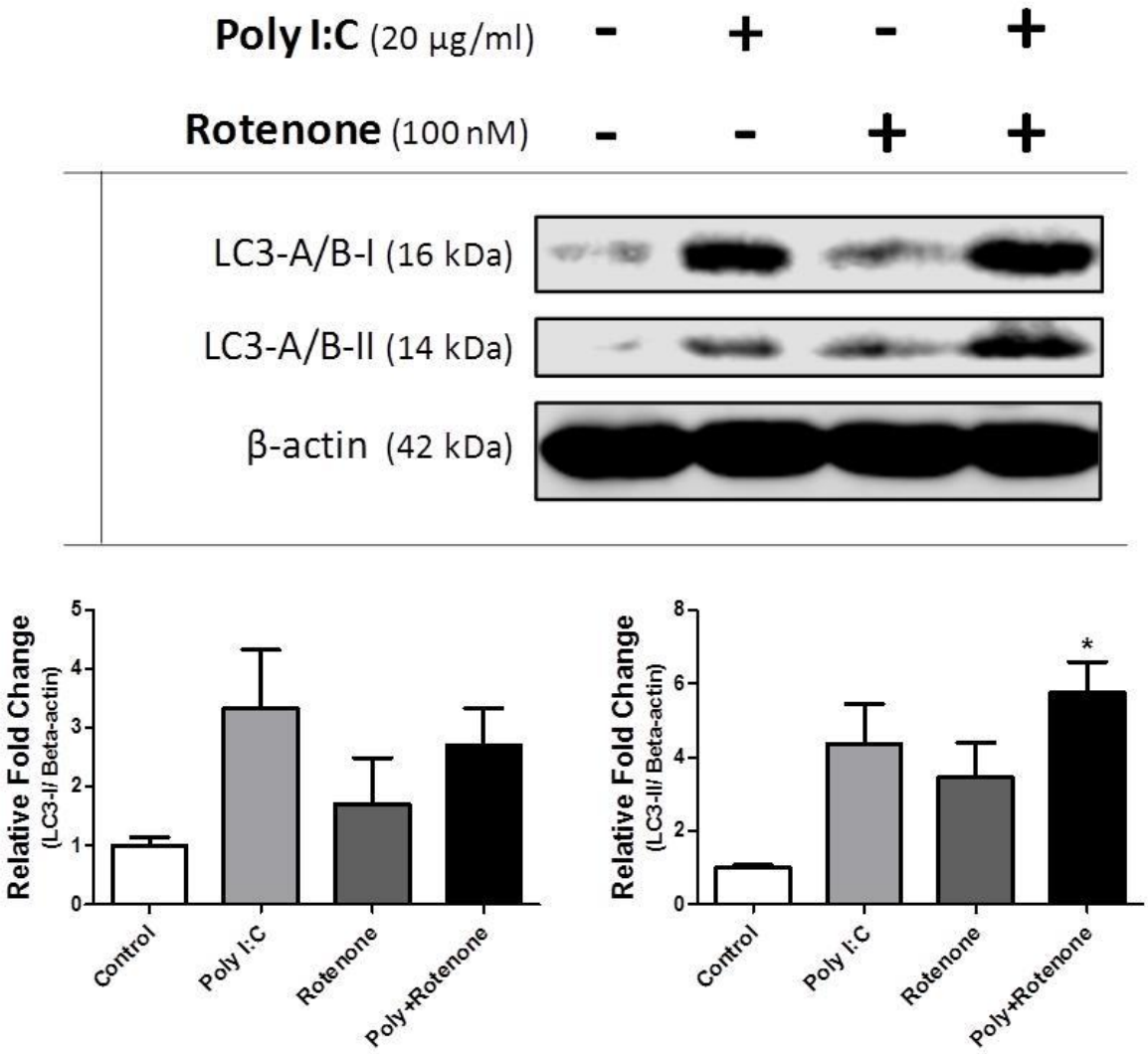

Figure 4.16. Poly I:C Priming Rotenone in E14 VM Primary Cells: LC3-a/b-I/II. Following 24 hr poly I:C priming (20 µg/ml) in combination with rotenone (100 nM for 24 hr), E14 rat VM cells were extracted, lysed, and probed for LC3-a/b-I/II. Analysis was conducted using One-way ANOVA, followed by SNK *post-hoc* test. Data are presented as means and standard error of the means. *$p < 0.05$ vs Control

4.4.4.3 Poly I:C Priming FN075 in VM Cells

Finally, viral-like poly I:C priming in combination with FN075 was investigated in primary rat VM cells to determine if poly I:C priming led to alterations in synaptic and autophagy markers. Interestingly, cells which were treated with poly I:C and FN075 were found to have a 3-fold increase in relative TH mRNA expression ($F_{(3,8)} = 8.4$, $p < 0.01$, see Fig. 4.17). Along with an increase in TH mRNA, these cells also expressed a significant 1.5-fold increase in α-synuclein mRNA expression ($F_{(3,8)} = 7.5$, $p < 0.05$). As expected, FN075 induced a significant 4.6-fold increase in filamentous α-synuclein expression in rat primary VM cells ($F_{(3,23)} = 12.5$, $p < 0.001$, see Fig. 4.18). Unexpectedly, priming with poly I:C before FN075 treatment attenuated the FN075 induced expression of filamentous α-synuclein (see Fig. 4.18), despite the increase in α-synuclein mRNA in this group.

Synapse related markers were also investigated after poly I:C priming in combination with FN075 in rat VM cells. Although synaptophysin mRNA expression was not found to change due to poly I:C or FN075 ($F_{(3,8)} = 1.9$, $p > 0.05$, see Fig. 4.17), poly I:C was found to increase relative synaptophysin protein expression when compared to the FN075 alone group ($F_{(3,8)} = 5.5$, $p < 0.05$, see Fig. 4.19). Conversely, poly I:C and FN075 was found to reduce relative PSD-95 mRNA expression by 0.7-fold ($F_{(3,8)} = 22.8$, $p < 0.001$, see Fig. 4.17). The effect of poly I:C on PSD-95 mRNA expression may have not been present in previous experiments due to the timing of the cell extraction. In this experiment, the FN075 treatment was extended to 48 hr, resulting in a total 72 hr poly I:C treatment compared to a 48 hr treatment in previous experiments. Despite this decrease in PSD-95 mRNA, neither poly I:C nor FN075 decreased PSD-95 protein expression (see Fig. 4.19). However, there was a significant

combined effect, with poly I:C in combination with FN075 producing a 1.5-fold increase in relative PSD-95 protein expression ($F_{(3,8)} = 8.6$, $p < 0.01$).

Unlike the poly I:C/rotenone combination experiments, priming with poly I:C in combination FN075 resulted in fewer changes to autophagic markers. Immunostaining found FN075 to result in a 2.6-fold, but statistically insignificant, increase in p62 in rat primary VM cells (see Fig. 4.18). However, poly I:C priming exacerbated this effect, leading to a 2.7-fold significant increase in p62 ($K = 13.4$, $p < 0.001$). Conversely, poly I:C priming in combination with FN075 in these cells led to a 0.6-fold (see Fig. 4.20), albeit statistically insignificant, decrease in the active form of LC3-a/b-II ($F_{(3,8)} = 2.9$, $p > 0.05$). There was also no significant change in LC3-a/b-I expression after poly I:C or FN075 treatment ($F_{(3,8)} = 1.9$, $p > 0.05$).

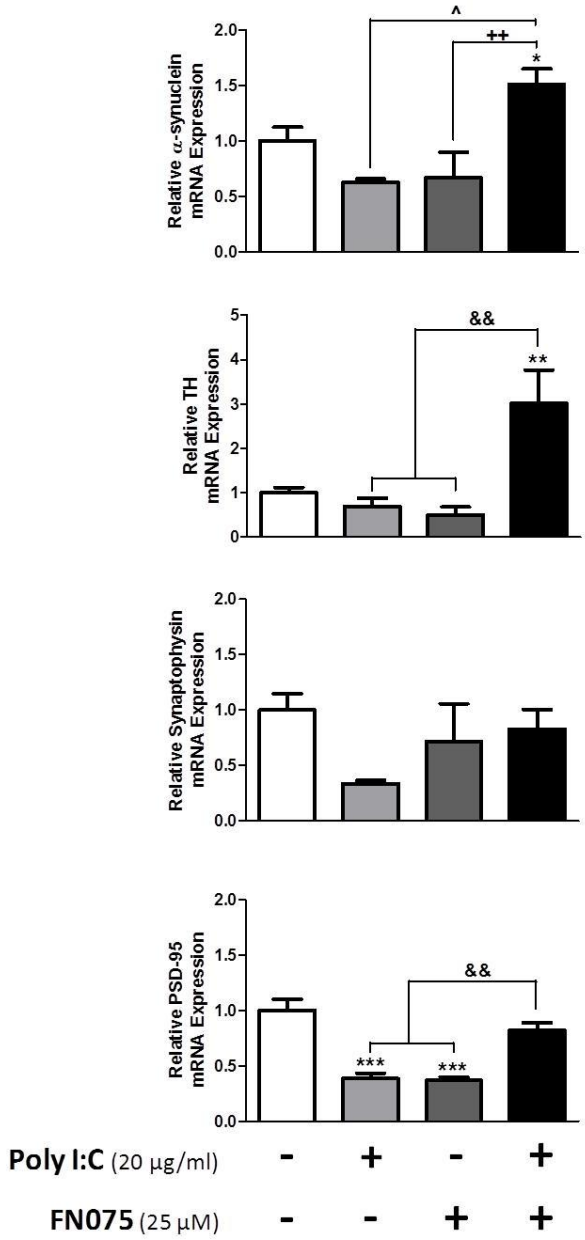

Figure 4.17. Poly I:C Priming FN075 in E14 VM Primary Cells: Synaptic Related mRNA Expression. E14 rat VM cells were primed with poly I:C (20 µg/ml) for 24 hr prior to a FN075 (25 µM) 48 hr treatment. Cells were extracted, lysed for mRNA, and probed with synapse related primers. The data was transformed by calculating the relative change in ΔCp values. Analysis was conducted using One-way ANOVA, followed by SNK *post-hoc* test. Data are presented as means and standard error of the means. *$p < 0.05$ vs Control, **$p < 0.01$ vs Control, ***$p < 0.001$ vs Control, ^$p < 0.05$ vs poly I:C, $^{++}p < 0.01$ vs FN075, $^{\&\&}p < 0.01$ vs poly I:C+FN075

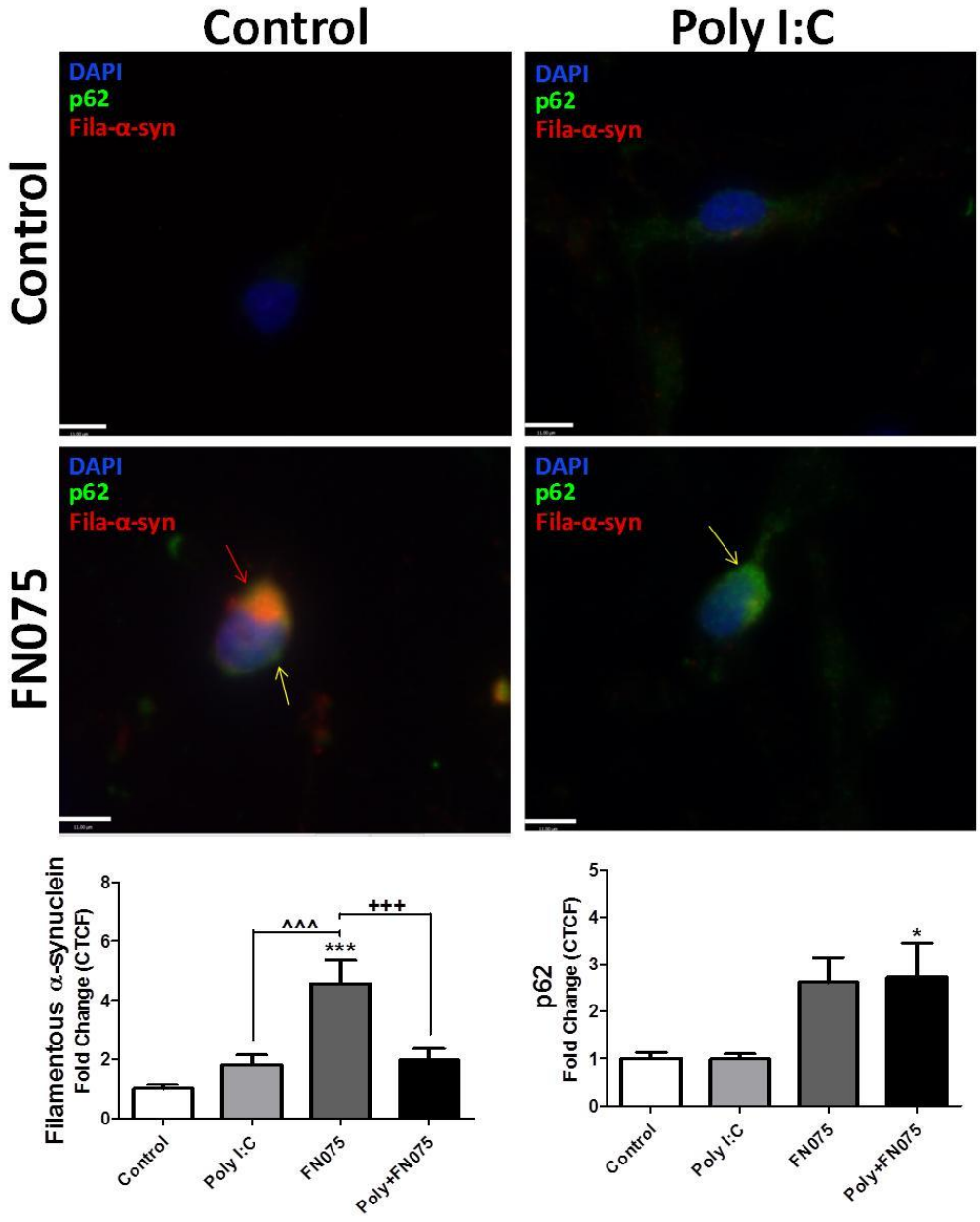

Figure 4.18. Poly I:C Priming FN075 in E14 VM Primary Cells: Filamentous-α-synuclein and p62. Following poly I:C priming (20 µg/ml for 24 hr) in combination with FN075 (25 µM for 48 hr), E14 rat VM cells were fixed with 4% PFA, permeabilised wiTriton-X100, and immunostained for filamentous α-synuclein (red), p62 (green), and DAPI (blue). FN075 treatment resulted in increases in p62 (yellow arrows) and filamentous α-synuclein (red arrows). Images were collected with an Olympus microscope using the 40X objective lens. Analysis was conducted using One-way ANOVA, followed by SNK *post-hoc* test. Data are presented as means and standard error of the means. Scale bar = 11 µm. *$p < 0.05$ vs Control, ***$p < 0.001$ vs Control, ^^^$p < 0.001$ vs poly I:C, $^{+++}p < 0.001$ vs FN075

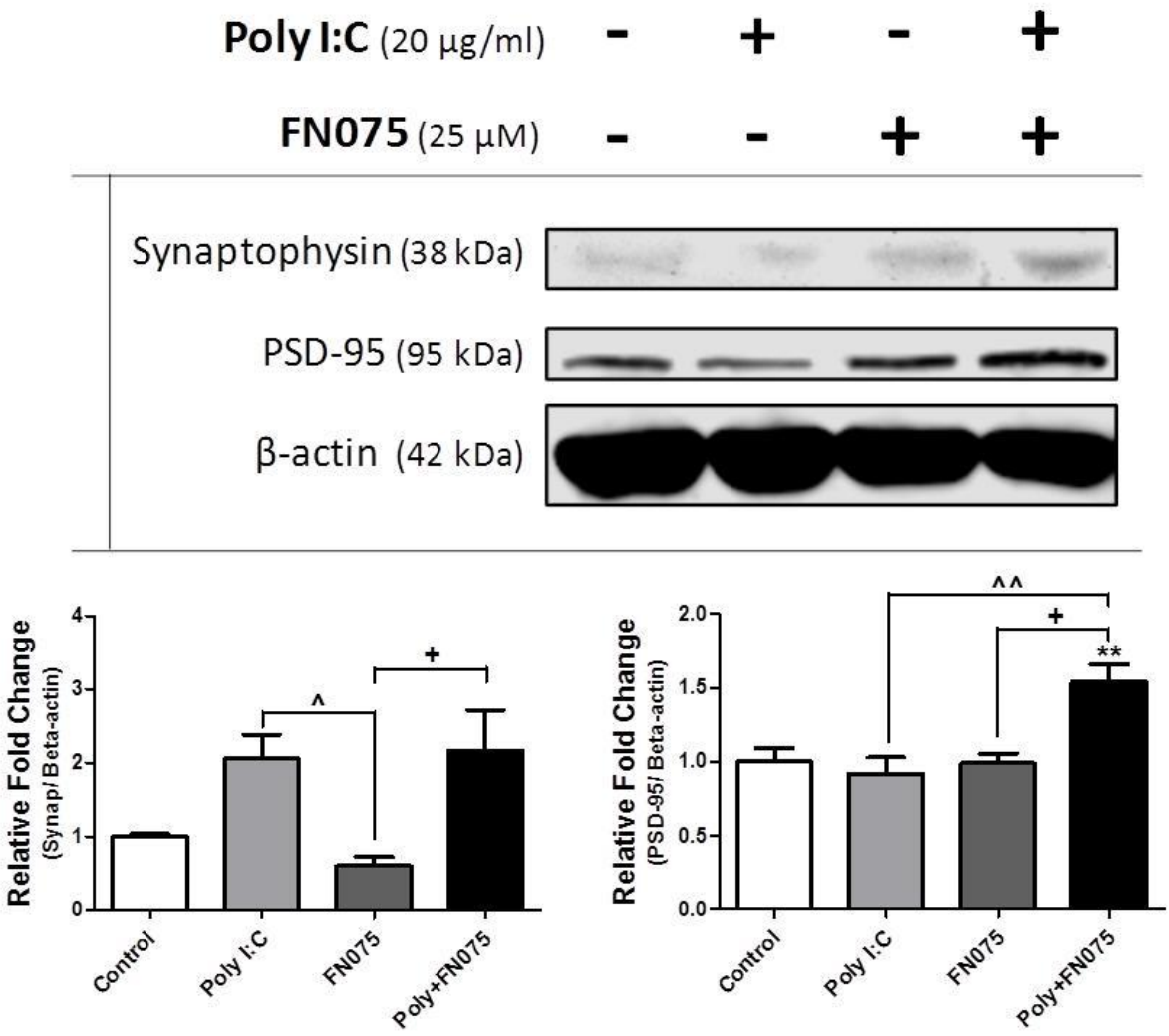

Figure 4.19. Poly I:C Priming FN075 in E14 VM Primary Cells: Synapse Related Proteins. Following 24 hr poly I:C priming (20 µg/ml) in combination with FN075 (25 µM for 48 hr), E14 rat VM cells were extracted, lysed, and probed for synapse related proteins. Analysis was conducted using One-way ANOVA, followed by SNK *post-hoc* test. Data are presented as means and standard error of the means. **$p < 0.01$ vs Control, ^$p < 0.05$ vs poly I:C, ^^$p < 0.01$ vs poly I:C, $^{+}p < 0.05$ vs FN075

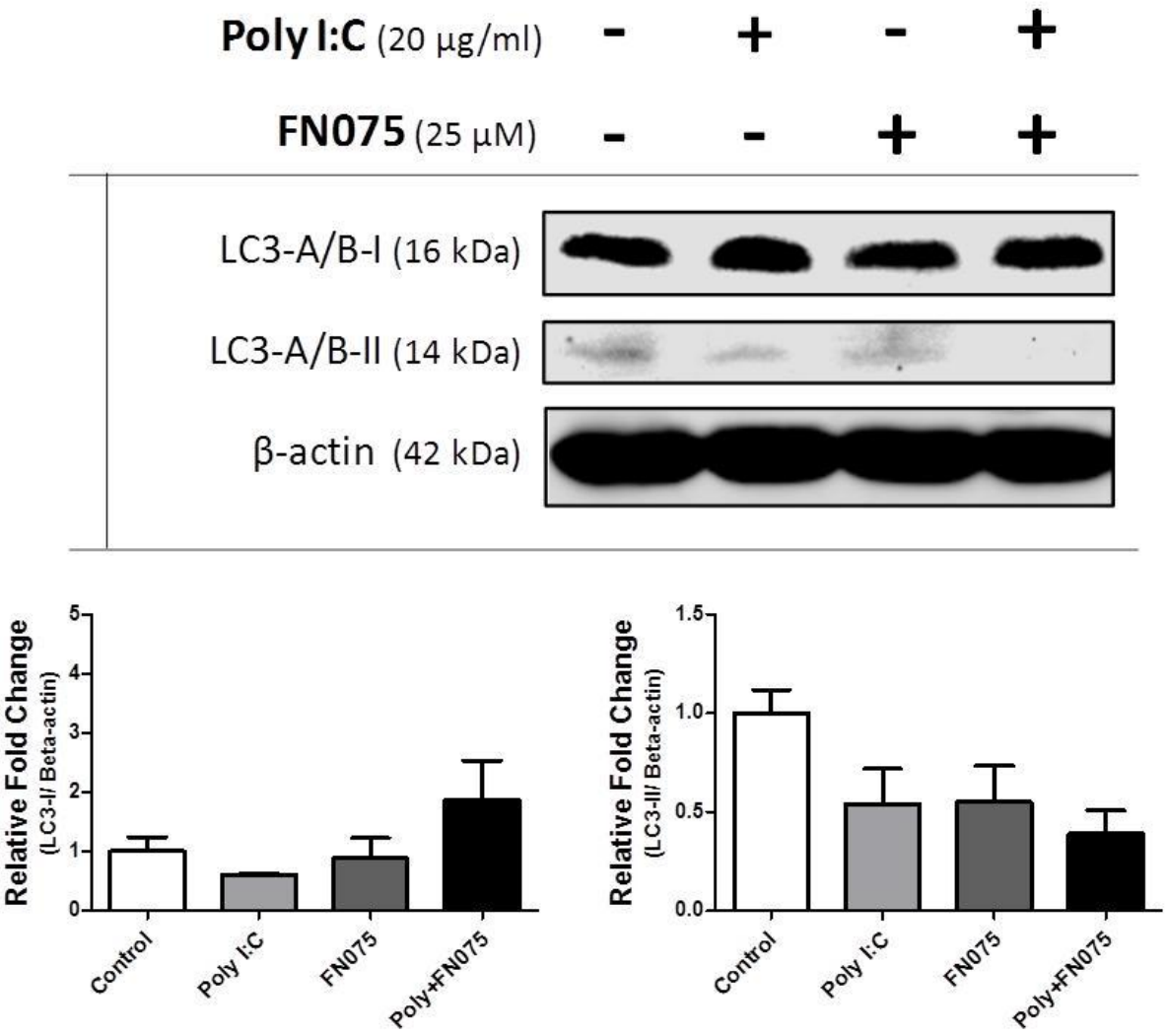

Figure 4.20. Poly I:C Priming FN075 in E14 VM Primary Cells: LC3-a/b-I/II. Following 24 hr poly I:C priming (20 µg/ml) in combination with FN075 (25 µM for 48 hr), E14 rat VM cells were extracted, lysed, and probed for LC3-a/b-I/II. Analysis was conducted using One-way ANOVA, followed by SNK *post-hoc* test. Data are presented as means and standard error of the means.

4.5 DISCUSSION

The results of this chapter further support our hypothesis that viral-like poly I:C priming might exacerbate neurodegeneration and neuropathological features common in PD. As expected, poly I:C priming in primary rat VM mixed cultures led to NF-κB nuclear translocation and excessive cytokine release. This finding was not surprising due to the pro-inflammatory nature of the glial cells present in the mixed culture. However, since very few experiments have been conducted using primary rat VM cells, these results are relatively novel. Previous experiments have mostly used LPS (a TLR4 ligand) to induce an inflammatory response in primary rat VM cells, which led to significant dopaminergic cell death in these cultures (Jeohn et al., 2002, Peng et al., 2005). Along with a pro-inflammatory response, poly I:C was also able to induce significant dopaminergic cell loss and reduce cell viability. It is worth noting that although poly I:C induced a significant reduction in cell viability, the assay is not able to distinguish between different cell types. Although immunostaining was able to confirm poly I:C induced dopaminergic neurodegeneration in the mixed VM cell cultures, it is unclear if other neuronal or glial cell types undergo cell death after poly I:C treatment.

Toxin	**6-OHDA**			**Rotenone**			**FN075**		
Result	P	6	P+6	P	R	P+R	P	F	P+F
TH	↓	↓↓	↓↓	↓	↓↓	↓↓	↓	↓	↓
α-syn	NC	↑	↑↑	NC	↑	NC	NC	↑	NC
p62	NC	↑	↑	NC	↑	NC	NC	↑	↑↑
LC3	NC	NC	NC	NC	NC	NC	NC	NC	↑
PSD-95	NC	NC	NC	NC	NC	NC	NC	NC	↑
Synap	↑	NC	NC	↑	NC	NC	↑	↓	↑↑

Table 4.1. Summary of Protein Changes.

In the poly I:C priming experiments, poly I:C was found to exacerbate 6-OHDA and rotenone induced decreases in cell viability. However, no poly I:C priming combination found poly I:C to exacerbate neurotoxin induced dopaminergic neurodegeneration. This finding suggests that poly I:C exacerbation of cell death with 6-OHDA and rotenone as measured by the MTT assay is due to non-dopaminergic cell death. Since the VM dissection includes tissue which matures into other brain regions besides the SN, the VM primary cultures include other neuronal cell types. The death of these cells might explain the synergistic effect seen after poly I:C priming in combination with 6-OHDA or rotenone, but the fact that some glial cells (such as astrocytes) continue to replicate in cell culture (compared to the differentiated neurons) further confounds the interpretation of these results. However, poly I:C treatment/poly I:C induced inflammation led to consistent changes in synaptic and autophagy related proteins. Poly I:C treatment appeared to increase synaptophysin expression across all groups. Contrary to the SH-SY5Y findings from Chapter 3, priming with poly I:C in combination with FN075 led to a further increase in synaptophysin. More consistent with the findings in the neuroblastoma cell line, poly I:C priming in combination with FN075 resulted in an increase PSD-95. As previously mentioned, few primary VM experiments have investigated viral-like inflammation. However, previous studies investigating the effects of LPS in primary rat VM cells found LPS priming to exacerbate neurotoxin induced cell death, which was suggested to be at least partially NMDA mediated (McNaught et al., 2002). The association between PSD-95 and NMDAR may contribute to the increase in PSD-95 seen in these cells after poly I:C priming before FN075 treatment.

Similar to the findings in SH-SY5Y cells from chapter 3 experiments, there were only consistent changes in p62 expression, not LC3-a/b-I/II. The only significant

changes in LC3-a/b-II were due to poly I:C priming in combination with rotenone. However, all the neurotoxins (6-OHDA, rotenone, and FN075) were found to increase p62 expression, similar to the SH-SY5Y findings. Interestingly, priming with poly I:C attenuated this increase in p62 expression when poly I:C priming was in combination with rotenone, which was also similar to the SH-SY5Y findings. It is worth noting that this is also the only combination which led to increases in LC3-a/b-I/II. Previous experiments investigating ubiquitin-dependent protein degradation in primary rat VM cells found proteasomal inhibition to lead to α-synuclein cytoplasmic inclusions and apoptosis in TH^+ neurons (Rideout et al., 2005). It is possible that a neurotoxin induced increase in p62 is meant to be neuroprotective. However, the poly I:C priming combination (poly I:C in combination with FN075) which found the largest increase in p62 expression also found significant changes in synaptic related proteins, with increases in both synaptophysin and PSD-95. With this in mind, it is unclear if these changes in protein expression (autophagy or synaptic) are neuroprotective or neurotoxic.

As previously mentioned, the cells used in this study are a mixed population. Although primary mixed cells are helpful for examining the effect of a compound in a system of cells which interact with each other, there are technical limitations to consider. Besides immunostaining for TH, the experiments conducted in this chapter did not distinguish between cell type for mRNA or protein analysis. Therefore, the results cannot be attributed to changes in dopaminergic cells. It is suggested that future studies use a technique such as cell sorting to collect TH immunopositive cells for protein analysis.

Although poly I:C priming was found to alter cell death, autophagy, and synaptic protein expression in primary rat VM cells, the effects seem to be context specific, with no poly I:C+neurotoxin combination exhibiting any consistency in molecular changes.

More sophisticated techniques for measuring alterations in dopaminergic neurons only may be able to better explore the effects of poly I:C in primary VM cultures.

Chapter Five: *In vivo* Results

CHAPTER FIVE

5.1 INTRODUCTION

Since Chapter 3 and Chapter 4 found viral-like poly I:C priming to alter the neurodegenerative effects of neurotoxins used in pre-clinical models of PD in cell culture, further investigation was conducted in a living animal system. Although all poly I:C priming combinations demonstrated significant changes to cell death, synapse, and autophagy related markers, suggesting viral infections may contribute to the neurotoxicity of PD related neuropathology, the poly I:C and FN075 combination was chosen for *in vivo* experimentation. Exploring the effects of viral-like poly I:C priming in combination with FN075 induced α-synuclein aggregation was chosen because of the novel features of FN075. Also, unlike 6-OHDA or MPP^+, viral-related neuroinflammation in combination with α-synuclein aggregation has yet to be investigated *in vivo* (Deleidi et al., 2010, Sadasivan et al., 2017).

The E14 primary rat VM cells were harvested from Sprague-Dawley rats for all Chapter 4 experiments. Therefore, it was decided to use Sprague-Dawley rats for *in vivo* experimentation. Rats are the most commonly used animal for pre-clincal experiments (Fagundes and Taha, 2004). Sprague-Dawley rats were obtained and further developed by Charles River Laboratories in 1950 for experimental research (White and Cham, 1998). Although rats are not responsive to MPP^+ treatment (Bové and Perier, 2012), it has been suggested that rats are preferable to mice to study α-synuclein pathology (Nuber et al., 2013).

Similar to Chapter 3 and 4, the poly I:C priming was conducted (via uni-lateral injection of poly I:C into the SN) prior to FN075 administration. After poly I:C priming, FN075 was intra-nigrally injected to induce α-synuclein 2 weeks post poly I:C injection.

Viral-like poly I:C priming induced modulation of neurodegeneration, synaptic function, and autophagy in the SN were all investigated by measuring protein changes in the SN using immunohistochemistry.

5.2 METHODS

The methods used in this chapter did not differ in any way from those outlined in chapter two, unless otherwise stated.

5.3 EXPERIMENTAL DESIGN

Previous preliminary experiments conducted by other lab group members suggested the optimal dose to induce neuroinflammation in the rat SN was 30 µg of poly I:C. Therefore, Sprague-Dawley rats received intra-nigral injection of poly I:C, followed 2 weeks later by intra-nigral injection of FN075 (1.9 µg), resulting in four distinct treatment groups (see Fig. 5.1). Behavioural analyses (Stepping Test and Whisker Test) were conducted throughout the experiment (see Fig. 5.1). At 8 weeks post FN075 injection, rat brains were extracted and fixed with 4% PFA for immunohistochemical analysis. FN075 induced α-synuclein aggregation was confirmed by measuring relative density of filamentous α-synuclein. Cell death was assessed by measuring the percentage of TH^+ neurons in the SN compared to the uninjected contralateral side. The percentage of $GFAP^+$ astrocytes and $OX42^+$ microglia in the SN, and the relative density of $GFAP^+$ astrocytes and $OX42^+$ microglia in the STR were quantified to determine changes in neuroinflammation. Pre-synaptic synaptophysin and post-synaptic PSD-95 proteins were probed to investigate changes in synaptic function. Relative density was measured for both, but synaptophysin inclusions were also quantified. Changes in autophagy after poly I:C priming in combination with FN075 were determined by measuring $p65^+$ cells within the SN. The experimental design is detailed in Figure 5.2.

A

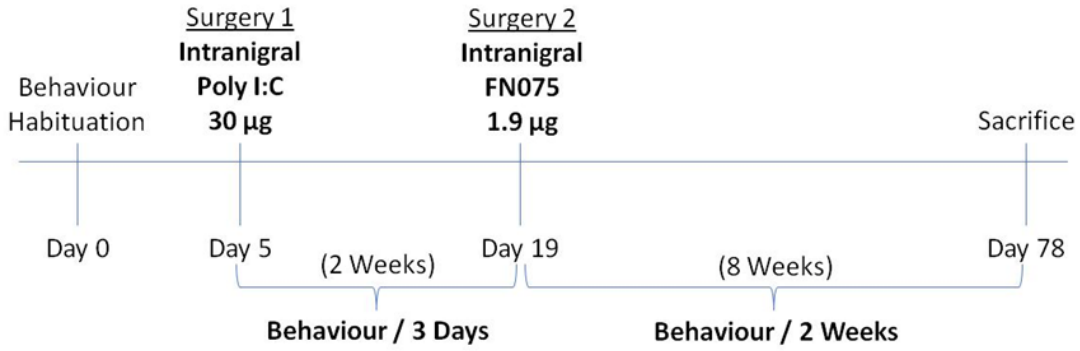

B

Group	Poly I:C Injection	FN075 Injection	N
Control	Vehicle	Vehicle	7
Poly I:C	Poly I:C	Vehicle	8
FN075	Vehicle	FN075	8
Poly I:C & FN075	Poly I:C	FN075	8

Figure 5.1. Surgery Groups and Timeline. (A) After behavioural habituation and baseline assessment, male Sprague-Dawley rats were performance matched into two groups for intra-nigral infusion of poly I:C (30 µg in 4 µl) or vehicle. They were then re-tested on the motor tests every 3 days for 2 wk after which they were again performance matched for subsequent intra-nigral infusion of FN075 (1.9 µg in 4 µl) or vehicle to give four final groups (B). Motor function testing resumed 1 wk after surgery and continued every 2 wk for 8 wk, after which rats were sacrificed for quantitative histology.

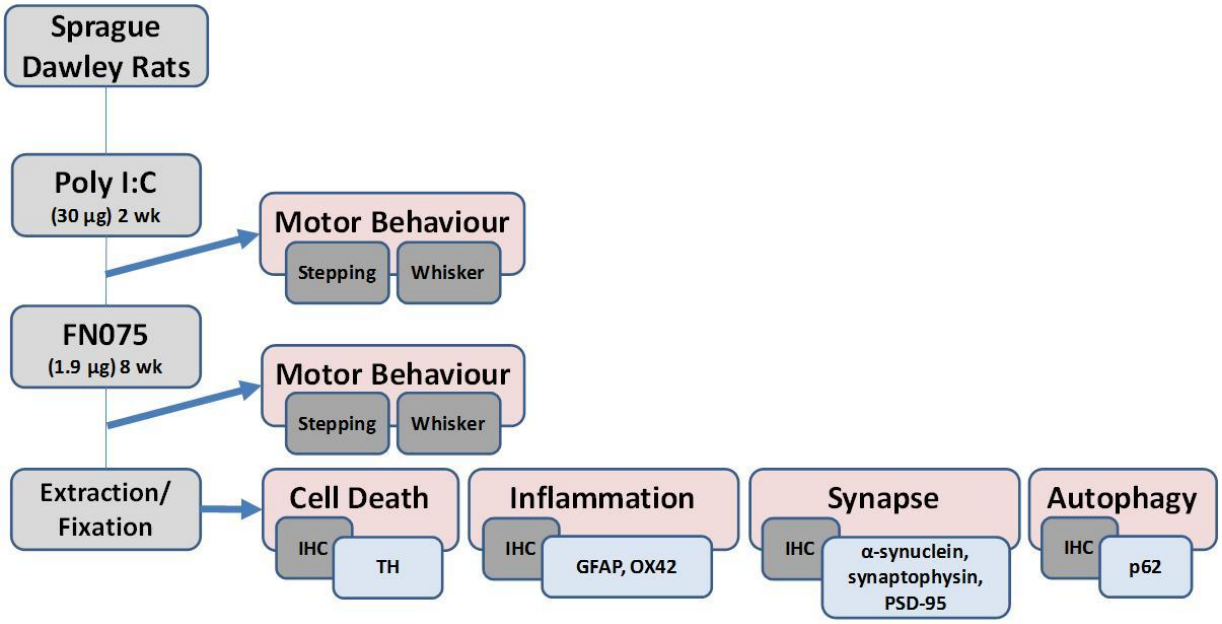

Figure 5.2. Chapter 5 Experimental Design. Sprague-Dawley rats received a unilateral intra-nigral injection of poly I:C (30 µg), followed 2 wk later by a subsequent intra-nigral injection of FN075 (1.9 µg). At 8 wk post FN075 injection, rat brains were extracted and fixed with PFA for IHC analysis.

5.4 RESULTS

5.4.1. Motor Dysfunction After Sequential Poly I:C and FN075 Administration

Sprague-Dawley rats received a uni-lateral intra-nigral injection of poly I:C (30 µg), followed 2 weeks later by a subsequent uni-lateral intra-nigral injection of FN075 (1.9 µg). After intra-nigral injection of poly I:C/vehicle and FN075/vehicle, behavioural tests were administered to assess motor function. Initially, there was a transient motor deficit due to intra-nigral administration of poly I:C ($p < 0.05$, see Fig. 5.3 and Fig. 5.4). Two weeks post-poly I:C injection, there was no significant motor deficit ($p > 0.05$, see Fig. 5.3 and Fig. 5.4). Following intra-nigral FN075, it was found that poly I:C priming in combination with FN075 led to significant motor deficits (see Fig. 5.3 and Fig. 5.4). For the Stepping Test of forelimb akinesia, there was no significant main effect of treatment ($F_{(3,108)} = 2.0$, $p > 0.05$) but there was a significant main effect of time ($F_{(4,108)} = 6.6$, $p < 0.001$). There was also a significant interaction between treatment and time ($F_{(12,108)} = 3.7$, $p < 0.001$). According to Bonferroni *post-hoc* tests, the group which received subsequent injections of poly I:C and FN075 made 5-6 fewer (or ~50% fewer) contralateral forepaw adjustments during the Stepping Test ($p < 0.05$, $p < 0.01$) by week 7/9 compared to the all other groups (see Fig. 5.3). This effect was unique to the poly I:C primed group, with no reduction in forepaw adjustments after injection of poly I:C alone ($p > 0.05$) or FN075 alone ($p > 0.05$). Similarly, poly I:C primed rats which received FN075 exhibited significant motor deficits at week 7 ($K = 14.3$, $p < 0.01$) and week 9 ($K = 13.2$, $p < 0.01$) (Fig. 5.4). Neither poly I:C ($p > 0.05$) nor FN075 ($p > 0.05$) alone induced any motor deficits in this test.

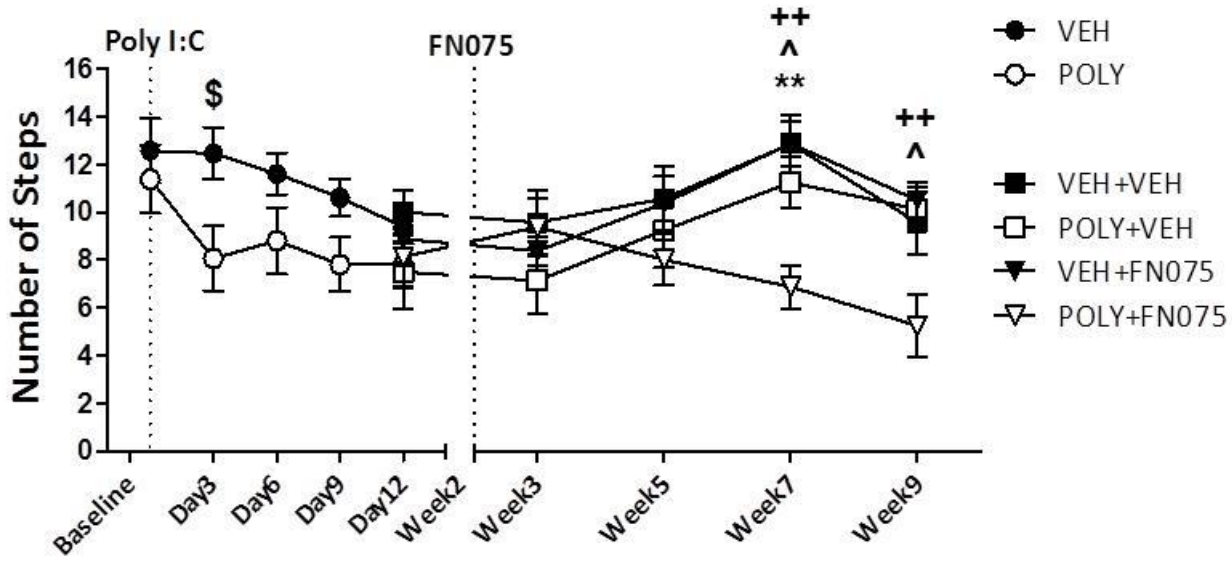

Figure 5.3. Contralateral Forelimb Akinesia Stepping Test. After intra-nigral injection of poly I:C, the Stepping Test was conducted every 3 days. Proceeding FN075 intra-nigral injection 2 weeks after poly I:C injection, the Stepping Test was assessed every 2 weeks. The unrestrained contralateral forelimb was guided across a 90 cm table top for 5 s and the number of forepaw adjustments were recorded. Analysis was conducted using a Two-way ANOVA, followed by Bonferroni *post-hoc* test. Data are presented as means and standard errors of the mean. **$p < 0.01$ vs Control, ^$p < 0.05$ vs poly I:C, $^{++}p < 0.01$ vs FN075, $^{\$}p < 0.05$ vs Control

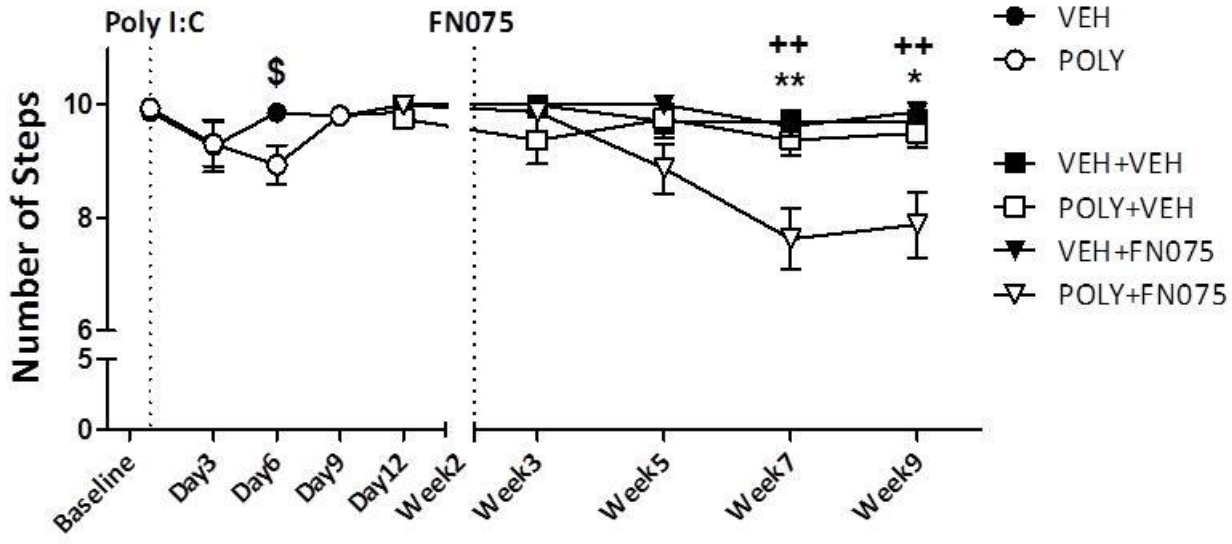

Figure 5.4. Contralateral Forelimb Whisker Test. After intra-nigral injection of poly I:C, the Whisker Test was conducted every 3 days. Proceeding FN075 intra-nigral injection 2 weeks after poly I:C injection, the Whisker Test was assessed every 2 weeks. The number of vibrissae-elicited forelimb placement steps (out of 10) when the rat's whiskers were brushed against the side of a table top were recorded. Analysis was conducted using a Kruskal-Wallis test for each time point, followed by Dunn's multiple comparison *post-hoc* test. Data are presented as means and standard errors of the mean. *$p < 0.05$ vs Control, **$p < 0.01$ vs Control, $^{++}p < 0.01$ vs FN075, $^{\$}p < 0.05$ vs Control

5.4.2. FN075 Promotes Filamentous α-synuclein Aggregation *In vivo*

As expected from *in vitro* and cell culture experiments, IHC assessment found intra-nigral injection of FN075 to induce significant increases in filamentous α-synuclein in the rat SN ($F_{(3,11)}$ = 21.1, $p < 0.0001$). At 8 wk post-FN075 injection, there was approximately a 10% increase in the density of filamentous α-synuclein in the injected SN compared to groups not injected with FN075 (see Fig. 5.5). It is worth noting that poly I:C priming did not modify the FN075-induced α-synuclein aggregation as measured by the filamentous-specific-α-synuclein antibody ($p > 0.05$). Also, these nigral α-synuclein aggregates did not appear to precipitate α-synuclein aggregation in the striatum at the 8 week time point ($F_{(3,11)}$ = 0.5, $p > 0.05$, see Fig. 5.6), with no significant changes in the density of filamentous α-synuclein after poly I:C or FN075 treatment. The lack of filamentous α-synuclein in the rat STR suggests that although FN075 was able to induce α-synuclein aggregation at the site of injection, this effect was not spread to innervating regions.

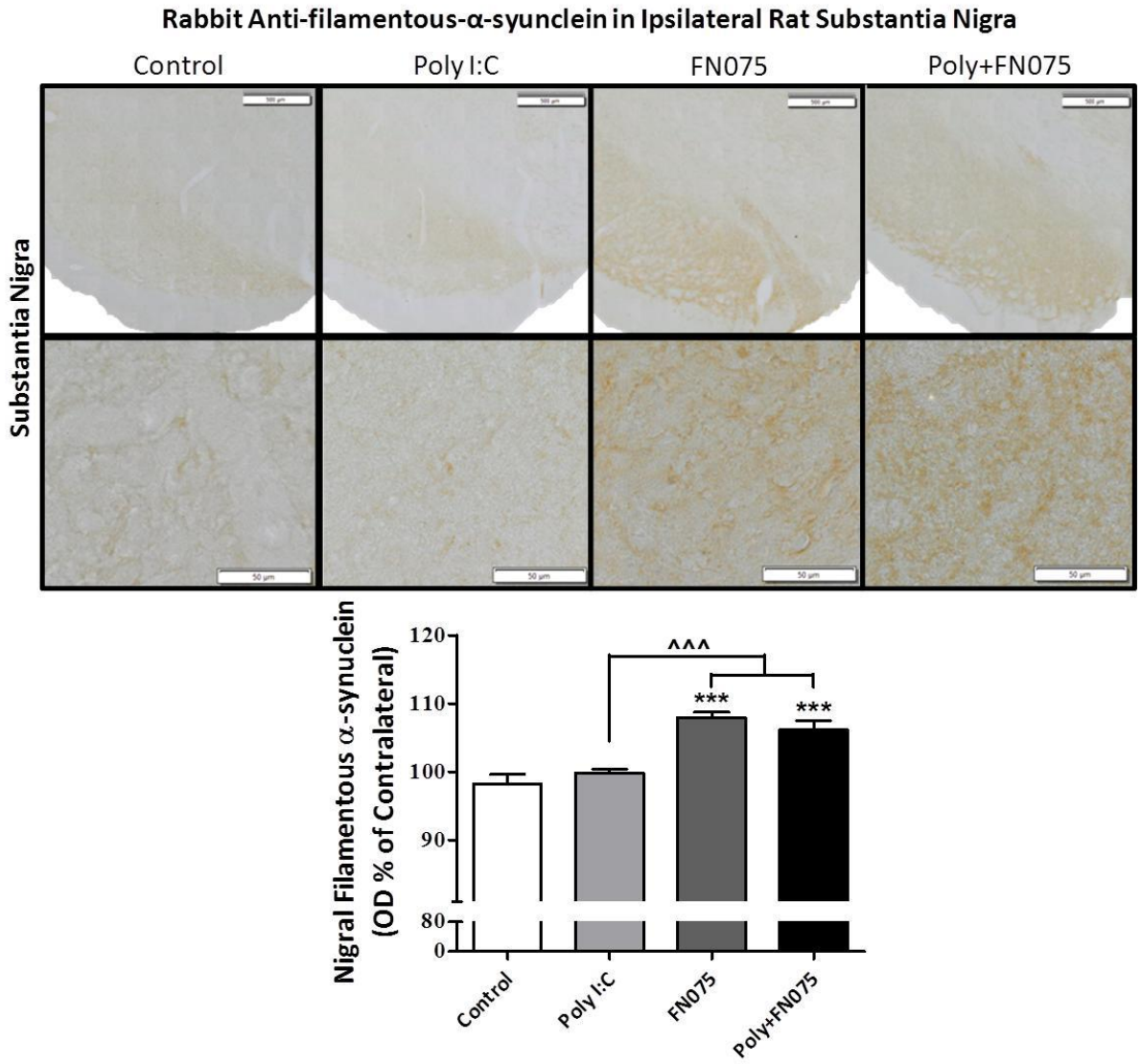

Figure 5.5. Filamentous α-synuclein in the Rat Substantia Nigra. After sequential intra-nigral injection of poly I:C and FN075, brains were 4% PFA fixed for free-floating IHC-DAB analysis. SN tissue (30 µm) was immunostained for filamentous-α-synuclein. Mounted tissue was imaged using an Olympus VS120 slide scanner. Data was quantified by comparing the nigral optical density to the contralateral (uninjected side of the brain) SN. Analysis was conducted using One-way ANOVA, followed by SNK *post-hoc* test. Data are presented as means and standard errors of the mean. Scale bar in whole SN = 500 µm. Scale bar in SN = 50 µm. ***$p < 0.001$ vs Control, ^^^$p < 0.001$ vs poly I:C

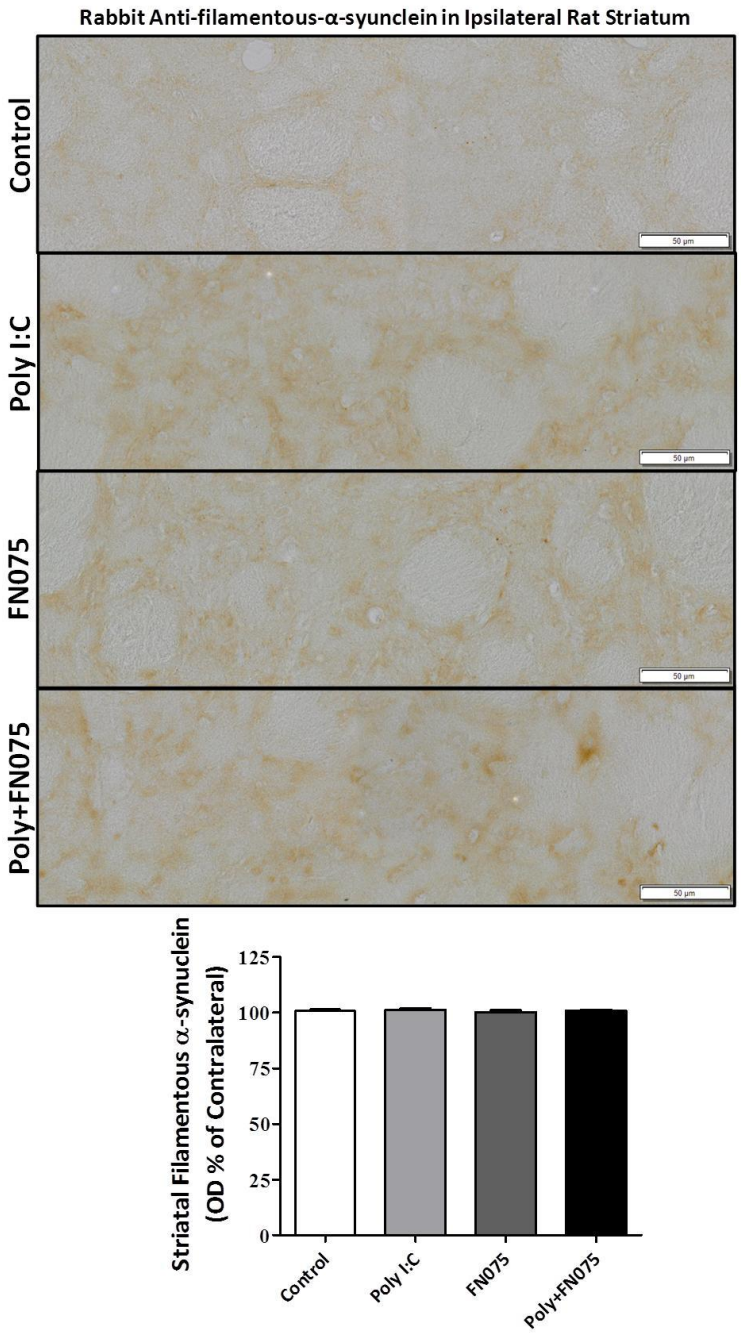

Figure 5.6. Filamentous α-synuclein in the Rat Striatum. After sequential intra-nigral injection of poly I:C and FN075, brains were 4% PFA fixed for free-floating IHC-DAB analysis. STR tissue (30 µm) was immunostained for filamentous-α-synuclein. Mounted tissue was imaged using an Olympus VS120 slide scanner. Data was quantified by comparing the striatal optical density to the contralateral (uninjected side of the brain) STR. Analysis was conducted using One-way ANOVA, followed by SNK *post-hoc* test. Data are presented as means and standard errors of the mean. Scale bar = 50 µm.

5.4.3. Poly I:C Priming of FN075 Precipitates Nigral Neurodegeneration *In vivo*

Nigrostriatal integrity was assessed by quantifying the neurodegenerative effects of poly I:C and/or FN075. Nigral and striatal rat tissue immmunostained for tyrosine hydroxylase determined that neither poly I:C ($p > 0.05$) nor FN075 ($p > 0.05$) alone induced nigral or striatal dopaminergic neurodegeneration (see Fig. 5.7 and Fig. 5.8). Instead, when poly I:C and FN075 were sequentially administered in the SN, a pronounced synergistic reduction in dopaminergic neurons was found ($F_{(3,11)} = 5.5$, $p = 0.015$, see Fig. 5.6). Poly I:C priming in combination with FN075 induced α-synuclein aggregation resulted in a 32% decrease in TH^+ neurons compared to the control group ($p < 0.05$). Although there was a significant reduction in TH^+ neurons in the SN at the 8 wk time point, this did not correspond with a decrease in TH^+ nerve terminals innervating the STR ($F_{(3,11)} = 1.0$, $p > 0.05$, see Fig. 5.8), with no changes in TH density after poly I:C or FN075 treatment.

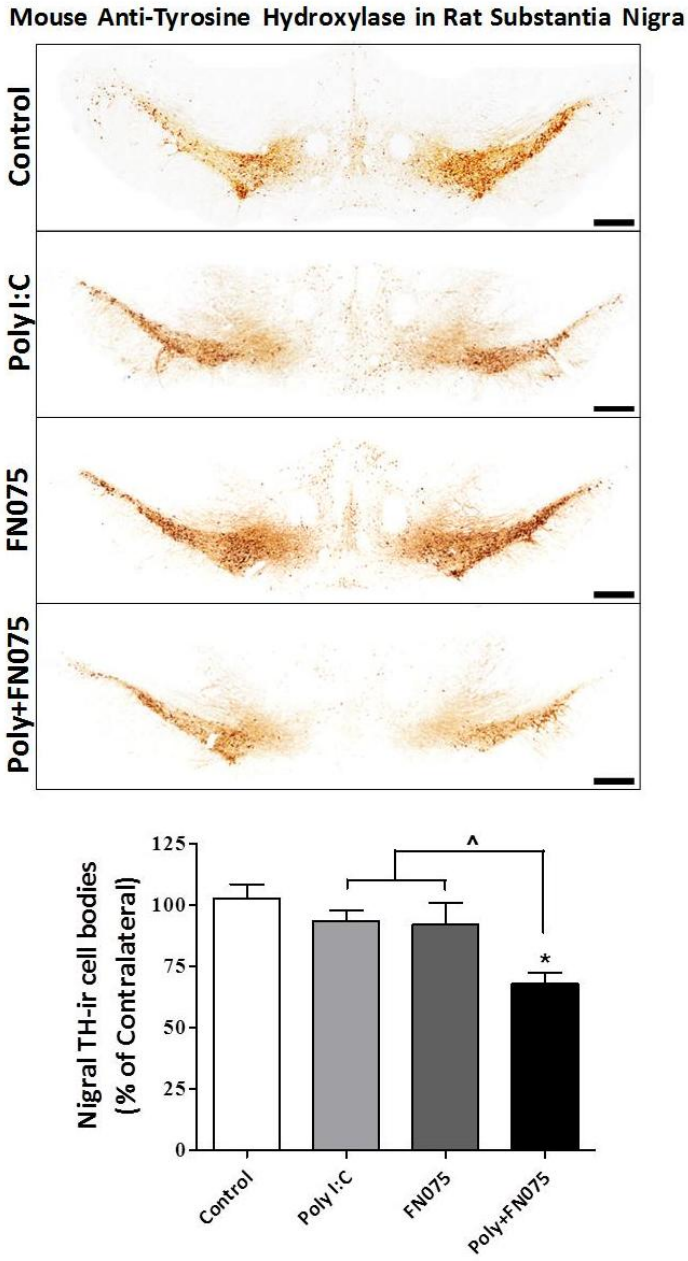

Figure 5.7. Nigral TH$^+$ Cell Bodies. After sequential intra-nigral injection of poly I:C and FN075, brains were 4% PFA fixed for free-floating IHC-DAB analysis. SN tissue (30 µm) was immunostained for tyrosine hydroxylase. Mounted tissue was imaged using an Olympus VS120 slide scanner. Data was quantified by comparing the number of nigral TH$^+$ cell bodies to the contralateral (uninjected side of the brain) SN. Above, the right SN image is ipsilateral. Analysis was conducted using One-way ANOVA, followed by SNK *post-hoc* test. Data are presented as means and standard errors of the mean. Scale = 500 µm. *$p < 0.05$ vs Control, ^$p < 0.05$ vs poly I:C

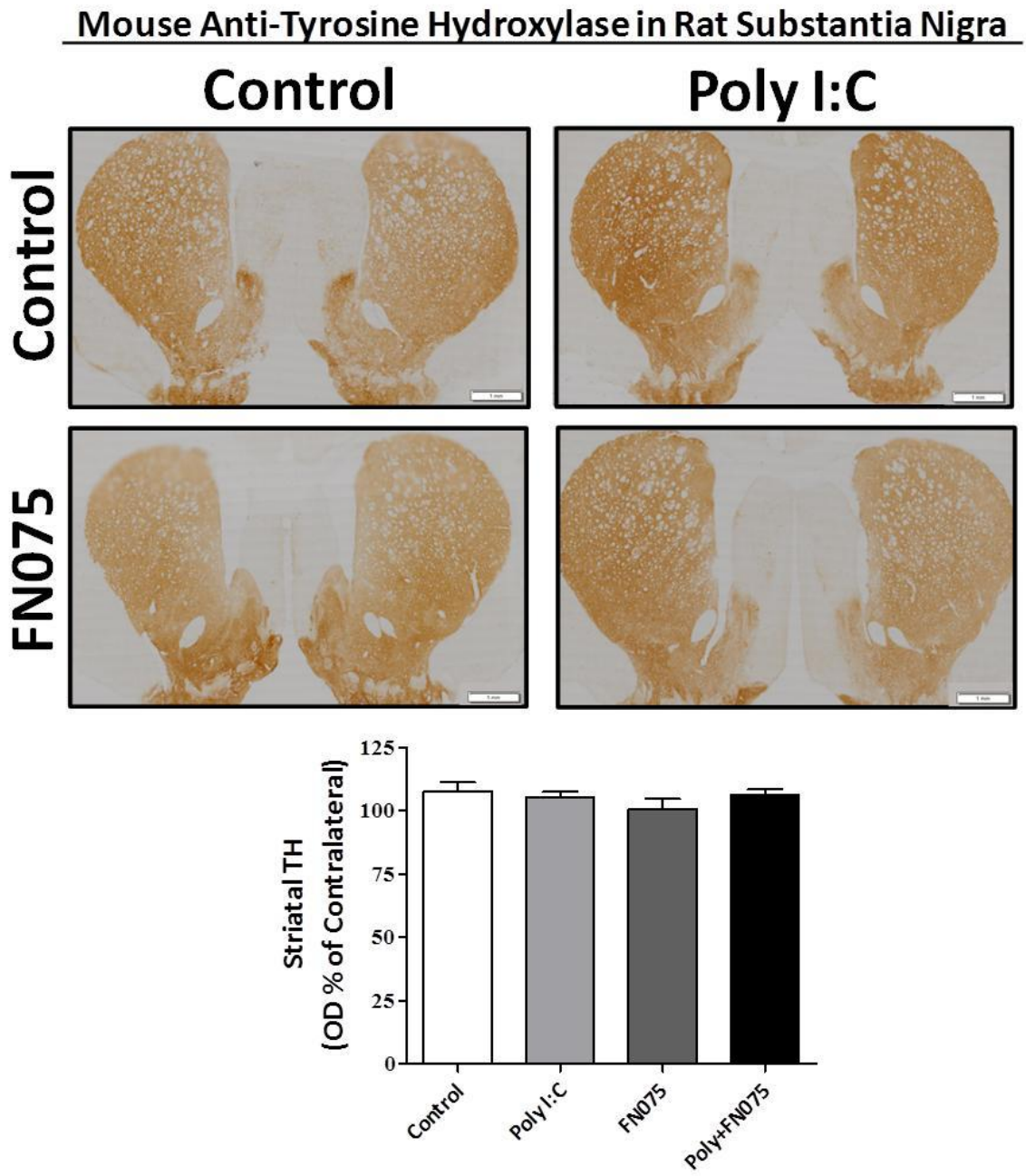

Figure 5.8. Striatal TH$^+$ Nerve Terminals. After sequential intra-nigral injection of poly I:C and FN075, brains were 4% PFA fixed for free-floating IHC-DAB analysis. STR tissue (30 µm) was immunostained for tyrosine hydroxylase. Mounted tissue was imaged using an Olympus VS120 slide scanner. Data was quantified by comparing the striatal optical density to the contralateral (uninjected side of the brain) STR. Above, the left STR image is ipsilateral. Analysis was conducted using One-way ANOVA, followed by SNK *post-hoc* test. Data are presented as means and standard errors of the mean. Scale = 1 mm.

5.4.4. Poly I:C Priming of FN075 Exacerbates Neuroinflammation *In vivo*

Proceeding on from assessing the neurodegenerative effects of viral-like poly I:C priming with FN075-induced α-synuclein aggregation, neuroinflammation was examined. Glial cells which mediate neuroinflammation (astrocytes and microglia) were measured by staining for astrocyte (GFAP) and microglia (OX42) markers (see Fig. 5.9-5.12). Quantification of astrocytic ($GFAP^+$) cell bodies in the SN found poly I:C priming in combination with intra-nigral injection of FN075 to induce a 65% increase astrocytosis in this region ($F_{(3,11)} = 7.8$, $p < 0.01$, see Fig. 5.9). There was also a 36% increase in $GFAP^+$ astrocytes in the SN after poly I:C intra-nigral injection, but *post-hoc* analysis did not find this change to be significant ($p > 0.05$). In contrast, poly I:C injection did not change the number of $OX42^+$ microglia in the SN (see Fig. 5.10). However, administration of FN075 did significantly increase $OX42^+$ microglial cells in the SN by approximately 35% ($p < 0.05$). Intriguingly, priming the SN with poly I:C exacerbated the effect of FN075 on nigral microgliosis ($F_{(3,11)} = 16.2$, $p < 0.001$). Similar to the level of astrogliosis, there was over a 60% increase in $OX42^+$ microglia in the region when viral-like poly I:C priming was combined with FN075 induced α-synuclein aggregation ($p < 0.001$, see Fig. 5.11). Unlike the neuroinflammation seen in the SN, there was no change in astroglial ($F_{(3,11)} = 1.3$, $p > 0.05$) or microglial ($F_{(3,11)} = 1.2$, $p > 0.05$) density in the STR (see Fig. 5.10 and Fig. 5.12).

Due to the numerous neuropathological changes in the SN after poly I:C priming, a correlation analysis was conducted. Quantified pathological features relating to α-synuclein aggregation, nigral neurodegeneration, and neuroinflammation were analysed (see Fig. 5.13). Nigral microgliosis was found to significantly correlate with other features in the SN, with an increase in microgliosis correlating with an increase in filamentous α-synuclein density ($r = 0.748$, $p < 0.01$) and a decrease in TH^+ cell bodies

($r = -0.709$, $p < 0.003$). In contrast, filamentous α-synuclein density was not directly correlated with the number of TH^+ cell bodies in the SN ($r = -0.368$, $p > 0.05$). Similar to microgliosis, an increase in astrogliosis was associated with a slight decrease in TH^+ cell bodies, but this did not reach statistical significance ($r = -0.507$, $p = 0.054$).

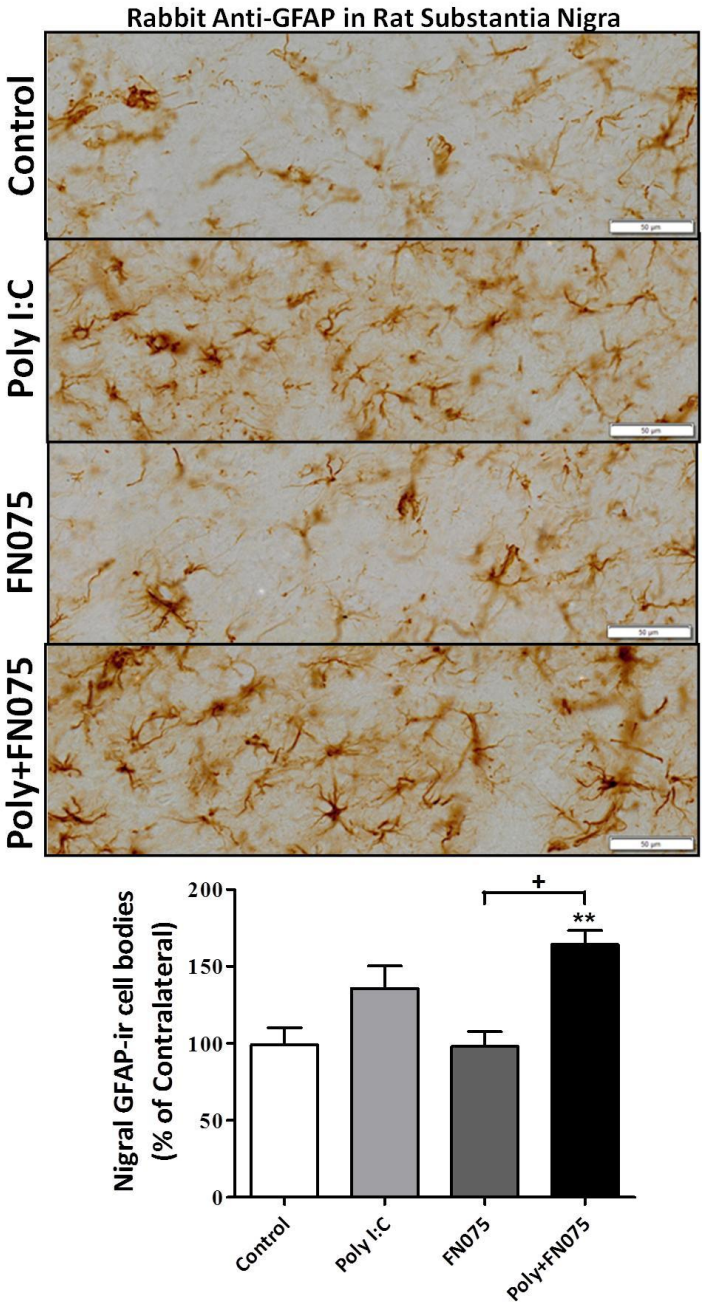

Figure 5.9. Nigral GFAP$^+$ Cell Bodies. After sequential intra-nigral injection of poly I:C and FN075, brains were 4% PFA fixed for free-floating IHC-DAB analysis. SN tissue (30 µm) was immunostained for astrocytic GFAP. Mounted tissue was imaged using an Olympus VS120 slide scanner. Data was quantified by comparing the number of nigral GFAP$^+$ cell bodies to the contralateral (uninjected side of the brain) SN. Analysis was conducted using One-way ANOVA, followed by SNK *post-hoc* test. Data are presented as means and standard errors of the mean. Scale = 50 µm. **$p < 0.01$ vs Control, $^+p < 0.05$ vs FN075

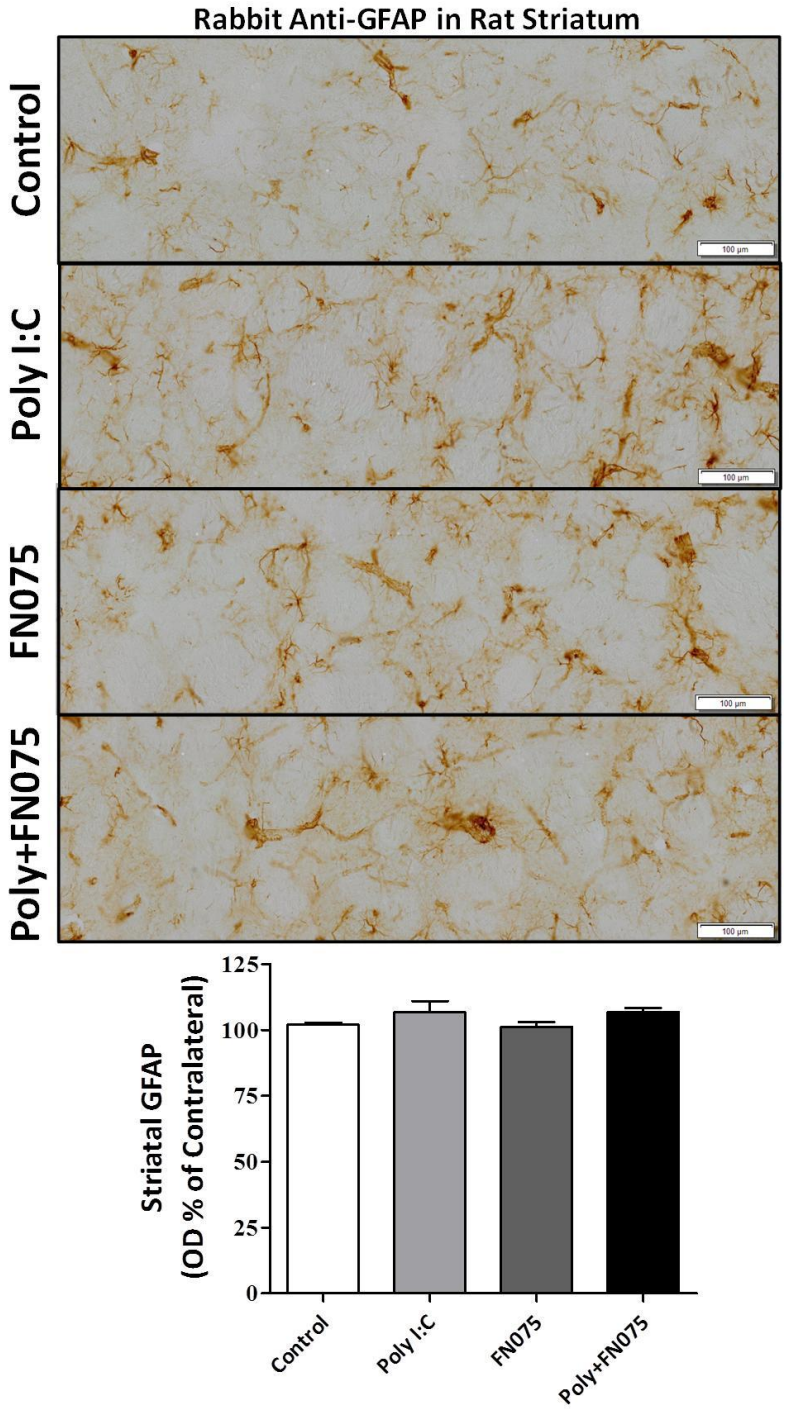

Figure 5.10. Striatal GFAP$^+$ Cell Bodies. After sequential intra-nigral injection of poly I:C and FN075, brains were 4% PFA fixed for free-floating IHC-DAB analysis. STR tissue (30 µm) was immunostained for astrocytic GFAP. Mounted tissue was imaged using an Olympus VS120 slide scanner. Data was quantified by comparing the striatal optical density to the contralateral (uninjected side of the brain) STR. Analysis was conducted using One-way ANOVA, followed by SNK *post-hoc* test. Data are presented as means and standard errors of the mean. Scale = 100 µm.

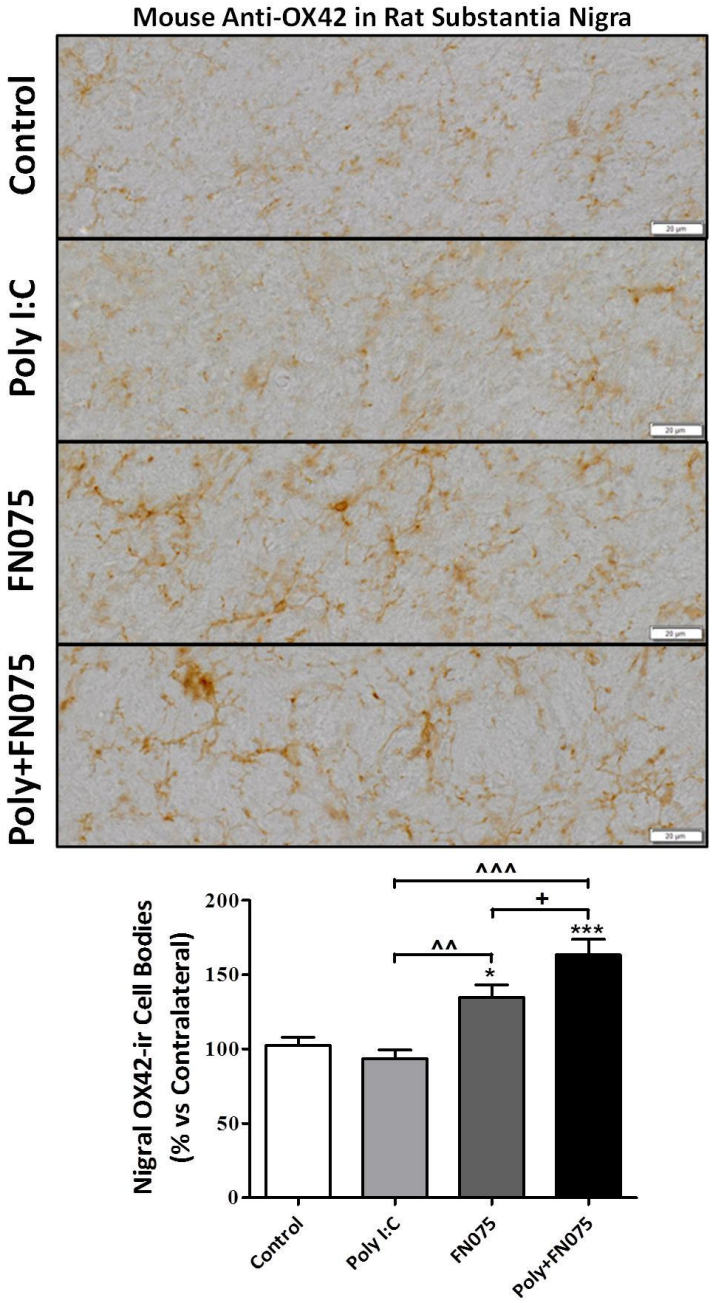

Figure 5.11. Nigral OX42$^+$ Cell Bodies. After sequential intra-nigral injection of poly I:C and FN075, brains were 4% PFA fixed for free-floating IHC-DAB analysis. SN tissue (30 µm) was immunostained for microglial marker OX42. Mounted tissue was imaged using an Olympus VS120 slide scanner. Data was quantified by comparing the number of nigral OX42$^+$ cell bodies to the contralateral (uninjected side of the brain) SN. Analysis was conducted using One-way ANOVA, followed by SNK *post-hoc* test. Data are presented as means and standard errors of the mean. Scale = 20 µm. *$p < 0.05$ vs Control, ***$p < 0.001$ vs Control, ^^$p < 0.01$ vs poly I:C, ^^^$p < 0.001$ vs poly I:C, $^+p < 0.05$ vs FN075

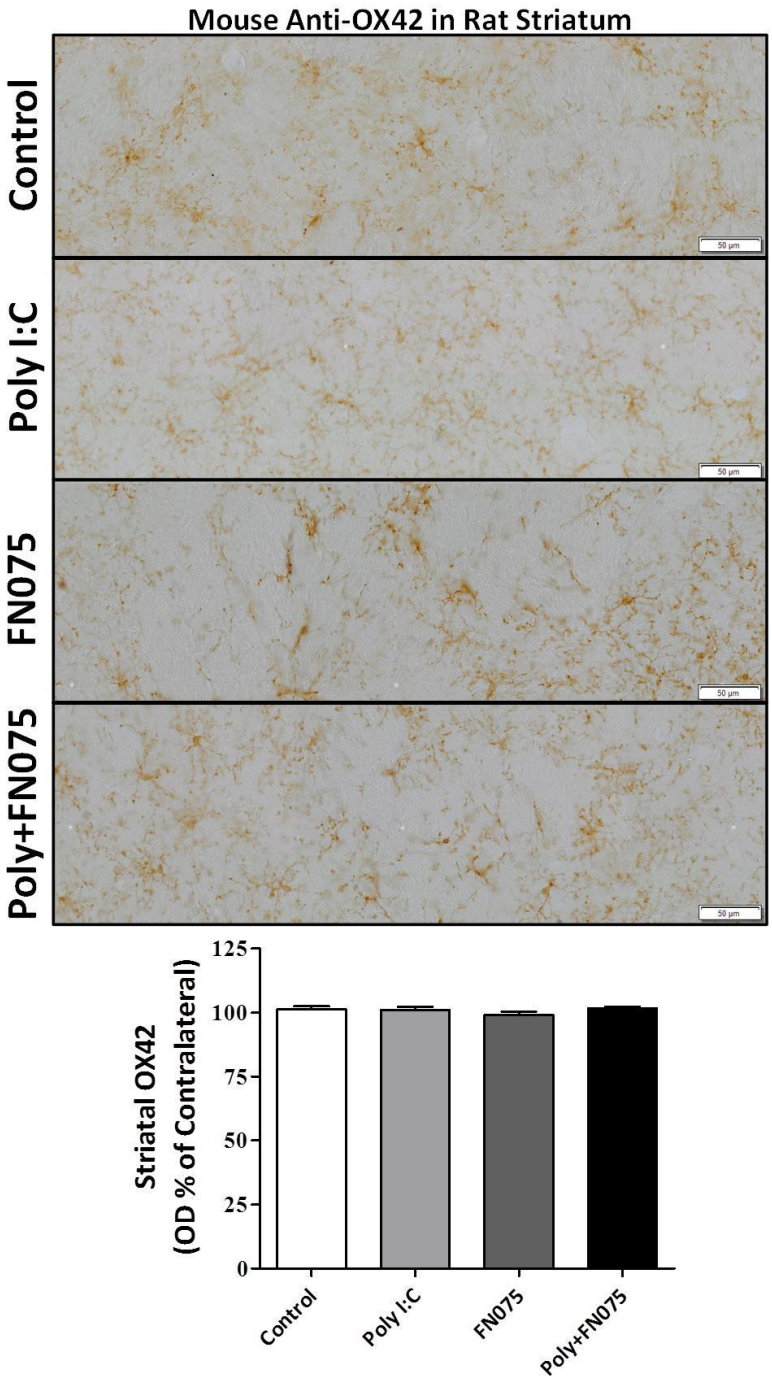

Figure 5.12. Striatal OX42^{+} Cell Bodies. After sequential intra-nigral injection of poly I:C and FN075, brains were 4% PFA fixed for free-floating IHC-DAB analysis. STR tissue (30 µm) was immunostained for microglial marker OX42. Mounted tissue was imaged using an Olympus VS120 slide scanner. Data was quantified by comparing the striatal optical density to the contralateral (uninjected side of the brain) STR. Analysis was conducted using One-way ANOVA, followed by SNK *post-hoc* test. Data are presented as means and standard errors of the mean. Scale = 50 µm.

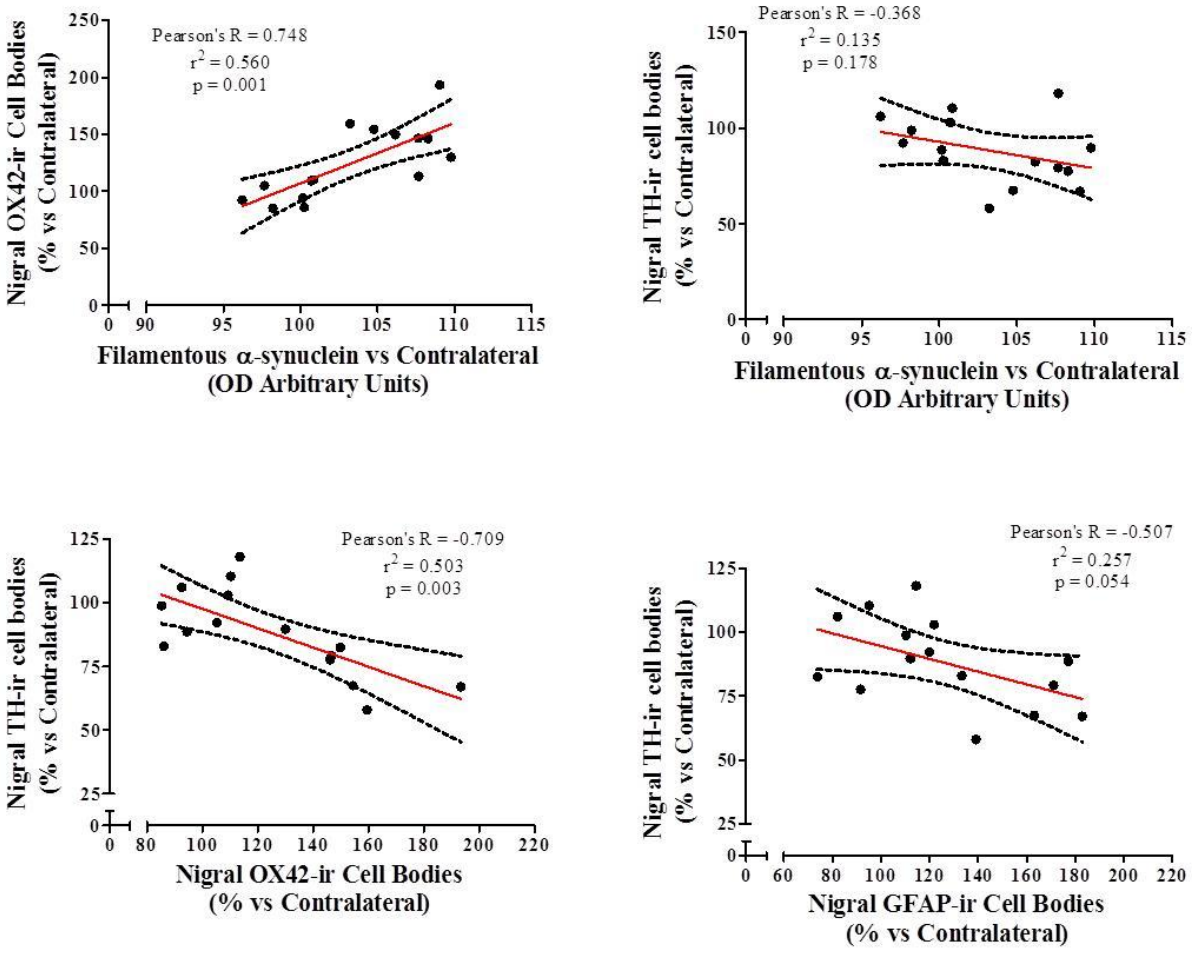

Figure 5.13. Neuropathological Correlations. Quantified nigral metrics (filamentous-α-synuclein density and TH^+, $GFAP^+$ and $OX42^+$ cell bodies) were assessed for correlational relationships. Each dot denotes an individual rat. Red lines indicate linear regression, with black dotted lines signifying 95% CI. Analysis was conducted using Pearson's Correlation test.

5.4.5. Synaptic and Autophagy Changes After Poly I:C Priming *In vivo*

The significant neurodegenerative and neuroinflammatory effects of viral-like poly I:C priming in combination with FN075-induced α-synuclein aggregation prompted further investigation into potential changes in synaptic and autophagy related proteins. Synaptophysin and PSD-95, key mediators of pre- and post-synaptic neuronal activity, were examined to determine if changes in these proteins occurred with viral-like poly I:C priming, possibly in association with nigral neurodegeneration. As previously mentioned, the autophagy process is critical for the clearance of mis-folded or abnormal protein aggregates (such as α-synuclein). With this in mind, autophagy related p62 was also examined in the SN to determine any changes in relation to neuroinflammation or α-synuclein aggregation.

There was no change in the density of synaptophysin ($F_{(3,11)} = 0.3$, $p > 0.05$) or PSD-95 ($F_{(3,11)} = 1.3$, $p > 0.05$) in the SN due to poly I:C or FN075 administration (see Fig. 5.14 and Fig. 5.15). However, the total area of synaptophysin inclusions in a FOV in the SN of the treated rats was quantified. Interestingly, a significant 4-fold increase in synaptophysin inclusions was found in the SN of rats primed with poly I:C previous to FN075 injection ($K = 9.1$, $p < 0.05$, see Fig. 5.14). Although intra-nigral injection of FN075 alone was found to induce over a 5-fold increase in synaptophysin inclusions, this increase was not found to be significant ($p > 0.05$), likely due to the wide variation of the existence of synaptophysin inclusions among the rats in this group (see Fig. 5.14).

Staining for the autophagy related protein p62 was quantified by counting the number of $p62^+$ cell bodies within the whole SN region of treated rats (see Fig. 5.16). Intra-nigral injection of poly I:C induced over a 50% increase in the number of $p62^+$ nigral cell bodies ($F_{(3,11)} = 7.9$, $p < 0.01$) when compared to the untreated control group ($p < 0.05$). Administration of FN075 did not significantly change p62 staining in the SN

(117%, $p > 0.05$). Surprisingly, poly I:C priming in combination with FN075 intra-nigral injection resulted in over a 25% decrease in the number of $p62^{+}$ nigral cell bodies (see Fig. 5.16). Although this decrease in p62 cell bodies was not found to be significantly reduced when compared to the untreated control group, the 80% reduction compared to the poly I:C alone group was significant ($p < 0.01$).

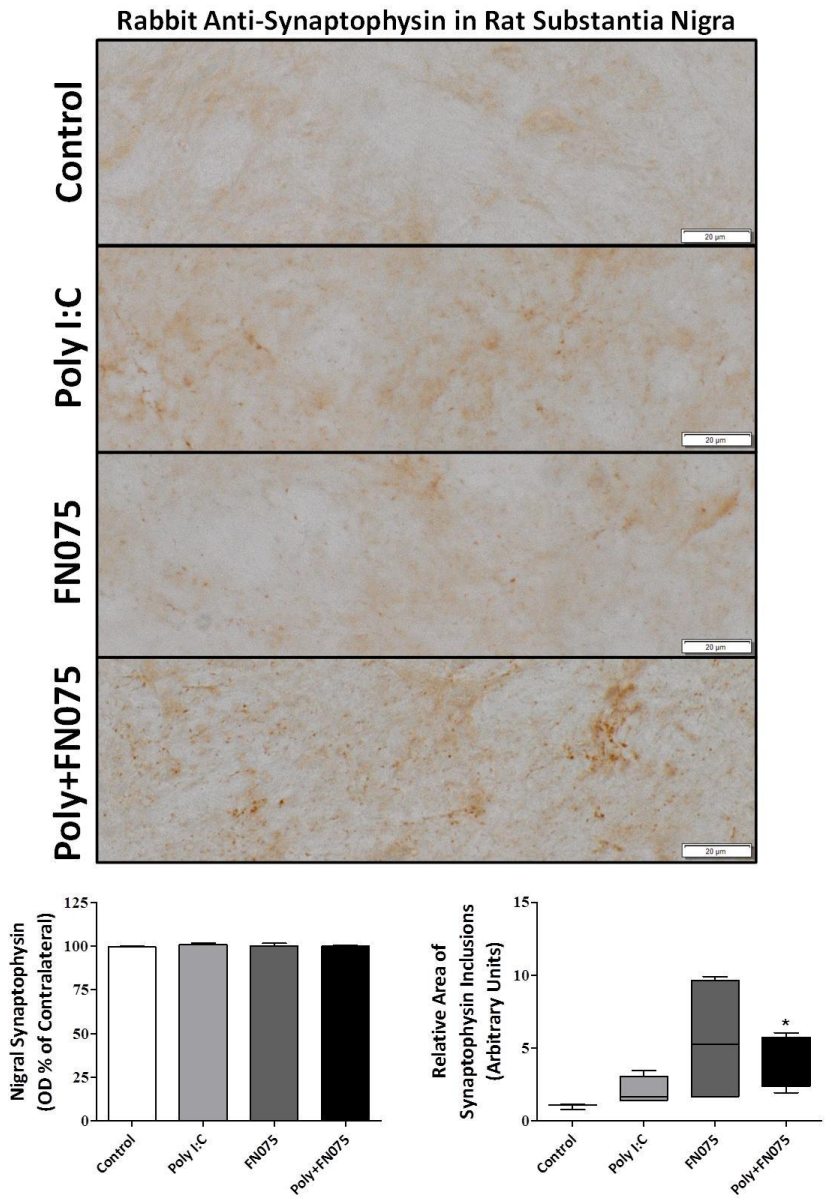

Figure 5.14. Nigral Synaptophysin Expression. After sequential intra-nigral injection of poly I:C and FN075, brains were 4% PFA fixed for free-floating IHC-DAB analysis. SN tissue (30 µm) was immunostained for synaptophysin. Mounted tissue was imaged using an Olympus VS120 slide scanner. Data was quantified by comparing the nigral optical density to the contralateral (uninjected side of the brain) SN and by measuring the relative area of synaptophysin inclusions. Analysis was conducted using One-way ANOVA (SNK *post-hoc* test) or Kruskal-Wallis (Dunn's Multiple Comparison *post-hoc* test) as appropriate. Data for density are presented as means and standard errors of the mean. Data for relative synaptophysin inclusion area are presented as median ± min and max Scale bar = 20 µm. *$p < 0.001$ vs Control

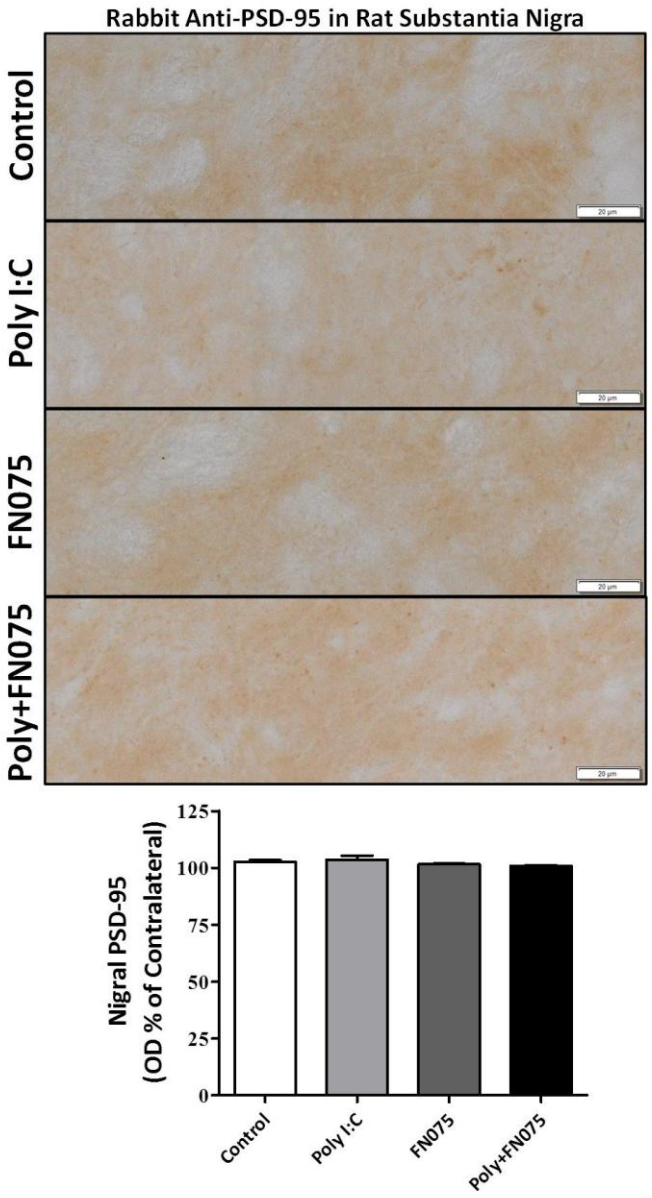

Figure 5.15. Nigral PSD-95 Expression. After sequential intra-nigral injection of poly I:C and FN075, brains were 4% PFA fixed for free-floating IHC-DAB analysis. SN tissue (30 µm) was immunostained for PSD-95. Mounted tissue was imaged using an Olympus VS120 slide scanner. Data was quantified by comparing the nigral optical density to the contralateral (uninjected side of the brain) SN. Analysis was conducted using One-way ANOVA, followed by SNK *post-hoc* test. Data are presented as means and standard errors of the mean. Scale = 20 µm.

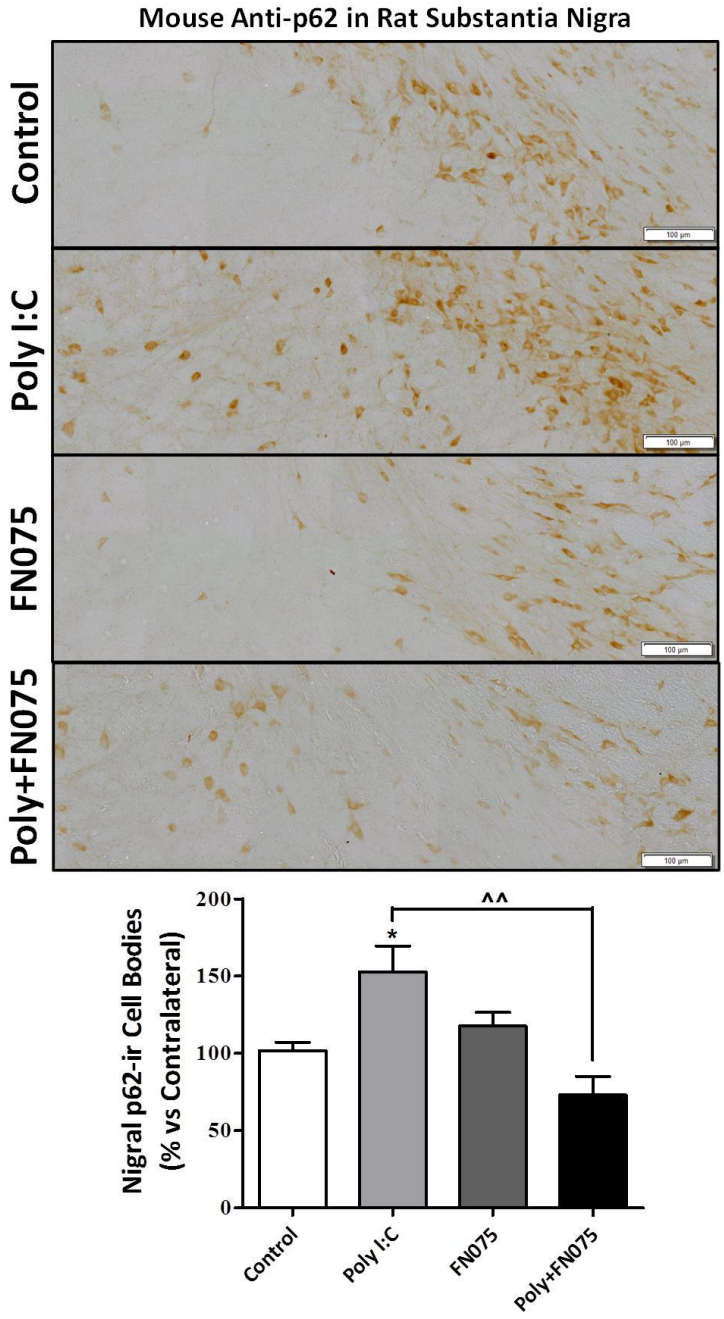

Figure 5.16. Nigral p62 Expression. After sequential intra-nigral injection of poly I:C and FN075, brains were 4% PFA fixed for free-floating IHC-DAB analysis. SN tissue (30 µm) was immunostained for p62. Mounted tissue was imaged using an Olympus VS120 slide scanner. Data was quantified by comparing the number of nigral $p62^{+}$ cell bodies to the contralateral (uninjected side of the brain) SN. Analysis was conducted using One-way ANOVA, followed by SNK *post-hoc* test. Data are presented as means and standard errors of the mean. Scale = 100 µm. *$p < 0.05$ vs Control, ^^$p < 0.01$ vs poly I:C

5.5 DISCUSSION

This chapter sought to further investigate the potential pathological interaction between viral-mediated neuroinflammation and α-synuclein aggregation. Adult rats were primed with the viral mimetic poly I:C via direct intra-nigral injection, followed 2 weeks later by injection of the α-synuclein aggregate promoter, FN075, at the same nigral site. Strikingly, viral-mediated priming caused a significant increase in α-synuclein mediated nigral neuroinflammation and neurodegeneration, which led to a significant impairment in the rats' motor function.

Toxin	**FN075**		
Result	P	F	P+F
TH	NC	NC	↓
α-syn	NC	↑	↑
GFAP	↑	NC	↑↑
OX42	NC	↑	↑↑
Syanptophysin	NC	NC	Inclusions
PSD-95	NC	NC	NC
p62	↑	NC	NC

Table 5.1. Summary of IHC Protein and Cell Changes.

Earlier *in vivo* studies reported intra-nigral or intra-striatal injection of poly I:C to produce microgliosis and astrogliosis (Deleidi et al., 2010, Concannon et al., 2016, McCabe et al., 2017). The poly I:C induced neuroinflammation in these studies was not sufficient to induce neurodegeneration, but did prime the sensitisation of neurons to other neurotoxins (Deleidi et al., 2010). However, in the present study poly I:C did not induce significant microglosis or astrogliosis, but this finding may be due to the much later time-point of 10 weeks compared to previous studies (Concannon et al., 2016, Deleidi et al., 2010, McCabe et al., 2017).

In this study FN075 was used to induce α-synuclein aggregation *in vivo*. FN075 has previously been found to promote fibril formation of purified monomeric α-synuclein via accelerated formation of the soluble oligomers observed prior to α-synuclein fibrillisation (Horvath et al., 2012, Pedersen et al., 2015). *In vivo*, murine intra-nigral injection of FN075 produced motor function impairment and dopaminergic neuronal loss, while Drosophila studies found significant effects regarding movement, lifespan, and the fraction of α-synuclein present as soluble oligomers (Chermenina et al., 2015, Pokrzywa et al., 2017). The experiment in from this chapter was the first to test this compound in rats. Using an α-synuclein filament specific antibody, α-synuclein aggregation was able to be detected in the rat SN *in vivo*. The approximately 10% relative increase in α-synuclein aggregates after FN075 intra-nigral injection corroborates previous *in vivo* research using FN075. Chermenina *et al*. found the α-synuclein knock-out mice to not exhibit any of the deleterious effects seen in the normal mice after intra-nigral injection of FN075, suggesting that FN075 induced neurotoxicity derives from the induction of α-synuclein aggregation *in vivo* (Chermenina et al., 2015). It is worth noting that filamentous α-synuclein aggregates were detected at 8 weeks post-FN075 injection in this study, much earlier than when Chermenina *et al*. tested the knock-out mouse model for rescue of nigral dopaminergic neurons (Chermenina et al., 2015). The successful induction of α-synuclein aggregation by FN075 was also associated with significant microgliosis and astrogliosis. Although previous studies using FN075 have not investigated microgliosis, there are multiple reports of α-synuclein aggregation/abnormalities producing a pro-inflammatory microglial response (Drouin-Ouellet et al., 2015, Kim et al., 2013a, Watson et al., 2012, Barkholt et al., 2012).

The most pronounced and important results from this study were those found after sequential intra-nigral injection of poly I:C and FN075. Viral-mediated neuroinflammation in combination with α-synuclein aggregation in the SN resulted in 32% dopaminergic neuronal cell loss, excessive gliosis, and significant motor deficits. Previously, other dual-hit model studies have found comparable results (Field et al., 2010, Kirik et al., 2002, Sadasivan et al., 2017). MPTP administration to H1N1 infected mice resulted in exacerbated TH positive cell loss in the SN, while microgliosis was primarily mediated by MPTP (Sadasivan et al., 2017). Also, systemic poly I:C in ME7 prion diseased mice worsened neurodegeneration compared to saline injected mice (Field et al., 2010).

It is worth noting that the neurodegeneration in our model was seen at 8 weeks post-FN075 injection. Other synucleinopathy models, such as over-expression of α-synuclein, have found neurodegeneration (along with α-synuclein aggregation) at this time point, but significant neurodegeneration only occurred in combination with viral-like priming in our model (Kirik et al., 2002). It is also worth noting that the dopaminergic cell loss in the SN did not correspond with a decrease in TH density in the innervating dopaminergic terminals of the STR (as measured by optical density). This finding is contradictory, especially considering the motor deficits seen in the group which had dopaminergic cell loss in the SN. It is possible that a more sensitive technique may find differences in the terminals that was missed. To confirm degeneration in the SN and further investigate innervation in the STR, other dopaminergic markers (such as DAT) and neuronal markers (such as NeuN or βIII-tubulin) should be measured.

The findings from the present study and other viral-related dual-hit models suggest that an interaction between viral-related inflammation and pathogenic α-synuclein aggregates may promote early or exacerbated neurodegeneration.

Chapter Six: General Discussion

CHAPTER SIX

6.1 SUMMARY OF FINDINGS

To possibly explain the epidemiological association between viral infections and PD, this research investigated the potential viral-mediated contribution to PD-related pathology. The general experimental design was similar across the cell culture and *in vivo* pre-clinical models, with synthetic viral-like dsRNA priming before treatment with neurotoxins used to model PD. The aim of this study was to investigate the potential influence viral infections might have on the neurodegenerative effects of PD related neuropathology using multiple models of PD. We hypothesised that viral infections may exacerbate the neurodegenerative effects of other underlying contributors to PD development.

Chapter 3 experiments were conducted using SH-SY5Y human neurblastoma cells. These experiments found clear patterns in poly I:C mediated alterations to neuronal cell death, autophagy, and synaptic protein expression. As summarised in Table 6.1, poly I:C consistently increased cleaved caspase-3 expression. This finding is not surprising since poly I:C induces IFN up-regulation, leading to caspase mediated apoptosis (Ludwiczek et al., 2001). In a model of chronic neurodegeneration, poly I:C mediated increases in IFN resulted in activated caspase-3 and TUNEL positive apoptotic cells, along with increased neurodegeneration (Field et al., 2010). Conversely, poly I:C mediated increases in $TUNEL^{+}$ staining was dependent on the neurotoxin combination (see Table 6.1). However, it is worth noting that the study by Field *et al.* combined poly I:C with protein aggregation (similar to the poly I:C+FN075 combination) (Field et al., 2010). It is possible that viral mediated inflammation in combination with protein aggregation determines if apoptotic cell death occurs.

A relatively consistent finding across Chapters 3 and 4 was an increase in PSD-95 expression when poly I:C mediated inflammation was combined with neurotoxins used for modeling PD (see Tables 6.1 and 6.2). Although poly I:C appeared to increase PSD-95 in primary rat cells, the only significant increases in PSD-95 were found when poly I:C was combined with other neurotoxins (such as 6-OHDA, rotenone, or FN075-induced α-synuclein aggregation). Also, poly I:C priming in combination with other neurotoxins resulted in changes in synaptophysin expression, but these findings did not show any consistent pattern (see Tables 6.1 and 6.2). In SH-SY5Y cells, poly I:C priming in combination with FN075 resulted in decreased synaptophysin expression, while the same experiment increased synaptophysin expression in primary rat VM cells. Further confounding the poly I:C priming effects on synaptophysin, poly I:C priming in combination with FN075 *in vivo* led to synaptophysin inclusions but no change in overall synaptophysin expression (see Table 6.3). These findings are similar to a previous *in vivo* study which found poly I:C priming in the rat SN to exacerbate 6-OHDA induced neurodegeneration, along with alterations to PSD-95 and synaptophysin expression (Deleidi et al., 2010). It is possible that changes in synaptic proteins precede synapse dysfunction and eventual neurodegeneration.

There were also some consistent changes in autophagy in cell culture experiments. Neurotoxin treatment (whether 6-OHDA, rotenone, MPP+, or FN075) overall led to increases in p62 expression (see Tables 6.1 and 6.2). Interestingly, priming with poly I:C often attenuated this neurotoxin induced increase in p62 expression. Although it is difficult to know if p62 accumulation signifies an increase or decrease in autophagic flux without pharmacological inhibition of autophagosome degradation, an increase in p62 accumulation is generally associated with autophagy inhibition or disruption (Bjørkøy et al., 2009, Klionsky et al., 2016). Thus, our findings suggest that

neurotoxin disruption of autophagic flux is inhibited when neurons are primed with viral-like poly I:C induced inflammation. Conversely, *in vivo* poly I:C increased p62 positive cells, suggesting poly I:C mediated inflammation in the brain may reduce autophagic flux. Autophagy inhibition may exacerbate PD related pathology if autophagic clearance of abnormal proteins (such as α-synuclein aggregates) is impaired.

Finally, the findings from Chapter 5 suggest poly I:C priming exacerbates neuroinflammation *in vivo*. Astrogliosis and microgliosis were both increased when poly I:C priming was combined with FN075 induced α-synuclein aggregation (see Table 6.3). Although the intricate dynamics regarding α-synuclein aggregation, neuroinflammation, and neurodegeneration in the CNS have yet to be fully understood. Based on the sequential design of our study and similar dual-hit studies, it is possible that pro-inflammatory astrocytes and microglia may work synergistically to induce neuronal cell death (Sadasivan et al., 2017, Suzumura et al., 2006). A study by Jack *et al*. found that although TLR3 expression is enriched in astrocytes, treatment with poly I:C increased TLR2 expression in human microglia (Jack et al., 2005). Oligomeric α-synuclein is a known endogenous ligand for TLR2, which has been found to mediate oligomeric α-synuclein induced microglia activation. As such, intra-nigral injection with poly I:C in this study may have primed the microglia for an exacerbated response to FN075 induced α-synuclein aggregates (Daniele et al., 2015, Kim et al., 2013a). Indeed, in this study viral-like priming before FN075 injection resulted in more OX42 positive microglia compared to the FN075 only group. Along with microgliosis, viral-like priming with FN075 resulted in significant astrogliosis in the rat SN. Time-course studies investigating the effects of intra-striatal poly I:C in Sprague-Dawley rats found an up-regulation of TLR3 2 weeks post-injection and astrogliosis at 4 weeks post-injection (Concannon et al., 2016, McCabe et al., 2017). Although astrogliosis alone does not

seem to cause neurodegeneration, the combination of astrogliosis and microglia activation might produce a microenvironment which leads to excessive neuroinflammation and neurodegeneration.

Toxin	**6-OHDA**			**Rotenone**			**MPP+**			**FN075**		
Result	P	6	P+6	P	R	P+R	P	M	P+M	P	F	P+F
TUNEL	NC	NC	NC	NC	NC	NC	NC	↑	↑↑	↑	↑	↑↑
cCASP3	↑	NC	↑	↑	NC	↑	↑↑	NC	↑	↑↑	NC	↑
cPARP	NC	NC	NC	NC	NC	NC	↑	NC	↑	NC	NC	NC
p62	NC	↑	NC	NC	↑	NC	NC	↑	↑↑	NC	↑	NC
LC3	NC	↑	NC	NC	NC	NC	NC	↓	NC	↓	↑	↓
PSD-95	NC	NC	↑	NC	NC	↑	NC	NC	↑	NC	NC	↑
Synap	NC	NC	↑	NC	NC	NC	NC	NC	↓	↓	↓	↓↓

Table 6.1. Summary of Protein/TUNEL Assay Changes from Chapter 3.

Toxin	**6-OHDA**			**Rotenone**			**FN075**		
Result	P	6	P+6	P	R	P+R	P	F	P+F
TH	↓	↓↓	↓↓	↓	↓↓	↓↓	↓	↓	↓
α-syn	NC	↑	↑↑	NC	↑	NC	NC	↑	NC
p62	NC	↑	↑	NC	↑	NC	NC	↑	↑↑
LC3	NC	NC	NC	NC	NC	NC	NC	NC	↑
PSD-95	NC	NC	NC	NC	NC	NC	NC	NC	↑
Synap	↑	NC	NC	↑	NC	NC	↑	↓	↑↑

Table 6.2. Summary of Protein Changes from Chapter 4.

Toxin	**FN075**		
Result	P	F	P+F
TH	NC	NC	↓
α-syn	NC	↑	↑
GFAP	↑	NC	↑↑
OX42	NC	↑	↑↑
Syanptophysin	NC	NC	Inclusions
PSD-95	NC	NC	NC
p62	↑	NC	NC

Table 6.3. Summary of IHC Protein and Cell Changes from Chapter 5.

6.2 CONTRIBUTIONS AND IMPLICATIONS

As previously mentioned throughout this thesis, the molecular/cellular consequences and potential contribution to PD pathology is unknown. The results from the preceding experiments attempted to investigate the neurodegenerative effects of viral infections when combined with PD-related pathology induced by pre-clinical models of PD. Our findings confirm our suspicions that viral infections can modulate cell death, autophagy, and synaptic proteins in neurons, and contribute to the examination of viral infections in PD pathology.

The consistent and significant increase in PSD-95 due to viral-like priming suggests that PSD-95 is profoundly influenced by inflammation and PD pathology. Previous research has already described PSD-95 as an important modulator of synaptic development due to its regulation of synapse stabilisation and plasticity (Ehrlich et al., 2007, El-Husseini et al., 2000). The neuropathological consequences of increased PSD-95 expression may contribute to PD and PD symptomology. Increases in PSD-95 results in recruitment of AMPARs to the synapse, leading to increases in LTP (Schnell et al.,

2002). Also, PSD-95 over-expression enhanced excitatory synapses while simultaneously decreasing inhibitory synapses (Prange et al., 2004). PSD-95 mediated alteration of the excitatory-to-inhibitory ratio could lead to excitotoxicity and PD motor dysfunction. Specifically, increases in PSD-95 was found to exacerbate dyskinesia in dyskinetic parkinsonian monkeys, with alleviation of dyskinsia when PSD-95 was decreased in these monkeys (Porras et al., 2012). Further analysis suggested that this effect was due to the interaction between PSD-95 and DR1 (Porras et al., 2012).

Expanding from the previous research and the findings in this thesis, it is proposed that viruses or viral-mediated inflammation has the potential to increase PSD-95 in neurons. It is possible that underlying PD-related pathology may synergistically combine with this viral mediated increase in PSD-95 to contribute to PD symptomology. Indeed, PSD-95 has been found to be increased in the hippocampus and striatum of PD patients (Fourie et al., 2014). It is possible that this finding in *post-mortem* PD patients is associated with previous viral infections during the patients' lives.

The results of the *in vivo* study from this thesis also may contribute to the better understanding of the consequences of viral infections in neurodegenerative diseases. Although inflammation and gliosis have been described in neurodegenerative diseases, the underlying contributors to this inflammation have yet to be fully understood. A recent study by Liddlelow *et al*. found activated microglia to push astrocytes towards a pro-inflammatory A1 phenotype, which led to dopaminergic specific neurodegeneration (Liddelow et al., 2017). It is possible that the poly I:C related astrogliosis in the rat SN in our study may not have been neurotoxic until combined with activated microglia promoted by FN075 induced oligomeric α-synuclein. Further investigation is warranted

to determine the relevant astrocyte-microglia cross-talk events in our model and more broadly in neurodegenerative diseases.

6.3 FUTURE RECOMMENDATIONS

Expanding on from the studies described in this thesis, it is suggested that further investigation should be conducted into the relationship between inflammation and PSD-95 expression. Now that an innate immune response can elicit alterations to synaptic related proteins, actual viruses should be investigated to determine if the epidemiological association is due to specific viruses or if this is a general viral induced inflammatory effect. Also, there is a strong need for a better understanding of glial-neuronal crosstalk. It is now known that astrocytes have more than one phenotypic state, with a pro-inflammatory and anti-inflammatory potential. Further investigation into the effects of these glial phenotypes and their response to viral infections should be conducted. Finally, autophagy processes in relation to viral mediated neuroinflammation need to be investigated further to determine if there is an increase or decrease in autophagic flux in response to viral infections.

Future experiments that could investigate the above would require techniques not described in this thesis. Electrophysiology can be used to determine if a poly I:C related change in PSD-95 protein expression corresponds to changes in synaptic activity and LTP. A cell sorter would be a useful tool for isolating dopaminergic neurons and glial cells from VM primary cultures and gross tissue. This technique would help to distinguish protein or mRNA changes in specific cell types. More sophisticated techniques could also be used to better understand the autophagy modulation in certain conditions described in this thesis. LC3 reporter cell lines in combination with an autophagy inhibitor (such as bafilomycin or chloroquine) could be used to determine if

autophagy is increasing or decreasing with poly I:C priming. Performing some of these suggested experiments would significantly add to the data presented in this thesis.

6.4 CONCLUSION

Although the findings from these studies are not conclusive, they strongly support a role of viral infections in PD pathology. The epidemiological association between viral infections and PD is likely not due to chance and may represent a potential novel therapeutic strategy for modifying PD pathology or disease progression.

References

References

ABBAS, A. K., LICHTMAN, A. H. & PILLAI, S. 2014. *Basic immunology: functions and disorders of the immune system*, Elsevier Health Sciences.

ABBOTT, N. J. & FRIEDMAN, A. 2012. Overview and introduction: the blood–brain barrier in health and disease. *Epilepsia,* 53**,** 1-6.

ABELIOVICH, A., SCHMITZ, Y., FARIÑAS, I., CHOI-LUNDBERG, D., HO, W.-H., CASTILLO, P. E., SHINSKY, N., VERDUGO, J. M. G., ARMANINI, M. & RYAN, A. 2000. Mice lacking α-synuclein display functional deficits in the nigrostriatal dopamine system. *Neuron,* 25**,** 239-252.

ADAMS, D. J., SHEN, C., LEVENGA, J., BASTA, T., EISENBERG, S. P., MAPES, J., HAMPTON, L., GROUNDS, K., HOEFFER, C. A. & STOWELL, M. H. 2017. Synaptophysin is a β-Amyloid Target that Regulates Synaptic Plasticity and Seizure Susceptibility in an Alzhiemer's Model. *bioRxiv***,** 129551.

ADAMS, E. R. 2015. Molecular Diagnostics—current Research and Applications. *Clinical Infectious Diseases,* 60**,** 1877.

AFONINA, INNA S., MÜLLER, C., MARTIN, SEAMUS J. & BEYAERT, R. 2015. Proteolytic Processing of Interleukin-1 Family Cytokines: Variations on a Common Theme. *Immunity,* 42**,** 991-1004.

AHMED, I., TAMOUZA, R., DELORD, M., KRISHNAMOORTHY, R., TZOURIO, C., MULOT, C., NACFER, M., LAMBERT, J.-C., BEAUNE, P., LAURENT-PUIG, P., LORIOT, M.-A., CHARRON, D. & ELBAZ, A. 2012. Association between Parkinson's disease and the HLA-DRB1 locus. *Movement Disorders,* 27**,** 1104-1110.

ALAM, M., MAYERHOFER, A. & SCHMIDT, W. 2004. The neurobehavioral changes induced by bilateral rotenone lesion in medial forebrain bundle of rats are reversed by L-DOPA. *Behavioural brain research,* 151**,** 117-124.

ALBERIO, T. & FASANO, M. 2011. Proteomics in Parkinson's disease: An unbiased approach towards peripheral biomarkers and new therapies. *Journal of biotechnology,* 156**,** 325-337.

ALEXANDER, D. E., WARD, S. L., MIZUSHIMA, N., LEVINE, B. & LEIB, D. A. 2007. Analysis of the Role of Autophagy in Replication of Herpes Simplex Virus in Cell Culture. *Journal of virology,* 81**,** 12128-12134.

ALEXOPOULOU, L., HOLT, A. C., MEDZHITOV, R. & FLAVELL, R. A. 2001. Recognition of double-stranded RNA and activation of NF-κB by Toll-like receptor 3. *Nature,* 413**,** 732-738.

ALLEN, N. J., BENNETT, M. L., FOO, L. C., WANG, G. X., CHAKRABORTY, C., SMITH, S. J. & BARRES, B. A. 2012. Astrocyte glypicans 4 and 6 promote formation of excitatory synapses via GluA1 AMPA receptors. *Nature,* 486**,** 410.

ANDERSON, J. P., WALKER, D. E., GOLDSTEIN, J. M., DE LAAT, R., BANDUCCI, K., CACCAVELLO, R. J., BARBOUR, R., HUANG, J., KLING, K., LEE, M., DIEP, L., KEIM, P. S., SHEN, X., CHATAWAY, T., SCHLOSSMACHER, M. G., SEUBERT, P., SCHENK, D., SINHA, S., GAI, W. P. & CHILCOTE, T. J. 2006. Phosphorylation of Ser-129 Is the Dominant Pathological Modification of α-Synuclein in Familial and Sporadic Lewy Body Disease. *Journal of Biological Chemistry,* 281**,** 29739-29752.

ANDERSON, L., VILENSKY, J. & DUVOISIN, R. 2009. Neuropathology of acute phase encephalitis lethargica: a review of cases from the epidemic period. *Neuropathology and applied neurobiology,* 35**,** 462-472.

ANDERSSON, V., HANZÉN, S., LIU, B., MOLIN, M. & NYSTRÖM, T. 2013. Enhancing protein disaggregation restores proteasome activity in aged cells. *Aging (Albany NY),* 5**,** 802.

ANGOT, E., STEINER, J. A., LEMA TOMÉ, C. M., EKSTRÖM, P., MATTSSON, B., BJÖRKLUND, A. & BRUNDIN, P. 2012. Alpha-Synuclein Cell-to-Cell Transfer and Seeding in Grafted Dopaminergic Neurons In Vivo. *PloS one,* 7**,** e39465.

ANTROBUS, R. & BOUTELL, C. 2008. Identification of a novel higher molecular weight isoform of USP7/HAUSP that interacts with the Herpes simplex virus type-1 immediate early protein ICP0. *Virus research,* 137**,** 64-71.

ARMAN, A., ISıK, N., COKER, A., CANDAN, F., BECIT, K. S. & LIST, E. O. 2010. Association between sporadic Parkinson disease and interleukin-1β-511 gene polymorphisms in the Turkish population. *European cytokine network,* 21**,** 116-121.

ATCC. 2016. *SH-SY5Y (ATCC CRL-2266)* [Online]. Available: https://www.lgcstandards-atcc.org/Products/All/CRL-2266.aspx?geo_country=ie [Accessed 06/08/2018 2018].

BABA, M., NAKAJO, S., TU, P.-H., TOMITA, T., NAKAYA, K., LEE, V., TROJANOWSKI, J. Q. & IWATSUBO, T. 1998. Aggregation of alpha-synuclein in Lewy bodies of sporadic Parkinson's disease and dementia with Lewy bodies. *The American journal of pathology,* 152**,** 879.

BALACHANDRAN, S., KIM, C. N., YEH, W. C., MAK, T. W., BHALLA, K. & BARBER, G. N. 1998a. Activation of the dsRNA-dependent protein kinase, PKR, induces apoptosis through FADD-mediated death signaling. *The EMBO Journal,* 17**,** 6888-6902.

BALACHANDRAN, S., KIM, C. N., YEH, W. C., MAK, T. W., BHALLA, K. & BARBER, G. N. 1998b. Activation of the dsRNA-dependent protein kinase, PKR, induces apoptosis through FADD-mediated death signaling. *The EMBO journal,* 17**,** 6888-6902.

BALACHANDRAN, S., ROBERTS, P. C., BROWN, L. E., TRUONG, H., PATTNAIK, A. K., ARCHER, D. R. & BARBER, G. N. 2000. Essential role for the dsRNA-dependent protein kinase PKR in innate immunity to viral infection. *Immunity,* 13**,** 129-141.

BANATI, R. B., GEHRMANN, J., SCHUBERT, P. & KREUTZBERG, G. W. 1993. Cytotoxicity of microglia. *Glia,* 7**,** 111-118.

BARBOUR, R., KLING, K., ANDERSON, J. P., BANDUCCI, K., COLE, T., DIEP, L., FOX, M., GOLDSTEIN, J. M., SORIANO, F. & SEUBERT, P. 2008. Red blood cells are the major source of alpha-synuclein in blood. *Neurodegenerative Diseases,* 5**,** 55-59.

BARKHOLT, P., SANCHEZ-GUAJARDO, V., KIRIK, D. & ROMERO-RAMOS, M. 2012. Long-term polarization of microglia upon α-synuclein overexpression in nonhuman primates. *Neuroscience,* 208**,** 85-96.

BEATMAN, E. L., MASSEY, A., SHIVES, K. D., BURRACK, K. S., CHAMANIAN, M., MORRISON, T. E. & BECKHAM, J. D. 2015. Alpha-synuclein expression restricts RNA viral infections in the brain. *Journal of virology***,** JVI. 02949-15.

BELL, J. K., BOTOS, I., HALL, P. R., ASKINS, J., SHILOACH, J., DAVIES, D. R. & SEGAL, D. M. 2006. The molecular structure of the TLR3 extracellular domain. *Journal of endotoxin research,* 12**,** 375-378.

BENMOHAMED, L., SRIVASTAVA, R. & KHAN, A. A. 2016. The Herpes Simplex Virus LAT Gene is Associated with a Broader Repertoire of Virus-Specific

Exhausted CD8⁺ T Cells Retained Within The Trigeminal Ganglia of Latently Infected HLA Transgenic Rabbits. *The Journal of Immunology,* 196**,** 79.14-79.14.

BERNARD, V., GARDIOL, A., FAUCHEUX, B., BLOCH, B., AGID, Y. & HIRSCH, E. C. 1996. Expression of glutamate receptors in the human and rat basal ganglia: Effect of the dopaminergic denervation on AMPA receptor gene expression in the striatopallidal complex in parkinson's disease and rat with 6-OHDA lesion. *Journal of Comparative Neurology,* 368**,** 553-568.

BERTRAND, E., LECHOWICZ, W., SZPAK, G. & DYMECKI, J. 1997. Qualitative and quantitative analysis of locus coeruleus neurons in Parkinson's disease. *Folia neuropathologica,* 35**,** 80-86.

BHAK, G., LEE, J.-H., HAHN, J.-S. & PAIK, S. R. 2009. Granular assembly of α-synuclein leading to the accelerated amyloid fibril formation with shear stress. *PloS one,* 4**,** e4177.

BIEDLER, J. L., ROFFLER-TARLOV, S., SCHACHNER, M. & FREEDMAN, L. S. 1978. Multiple neurotransmitter synthesis by human neuroblastoma cell lines and clones. *Cancer research,* 38**,** 3751-3757.

BJÖRKLUND, A. & LINDVALL, O. 2017. Replacing dopamine neurons in Parkinson's disease: how did it happen? *Journal of Parkinson's disease,* 7**,** S21-S31.

BJØRKØY, G., LAMARK, T., PANKIV, S., ØVERVATN, A., BRECH, A. & JOHANSEN, T. 2009. Chapter 12 Monitoring Autophagic Degradation of p62/SQSTM1. *Methods in Enzymology.* Academic Press.

BOBYN, J., MANGANO, E. N., GANDHI, A., NELSON, E., MOLONEY, K., CLARKE, M. & HAYLEY, S. 2012. Viral-toxin interactions and Parkinson's disease: poly (I: C) priming enhanced the neurodegenerative effects of paraquat. *Journal of neuroinflammation,* 9**,** 86.

BOES, M. & MEYER-WENTRUP, F. 2015. TLR3 triggering regulates PD-L1 (CD274) expression in human neuroblastoma cells. *Cancer Letters,* 361**,** 49-56.

BONIFATI, V. 2012. Autosomal recessive parkinsonism. *Parkinsonism & related disorders,* 18**,** S4-S6.

BONIFATI, V. 2014. Genetics of Parkinson's disease – state of the art, 2013. *Parkinsonism & Related Disorders,* 20**,** S23-S28.

BOUSSET, L., PIERI, L., RUIZ-ARLANDIS, G., GATH, J., JENSEN, P. H., HABENSTEIN, B., MADIONA, K., OLIERIC, V., BÖCKMANN, A., MEIER, B. H. & MELKI, R. 2013. Structural and functional characterization of two alpha-synuclein strains. *Nature communications,* 4**,** 2575.

BOVÉ, J. & PERIER, C. 2012. Neurotoxin-based models of Parkinson's disease. *Neuroscience,* 211**,** 51-76.

BRAAK, H., RÜB, U., GAI, W. P. & DEL TREDICI, K. 2003. Idiopathic Parkinson's disease: possible routes by which vulnerable neuronal types may be subject to neuroinvasion by an unknown pathogen. *Journal of Neural Transmission,* 110**,** 517-536.

BRASK, J., CHAUHAN, A., HILL, R. H., LJUNGGREN, H.-G. & KRISTENSSON, K. 2005. Effects on synaptic activity in cultured hippocampal neurons by influenza A viral proteins. *Journal of Neurovirology,* 11**,** 395-402.

BRENNER, D., BLASER, H. & MAK, T. W. 2015. Regulation of tumour necrosis factor signalling: live or let die. *Nature Reviews Immunology,* 15**,** 362.

BREYDO, L., WU, J. W. & UVERSKY, V. N. 2012. α-Synuclein misfolding and Parkinson's disease. *Biochimica et Biophysica Acta (BBA)-Molecular Basis of Disease,* 1822**,** 261-285.

BRINKMANN, M. M., SPOONER, E., HOEBE, K., BEUTLER, B., PLOEGH, H. L. & KIM, Y.-M. 2007. The interaction between the ER membrane protein UNC93B and TLR3, 7, and 9 is crucial for TLR signaling. *The Journal of cell biology,* 177**,** 265-275.

BSIBSI, M., PERSOON-DEEN, C., VERWER, R. W., MEEUWSEN, S., RAVID, R. & VAN NOORT, J. M. 2006. Toll-like receptor 3 on adult human astrocytes triggers production of neuroprotective mediators. *Glia,* 53**,** 688-695.

BSIBSI, M., RAVID, R., GVERIC, D. & VAN NOORT, J. M. 2002. Broad expression of Toll-like receptors in the human central nervous system. *Journal of Neuropathology & Experimental Neurology,* 61**,** 1013-1021.

BU, X.-L., YAO, X.-Q., JIAO, S.-S., ZENG, F., LIU, Y.-H., XIANG, Y., LIANG, C.-R., WANG, Q.-H., WANG, X., CAO, H.-Y., YI, X., DENG, B., LIU, C.-H., XU, J., ZHANG, L.-L., GAO, C.-Y., XU, Z.-Q., ZHANG, M., WANG, L., TAN, X.-L., XU, X., ZHOU, H.-D. & WANG, Y.-J. 2015. A study on the association between infectious burden and Alzheimer's disease. *European journal of neurology,* 22**,** 1519-1525.

CABIN, D. E., SHIMAZU, K., MURPHY, D., COLE, N. B., GOTTSCHALK, W., MCILWAIN, K. L., ORRISON, B., CHEN, A., ELLIS, C. E. & PAYLOR, R. 2002. Synaptic vesicle depletion correlates with attenuated synaptic responses to prolonged repetitive stimulation in mice lacking α-synuclein. *Journal of Neuroscience,* 22**,** 8797-8807.

CAGGIU, E., PAULUS, K., ARRU, G., PIREDDA, R., SECHI, G. P. & SECHI, L. A. 2016. Humoral cross reactivity between α-synuclein and herpes simplex-1 epitope in Parkinson's disease, a triggering role in the disease? *Journal of neuroimmunology,* 291**,** 110-114.

CANNON, J. R., TAPIAS, V., NA, H. M., HONICK, A. S., DROLET, R. E. & GREENAMYRE, J. T. 2009. A highly reproducible rotenone model of Parkinson's disease. *Neurobiology of disease,* 34**,** 279-290.

CARPENTIER, P. A., BEGOLKA, W. S., OLSON, J. K., ELHOFY, A., KARPUS, W. J. & MILLER, S. D. 2005. Differential activation of astrocytes by innate and adaptive immune stimuli. *Glia,* 49**,** 360-374.

CARR, D. J., NOISAKRAN, S., HALFORD, W. P., LUKACS, N., ASENSIO, V. & CAMPBELL, I. L. 1998. Cytokine and chemokine production in HSV-1 latently infected trigeminal ganglion cell cultures: effects of hyperthermic stress. *Journal of neuroimmunology,* 85**,** 111-121.

CAUDLE, W. M., COLEBROOKE, R. E., EMSON, P. C. & MILLER, G. W. 2008. Altered vesicular dopamine storage in Parkinson's disease: a premature demise. *Trends in neurosciences,* 31**,** 303-308.

CEGELSKI, L., PINKNER, J. S., HAMMER, N. D., CUSUMANO, C. K., HUNG, C. S., CHORELL, E., ÅBERG, V., WALKER, J. N., SEED, P. C. & ALMQVIST, F. 2009. Small-molecule inhibitors target Escherichia coli amyloid biogenesis and biofilm formation. *Nature chemical biology,* 5**,** 913-919.

CHANG, Z. 2010. Important aspects of Toll-like receptors, ligands and their signaling pathways. *Inflammation research,* 59**,** 791-808.

CHATTOPADHYAY, S., YAMASHITA, M., ZHANG, Y. & SEN, G. C. 2011. The IRF-3/Bax mediated apoptotic pathway, activated by viral cytoplasmic RNA and DNA, inhibits virus replication. *Journal of virology.*

CHERMENINA, M., CHORELL, E., POKRZYWA, M., ANTTI, H., ALMQVIST, F., STRÖMBERG, I. & WITTUNG-STAFSHEDE, P. 2015. Single injection of

small-molecule amyloid accelerator results in cell death of nigral dopamine neurons in mice. *NPJ Parkinson's disease,* 1**,** 15024.

CHESHIRE, P., AYTON, S., BERTRAM, K. L., LING, H., LI, A., MCLEAN, C., HALLIDAY, G. M., O'SULLIVAN, S. S., REVESZ, T., FINKELSTEIN, D. I., STOREY, E. & WILLIAMS, D. R. 2015. Serotonergic markers in Parkinson's disease and levodopa-induced dyskinesias. *Movement Disorders,* 30**,** 796-804.

CHOE, J., KELKER, M. S. & WILSON, I. A. 2005. Crystal structure of human toll-like receptor 3 (TLR3) ectodomain. *science,* 309**,** 581-585.

CHU, Y. & KORDOWER, J. H. 2010. Lewy body pathology in fetal grafts. *Annals of the New York Academy of Sciences,* 1184**,** 55-67.

CLAYTON, K. B. & SULLIVAN, A. M. 2007. Differential effects of GDF5 on the medial and lateral rat ventral mesencephalon. *Neuroscience letters,* 427**,** 132-137.

CLINTON, S. M., HAROUTUNIAN, V. & MEADOR-WOODRUFF, J. H. 2006. Up-regulation of NMDA receptor subunit and post-synaptic density protein expression in the thalamus of elderly patients with schizophrenia. *Journal of neurochemistry,* 98**,** 1114-1125.

CONCANNON, R. M., OKINE, B. N., FINN, D. P. & DOWD, E. 2016. Upregulation of the cannabinoid CB2 receptor in environmental and viral inflammation-driven rat models of Parkinson's disease. *Experimental neurology,* 283**,** 204-212.

COUSINS, S. L. & STEPHENSON, F. A. 2012. Identification of NMDA receptor subtype-specific binding sites that mediate direct interactions with the scaffold protein, PSD-95. *Journal of Biological Chemistry*.

COX, D., CARVER, J. A. & ECROYD, H. 2014. Preventing α-synuclein aggregation: The role of the small heat-shock molecular chaperone proteins. *Biochimica et Biophysica Acta (BBA) - Molecular Basis of Disease,* 1842**,** 1830-1843.

CREMADES, N., COHEN, S. I., DEAS, E., ABRAMOV, A. Y., CHEN, A. Y., ORTE, A., SANDAL, M., CLARKE, R. W., DUNNE, P. & APRILE, F. A. 2012. Direct observation of the interconversion of normal and toxic forms of α-synuclein. *Cell,* 149**,** 1048-1059.

CUERVO, A. M. 2010. Chaperone-mediated autophagy: selectivity pays off. *Trends in Endocrinology & Metabolism,* 21**,** 142-150.

DALE, R. C., CHURCH, A. J., SURTEES, R. A., LEES, A. J., ADCOCK, J. E., HARDING, B., NEVILLE, B. G. & GIOVANNONI, G. 2004. Encephalitis lethargica syndrome: 20 new cases and evidence of basal ganglia autoimmunity. *Brain,* 127**,** 21-33.

DALE, R. C., IRANI, S. R., BRILOT, F., PILLAI, S., WEBSTER, R., GILL, D., LANG, B. & VINCENT, A. 2009. N-methyl-D-aspartate receptor antibodies in pediatric dyskinetic encephalitis lethargica. *Annals of Neurology: Official Journal of the American Neurological Association and the Child Neurology Society,* 66**,** 704-709.

DANIELE, S. G., BÉRAUD, D., DAVENPORT, C., CHENG, K., YIN, H. & MAGUIRE-ZEISS, K. A. 2015. Activation of MyD88-dependent TLR1/2 signaling by misfolded α-synuclein, a protein linked to neurodegenerative disorders. *Sci. Signal.,* 8**,** ra45-ra45.

DAUGHERTY, A. & RAZ, N. 2013. Age-related differences in iron content of subcortical nuclei observed in vivo: a meta-analysis. *Neuroimage,* 70**,** 113-121.

DAY, M., WANG, Z., DING, J., AN, X., INGHAM, C. A., SHERING, A. F., WOKOSIN, D., ILIJIC, E., SUN, Z. & SAMPSON, A. R. 2006. Selective

elimination of glutamatergic synapses on striatopallidal neurons in Parkinson disease models. *Nature neuroscience,* 9**,** 251.

DE JONG , M. D., CAM , B. V., QUI , P. T., HIEN , V. M., THANH , T. T., HUE , N. B., BELD , M., PHUONG , L. T., KHANH , T. H., CHAU , N. V. V., HIEN , T. T., HA , D. Q. & FARRAR , J. 2005. Fatal Avian Influenza A (H5N1) in a Child Presenting with Diarrhea Followed by Coma. *New England Journal of Medicine,* 352**,** 686-691.

DE LA FUENTE-FERNÁNDEZ, R. 2013. Imaging of dopamine in PD and implications for motor and neuropsychiatric manifestations of PD. *Frontiers in neurology,* 4**,** 90.

DE LAU, L. M. & BRETELER, M. M. 2006. Epidemiology of Parkinson's disease. *The Lancet Neurology,* 5**,** 525-535.

DEL TREDICI, K. & BRAAK, H. 2016. Review: Sporadic Parkinson's disease: development and distribution of α-synuclein pathology. *Neuropathology and applied neurobiology,* 42**,** 33-50.

DELEIDI, M., HALLETT, P. J., KOPRICH, J. B., CHUNG, C.-Y. & ISACSON, O. 2010. The Toll-like receptor-3 agonist polyinosinic: polycytidylic acid triggers nigrostriatal dopaminergic degeneration. *Journal of Neuroscience,* 30**,** 16091-16101.

DELEIDI, M. & ISACSON, O. 2012. Viral and Inflammatory Triggers of Neurodegenerative Diseases. *Science translational medicine,* 4**,** 121ps3-121ps3.

DESPLATS, P., LEE, H.-J., BAE, E.-J., PATRICK, C., ROCKENSTEIN, E., CREWS, L., SPENCER, B., MASLIAH, E. & LEE, S.-J. 2009. Inclusion formation and neuronal cell death through neuron-to-neuron transmission of α-synuclein. *Proceedings of the National Academy of Sciences of the United States of America,* 106**,** 13010-13015.

DEVOS, D., DEFEBVRE, L. & BORDET, R. 2010. Dopaminergic and non-dopaminergic pharmacological hypotheses for gait disorders in Parkinson's disease. *Fundamental & clinical pharmacology,* 24**,** 407-421.

DINARELLO, C. A. 2009. Immunological and inflammatory functions of the interleukin-1 family. *Annual review of immunology,* 27**,** 519-550.

DINARELLO, C. A. 2018. Introduction to the interleukin-1 family of cytokines and receptors: Drivers of innate inflammation and acquired immunity. *Immunological reviews,* 281**,** 5-7.

DING, T. T., LEE, S.-J., ROCHET, J.-C. & LANSBURY, P. T. 2002. Annular α-synuclein protofibrils are produced when spherical protofibrils are incubated in solution or bound to brain-derived membranes. *Biochemistry,* 41**,** 10209-10217.

DROUIN-OUELLET, J., ST-AMOUR, I., SAINT-PIERRE, M., LAMONTAGNE-PROULX, J., KRIZ, J., BARKER, R. A. & CICCHETTI, F. 2015. Toll-like receptor expression in the blood and brain of patients and a mouse model of Parkinson's disease. *International Journal of Neuropsychopharmacology,* 18**,** pyu103.

DUTTON, R., BRADLEY, L. & SWAIN, S. 1998. T cell memory. *Annual review of immunology,* 16**,** 201-223.

EBRAHIMIE, E., NUROLLAH, Z., EBRAHIMI, M., HEMMATZADEH, F. & IGNJATOVIC, J. 2015. Unique ability of pandemic influenza to downregulate the genes involved in neuronal disorders. *Molecular Biology Reports,* 42**,** 1377-1390.

EHRLICH, I., KLEIN, M., RUMPEL, S. & MALINOW, R. 2007. PSD-95 is required for activity-driven synapse stabilization. *Proceedings of the National Academy of Sciences,* 104**,** 4176-4181.

EJLERSKOV, P., HULTBERG, JEANETTE G., WANG, J., CARLSSON, R., AMBJØRN, M., KUSS, M., LIU, Y., PORCU, G., KOLKOVA, K., FRIIS RUNDSTEN, C., RUSCHER, K., PAKKENBERG, B., GOLDMANN, T., LORETH, D., PRINZ, M., RUBINSZTEIN, DAVID C. & ISSAZADEH-NAVIKAS, S. 2015. Lack of Neuronal IFN-β-IFNAR Causes Lewy Body- and Parkinson's Disease-like Dementia. *Cell,* 163**,** 324-339.

EL-HUSSEINI, A. E.-D., SCHNELL, E., CHETKOVICH, D. M., NICOLL, R. A. & BREDT, D. S. 2000. PSD-95 Involvement in Maturation of Excitatory Synapses. *science,* 290**,** 1364-1368.

ELIZAN, T. S., MADDEN, D. L., NOBLE, G. R., HERRMANN, K. L., GARDNER, J., SCHWARTZ, J., SMITH, H., SEVER, J. L. & YAHR, M. D. 1979. Viral antibodies in serum and CSF of Parkinsonian patients and controls. *Archives of neurology,* 36**,** 529-534.

ESCALANTE, C. R., NISTAL-VILLÁN, E., SHEN, L., GARCÍA-SASTRE, A. & AGGARWAL, A. K. 2007. Structure of IRF-3 bound to the PRDIII-I regulatory element of the human interferon-β enhancer. *Molecular cell,* 26**,** 703-716.

ESIRI, M. M. 1982. Herpes simplex encephalitis: an immunohistological study of the distribution of viral antigen within the brain. *Journal of the neurological sciences,* 54**,** 209-226.

FAGUNDES, D. J. & TAHA, M. O. 2004. Animal disease model: choice´ s criteria and current animals specimens. *Acta Cirurgica Brasileira,* 19**,** 59-65.

FALVO, J. V., PAREKH, B. S., LIN, C. H., FRAENKEL, E. & MANIATIS, T. 2000. Assembly of a functional beta interferon enhanceosome is dependent on ATF-2–c-Jun heterodimer orientation. *Molecular and cellular biology,* 20**,** 4814-4825.

FARINA, C., KRUMBHOLZ, M., GIESE, T., HARTMANN, G., ALOISI, F. & MEINL, E. 2005. Preferential expression and function of Toll-like receptor 3 in human astrocytes. *Journal of neuroimmunology,* 159**,** 12-19.

FEARNLEY, J. M. & LEES, A. J. 1991. Ageing and Parkinson's disease: substantia nigra regional selectivity. *Brain,* 114**,** 2283-2301.

FERRINGTON, D. A., HUSOM, A. D. & THOMPSON, L. V. 2005. Altered proteasome structure, function, and oxidation in aged muscle. *The FASEB journal,* 19**,** 644-646.

FIELD, R., CAMPION, S., WARREN, C., MURRAY, C. & CUNNINGHAM, C. 2010. Systemic challenge with the TLR3 agonist poly I: C induces amplified IFNα/β and IL-1β responses in the diseased brain and exacerbates chronic neurodegeneration. *Brain, Behavior, and Immunity,* 24**,** 996-1007.

FINLEY, D. 2009. Recognition and processing of ubiquitin-protein conjugates by the proteasome. *Annual review of biochemistry,* 78**,** 477-513.

FITZGERALD, K. A., MCWHIRTER, S. M., FAIA, K. L., ROWE, D. C., LATZ, E., GOLENBOCK, D. T., COYLE, A. J., LIAO, S.-M. & MANIATIS, T. 2003. IKKε and TBK1 are essential components of the IRF3 signaling pathway. *Nature immunology,* 4**,** 491.

FLAGMEIER, P., MEISL, G., VENDRUSCOLO, M., KNOWLES, T. P. J., DOBSON, C. M., BUELL, A. K. & GALVAGNION, C. 2016. Mutations associated with familial Parkinson's disease alter the initiation and amplification steps of α-synuclein aggregation. *Proceedings of the National Academy of Sciences of the United States of America,* 113**,** 10328-10333.

FORREST, C. M., KHALIL, O. S., PISAR, M., SMITH, R. A., DARLINGTON, L. G. & STONE, T. W. 2012. Prenatal activation of Toll-like receptors-3 by administration of the viral mimetic poly (I: C) changes synaptic proteins, N-methyl-D-aspartate receptors and neurogenesis markers in offspring. *Molecular brain,* 5**,** 22.

FOURIE, C., KIM, E., WALDVOGEL, H., WONG, J., MCGREGOR, A., FAULL, R. & MONTGOMERY, J. 2014. Differential changes in postsynaptic density proteins in postmortem Huntington's disease and Parkinson's disease human brains. *Journal of neurodegenerative diseases,* 2014.

FRASER, N. W., LAWRENCE, W. C., WROBLEWSKA, Z., GILDEN, D. H. & KOPROWSKI, H. 1981. Herpes simplex type 1 DNA in human brain tissue. *Proceedings of the National Academy of Sciences,* 78**,** 6461-6465.

FRIEDMAN, L. G., LACHENMAYER, M. L., WANG, J., HE, L., POULOSE, S. M., KOMATSU, M., HOLSTEIN, G. R. & YUE, Z. 2012. Disrupted autophagy leads to dopaminergic axon and dendrite degeneration and promotes presynaptic accumulation of α-synuclein and LRRK2 in the brain. *Journal of Neuroscience,* 32**,** 7585-7593.

FUJIOKA, S., OGAKI, K., TACIK, P., UITTI, R. J., ROSS, O. A. & WSZOLEK, Z. K. 2014. Update on novel familial forms of Parkinson's disease and multiple system atrophy. *Parkinsonism & Related Disorders,* 20**,** S29-S34.

FUNAMI, K., MATSUMOTO, M., OSHIUMI, H., AKAZAWA, T., YAMAMOTO, A. & SEYA, T. 2004. The cytoplasmic 'linker region'in Toll-like receptor 3 controls receptor localization and signaling. *International immunology,* 16**,** 1143-1154.

GAI, W., HALLIDAY, G., BLUMBERGS, P., GEFFEN, L. & W BLESSING, W. 1991. Substance P-containing neurons in the mesopontine tegmentum are severely affected in Parkinson's disease. *Brain,* 114**,** 2253-2267.

GAMBOA, E. T., WOLF, A., YAHR, M. D., HARTER, D. H., DUFFY, P. E., BARDEN, H. & HSU, K. C. 1974. Influenza virus antigen in postencephalitic parkinsonism brain: detection by immunofluorescence. *Archives of neurology,* 31**,** 228-232.

GAO, H.-M. & HONG, J.-S. 2011. Gene–environment interactions: key to unraveling the mystery of Parkinson's disease. *Progress in neurobiology,* 94**,** 1-19.

GARCIA-REITBÖCK, P., ANICHTCHIK, O., BELLUCCI, A., IOVINO, M., BALLINI, C., FINEBERG, E., GHETTI, B., DELLA CORTE, L., SPANO, P. & TOFARIS, G. K. 2010. SNARE protein redistribution and synaptic failure in a transgenic mouse model of Parkinson's disease. *Brain,* 133**,** 2032-2044.

GARCIA, Y., BREEN, A., BURUGAPALLI, K., DOCKERY, P. & PANDIT, A. 2007. Stereological methods to assess tissue response for tissue-engineered scaffolds. *Biomaterials,* 28**,** 175-186.

GERLIER, D. & THOMASSET, N. 1986. Use of MTT colorimetric assay to measure cell activation. *Journal of Immunological Methods,* 94**,** 57-63.

GIBB, W. & LEES, A. 1988. A comparison of clinical and pathological features of young-and old-onset Parkinson's disease. *Neurology,* 38**,** 1402-1402.

GIGUÈRE, N., BURKE NANNI, S. & TRUDEAU, L.-E. 2018. On Cell Loss and Selective Vulnerability of Neuronal Populations in Parkinson's Disease. *Frontiers in neurology,* 9**,** 455.

GIORDANO, S., LEE, J., DARLEY-USMAR, V. M. & ZHANG, J. 2012. Distinct Effects of Rotenone, 1-methyl-4-phenylpyridinium and 6-hydroxydopamine on Cellular Bioenergetics and Cell Death. *PloS one,* 7**,** e44610.

GLABE, C. G. 2008. Structural classification of toxic amyloid oligomers. *Journal of Biological Chemistry,* 283**,** 29639-29643.

GOEDERT, M., SPILLANTINI, M. G., DEL TREDICI, K. & BRAAK, H. 2013. 100 years of Lewy pathology. *Nature Reviews Neurology,* 9**,** 13.

GORDON, L., MCQUAID, S. & COSBY, S. 1996. Detection of herpes simplex virus (types 1 and 2) and human herpesvirus 6 DNA in human brain tissue by polymerase chain reaction. *Clinical and diagnostic virology,* 6**,** 33-40.

GORDON, S. L., HARPER, C. B., SMILLIE, K. J. & COUSIN, M. A. 2016. A fine balance of synaptophysin levels underlies efficient retrieval of synaptobrevin II to synaptic vesicles. *PloS one,* 11**,** e0149457.

GOSAVI, N., LEE, H.-J., LEE, J. S., PATEL, S. & LEE, S.-J. 2002. Golgi fragmentation occurs in the cells with prefibrillar α-synuclein aggregates and precedes the formation of fibrillar inclusion. *Journal of Biological Chemistry,* 277**,** 48984-48992.

GRUNE, T., JUNG, T., MERKER, K. & DAVIES, K. J. A. 2004. Decreased proteolysis caused by protein aggregates, inclusion bodies, plaques, lipofuscin, ceroid, and 'aggresomes' during oxidative stress, aging, and disease. *The International Journal of Biochemistry & Cell Biology,* 36**,** 2519-2530.

GUO, J. L. & LEE, V. M. 2014. Cell-to-cell transmission of pathogenic proteins in neurodegenerative diseases. *Nature medicine,* 20**,** 130.

GUO, Y., DENG, X., ZHENG, W., XU, H., SONG, Z., LIANG, H., LEI, J., JIANG, X., LUO, Z. & DENG, H. 2011. HLA rs3129882 variant in Chinese Han patients with late-onset sporadic Parkinson disease. *Neuroscience letters,* 501**,** 185-187.

HAKIMI, M., SELVANANTHAM, T., SWINTON, E., PADMORE, R. F., TONG, Y., KABBACH, G., VENDEROVA, K., GIRARDIN, S. E., BULMAN, D. E., SCHERZER, C. R., LAVOIE, M. J., GRIS, D., PARK, D. S., ANGEL, J. B., SHEN, J., PHILPOTT, D. J. & SCHLOSSMACHER, M. G. 2011. Parkinson's disease-linked LRRK2 is expressed in circulating and tissue immune cells and upregulated following recognition of microbial structures. *Journal of Neural Transmission,* 118**,** 795-808.

HALFORD, W. P., GEBHARDT, B. M. & CARR, D. J. 1996. Persistent cytokine expression in trigeminal ganglion latently infected with herpes simplex virus type 1. *The Journal of Immunology,* 157**,** 3542-3549.

HALLIDAY, G. M. & MCCANN, H. 2008. Human-based studies on α-synuclein deposition and relationship to Parkinson's disease symptoms. *Experimental neurology,* 209**,** 12-21.

HAMZA, T. H., ZABETIAN, C. P., TENESA, A., LAEDERACH, A., MONTIMURRO, J., YEAROUT, D., KAY, D. M., DOHENY, K. F., PASCHALL, J., PUGH, E., KUSEL, V. I., COLLURA, R., ROBERTS, J., GRIFFITH, A., SAMII, A., SCOTT, W. K., NUTT, J., FACTOR, S. A. & PAYAMI, H. 2010. Common genetic variation in the HLA region is associated with late-onset sporadic Parkinson's disease. *Nature genetics,* 42**,** 781-785.

HARRIS, M. A., TSUI, J. K., MARION, S. A., SHEN, H. & TESCHKE, K. 2012. Association of Parkinson's disease with infections and occupational exposure to possible vectors. *Movement Disorders,* 27**,** 1111-1117.

HAUWEL, M., FURON, E., CANOVA, C., GRIFFITHS, M., NEAL, J. & GASQUE, P. 2005. Innate (inherent) control of brain infection, brain inflammation and brain repair: the role of microglia, astrocytes,"protective" glial stem cells and stromal ependymal cells. *Brain research reviews,* 48**,** 220-233.

HAWKES, C. H., DEL TREDICI, K. & BRAAK, H. 2007. Parkinson's disease: a dual-hit hypothesis. *Neuropathology and applied neurobiology,* 33**,** 599-614.

HE, B., GROSS, M. & ROIZMAN, B. 1997. The γ134. 5 protein of herpes simplex virus 1 complexes with protein phosphatase 1α to dephosphorylate the α subunit of the eukaryotic translation initiation factor 2 and preclude the shutoff of protein synthesis by double-stranded RNA-activated protein kinase. *Proceedings of the National Academy of Sciences,* 94**,** 843-848.

HEIKKILA, R. E., NICKLAS, W. J., VYAS, I. & DUVOISIN, R. C. 1985. Dopaminergic toxicity of rotenone and the 1-methyl-4-phenylpyridinium ion after their stereotaxic administration to rats: implication for the mechanism of 1-methyl-4-phenyl-1, 2, 3, 6-tetrahydropyridine toxicity. *Neuroscience letters,* 62**,** 389-394.

HEINRICH, P. C., CASTELL, J. V. & ANDUS, T. 1990. Interleukin-6 and the acute phase response. *Biochemical journal,* 265**,** 621.

HEMLING, N., RÖYTTÄ, M., RINNE, J., PÖLLÄNEN, P., BROBERG, E., TAPIO, V., VAHLBERG, T. & HUKKANEN, V. 2003. Herpesviruses in brains in Alzheimer's and Parkinson's diseases. *Annals of neurology,* 54**,** 267-271.

HENNESSY, C. & MCKERNAN, D. P. 2016. Epigenetics and innate immunity: the 'unTolld'story. *Immunology and cell biology,* 94**,** 631-639.

HEO, S. R., HAN, A. M., KWON, Y. K. & JOUNG, I. 2009. p62 protects SH-SY5Y neuroblastoma cells against H2O2-induced injury through the PDK1/Akt pathway. *Neuroscience letters,* 450**,** 45-50.

HEUSINKVELD, H. J. & WESTERINK, R. H. S. 2017. Comparison of different in vitro cell models for the assessment of pesticide-induced dopaminergic neurotoxicity. *Toxicology in Vitro,* 45**,** 81-88.

HINDLE, J. V. 2010. Ageing, neurodegeneration and Parkinson's disease. *Age and ageing,* 39**,** 156-161.

HIRSCH, E. C., GRAYBIEL, A. M., DUYCKAERTS, C. & JAVOY-AGID, F. 1987. Neuronal loss in the pedunculopontine tegmental nucleus in Parkinson disease and in progressive supranuclear palsy. *Proceedings of the National Academy of Sciences,* 84**,** 5976-5980.

HOBAN, D. B., CONNAUGHTON, E., CONNAUGHTON, C., HOGAN, G., THORNTON, C., MULCAHY, P., MOLONEY, T. C. & DOWD, E. 2013. Further characterisation of the LPS model of Parkinson's disease: a comparison of intra-nigral and intra-striatal lipopolysaccharide administration on motor function, microgliosis and nigrostriatal neurodegeneration in the rat. *Brain, Behavior, and Immunity,* 27**,** 91-100.

HORVATH, I., WEISE, C. F., ANDERSSON, E. K., CHORELL, E., SELLSTEDT, M., BENGTSSON, C., OLOFSSON, A., HULTGREN, S. J., CHAPMAN, M. & WOLF-WATZ, M. 2012. Mechanisms of protein oligomerization: inhibitor of functional amyloids templates α-synuclein fibrillation. *Journal of the American Chemical Society,* 134**,** 3439-3444.

HUNOT, S., BOISSIERE, F., FAUCHEUX, B., BRUGG, B., MOUATT-PRIGENT, A., AGID, Y. & HIRSCH, E. 1996. Nitric oxide synthase and neuronal vulnerability in Parkinson's disease. *Neuroscience,* 72**,** 355-363.

IRRCHER, I., ALEYASIN, H., SEIFERT, E., HEWITT, S., CHHABRA, S., PHILLIPS, M., LUTZ, A., ROUSSEAUX, M., BEVILACQUA, L. & JAHANI-ASL, A. 2010. Loss of the Parkinson's disease-linked gene DJ-1 perturbs mitochondrial dynamics. *Human molecular genetics,* 19**,** 3734-3746.

ISAACS, A. & LINDENMANN, J. 1957. Virus interference. I. The interferon. *Proceedings of the Royal Society of London B: Biological Sciences,* 147**,** 258-267.

ITZHAKI, R. F., LATHE, R., BALIN, B. J., BALL, M. J., BEARER, E. L., BRAAK, H., BULLIDO, M. J., CARTER, C., CLERICI, M. & COSBY, S. L. 2016. Microbes and Alzheimer's disease. *Journal of Alzheimer's disease: JAD,* 51**,** 979.

JACK, C. S., ARBOUR, N., MANUSOW, J., MONTGRAIN, V., BLAIN, M., MCCREA, E., SHAPIRO, A. & ANTEL, J. P. 2005. TLR signaling tailors innate immune responses in human microglia and astrocytes. *The Journal of Immunology,* 175**,** 4320-4330.

JAMIESON, G. A., MAITLAND, N. J., WILCOCK, G. K., YATES, C. M. & ITZHAKI, R. F. 1992. Herpes simplex virus type 1 DNA is present in specific regions of brain from aged people with and without senile dementia of the Alzheimer type. *The Journal of Pathology,* 167**,** 365-368.

JANG, H., BOLTZ, D., MCCLAREN, J., PANI, A. K., SMEYNE, M., KORFF, A., WEBSTER, R. & SMEYNE, R. J. 2012. Inflammatory effects of highly pathogenic H5N1 influenza virus infection in the CNS of mice. *Journal of Neuroscience,* 32**,** 1545-1559.

JANG, H., BOLTZ, D., STURM-RAMIREZ, K., SHEPHERD, K. R., JIAO, Y., WEBSTER, R. & SMEYNE, R. J. 2009. Highly pathogenic H5N1 influenza virus can enter the central nervous system and induce neuroinflammation and neurodegeneration. *Proceedings of the National Academy of Sciences,* 106**,** 14063-14068.

JAROSINSKI, K. W., WHITNEY, L. W. & MASSA, P. T. 2001. Specific deficiency in nuclear factor-κB activation in neurons of the central nervous system. *Laboratory investigation,* 81**,** 1275.

JAVITCH, J. A., D'AMATO, R. J., STRITTMATTER, S. M. & SNYDER, S. H. 1985. Parkinsonism-inducing neurotoxin, N-methyl-4-phenyl-1, 2, 3, 6-tetrahydropyridine: uptake of the metabolite N-methyl-4-phenylpyridine by dopamine neurons explains selective toxicity. *Proceedings of the National Academy of Sciences,* 82**,** 2173-2177.

JAVOY, F., SOTELO, C., HERBET, A. & AGID, Y. 1976. Specificity of dopaminergic neuronal degeneration induced by intracerebral injection of 6-hydroxydopamine in the nigrostriatal dopamine system. *Brain Research,* 102**,** 201-215.

JEOHN, G.-H., COOPER, C. L., WILSON, B., CHANG, R. C., JANG, K.-J., KIM, H.-C., LIU, B. & HONG, J.-S. 2002. p38 MAP kinase is involved in lipopolysaccharide-induced dopaminergic neuronal cell death in rat mesencephalic neuron-glia cultures. *Annals of the New York Academy of Sciences,* 962**,** 332-346.

JONSSON, G. 1980. Chemical neurotoxins as denervation tools in neurobiology. *Annual review of neuroscience,* 3**,** 169-187.

JORDAN, T. X. & RANDALL, G. 2012. Manipulation or capitulation: virus interactions with autophagy. *Microbes and infection,* 14**,** 126-139.

KABEYA, Y., MIZUSHIMA, N., UENO, T., YAMAMOTO, A., KIRISAKO, T., NODA, T., KOMINAMI, E., OHSUMI, Y. & YOSHIMORI, T. 2000. LC3, a mammalian homologue of yeast Apg8p, is localized in autophagosome membranes after processing. *The EMBO Journal,* 19**,** 5720-5728.

KANDEL, E. R., SCHWARTZ, J. H., JESSELL, T. M., SIEGELBAUM, S. A. & HUDSPETH, A. J. 2000. *Principles of neural science,* McGraw-hill New York.

KANG, R., ZEH, H., LOTZE, M. & TANG, D. 2011. The Beclin 1 network regulates autophagy and apoptosis. *Cell Death & Differentiation,* 18**,** 571-580.

KARUNAKARAN, S., SAEED, U., MISHRA, M., VALLI, R. K., JOSHI, S. D., MEKA, D. P., SETH, P. & RAVINDRANATH, V. 2008. Selective activation of p38 mitogen-activated protein kinase in dopaminergic neurons of substantia nigra leads to nuclear translocation of p53 in 1-methyl-4-phenyl-1, 2, 3, 6-tetrahydropyridine-treated mice. *Journal of Neuroscience,* 28**,** 12500-12509.

KAVOURAS, J. H., PRANDOVSZKY, E., VALYI-NAGY, K., KOVACS, S. K., TIWARI, V., KOVACS, M., SHUKLA, D. & VALYI-NAGY, T. 2007. Herpes simplex virus type 1 infection induces oxidative stress and the release of bioactive lipid peroxidation by-products in mouse P19N neural cell cultures. *Journal of Neurovirology,* 13**,** 416-425.

KAWAI, T. & AKIRA, S. 2006. Innate immune recognition of viral infection. *Nature immunology,* 7**,** 131.

KHANLOU, N., MOORE, D. J., CHANA, G., CHERNER, M., LAZZARETTO, D., DAWES, S., GRANT, I., MASLIAH, E., EVERALL, I. P. & GROUP, H. 2009. Increased frequency of α-synuclein in the substantia nigra in human immunodeficiency virus infection. *Journal of Neurovirology,* 15**,** 131-138.

KHANNA, K. M., BONNEAU, R. H., KINCHINGTON, P. R. & HENDRICKS, R. L. 2003. Herpes Simplex Virus-Specific Memory CD8+ T Cells Are Selectively Activated and Retained in Latently Infected Sensory Ganglia. *Immunity,* 18**,** 593-603.

KIM, C., HO, D.-H., SUK, J.-E., YOU, S., MICHAEL, S., KANG, J., LEE, S. J., MASLIAH, E., HWANG, D. & LEE, H.-J. 2013a. Neuron-released oligomeric α-synuclein is an endogenous agonist of TLR2 for paracrine activation of microglia. *Nature communications,* 4**,** 1562.

KIM, C., LEE, H.-J., MASLIAH, E. & LEE, S.-J. 2016. Non-cell-autonomous Neurotoxicity of α-synuclein Through Microglial Toll-like Receptor 2. *Experimental neurobiology,* 25**,** 113-119.

KIM, J., HUH, J., HWANG, M., KWON, E.-H., JUNG, D.-J., BRINKMANN, M. M., JANG, M. H., PLOEGH, H. L. & KIM, Y.-M. 2013b. Acidic amino acid residues in the juxtamembrane region of the nucleotide-sensing TLRs are important for UNC93B1 binding and signaling. *The Journal of Immunology***,** 1202767.

KIMURA, A. & KISHIMOTO, T. 2010. IL-6: regulator of Treg/Th17 balance. *European journal of immunology,* 40**,** 1830-1835.

KIRIK, D., ANNETT, L. E., BURGER, C., MUZYCZKA, N., MANDEL, R. J. & BJÖRKLUND, A. 2003. Nigrostriatal α-synucleinopathy induced by viral vector-mediated overexpression of human α-synuclein: a new primate model of Parkinson's disease. *Proceedings of the National Academy of Sciences,* 100**,** 2884-2889.

KIRIK, D., ROSENBLAD, C., BURGER, C., LUNDBERG, C., JOHANSEN, T. E., MUZYCZKA, N., MANDEL, R. J. & BJÖRKLUND, A. 2002. Parkinson-Like Neurodegeneration Induced by Targeted Overexpression of α-Synuclein in the Nigrostriatal System. *The Journal of Neuroscience,* 22**,** 2780-2791.

KISHIMOTO, T. 1989. The biology of interleukin-6. *Blood,* 74**,** 1-10.

KLEINE, T., HACKLER, R. & ZÖFEL, P. 1992. Age-related alterations of the blood-brain-barrier (bbb) permeability to protein molecules of different size. *Zeitschrift fur Gerontologie,* 26**,** 256-259.

KLIONSKY, D. J., ABDELMOHSEN, K., ABE, A., ABEDIN, M. J., ABELIOVICH, H., ACEVEDO AROZENA, A., ADACHI, H., ADAMS, C. M., ADAMS, P. D. & ADELI, K. 2016. Guidelines for the use and interpretation of assays for monitoring autophagy. *Autophagy,* 12**,** 1-222.

KOMATSU, M., WAGURI, S., CHIBA, T., MURATA, S., IWATA, J.-I., TANIDA, I., UENO, T., KOIKE, M., UCHIYAMA, Y. & KOMINAMI, E. 2006. Loss of autophagy in the central nervous system causes neurodegeneration in mice. *Nature,* 441**,** 880-884.

KOPRICH, J. B., JOHNSTON, T. H., HUOT, P., REYES, M. G., ESPINOSA, M. & BROTCHIE, J. M. 2011. Progressive neurodegeneration or endogenous compensation in an animal model of Parkinson's disease produced by decreasing doses of alpha-synuclein. *PloS one,* 6**,** e17698.

KOPRICH, J. B., KALIA, L. V. & BROTCHIE, J. M. 2017. Animal models of α-synucleinopathy for Parkinson disease drug development. *Nature Reviews Neuroscience,* 18**,** 515.

KORDOWER, J. H., CHU, Y., HAUSER, R. A., FREEMAN, T. B. & OLANOW, C. W. 2008a. Lewy body–like pathology in long-term embryonic nigral transplants in Parkinson's disease. *Nature medicine,* 14**,** 504.

KORDOWER, J. H., CHU, Y., HAUSER, R. A., OLANOW, C. W. & FREEMAN, T. B. 2008b. Transplanted dopaminergic neurons develop PD pathologic changes: A second case report. *Movement Disorders,* 23**,** 2303-2306.

KORDOWER, J. H., DODIYA, H. B., KORDOWER, A. M., TERPSTRA, B., PAUMIER, K., MADHAVAN, L., SORTWELL, C., STEECE-COLLIER, K. & COLLIER, T. J. 2011. TRANSFER OF HOST-DERIVED ALPHA SYNUCLEIN TO GRAFTED DOPAMINERGIC NEURONS IN RAT. *Neurobiology of disease,* 43**,** 552-557.

KOUROUPI, G., TAOUFIK, E., VLACHOS, I. S., TSIORAS, K., ANTONIOU, N., PAPASTEFANAKI, F., CHRONI-TZARTOU, D., WRASIDLO, W., BOHL, D. & STELLAS, D. 2017. Defective synaptic connectivity and axonal neuropathology in a human iPSC-based model of familial Parkinson's disease. *Proceedings of the National Academy of Sciences,* 114**,** E3679-E3688.

KOUTI, L., NOROOZIAN, M., AKHONDZADEH, S., ABDOLLAHI, M., JAVADI, M., FARAMARZI, M., MOUSAVI, S. & GHAELI, P. 2013. Nitric oxide and peroxynitrite serum levels in Parkinson's disease: correlation of oxidative stress and the severity of the disease. *Eur Rev Med Pharmacol Sci,* 17**,** 964-970.

KROKSVEEN, A., OPSAHL, J., AYE, T., ULVIK, R. & BERVEN, F. 2011. Proteomics of human cerebrospinal fluid: discovery and verification of biomarker candidates in neurodegenerative diseases using quantitative proteomics. *Journal of proteomics,* 74**,** 371-388.

KRÜGER, R., KUHN, W., MÜLLER, T., WOITALLA, D., GRAEBER, M., KÖSEL, S., PRZUNTEK, H., EPPLEN, J. T., SCHOLS, L. & RIESS, O. 1998. AlaSOPro mutation in the gene encoding α-synuclein in Parkinson's disease. *Nature genetics,* 18**,** 106-108.

KUIKEN, T. & TAUBENBERGER, J. K. 2008. Pathology of human influenza revisited. *Vaccine,* 26**,** D59-D66.

KUMAR, S. P., CHANDY, M. L., SHANAVAS, M., KHAN, S. & SURESH, K. 2016. Pathogenesis and life cycle of herpes simplex virus infection-stages of primary, latency and recurrence. *Journal of Oral and Maxillofacial Surgery, Medicine, and Pathology,* 28**,** 350-353.

KUROWSKA, Z., ENGLUND, E., WIDNER, H., LINDVALL, O., LI, J.-Y. & BRUNDIN, P. 2011. Signs of degeneration in 12–22-year old grafts of mesencephalic dopamine neurons in patients with Parkinson's disease. *Journal of Parkinson's disease,* 1**,** 83-92.

LAFAILLE, F. G., PESSACH, I. M., ZHANG, S.-Y., CIANCANELLI, M. J., HERMAN, M., ABHYANKAR, A., YING, S.-W., KEROS, S., GOLDSTEIN, P. A. & MOSTOSLAVSKY, G. 2012. Impaired intrinsic immunity to HSV-1 in human iPSC-derived TLR3-deficient CNS cells. *Nature,* 491**,** 769.

LAI, B., MARION, S., TESCHKE, K. & TSUI, J. 2002. Occupational and environmental risk factors for Parkinson's disease. *Parkinsonism & related disorders,* 8**,** 297-309.

LANGSTON, J. W., IRWIN, I., LANGSTON, E. B. & FORNO, L. S. 1984. Pargyline prevents MPTP-induced parkinsonism in primates. *science,* 225**,** 1480-1482.

LAROUCHE, A., BERUBE, P., SARRET, P. & GRIGNON, S. 2008. Subacute H2O2, but not poly (IC), upregulates dopamine D2 receptors in retinoic acid differentiated SH-SY5Y neuroblastoma. *Synapse,* 62**,** 70-73.

LASHUEL, H. A., HARTLEY, D., PETRE, B. M., WALZ, T. & LANSBURY JR, P. T. 2002. Neurodegenerative disease: amyloid pores from pathogenic mutations. *Nature,* 418**,** 291.

LASHUEL, H. A., OVERK, C. R., OUESLATI, A. & MASLIAH, E. 2013. The many faces of α-synuclein: from structure and toxicity to therapeutic target. *Nature Reviews Neuroscience,* 14**,** 38.

LAU, Y.-F., TANG, L.-H. & OOI, E.-E. 2009. A TLR3 ligand that exhibits potent inhibition of influenza virus replication and has strong adjuvant activity has the potential for dual applications in an influenza pandemic. *Vaccine,* 27**,** 1354-1364.

LAUTENSCHLÄGER, J., KAMINSKI, C. F. & KAMINSKI SCHIERLE, G. S. 2017. Alpha-Synuclein - 2013; Regulator of Exocytosis, Endocytosis, or Both? *Trends in Cell Biology,* 27**,** 468-479.

LAWRIMORE, C. J. & CREWS, F. T. 2017. Ethanol, TLR 3, and TLR 4 Agonists Have Unique Innate Immune Responses in Neuron-Like SH-SY 5Y and Microglia-Like BV 2. *Alcoholism: Clinical and Experimental Research,* 41**,** 939-954.

LE GOFFIC, R., POTHLICHET, J., VITOUR, D., FUJITA, T., MEURS, E., CHIGNARD, M. & SI-TAHAR, M. 2007. Cutting Edge: Influenza A virus activates TLR3-dependent inflammatory and RIG-I-dependent antiviral responses in human lung epithelial cells. *The Journal of Immunology,* 178**,** 3368-3372.

LEE, H.-J., PATEL, S. & LEE, S.-J. 2005. Intravesicular Localization and Exocytosis of α-Synuclein and its Aggregates. *The Journal of Neuroscience,* 25**,** 6016-6024.

LEGER, A. J. S., JEON, S. & HENDRICKS, R. L. 2013. Broadening the Repertoire of Functional Herpes Simplex Virus Type 1–Specific CD8+ T Cells Reduces Viral Reactivation from Latency in Sensory Ganglia. *The Journal of Immunology,* 191**,** 2258-2265.

LEIB, D. A., ALEXANDER, D. E., COX, D., YIN, J. & FERGUSON, T. A. 2009. Interaction of ICP34. 5 with Beclin 1 modulates herpes simplex virus type 1 pathogenesis through control of CD4+ T-cell responses. *Journal of virology,* 83**,** 12164-12171.

LEONARD, J. N., GHIRLANDO, R., ASKINS, J., BELL, J. K., MARGULIES, D. H., DAVIES, D. R. & SEGAL, D. M. 2008. The TLR3 signaling complex forms by

cooperative receptor dimerization. *Proceedings of the National Academy of Sciences,* 105**,** 258-263.

LESAGE, S., ANHEIM, M., LETOURNEL, F., BOUSSET, L., HONORÉ, A., ROZAS, N., PIERI, L., MADIONA, K., DÜRR, A., MELKI, R., VERNY, C. & BRICE, A. 2013. G51D α-synuclein mutation causes a novel Parkinsonian–pyramidal syndrome. *Annals of neurology,* 73**,** 459-471.

LEVINE, B. 2005. Eating Oneself and Uninvited Guests: Autophagy-Related Pathways in Cellular Defense. *Cell,* 120**,** 159-162.

LI, J.-Y., ENGLUND, E., HOLTON, J. L., SOULET, D., HAGELL, P., LEES, A. J., LASHLEY, T., QUINN, N. P., REHNCRONA, S., BJÖRKLUND, A., WIDNER, H., REVESZ, T., LINDVALL, O. & BRUNDIN, P. 2008. Lewy bodies in grafted neurons in subjects with Parkinson's disease suggest host-to-graft disease propagation. *Nature medicine,* 14**,** 501.

LI, J.-Y., ENGLUND, E., WIDNER, H., REHNCRONA, S., BJÖRKLUND, A., LINDVALL, O. & BRUNDIN, P. 2010. Characterization of Lewy body pathology in 12- and 16-year-old intrastriatal mesencephalic grafts surviving in a patient with Parkinson's disease. *Movement Disorders,* 25**,** 1091-1096.

LIDDELOW, S. A., GUTTENPLAN, K. A., CLARKE, L. E., BENNETT, F. C., BOHLEN, C. J., SCHIRMER, L., BENNETT, M. L., MÜNCH, A. E., CHUNG, W.-S., PETERSON, T. C., WILTON, D. K., FROUIN, A., NAPIER, B. A., PANICKER, N., KUMAR, M., BUCKWALTER, M. S., ROWITCH, D. H., DAWSON, V. L., DAWSON, T. M., STEVENS, B. & BARRES, B. A. 2017. Neurotoxic reactive astrocytes are induced by activated microglia. *Nature,* 541**,** 481.

LIN, R., NOYCE, R. S., COLLINS, S. E., EVERETT, R. D. & MOSSMAN, K. L. 2004. The herpes simplex virus ICP0 RING finger domain inhibits IRF3-and IRF7-mediated activation of interferon-stimulated genes. *Journal of virology,* 78**,** 1675-1684.

LIOU, H., TSAI, M., CHEN, C., JENG, J., CHANG, Y., CHEN, S. & CHEN, R. 1997. Environmental risk factors and Parkinson's disease A case-control study in Taiwan. *Neurology,* 48**,** 1583-1588.

LIU, Y., QIANG, M., WEI, Y. & HE, R. 2011. A novel molecular mechanism for nitrated α-synuclein-induced cell death. *Journal of Molecular Cell Biology,* 3**,** 239-249.

LIVAK, K. & SCHMITTGEN, T. 2001. Analysis of relative gene expression data using real time quantitative PCR and the 2-Ct method. Methods25: 402–408.

LO, K., GEDDES, J., DANIELS, R. & OXFORD, J. 2003. Lack of detection of influenza genes in archived formalin-fixed, paraffin wax-embedded brain samples of encephalitis lethargica patients from 1916 to 1920. *Virchows Archiv,* 442**,** 591-596.

LOPES, F. M., DA MOTTA, L. L., DE BASTIANI, M. A., PFAFFENSELLER, B., AGUIAR, B. W., DE SOUZA, L. F., ZANATTA, G., VARGAS, D. M., SCHÖNHOFEN, P., LONDERO, G. F., DE MEDEIROS, L. M., FREIRE, V. N., DAFRE, A. L., CASTRO, M. A. A., PARSONS, R. B. & KLAMT, F. 2017. RA Differentiation Enhances Dopaminergic Features, Changes Redox Parameters, and Increases Dopamine Transporter Dependency in 6-Hydroxydopamine-Induced Neurotoxicity in SH-SY5Y Cells. *Neurotoxicity Research,* 31**,** 545-559.

LOPEZ-ALBEROLA, R., GEORGIOU, M., SFAKIANAKIS, G. N., SINGER, C. & PAPAPETROPOULOS, S. 2009. Contemporary encephalitis lethargica:

phenotype, laboratory findings and treatment outcomes. *Journal of neurology,* 256**,** 396-404.

LÖVHEIM, H., GILTHORPE, J., ADOLFSSON, R., NILSSON, L.-G. & ELGH, F. 2015. Reactivated herpes simplex infection increases the risk of Alzheimer's disease. *Alzheimer's & Dementia,* 11**,** 593-599.

LUCAS, M., CHAVES, F., TEIXEIRA, S., CARVALHO, D., PERESSUTTI, C., BITTENCOURT, J., VELASQUES, B., MENÉNDEZ-GONZÁLEZ, M., CAGY, M. & PIEDADE, R. 2013. Time perception impairs sensory-motor integration in Parkinson's disease. *International archives of medicine,* 6**,** 39.

LUDWICZEK, O., KASER, A., KOCH, R. O., VOGEL, W., CRUIKSHANK, W. W. & TILG, H. 2001. Activation of caspase-3 by interferon alpha causes interleukin-16 secretion but fails to modulate activation induced cell death. *European cytokine network,* 12**,** 478-486.

LUSSIGNOL, M., QUEVAL, C., BERNET-CAMARD, M.-F., COTTE-LAFFITTE, J., BEAU, I., CODOGNO, P. & ESCLATINE, A. 2013. The herpes simplex virus 1 Us11 protein inhibits autophagy through its interaction with the protein kinase PKR. *Journal of virology,* 87**,** 859-871.

LY, D. H., LOCKHART, D. J., LERNER, R. A. & SCHULTZ, P. G. 2000. Mitotic misregulation and human aging. *science,* 287**,** 2486-2492.

MA, C. S., DEENICK, E. K., BATTEN, M. & TANGYE, S. G. 2012. The origins, function, and regulation of T follicular helper cells. *Journal of Experimental Medicine,* 209**,** 1241-1253.

MADRAS, B. K., FAHEY, M. A., GOULET, M., LIN, Z., BENDOR, J., GOODRICH, C., MELTZER, P. C., ELMALEH, D. R., LIVNI, E. & BONAB, A. A. 2006. Dopamine transporter (DAT) inhibitors alleviate specific parkinsonian deficits in monkeys: association with DAT occupancy in vivo. *Journal of Pharmacology and Experimental Therapeutics,* 319**,** 570-585.

MANDEL, J., ADAMI, H.-O. & COLE, P. 2012. Paraquat and Parkinson's disease: an overview of the epidemiology and a review of two recent studies. *Regulatory Toxicology and Pharmacology,* 62**,** 385-392.

MANZANILLO, P. S., AYRES, J. S., WATSON, R. O., COLLINS, A. C., SOUZA, G., RAE, C. S., SCHNEIDER, D. S., NAKAMURA, K., SHILOH, M. U. & COX, J. S. 2013. The ubiquitin ligase parkin mediates resistance to intracellular pathogens. *Nature,* 501**,** 512.

MARCUS, P. I. & SEKELLICK, M. J. 1977. Defective interfering particles with covalently linked [±] RNA induce interferon. *Nature,* 266**,** 815-819.

MARFURT, C. F. & RAJCHERT, D. M. 1991. Trigeminal primary afferent projections to "non-trigeminal" areas of the rat central nervous system. *Journal of Comparative Neurology,* 303**,** 489-511.

MARKESBERY, W. R., JICHA, G. A., LIU, H. & SCHMITT, F. A. 2009. Lewy body pathology in normal elderly subjects. *Journal of Neuropathology & Experimental Neurology,* 68**,** 816-822.

MAROTEAUX, L. & SCHELLER, R. 1991. The rat brain synucleins; family of proteins transiently associated with neuronal membrane. *Molecular brain research,* 11**,** 335-343.

MARRAS, C., BECK, J. C., BOWER, J. H., ROBERTS, E., RITZ, B., ROSS, G. W., ABBOTT, R. D., SAVICA, R., VAN DEN EEDEN, S. K., WILLIS, A. W. & TANNER, C. M. 2018. Prevalence of Parkinson's disease across North America. *NPJ Parkinson's disease,* 4**,** 21.

MARTTILA, R., ARSTILA, P., NIKOSKELAINEN, J., HALONEN, P. & RINNE, U. 1977. Viral antibodies in the sera from patients with Parkinson disease. *European neurology,* 15**,** 25-33.

MARTTILA, R., KAPRIO, J., KOSKENVUO, M. & RINNE, U. 1988. Parkinson's disease in a nationwide twin cohort. *Neurology,* 38**,** 1217-1217.

MARTTILA, R. J. & RINNE, U. K. 1978. Herpes simplex virus antibodies in patients with Parkinson's disease. *Journal of the neurological sciences,* 35**,** 375-379.

MARTTILA, R. J., RINNE, U. K., HALONEN, P., MADDEN, D. L. & SEVER, J. L. 1981. Herpesviruses and Parkinsonism: herpes simplex virus types 1 and 2, and cytomegalovirus antibodies in serum and CSF. *Archives of neurology,* 38**,** 19-21.

MARTTILA, R. J., RINNE, U. K. & TIILIKAINEN, A. 1982. Virus antibodies in Parkinson's disease: Herpes simplex and measles virus antibodies in serum and CSF and their relation to HLA types. *Journal of the neurological sciences,* 54**,** 227-238.

MASSA, P. T., ALEYASIN, H., PARK, D. S., MAO, X. & BARGER, S. W. 2006. NFκB in neurons? The uncertainty principle in neurobiology. *Journal of neurochemistry,* 97**,** 607-618.

MATSUDA, K., SHIBATA, T., SAKODA, Y., KIDA, H., KIMURA, T., OCHIAI, K. & UMEMURA, T. 2005. In vitro demonstration of neural transmission of avian influenza A virus. *Journal of general virology,* 86**,** 1131-1139.

MATSUDA, N. & TANAKA, K. 2010. Does impairment of the ubiquitin-proteasome system or the autophagy-lysosome pathway predispose individuals to neurodegenerative disorders such as Parkinson's disease? *Journal of Alzheimer's Disease,* 19**,** 1-9.

MATSUMOTO, M., KIKKAWA, S., KOHASE, M., MIYAKE, K. & SEYA, T. 2002. Establishment of a monoclonal antibody against human Toll-like receptor 3 that blocks double-stranded RNA-mediated signaling. *Biochemical and biophysical research communications,* 293**,** 1364-1369.

MATSUMOTO, M. & SEYA, T. 2008. TLR3: interferon induction by double-stranded RNA including poly (I: C). *Advanced drug delivery reviews,* 60**,** 805-812.

MATTOS, J. P. D., ROSSO, A. L. Z. D., CORRÊA, R. B. & NOVIS, S. A. 2002. Movement disorders in 28 HIV-infected patients. *Arquivos de neuro-psiquiatria,* 60**,** 525-530.

MAYEUX, R., HONIG, L. S., TANG, M.-X., MANLY, J., STERN, Y., SCHUPF, N. & MEHTA, P. D. 2003. Plasma Aβ40 and Aβ42 and Alzheimer's disease Relation to age, mortality, and risk. *Neurology,* 61**,** 1185-1190.

MAZZIO, E. A., REAMS, R. R. & SOLIMAN, K. F. 2004. The role of oxidative stress, impaired glycolysis and mitochondrial respiratory redox failure in the cytotoxic effects of 6-hydroxydopamine in vitro. *Brain Research,* 1004**,** 29-44.

MBEFO, M. K., PALEOLOGOU, K. E., BOUCHARABA, A., OUESLATI, A., SCHELL, H., FOURNIER, M., OLSCHEWSKI, D., YIN, G., ZWECKSTETTER, M., MASLIAH, E., KAHLE, P. J., HIRLING, H. & LASHUEL, H. A. 2010. Phosphorylation of Synucleins by Members of the Polo-like Kinase Family. *The Journal of Biological Chemistry,* 285**,** 2807-2822.

MCALLISTER, C. S., LAKHDARI, O., DE CHAMBRUN, G. P., GAREAU, M. G., BROQUET, A., LEE, G. H., SHENOUDA, S., ECKMANN, L. & KAGNOFF, M. F. 2012. TLR3, TRIF, and caspase 8 determine double-stranded RNA-induced epithelial cell death and survival in vivo. *The Journal of Immunology***,** 1202756.

MCCABE, K., CONCANNON, R. M., MCKERNAN, D. P. & DOWD, E. 2017. Time-course of striatal Toll-like receptor expression in neurotoxic, environmental and inflammatory rat models of Parkinson's disease. *Journal of Neuroimmunology,* 310**,** 103-106.

MCCALL, S., HENRY, J. M., REID, A. H. & TAUBENBERGER, J. K. 2001. Influenza RNA not detected in archival brain tissues from acute encephalitis lethargica cases or in postencephalitic Parkinson cases. *Journal of Neuropathology & Experimental Neurology,* 60**,** 696-704.

MCNAUGHT, K. S. P., SHASHIDHARAN, P., PERL, D. P., JENNER, P. & OLANOW, C. W. 2002. Aggresome-related biogenesis of Lewy bodies. *European Journal of Neuroscience,* 16**,** 2136-2148.

MENAGER, P., ROUX, P., MEGRET, F., BOURGEOIS, J.-P., LE SOURD, A.-M., DANCKAERT, A., LAFAGE, M., PREHAUD, C. & LAFON, M. 2009. Toll-like receptor 3 (TLR3) plays a major role in the formation of rabies virus Negri Bodies. *PLoS pathogens,* 5**,** e1000315.

MENENDEZ, C. M., JINKINS, J. K. & CARR, D. J. 2016. Resident T cells are unable to control herpes simplex virus-1 activity in the brain ependymal region during latency. *The Journal of Immunology,* 197**,** 1262-1275.

MIKOLAENKO, I., PLETNIKOVA, O., KAWAS, C. H., O'BRIEN, R., RESNICK, S. M., CRAIN, B. & TRONCOSO, J. C. 2005. Alpha-synuclein lesions in normal aging, Parkinson disease, and Alzheimer disease: evidence from the Baltimore Longitudinal Study of Aging (BLSA). *Journal of Neuropathology & Experimental Neurology,* 64**,** 156-162.

MILLER, K. D., SCHNELL, M. J. & RALL, G. F. 2016. Keeping it in check: chronic viral infection and antiviral immunity in the brain. *Nature Reviews Neuroscience,* 17**,** 766-776.

MILLER, Y. I., CHOI, S.-H., WIESNER, P., FANG, L., HARKEWICZ, R., HARTVIGSEN, K., BOULLIER, A., GONEN, A., DIEHL, C. J., QUE, X., MONTANO, E., SHAW, P. X., TSIMIKAS, S., BINDER, C. J. & WITZTUM, J. L. 2011. Oxidation-Specific Epitopes Are Danger-Associated Molecular Patterns Recognized by Pattern Recognition Receptors of Innate Immunity. *Circulation Research,* 108**,** 235-248.

MIZUNO, Y., HATTORI, N., MORI, H., SUZUKI, T. & TANAKA, K. 2001. Parkin and Parkinson's disease. *Current opinion in neurology,* 14**,** 477-482.

MOCHIZUKI, H., CHOONG, C.-J. & MASLIAH, E. 2018. A refined concept: Alpha synuclein dysregulation disease. *Neurochemistry International*.

MOGI, M., HARADA, M., NARABAYASHI, H., INAGAKI, H., MINAMI, M. & NAGATSU, T. 1996. Interleukin (IL)-1β, IL-2, IL-4, IL-6 and transforming growth factor-α levels are elevated in ventricular cerebrospinal fluid in juvenile parkinsonism and Parkinson's disease. *Neuroscience letters,* 211**,** 13-16.

MORI, I., GOSHIMA, F., IMAI, Y., KOHSAKA, S., SUGIYAMA, T., YOSHIDA, T., YOKOCHI, T., NISHIYAMA, Y. & KIMURA, Y. 2002. Olfactory receptor neurons prevent dissemination of neurovirulent influenza A virus into the brain by undergoing virus-induced apoptosis. *Journal of general virology,* 83**,** 2109-2116.

MORI, I., KIMURA, Y., NAIKI, H., MATSUBARA, R., TAKEUCHI, T., YOKOCHI, T. & NISHIYAMA, Y. 2004. Reactivation of HSV-1 in the brain of patients with familial Alzheimer's disease. *Journal of medical virology,* 73**,** 605-611.

MORIARTY, N., PANDIT, A. & DOWD, E. 2017. Encapsulation of primary dopaminergic neurons in a GDNF-loaded collagen hydrogel increases their

survival, re-innervation and function after intra-striatal transplantation. *Scientific reports,* 7**,** 16033.

MOSLEY, B., URDAL, D., PRICKETT, K., LARSEN, A., COSMAN, D., CONLON, P., GILLIS, S. & DOWER, S. 1987. The interleukin-1 receptor binds the human interleukin-1 alpha precursor but not the interleukin-1 beta precursor. *Journal of Biological Chemistry,* 262**,** 2941-2944.

MOSSER, D. M. & EDWARDS, J. P. 2008. Exploring the full spectrum of macrophage activation. *Nature Reviews Immunology,* 8**,** 958-969.

MOUSTAFA, A. A., CHAKRAVARTHY, S., PHILLIPS, J. R., GUPTA, A., KERI, S., POLNER, B., FRANK, M. J. & JAHANSHAHI, M. 2016. Motor symptoms in Parkinson's disease: A unified framework. *Neuroscience & Biobehavioral Reviews,* 68**,** 727-740.

MUCHOWSKI, P. J. & WACKER, J. L. 2005. Modulation of neurodegeneration by molecular chaperones. *Nature Reviews Neuroscience,* 6**,** 11.

MULVEY, M., POPPERS, J., LADD, A. & MOHR, I. 1999. A herpesvirus ribosome-associated, RNA-binding protein confers a growth advantage upon mutants deficient in a GADD34-related function. *Journal of virology,* 73**,** 3375-3385.

MURPHY, D. D., RUETER, S. M., TROJANOWSKI, J. Q. & LEE, V. M.-Y. 2000. Synucleins are developmentally expressed, and α-synuclein regulates the size of the presynaptic vesicular pool in primary hippocampal neurons. *Journal of Neuroscience,* 20**,** 3214-3220.

MUZIO, M., BOSISIO, D., POLENTARUTTI, N., D'AMICO, G., STOPPACCIARO, A., MANCINELLI, R., VAN'T VEER, C., PENTON-ROL, G., RUCO, L. P. & ALLAVENA, P. 2000. Differential expression and regulation of toll-like receptors (TLR) in human leukocytes: selective expression of TLR3 in dendritic cells. *The Journal of Immunology,* 164**,** 5998-6004.

NAGATSU, T., MOGI, M., ICHINOSE, H. & TOGARI, A. 2000. Cytokines in Parkinson's disease. *Journal of Neural Transmission Supplementum,* 58**,** 143-152.

NEAL, J. B. 1942. Encephalitis. A Clinical Study. *Encephalitis. A Clinical Study.*

NEAL, J. B. & BENTLEY, I. A. 1932. Treatment of epidemic encephalitis: a review of the work of the Matheson Commission. *Archives of Neurology & Psychiatry,* 28**,** 897-907.

NESSA, B. N., TANAKA, T., KAMINO, K., SADIK, G., ANSAR, A. B., KIMURA, R., TANII, H., OKOCHI, M., MORIHARA, T. & TAGAMI, S. 2006. Toll-like receptor 3 mediated hyperphosphorylation of tau in human SH-SY5Y neuroblastoma cells. *Psychiatry and Clinical Neurosciences,* 60**,** S27-S33.

NICHOLSON, K. G., KENT, J., HAMMERSLEY, V. & CANCIO, E. 1997. Acute viral infections of upper respiratory tract in elderly people living in the community: comparative, prospective, population based study of disease burden. *BMJ,* 315**,** 1060-1064.

NICKLAS, W. J., YOUNGSTER, S. K., KINDT, M. V. & HEIKKILA, R. E. 1987. IV. MPTP, MPP+ and mitochondrial function. *Life sciences,* 40**,** 721-729.

NISHIYA, T., KAJITA, E., MIWA, S. & DEFRANCO, A. L. 2005. TLR3 and TLR7 are targeted to the same intracellular compartments by distinct regulatory elements. *Journal of Biological Chemistry*.

NIXON, R. A. 2013. The role of autophagy in neurodegenerative disease. *Nature medicine,* 19**,** 983.

NUBER, S., HARMUTH, F., KOHL, Z., ADAME, A., TREJO, M., SCHÖNIG, K., ZIMMERMANN, F., BAUER, C., CASADEI, N. & GIEL, C. 2013. A

progressive dopaminergic phenotype associated with neurotoxic conversion of α-synuclein in BAC-transgenic rats. *Brain,* 136**,** 412-432.

O'NEILL, L. A. J., GOLENBOCK, D. & BOWIE, A. G. 2013. The history of Toll-like receptors — redefining innate immunity. *Nature Reviews Immunology,* 13**,** 453.

OH-NISHI, A., OBAYASHI, S., SUGIHARA, I., MINAMIMOTO, T. & SUHARA, T. 2010. Maternal immune activation by polyriboinosinic-polyribocytidilic acid injection produces synaptic dysfunction but not neuronal loss in the hippocampus of juvenile rat offspring. *Brain Research,* 1363**,** 170-179.

OLANOW, C. W. & BRUNDIN, P. 2013. Parkinson's disease and alpha synuclein: is Parkinson's disease a prion-like disorder? *Movement Disorders,* 28**,** 31-40.

OLESEN, J., GUSTAVSSON, A., SVENSSON, M., WITTCHEN, H. U., JÖNSSON, B., GROUP, C. S. & COUNCIL, E. B. 2012. The economic cost of brain disorders in Europe. *European journal of neurology,* 19**,** 155-162.

OLGIATI, S., THOMAS, A., QUADRI, M., BREEDVELD, G. J., GRAAFLAND, J., EUSSEN, H., DOUBEN, H., DE KLEIN, A., ONOFRJ, M. & BONIFATI, V. 2015. Early-onset parkinsonism caused by alpha-synuclein gene triplication: Clinical and genetic findings in a novel family. *Parkinsonism & Related Disorders,* 21**,** 981-986.

OLSEN, L. K., DOWD, E. & MCKERNAN, D. P. 2018. A role for viral infections in Parkinson's etiology? *Neuronal Signaling,* 2**,** NS20170166.

OLSSON, J., LÖVHEIM, H., HONKALA, E., KARHUNEN, P. J., ELGH, F. & KOK, E. H. 2016. HSV presence in brains of individuals without dementia: the TASTY brain series. *Disease models & mechanisms,* 9**,** 1349-1355.

OLSSON, M., NIKKHAH, G., BENTLAGE, C. & BJORKLUND, A. 1995. Forelimb akinesia in the rat Parkinson model: differential effects of dopamine agonists and nigral transplants as assessed by a new stepping test. *Journal of Neuroscience,* 15**,** 3863-3875.

ORVEDAHL, A., ALEXANDER, D., TALLÓCZY, Z., SUN, Q., WEI, Y., ZHANG, W., BURNS, D., LEIB, D. A. & LEVINE, B. 2007. HSV-1 ICP34. 5 confers neurovirulence by targeting the Beclin 1 autophagy protein. *Cell host & microbe,* 1**,** 23-35.

ORVEDAHL, A. & LEVINE, B. 2008. Eating the enemy within: autophagy in infectious diseases. *Cell Death And Differentiation,* 16**,** 57.

OSHIUMI, H., SASAI, M., SHIDA, K., FUJITA, T., MATSUMOTO, M. & SEYA, T. 2003. TICACM-2: a bridging adapter recruiting to Toll-like receptor 4 TICAM-1 that induces interferon-β. *Journal of Biological Chemistry*.

PAN-MONTOJO, F., SCHWARZ, M., WINKLER, C., ARNHOLD, M., O'SULLIVAN, G. A., PAL, A., SAID, J., MARSICO, G., VERBAVATZ, J.-M. & RODRIGO-ANGULO, M. 2012. Environmental toxins trigger PD-like progression via increased alpha-synuclein release from enteric neurons in mice. *Scientific Reports,* 2**,** 898.

PANKIV, S., CLAUSEN, T. H., LAMARK, T., BRECH, A., BRUUN, J.-A., OUTZEN, H., ØVERVATN, A., BJØRKØY, G. & JOHANSEN, T. 2007. p62/SQSTM1 binds directly to Atg8/LC3 to facilitate degradation of ubiquitinated protein aggregates by autophagy. *Journal of Biological Chemistry*.

PANNE, D., MANIATIS, T. & HARRISON, S. C. 2007. An atomic model of the interferon-β enhanceosome. *Cell,* 129**,** 1111-1123.

PARK, C., LEE, S., CHO, I. H., LEE, H. K., KIM, D., CHOI, S. Y., OH, S. B., PARK, K., KIM, J. S. & LEE, S. J. 2006. TLR3-mediated signal induces proinflammatory cytokine and chemokine gene expression in astrocytes:

differential signaling mechanisms of TLR3-induced IP-10 and IL-8 gene expression. *Glia,* 53**,** 248-256.

PARK, C. H., ISHINAKA, M., TAKADA, A., KIDA, H., KIMURA, T., OCHIAI, K. & UMEMURA, T. 2002. The invasion routes of neurovirulent A/Hong Kong/483/97 (H5N1) influenza virus into the central nervous system after respiratory infection in mice. *Archives of Virology,* 147**,** 1425-1436.

PARK, J. H., LEE, J. E., SHIN, I. C. & KOH, H. C. 2013. Autophagy regulates chlorpyrifos-induced apoptosis in SH-SY5Y cells. *Toxicology and Applied Pharmacology,* 268**,** 55-67.

PARKIN, J. & COHEN, B. 2001. An overview of the immune system. *The Lancet,* 357**,** 1777-1789.

PARKINSON, J. 1817. An essay on the shaking palsy (Printed by Whittingham and Rowland for Sherwood, Neely, and Jones). London.

PARKINSON, J. 2002. An essay on the shaking palsy. *The Journal of neuropsychiatry and clinical neurosciences,* 14**,** 223-236.

PAXINOS, G. & ASHWELL, K. W. 2018. *Atlas of the developing rat nervous system*, Academic Press.

PEDERSEN, M. N., FODERÀ, V., HORVATH, I., VAN MAARSCHALKERWEERD, A., TOFT, K. N., WEISE, C., ALMQVIST, F., WOLF-WATZ, M., WITTUNG-STAFSHEDE, P. & VESTERGAARD, B. 2015. Direct correlation between ligand-induced α-synuclein oligomers and amyloid-like fibril growth. *Scientific reports,* 5**,** 10422.

PEELAERTS, W., BOUSSET, L., VAN DER PERREN, A., MOSKALYUK, A., PULIZZI, R., GIUGLIANO, M., VAN DEN HAUTE, C., MELKI, R. & BAEKELANDT, V. 2015. α-Synuclein strains cause distinct synucleinopathies after local and systemic administration. *Nature,* 522**,** 340.

PENG, G.-S., LI, G., TZENG, N.-S., CHEN, P.-S., CHUANG, D.-M., HSU, Y.-D., YANG, S. & HONG, J.-S. 2005. Valproate pretreatment protects dopaminergic neurons from LPS-induced neurotoxicity in rat primary midbrain cultures: role of microglia. *Molecular brain research,* 134**,** 162-169.

PERRONE, L. A., PLOWDEN, J. K., GARCÍA-SASTRE, A., KATZ, J. M. & TUMPEY, T. M. 2008. H5N1 and 1918 pandemic influenza virus infection results in early and excessive infiltration of macrophages and neutrophils in the lungs of mice. *PLoS pathogens,* 4**,** e1000115.

PIACENTINI, R., PUMA, D. D. L., RIPOLI, C., MARCOCCI, M. E., DE CHIARA, G., GARACI, E., PALAMARA, A. T. & GRASSI, C. 2015. Herpes Simplex Virus type-1 infection induces synaptic dysfunction in cultured cortical neurons via GSK-3 activation and intraneuronal amyloid-β protein accumulation. *Scientific Reports,* 5.

PICCONI, B., PICCOLI, G. & CALABRESI, P. 2012. Synaptic dysfunction in Parkinson's disease. *Synaptic Plasticity.* Springer.

PLOWEY, E. D., CHERRA III, S. J., LIU, Y. J. & CHU, C. T. 2008. Role of autophagy in G2019S-LRRK2-associated neurite shortening in differentiated SH-SY5Y cells. *Journal of neurochemistry,* 105**,** 1048-1056.

POHAR, J., PIRHER, N., BENČINA, M., MANČEK-KEBER, M. & JERALA, R. 2014. The ectodomain of TLR3 receptor is required for its plasma membrane translocation. *PloS one,* 9**,** e92391.

POKRZYWA, M., PAWEŁEK, K., KUCIA, W. E., SARBAK, S., CHORELL, E., ALMQVIST, F. & WITTUNG-STAFSHEDE, P. 2017. Effects of small-

molecule amyloid modulators on a Drosophila model of Parkinson's disease. *PloS one,* 12**,** e0184117.

POLYMEROPOULOS, M. H., LAVEDAN, C., LEROY, E., IDE, S. E., DEHEJIA, A., DUTRA, A., PIKE, B., ROOT, H., RUBENSTEIN, J. & BOYER, R. 1997. Mutation in the α-synuclein gene identified in families with Parkinson's disease. *science,* 276**,** 2045-2047.

POPPERS, J., MULVEY, M., KHOO, D. & MOHR, I. 2000. Inhibition of PKR activation by the proline-rich RNA binding domain of the herpes simplex virus type 1 Us11 protein. *Journal of virology,* 74**,** 11215-11221.

PORRAS, G., BERTHET, A., DEHAY, B., LI, Q., LADEPECHE, L., NORMAND, E., DOVERO, S., MARTINEZ, A., DOUDNIKOFF, E. & MARTIN-NÉGRIER, M.-L. 2012. PSD-95 expression controls L-DOPA dyskinesia through dopamine D1 receptor trafficking. *The Journal of clinical investigation,* 122**,** 3977-3989.

POSER, C. M., HUNTLEY, C. J. & POLAND, J. D. 1969. Para-encephalitic Parkinsonism: Report of an Acute Case Due to Coxsackie Virus Type B 2 and Re-Examination of the Etiologic Concepts of Postencephalitic Parkinsonism. *Acta Neurologica Scandinavica,* 45**,** 199-215.

PRANGE, O., WONG, T. P., GERROW, K., WANG, Y. T. & EL-HUSSEINI, A. 2004. A balance between excitatory and inhibitory synapses is controlled by PSD-95 and neuroligin. *Proceedings of the National Academy of Sciences of the United States of America,* 101**,** 13915-13920.

PRANZATELLI, M. R., MOTT, S. H., PAVLAKIS, S. G., CONRY, J. A. & TATE, E. D. 1994. Clinical spectrum of secondary parkinsonism in childhood: a reversible disorder. *Pediatric neurology,* 10**,** 131-140.

PRESTON, C. M., HARMAN, A. N. & NICHOLL, M. J. 2001. Activation of interferon response factor-3 in human cells infected with herpes simplex virus type 1 or human cytomegalovirus. *Journal of virology,* 75**,** 8909-8916.

PRINGPROA, K., RUNGSIWIWUT, R., TANTILERTCHAROEN, R., PRAPHET, R., PRUKSANANONDA, K., BAUMGÄRTNER, W. & THANAWONGNUWECH, R. 2015. Tropism and Induction of Cytokines in Human Embryonic-Stem Cells-Derived Neural Progenitors upon Inoculation with Highly- Pathogenic Avian H5N1 Influenza Virus. *PloS one,* 10**,** e0135850.

PROUKAKIS, C., HOULDEN, H. & SCHAPIRA, A. H. 2013. Somatic Alpha-Synuclein Mutations in Parkinson's Disease: Hypothesis and Preliminary Data. *Movement Disorders,* 28**,** 705-712.

PRZEDBORSKI, S., CHEN, Q., VILA, M., GIASSON, B. I., DJALDATTI, R., VUKOSAVIC, S., SOUZA, J. M., JACKSON-LEWIS, V., LEE, V. M. Y. & ISCHIROPOULOS, H. 2001. Oxidative post-translational modifications of α-synuclein in the 1-methyl-4-phenyl-1, 2, 3, 6-tetrahydropyridine (MPTP) mouse model of Parkinson's disease. *Journal of neurochemistry,* 76**,** 637-640.

PURVES, D., AUGUSTINE, G. J., FITZPATRICK, D., KATZ, L. C., LAMANTIA, A.-S., MCNAMARA, J. O. & WILLIAMS, S. M. 2001. Circuits within the basal ganglia system.

QI, R., HOOSE, S., SCHREITER, J., SAWANT, K. V., LAMB, R., RANJITH-KUMAR, C., MILLS, J., SAN MATEO, L., JORDAN, J. L. & KAO, C. C. 2010. Secretion of the human Toll-like receptor 3 ectodomain is affected by single nucleotide polymorphisms and regulated by Unc93b1. *Journal of Biological Chemistry***,** jbc. M110. 144402.

QI, R., SINGH, D. & KAO, C. C. 2012. Proteolytic processing regulates Toll-like receptor 3 stability and endosomal localization. *Journal of Biological Chemistry,* 287**,** 32617-32629.

QIN, Z., HU, D., HAN, S., REANEY, S. H., DI MONTE, D. A. & FINK, A. L. 2007. Effect of 4-Hydroxy-2-nonenal Modification on α-Synuclein Aggregation. *Journal of Biological Chemistry,* 282**,** 5862-5870.

RAIL, D., SCHOLTZ, C. & SWASH, M. 1981. Post-encephalitic parkinsonism: current experience. *Journal of Neurology, Neurosurgery & Psychiatry,* 44**,** 670-676.

RAJEWSKY, K. & SCHITTEK, B. 1990. Maintenance of B-cell memory by long-lived cells generated from proliferating precursors. *Nature,* 346**,** 749.

RAO, G., FISCH, L., SRINIVASAN, S., D'AMICO, F., OKADA, T., EATON, C. & ROBBINS, C. 2003. Does this patient have Parkinson disease? *Jama,* 289**,** 347-353.

RAVENHOLT, R. & FOEGE, W. 1982. 1918 influenza, encephalitis lethargica, parkinsonism. *The Lancet,* 320**,** 860-864.

REID, A. H., FANNING, T. G., HULTIN, J. V. & TAUBENBERGER, J. K. 1999. Origin and evolution of the 1918 "Spanish" influenza virus hemagglutinin gene. *Proceedings of the National Academy of Sciences,* 96**,** 1651-1656.

REID, A. H., FANNING, T. G., JANCZEWSKI, T. A. & TAUBENBERGER, J. K. 2000. Characterization of the 1918 "Spanish" influenza virus neuraminidase gene. *Proceedings of the National Academy of Sciences,* 97**,** 6785-6790.

REINACHER, M., BONIN, J., NARAYAN, O. & SCHOLTISSEK, C. 1983. Pathogenesis of neurovirulent influenza A virus infection in mice. Route of entry of virus into brain determines infection of different populations of cells. *Laboratory investigation; a journal of technical methods and pathology,* 49**,** 686-692.

REINERT, L. S., HARDER, L., HOLM, C. K., IVERSEN, M. B., HORAN, K. A., DAGNÆS-HANSEN, F., ULHØI, B. P., HOLM, T. H., MOGENSEN, T. H. & OWENS, T. 2012. TLR3 deficiency renders astrocytes permissive to herpes simplex virus infection and facilitates establishment of CNS infection in mice. *The Journal of clinical investigation,* 122**,** 1368-1376.

RIDEOUT, H. J., LANG-ROLLIN, I. C., SAVALLE, M. & STEFANIS, L. 2005. Dopaminergic neurons in rat ventral midbrain cultures undergo selective apoptosis and form inclusions, but do not up-regulate iHSP70, following proteasomal inhibition. *Journal of neurochemistry,* 93**,** 1304-1313.

ROCHET, J.-C., CONWAY, K. A. & LANSBURY, P. T. 2000. Inhibition of fibrillization and accumulation of prefibrillar oligomers in mixtures of human and mouse α-synuclein. *Biochemistry,* 39**,** 10619-10626.

ROCK, F. L., HARDIMAN, G., TIMANS, J. C., KASTELEIN, R. A. & BAZAN, J. F. 1998. A family of human receptors structurally related to Drosophila Toll. *Proceedings of the National Academy of Sciences,* 95**,** 588-593.

RODRÍGUEZ-LÁZARO, D. & HERNÁNDEZ, M. 2013. Introduction to the real-time polymerase chain reaction. *real-time PCR in food science*.

RODRIGUEZ, M., RODRIGUEZ-SABATE, C., MORALES, I., SANCHEZ, A. & SABATE, M. 2015. Parkinson's disease as a result of aging. *Aging cell,* 14**,** 293-308.

ROHN, T. T. & CATLIN, L. W. 2011. Immunolocalization of influenza A virus and markers of inflammation in the human Parkinson's disease brain. *PloS one,* 6**,** e20495.

ROSATO, P. C., KATZENELL, S., PESOLA, J. M., NORTH, B., COEN, D. M. & LEIB, D. A. 2016. Neuronal IFN signaling is dispensable for the establishment of HSV-1 latency. *Virology,* 497**,** 323-327.

ROSS, O. A., BRAITHWAITE, A. T., SKIPPER, L. M., KACHERGUS, J., HULIHAN, M. M., MIDDLETON, F. A., NISHIOKA, K., FUCHS, J., GASSER, T., MARAGANORE, D. M., ADLER, C. H., LARVOR, L., CHARTIER-HARLIN, M.-C., NILSSON, C., LANGSTON, J. W., GWINN, K., HATTORI, N. & FARRER, M. J. 2008. Genomic investigation of α-Synuclein multiplication and parkinsonism. *Annals of neurology,* 63**,** 10.1002/ana.21380.

ROSS, R. A. & BIEDLER, J. L. 1985. Presence and regulation of tyrosinase activity in human neuroblastoma cell variants in vitro. *Cancer research,* 45**,** 1628-1632.

SADASIVAN, S., SHARP, B., SCHULTZ-CHERRY, S. & SMEYNE, R. J. 2017. Synergistic effects of influenza and 1-methyl-4-phenyl-1, 2, 3, 6-tetrahydropyridine (MPTP) can be eliminated by the use of influenza therapeutics: experimental evidence for the multi-hit hypothesis. *NPJ Parkinson's disease,* 3**,** 18.

SAKAI, K. & GASH, D. M. 1994. Effect of bilateral 6-OHDA lesions of the substantia nigra on locomotor activity in the rat. *Brain Research,* 633**,** 144-150.

SAMJI, T. 2009. Influenza A: Understanding the Viral Life Cycle. *The Yale Journal of Biology and Medicine,* 82**,** 153-159.

SANTANA, S., RECUERO, M., BULLIDO, M. J., VALDIVIESO, F. & ALDUDO, J. 2012. Herpes simplex virus type I induces the accumulation of intracellular β-amyloid in autophagic compartments and the inhibition of the non-amyloidogenic pathway in human neuroblastoma cells. *Neurobiology of aging,* 33**,** 430. e19-430. e33.

SATAKE, W., NAKABAYASHI, Y., MIZUTA, I., HIROTA, Y., ITO, C., KUBO, M., KAWAGUCHI, T., TSUNODA, T., WATANABE, M., TAKEDA, A., TOMIYAMA, H., NAKASHIMA, K., HASEGAWA, K., OBATA, F., YOSHIKAWA, T., KAWAKAMI, H., SAKODA, S., YAMAMOTO, M., HATTORI, N., MURATA, M., NAKAMURA, Y. & TODA, T. 2009. Genome-wide association study identifies common variants at four loci as genetic risk factors for Parkinson's disease. *Nature genetics,* 41**,** 1303.

SATO, M., TANAKA, N., HATA, N., ODA, E. & TANIGUCHI, T. 1998. Involvement of the IRF family transcription factor IRF-3 in virus-induced activation of the IFN-β gene. *FEBS letters,* 425**,** 112-116.

SAUNDERS, J. A. H., ESTES, K. A., KOSLOSKI, L. M., ALLEN, H. E., DEMPSEY, K. M., TORRES-RUSSOTTO, D. R., MEZA, J. L., SANTAMARIA, P. M., BERTONI, J. M. & MURMAN, D. L. 2012. CD4+ regulatory and effector/memory T cell subsets profile motor dysfunction in Parkinson's disease. *Journal of Neuroimmune Pharmacology,* 7**,** 927-938.

SAWADA, M., IMAMURA, K. & NAGATSU, T. 2006. Role of cytokines in inflammatory process in Parkinson's disease. *Parkinson's Disease and Related Disorders***,** 373-381.

SCHALLERT, T., FLEMING, S. M., LEASURE, J. L., TILLERSON, J. L. & BLAND, S. T. 2000. CNS plasticity and assessment of forelimb sensorimotor outcome in unilateral rat models of stroke, cortical ablation, parkinsonism and spinal cord injury. *Neuropharmacology,* 39**,** 777-787.

SCHAPIRA, A. H. & JENNER, P. 2011. Etiology and pathogenesis of Parkinson's disease. *Movement Disorders,* 26**,** 1049-1055.

SCHERZER, C. R., GRASS, J. A., LIAO, Z., PEPIVANI, I., ZHENG, B., EKLUND, A. C., NEY, P. A., NG, J., MCGOLDRICK, M. & MOLLENHAUER, B. 2008. GATA transcription factors directly regulate the Parkinson's disease-linked gene α-synuclein. *Proceedings of the National Academy of Sciences*.

SCHMID, D., PYPAERT, M. & MÜNZ, C. 2007. Antigen-loading compartments for major histocompatibility complex class II molecules continuously receive input from autophagosomes. *Immunity,* 26**,** 79-92.

SCHNELL, E., SIZEMORE, M., KARIMZADEGAN, S., CHEN, L., BREDT, D. S. & NICOLL, R. A. 2002. Direct interactions between PSD-95 and stargazin control synaptic AMPA receptor number. *Proceedings of the National Academy of Sciences,* 99**,** 13902-13907.

SCHRODER, K., SWEET, M. J. & HUME, D. A. 2006. Signal integration between IFNγ and TLR signalling pathways in macrophages. *Immunobiology,* 211**,** 511-524.

SCHWARTZ, M. & SHECHTER, R. 2010. Systemic inflammatory cells fight off neurodegenerative disease. *Nature Reviews Neurology,* 6**,** 405.

SCOTT, D. A., TABAREAN, I., TANG, Y., CARTIER, A., MASLIAH, E. & ROY, S. 2010. A pathologic cascade leading to synaptic dysfunction in α-synuclein-induced neurodegeneration. *Journal of Neuroscience,* 30**,** 8083-8095.

SCUMPIA, P. O., KELLY, K. M., REEVES, W. H. & STEVENS, B. R. 2005. Double-stranded RNA signals antiviral and inflammatory programs and dysfunctional glutamate transport in TLR3-expressing astrocytes. *Glia,* 52**,** 153-162.

SEIDLER, A., HELLENBRAND, W., ROBRA, B.-P., VIEREGGE, P., NISCHAN, P., JOERG, J., OERTEL, W., ULM, G. & SCHNEIDER, E. 1996. Possible environmental, occupational, and other etiologic factors for Parkinson's disease A case-control study in Germany. *Neurology,* 46**,** 1275-1275.

SEONG, S.-Y. & MATZINGER, P. 2004. Hydrophobicity: an ancient damage-associated molecular pattern that initiates innate immune responses. *Nature Reviews Immunology,* 4**,** 469.

SHARMA, K., TRIPATHI, S., RANJAN, P., KUMAR, P., GARTEN, R., DEYDE, V., KATZ, J. M., COX, N. J., LAL, R. B., SAMBHARA, S. & LAL, S. K. 2011. Influenza A Virus Nucleoprotein Exploits Hsp40 to Inhibit PKR Activation. *PloS one,* 6**,** e20215.

SHERER, T. B., BETARBET, R., TESTA, C. M., SEO, B. B., RICHARDSON, J. R., KIM, J. H., MILLER, G. W., YAGI, T., MATSUNO-YAGI, A. & GREENAMYRE, J. T. 2003. Mechanism of toxicity in rotenone models of Parkinson's disease. *Journal of Neuroscience,* 23**,** 10756-10764.

SHOJI-KAWATA, S. & LEVINE, B. 2009. Autophagy, antiviral immunity, and viral countermeasures. *Biochimica et Biophysica Acta (BBA)-Molecular Cell Research,* 1793**,** 1478-1484.

SHOJI, H., KOGA, M., KUSUHARA, T., KAJI, M., AYABE, M., HINO, H. & HONDO, R. 1994. Differentiation of herpes simplex virus 1 and 2 in cerebrospinal fluid of patients with HSV encephalitis and meningitis by stringent hybridization of PCR-amplified DNAs. *Journal of neurology,* 241**,** 526-530.

SHTILERMAN, M. D., DING, T. T. & LANSBURY, P. T. 2002. Molecular crowding accelerates fibrillization of α-synuclein: could an increase in the cytoplasmic protein concentration induce Parkinson's disease? *Biochemistry,* 41**,** 3855-3860.

SILVA, A. M., WHITMORE, M., XU, Z., JIANG, Z., LI, X. & WILLIAMS, B. R. 2004. Protein kinase R (PKR) interacts with and activates mitogen activated

protein kinase kinase 6 (MKK6) in response to double stranded RNA stimulation. *Journal of Biological Chemistry*.

SINGER, H. S., HONG, J. J., YOON, D. Y. & WILLIAMS, P. N. 2005. Serum autoantibodies do not differentiate PANDAS and Tourette syndrome from controls. *Neurology,* 65**,** 1701-1707.

SORKIN, A. & VON ZASTROW, M. 2009. Endocytosis and signalling: intertwining molecular networks. *Nature reviews Molecular cell biology,* 10**,** 609.

SULZER, D., ALCALAY, R. N., GARRETTI, F., COTE, L., KANTER, E., AGIN-LIEBES, J., LIONG, C., MCMURTREY, C., HILDEBRAND, W. H., MAO, X., DAWSON, V. L., DAWSON, T. M., OSEROFF, C., PHAM, J., SIDNEY, J., DILLON, M. B., CARPENTER, C., WEISKOPF, D., PHILLIPS, E., MALLAL, S., PETERS, B., FRAZIER, A., LINDESTAM ARLEHAMN, C. S. & SETTE, A. 2017. T cells from patients with Parkinson's disease recognize α-synuclein peptides. *Nature,* 546**,** 656.

SUN, Q., SUN, L., LIU, H.-H., CHEN, X., SETH, R. B., FORMAN, J. & CHEN, Z. J. 2006. The specific and essential role of MAVS in antiviral innate immune responses. *Immunity,* 24**,** 633-642.

SUZUMURA, A., TAKEUCHI, H., ZHANG, G., KUNO, R. & MIZUNO, T. 2006. Roles of glia-derived cytokines on neuronal degeneration and regeneration. *Annals of the New York Academy of Sciences,* 1088**,** 219-229.

TABETA, K., HOEBE, K., JANSSEN, E. M., DU, X., GEORGEL, P., CROZAT, K., MUDD, S., MANN, N., SOVATH, S. & GOODE, J. 2006. The Unc93b1 mutation 3d disrupts exogenous antigen presentation and signaling via Toll-like receptors 3, 7 and 9. *Nature immunology,* 7**,** 156.

TAKAHASHI, M., YAMADA, T., NAKAJIMA, S., NAKAJIMA, K., YAMAMOTO, T. & OKADA, H. 1995. The substantia nigra is a major target for neurovirulent influenza A virus. *The Journal of Experimental Medicine,* 181**,** 2161-2169.

TALLÓCZY, Z., VIRGIN, I., HERBERT & LEVINE, B. 2006. PKR-dependent xenophagic degradation of herpes simplex virus type 1. *Autophagy,* 2**,** 24-29.

TANAKA, K. & MATSUDA, N. 2014. Proteostasis and neurodegeneration: the roles of proteasomal degradation and autophagy. *Biochimica et Biophysica Acta (BBA)-Molecular Cell Research,* 1843**,** 197-204.

TANAKA, T. & KISHIMOTO, T. 2014. The Biology and Medical Implications of Interleukin-6. *Cancer Immunology Research,* 2**,** 288-294.

TANAKA, T., NARAZAKI, M. & KISHIMOTO, T. 2012. Therapeutic targeting of the interleukin-6 receptor. *Annual review of pharmacology and toxicology,* 52**,** 199-219.

TANNER, C. M., KAMEL, F., ROSS, G. W., HOPPIN, J. A., GOLDMAN, S. M., KORELL, M., MARRAS, C., BHUDHIKANOK, G. S., KASTEN, M., CHADE, A. R., COMYNS, K., RICHARDS, M. B., MENG, C., PRIESTLEY, B., FERNANDEZ, H. H., CAMBI, F., UMBACH, D. M., BLAIR, A., SANDLER, D. P. & LANGSTON, J. W. 2011. Rotenone, Paraquat, and Parkinson's Disease. *Environmental Health Perspectives,* 119**,** 866-872.

TAUBENBERGER, J. K., REID, A. H., KRAFFT, A. E., BIJWAARD, K. E. & FANNING, T. G. 1997. Initial genetic characterization of the 1918 "Spanish" influenza virus. *science,* 275**,** 1793-1796.

THANOS, D. & MANIATIS, T. 1995. NF-κB: a lesson in family values. *Cell,* 80**,** 529-532.

THEIL, D., DERFUSS, T., PARIPOVIC, I., HERBERGER, S., MEINL, E., SCHUELER, O., STRUPP, M., ARBUSOW, V. & BRANDT, T. 2003. Latent

herpesvirus infection in human trigeminal ganglia causes chronic immune response. *The American journal of pathology,* 163**,** 2179-2184.

THULASI RAMAN, S. N. & ZHOU, Y. 2016. Networks of Host Factors that Interact with NS1 Protein of Influenza A Virus. *Frontiers in Microbiology,* 7**,** 654.

TSE, W., CERSOSIMO, M. G., GRACIES, J.-M., MORGELLO, S., OLANOW, C. W. & KOLLER, W. 2004. Movement disorders and AIDS: a review. *Parkinsonism & Related Disorders,* 10**,** 323-334.

TURVEY, S. E. & BROIDE, D. H. 2010. Innate immunity. *Journal of Allergy and Clinical Immunology,* 125**,** S24-S32.

TYEDMERS, J., MOGK, A. & BUKAU, B. 2010. Cellular strategies for controlling protein aggregation. *Nature reviews Molecular cell biology,* 11**,** 777.

ULBRICH, F., KAUFMANN, K., ROESSLEIN, M., WELLNER, F., AUWÄRTER, V., KEMPF, J., LOOP, T., BUERKLE, H. & GOEBEL, U. 2015. Argon Mediates Anti-Apoptotic Signaling and Neuroprotection via Inhibition of Toll-Like Receptor 2 and 4. *PloS one,* 10**,** e0143887.

UNGERSTEDT, U. 1968. 6-Hydroxy-dopamine induced degeneration of central monoamine neurons. *European journal of pharmacology,* 5**,** 107-110.

UVERSKY, V. N., LI, J., BOWER, K. & FINK, A. L. 2002. Synergistic effects of pesticides and metals on the fibrillation of α-synuclein: implications for Parkinson's disease. *Neurotoxicology,* 23**,** 527-536.

VALIATHAN, R., ASHMAN, M. & ASTHANA, D. 2016. Effects of ageing on the immune system: infants to elderly. *Scandinavian journal of immunology,* 83**,** 255-266.

VALYI-NAGY, T., OLSON, S. J., VALYI-NAGY, K., MONTINE, T. J. & DERMODY, T. S. 2000. Herpes simplex virus type 1 latency in the murine nervous system is associated with oxidative damage to neurons. *Virology,* 278**,** 309-321.

VAN RIEL, D., VERDIJK, R. & KUIKEN, T. 2015. The olfactory nerve: a shortcut for influenza and other viral diseases into the central nervous system. *The Journal of Pathology,* 235**,** 277-287.

VICKERS, C. A., STEPHENS, B., BOWEN, J., ARBUTHNOTT, G. W., GRANT, S. G. N. & INGHAM, C. A. 2006. Neurone specific regulation of dendritic spines in vivo by post synaptic density 95 protein (PSD-95). *Brain Research,* 1090**,** 89-98.

VICTOR, F. & GOTTLIEB, A. 2002. TNF-alpha and apoptosis: implications for the pathogenesis and treatment of psoriasis. *Journal of drugs in dermatology: JDD,* 1**,** 264-275.

VILCHEZ, D., SAEZ, I. & DILLIN, A. 2014. The role of protein clearance mechanisms in organismal ageing and age-related diseases. *Nature communications,* 5**,** 5659.

VINCENT, A., BUCKLEY, C., SCHOTT, J. M., BAKER, I., DEWAR, B. K., DETERT, N., CLOVER, L., PARKINSON, A., BIEN, C. G. & OMER, S. 2004. Potassium channel antibody-associated encephalopathy: a potentially immunotherapy-responsive form of limbic encephalitis. *Brain,* 127**,** 701-712.

VLAJINAC, H., DZOLJIC, E., MAKSIMOVIC, J., MARINKOVIC, J., SIPETIC, S. & KOSTIC, V. 2013. Infections as a risk factor for Parkinson's disease: a case–control study. *International Journal of Neuroscience,* 123**,** 329-332.

VOLPICELLI-DALEY, L. A., LUK, K. C., PATEL, T. P., TANIK, S. A., RIDDLE, D. M., STIEBER, A., MEANEY, D. F., TROJANOWSKI, J. Q. & LEE, V. M.-Y. 2011. Exogenous α-synuclein fibrils induce Lewy body pathology leading to synaptic dysfunction and neuron death. *Neuron,* 72**,** 57-71.

VON ECONOMO, C. 1931. *Encephalitis Lethargica: Its Sequelae and Treatment,* London, Oxford University Press.

WALTERS, J. H. 1960. Postencephalitic Parkinson syndrome after meningoencephalitis due to coxsackie virus group B, type 2. *New England Journal of Medicine,* 263**,** 744-747.

WANG, B. X., WEI, L., KOTRA, L. P., BROWN, E. G. & FISH, E. N. 2017. A Conserved Residue, Tyrosine (Y) 84, in H5N1 Influenza A Virus NS1 Regulates IFN Signaling Responses to Enhance Viral Infection. *Viruses,* 9**,** 107.

WATSON, M. B., RICHTER, F., LEE, S. K., GABBY, L., WU, J., MASLIAH, E., EFFROS, R. B. & CHESSELET, M.-F. 2012. Regionally-specific microglial activation in young mice over-expressing human wildtype alpha-synuclein. *Experimental neurology,* 237**,** 318-334.

WETMUR, J. G., SCHWARTZ, J. & ELIZAN, T. S. 1979. Nucleic acid homology studies of viral nucleic acids in idiopathic Parkinson's disease. *Archives of neurology,* 36**,** 462-464.

WHITE, W. J. & CHAM, S. 1998. The Development and Maintenance of the Crl: CH!! J (SD) IGSBR Rat Breeding System.

WIEDENMANN, B. & FRANKE, W. W. 1985. Identification and localization of synaptophysin, an integral membrane glycoprotein of Mr 38,000 characteristic of presynaptic vesicles. *Cell,* 41**,** 1017-1028.

WINNER, B., JAPPELLI, R., MAJI, S. K., DESPLATS, P. A., BOYER, L., AIGNER, S., HETZER, C., LOHER, T., VILAR, M. & CAMPIONI, S. 2011. In vivo demonstration that α-synuclein oligomers are toxic. *Proceedings of the National Academy of Sciences,* 108**,** 4194-4199.

WONG, E. & CUERVO, A. M. 2010. Integration of clearance mechanisms: the proteasome and autophagy. *Cold Spring Harbor perspectives in biology***,** a006734.

WOOD, S. J., WYPYCH, J., STEAVENSON, S., LOUIS, J.-C., CITRON, M. & BIERE, A. L. 1999. α-Synuclein fibrillogenesis Is nucleation-dependent Implications for the pathogenesis of Parkinson′ s disease. *Journal of Biological Chemistry,* 274**,** 19509-19512.

WOZNIAK, M. A., FROST, A. L. & ITZHAKI, R. F. 2009. Alzheimer's disease-specific tau phosphorylation is induced by herpes simplex virus type 1. *Journal of Alzheimer's Disease,* 16**,** 341-350.

WU, X.-F., BLOCK, M. L., ZHANG, W., QIN, L., WILSON, B., ZHANG, W.-Q., VERONESI, B. & HONG, J.-S. 2005. The role of microglia in paraquat-induced dopaminergic neurotoxicity. *Antioxidants & redox signaling,* 7**,** 654-661.

XICOY, H., WIERINGA, B. & MARTENS, G. J. M. 2017. The SH-SY5Y cell line in Parkinson's disease research: a systematic review. *Molecular Neurodegeneration,* 12**,** 10.

XU, J., KAO, S.-Y., LEE, F. J., SONG, W., JIN, L.-W. & YANKNER, B. A. 2002. Dopamine-dependent neurotoxicity of α-synuclein: a mechanism for selective neurodegeneration in Parkinson disease. *Nature medicine,* 8**,** 600.

YAMADA, T., YAMANAKA, I., TAKAHASHI, M. & NAKAJIMA, S. 1996. Invasion of brain by neurovirulent influenza A virus after intranasal inoculation. *Parkinsonism & related disorders,* 2**,** 187-193.

YAMAMOTO, R., ISEKI, E., MURAYAMA, N., MINEGISHI, M., MARUI, W., TOGO, T., KATSUSE, O., KATO, M., IWATSUBO, T. & KOSAKA, K. 2006. Investigation of Lewy pathology in the visual pathway of brains of dementia with Lewy bodies. *Journal of the neurological sciences,* 246**,** 95-101.

YAVICH, L., JÄKÄLÄ, P. & TANILA, H. 2006. Abnormal compartmentalization of norepinephrine in mouse dentate gyrus in α-synuclein knockout and A30P transgenic mice. *Journal of neurochemistry,* 99**,** 724-732.

YORDY, B., IIJIMA, N., HUTTNER, A., LEIB, D. & IWASAKI, A. 2012. A neuron-specific role for autophagy in antiviral defense against herpes simplex virus. *Cell host & microbe,* 12**,** 334-345.

ZARRANZ, J. J., ALEGRE, J., GÓMEZ-ESTEBAN, J. C., LEZCANO, E., ROS, R., AMPUERO, I., VIDAL, L., HOENICKA, J., RODRIGUEZ, O. & ATARÉS, B. 2004. The new mutation, E46K, of α-synuclein causes parkinson and Lewy body dementia. *Annals of Neurology: Official Journal of the American Neurological Association and the Child Neurology Society,* 55**,** 164-173.

ZHANG, H., LI, W., WANG, G., SU, Y., ZHANG, C., CHEN, X., XU, Y. & LI, K. 2011. The distinct binding properties between avian/human influenza A virus NS1 and Postsynaptic density protein-95 (PSD-95), and inhibition of nitric oxide production. *Virology journal,* 8**,** 298.

ZHANG, J., PERRY, G., SMITH, M. A., ROBERTSON, D., OLSON, S. J., GRAHAM, D. G. & MONTINE, T. J. 1999. Parkinson's disease is associated with oxidative damage to cytoplasmic DNA and RNA in substantia nigra neurons. *The American journal of pathology,* 154**,** 1423-1429.

ZHANG, W., WANG, T., PEI, Z., MILLER, D. S., WU, X., BLOCK, M. L., WILSON, B., ZHANG, W., ZHOU, Y. & HONG, J.-S. 2005. Aggregated α-synuclein activates microglia: a process leading to disease progression in Parkinson's disease. *The FASEB journal,* 19**,** 533-542.

ZHAO, Y., RIVIECCIO, M. A., LUTZ, S., SCEMES, E. & BROSNAN, C. F. 2006. The TLR3 ligand poly I:C downregulates connexin 43 expression and function in astrocytes by a mechanism involving the NF-κB and PI3 kinase pathways. *Glia,* 54**,** 775-785.

ZHOU, L., WANG, X., WANG, Y. J., ZHOU, Y., HU, S., YE, L., HOU, W., LI, H. & HO, W. Z. 2009. Activation of Toll-like receptor-3 induces interferon-λ expression in human neuronal cells. *Neuroscience,* 159**,** 629-637.

ZHU, Y., CHEN, X., LIU, Z., PENG, Y.-P. & QIU, Y.-H. 2015. Interleukin-10 protection against lipopolysaccharide-induced neuro-inflammation and neurotoxicity in ventral mesencephalic cultures. *International journal of molecular sciences,* 17**,** 25.

ZIMPRICH, A., BISKUP, S., LEITNER, P., LICHTNER, P., FARRER, M., LINCOLN, S., KACHERGUS, J., HULIHAN, M., UITTI, R. J., CALNE, D. B., STOESSL, A. J., PFEIFFER, R. F., PATENGE, N., CARBAJAL, I. C., VIEREGGE, P., ASMUS, F., MÜLLER-MYHSOK, B., DICKSON, D. W., MEITINGER, T., STROM, T. M., WSZOLEK, Z. K. & GASSER, T. 2004. Mutations in LRRK2 Cause Autosomal-Dominant Parkinsonism with Pleomorphic Pathology. *Neuron,* 44**,** 601-607.

Appendix

Appendix A.

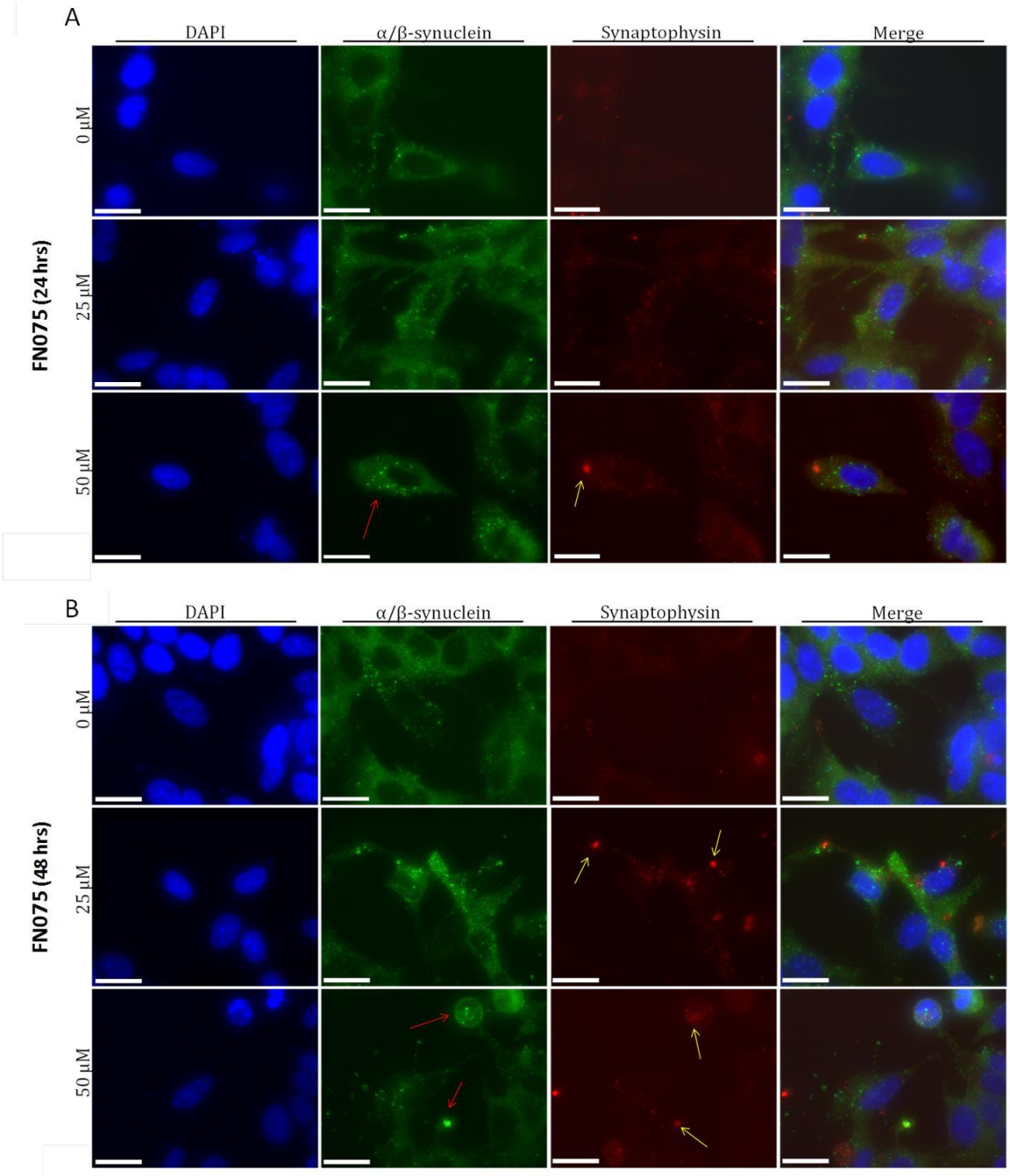

Figure 1. FN075 induced α-synuclein aggregation *in vitro*. (**A** and **B**) SH-SY5Y cells were incubated with FN075 (0-50 µM) for 24 or 48 hr. Qualitative α-synuclein and synaptophysin intra-cellular protein inclusions (red and yellow arrows, respectively) were visible after FN075 treatment. Scale bar = 20 µm